Pentopyranosyl Oligonucleotide Systems

9th Communication[1])

The β-D-Ribopyranosyl-(4′ → 2′)-oligonucleotide System ('Pyranosyl-RNA'): Synthesis and Resumé of Base-Pairing Properties

by **Stefan Pitsch**[2a]), **Sebastian Wendeborn**[2b]), **Ramanarayanan Krishnamurthy***[2c]), **Armin Holzner**[2d]), **Mark Minton**[2e]), **Martin Bolli**[2f]), **Christian Miculca**[2g]), **Norbert Windhab**[2h]), **Ronald Micura**[2i]), **Michael Stanek**[2k]), **Bernhard Jaun,** and **Albert Eschenmoser***

Laboratory of Organic Chemistry, Swiss Federal Institute of Technology (ETH), Hönggerberg, HCI H309, CH-8093 Zürich

and

The *Skaggs* Institute for Chemical Biology at The *Scripps* Research Institute (TSRI), 10550 North Torrey Pines Road, La Jolla, CA-92037, USA

Dulio Arigoni zu seinem 75. Geburtstag gewidmet, in Erinnerung an gute alte Zeiten

Pyranosyl-RNA ('p-RNA') is an oligonucleotide system isomeric to natural RNA and composed of the very same building blocks as RNA. Its generational, chemical, and informational properties are deemed to be those of an alternative nucleic acid system that could have been a candidate in Nature's evolutionary choice of the molecular basis of genetic function. We consider the study of the chemistry of p-RNA as etiologically relevant in the sense that knowledge of its structural, chemical, and informational properties on the chemical level offers both a perspective and reference points for the recognition of specific structural assets of the RNA structure that made it the (supposedly) superior system among possible alternatives and, therefore, the system that became part of biology as we know it today. The paper describes the chemical synthesis of β-D- (and L)-ribopyranosyl-(4′ → 2′)-oligonucleotide sequences, presents a resume of their structural and chemical properties, and cautiously discusses what we may and may not have learned from the pyranosyl isomer of RNA with respect to the conundrum of RNA's origin.

---

[1]) For communications No. 1–8 see [1–8]. The label '*Chemistry of Pyranosyl-RNA*' previously used for the series of papers on p-RNA [1–8] has been changed (see [9]) into '*Pentopyranosyl Oligonucleotide Systems*' as a consequence of the extension of our work on p-RNA to a whole family of diastereoisomeric pentopyranosyl oligonucleotides. In [9], the present paper had been assigned No. 9 in this series. The follow-up papers No. 10 [9], 11 [10], 12 [11], and 13 [12] in the series have already appeared. The present paper also is communication No. 30 in the series '*Chemistry of α-Aminonitriles*'. The assignment of papers in this latter series is as follows: No. 29 is [13], [14] counts as No. 28, [15] is No. 27, [16] is No. 26, [17] counts as No. 25, [8] is No. 24, [7] counts as No. 23, [18] is No. 22, [5] No. 21, [6] No. 20, [4] counts as No. 19, [3] is No. 18, [19] No. 17, [2] No. 16, [20] No. 15, [21] No. 14, [22] No. 13, [23] No. 12, and [1] is No. 11; the communication assigned to be No. 10 [24] has not appeared yet; [25] is No. 9, [26] No. 8, [27] No. 7, [28] No. 6, [29] No. 5, [30] No. 4, [31] No. 3, [32] No. 2, and [33] is No. 1.

[2]) Postdoctorates: a) ETH September 1992 – February 1995; b) ETH November 1992 – December 1993; c) ETH July 1992 – December 1994 and TSRI 1996 –; d) ETH April 1992 – October 1993; e) ETH September 1993 – April 1994; f) ETH and TSRI January 1995 – June 1997; g) Universität Frankfurt October 1993 – März 1995; h) Universität Frankfurt 1993–1995; i) ETH and TSRI January 1996 – June 1998; k) TSRI June 1998 – June 1999.

1. Introduction. – The β-D-Ribopyranosyl-(4′ → 2′)-oligonucleotide system ('pyranosyl-RNA' or 'p-RNA') is a constitutional isomer of RNA, containing its D-ribose building block in the pyranose (instead of the furanose) form, and the phosphodiester linkage between the D-ribose C-atoms C(4′) and C(2′) (instead of C(5′) and C(3′)). From a chemical point of view, the *type* of generational chemistry that allows the molecular structure of contemporary RNA to be derived from its building blocks (D-ribose, phosphate and nucleobases) might equally give rise to (and have given rise to) the pyranosyl isomer of RNA. Therefore, this latter system is deemed to have been a potentially natural, evolutionary alternative to RNA. Why, then, did Nature choose the furanose and not the pyranose form of RNA as an informational molecular system? Any comment to this question has as its absolute pre-requisite a knowledge of p-RNA's chemical properties, a quest primarily directed to the property that constitutes the chemical basis of RNA's role in Biology, namely, its capability to undergo informational *Watson–Crick* pairing. Thus, the study of the chemistry of the pyranosyl isomer of RNA must be part of any experimental approach to a chemical etiology of the structure type of the natural nucleic acids.

In a series of preliminary communications in this and other journals [1–8], we had reported on the synthesis, the structure, and the chemical properties of p-RNA. These studies were later extended to a whole family of pentopyranosyl oligonucleotide systems [15–17], all of them representing potentially natural nucleic acid alternatives according to the criteria previously defined [34–40]. While our preliminary communications on these latter studies have been complemented recently by full papers in this journal reporting in detail the procedures used in synthesis, purification, and characterization of the pentopyranosyl oligonucleotides investigated [9–12], the corresponding paper on p-RNA, describing the synthesis of β-D-ribopyranosyl-(4′ → 2′)-oligonucleotides in detail, had been unduly postponed. The present paper closes this gap.

Work on the pyranosyl-isomer of RNA was initiated in 1992 as a consequence of observations we had made in studies on the properties of hexopyranosyl-(6′ → 4′) alternatives of RNA. We had found that none of the three investigated members of the hexopyranosyl-(6′ → 4′) family, namely, oligonucleotides of the β-allo-, β-altro- and β-glucopyranosyl series (*Fig. 1*), possesses a capacity for *Watson–Crick* pairing that would be comparable in strength, selectivity, and informational consistency to that of corresponding RNA oligonucleotides [24][36–38][41][42]. This had led us to conclude that, for functional reasons, such hexopyranosyl-(6′ → 4′) analogues of RNA could *not* have acted as evolutionary competitors of the RNA structure[3]). The inability of these potentially natural (fully hydroxylated) hexopyranosyl systems to undergo efficient *Watson–Crick* base pairing was in sharp contrast to the remarkable pairing capability of the 'unnatural' 2′,3′-dideoxy model system homo-DNA (*Fig. 1*), which we had investigated before, and whose base-pairing strength in both the

---

[3]) In a strict sense, this conclusion is valid only for the three investigated members from the eight diastereoisomers of the hexopyranosyl-(6′ → 4′)-oligonucleotide family containing their nucleobases in equatorial positions. Analogous intrastrand steric hindrance in the pairing conformation is, however, to be expected for (most of) the remaining members. For pairing properties of hexapyranosyl oligonucleotide systems with non-nucleosidic ('unnatural') structure, see [43–45].

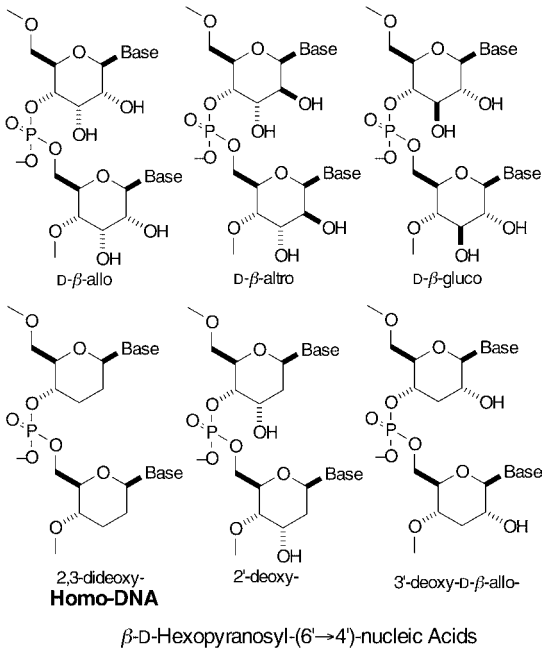

Fig. 1. *Members of the family of β-D-hexopyranosyl-(6′ → 4′)-oligonucleotides dealt with in previous studies*

Watson–Crick and (reverse) *Hoogsteen* mode had been found to be greater than that of either DNA or RNA[4]). This contrast has been rationalized as resulting from intrastrand steric hindrance in the pairing conformation of the fully hydroxylated

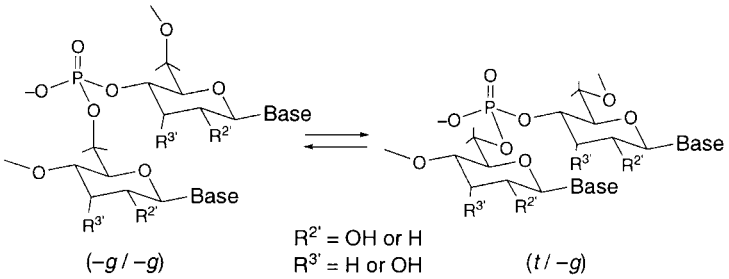

Fig. 2. *The two pairing-conformations of the homo-DNA system as deduced by qualitative conformational analysis* [29] *and observed by NMR structure determination* [26].

---

[4]) The criterion for deciding whether a RNA analogue is to be deemed a 'potentially natural' nucleic acid alternative refers to whether the structure of an analogue can be derived from a $(CH_2O)_n$ aldose sugar ($n = 4-6$) by the same type of (potentially natural) chemistry that allows the structure of RNA to be derived from ribose [29][40].

hexopyranosyl systems. Such hindrance is expected to occur between an equatorial 2′-OH group of a pyranosyl unit and the neighboring (downstream-positioned) nucleobase; it is clearly to be inferred from model considerations based on homo-DNA's two types of pairing conformations ($-g/-g$ and $t/-g$), which were derived by qualitative conformational analysis [29][5]) (*Fig. 2*), and were found to co-exist in a homo-DNA duplex by an NMR structure analysis by *Otting et al* [26]. The results of experimental studies on 2′-deoxy- and 3′-deoxyallopyranosyl model systems [24][46][47] (*Table 1*) corroborated this interpretation.

Table 1. *Relative Base-Pairing Strengths in β-*D*-*A*llopyranosyl-Oligonucleotide Derivatives*

$R^{3'}$	$R^{2'}$	Relative pairing strength
OH	OH	very weak [41][38]
H	H	very strong [25]
OH	H	strong [46][38][37]
H	OH	weak [46][38][37]

It was this insight into the consequences of the steric bulk of fully hydroxylated (6′ → 4′)-hexopyranosyl building blocks that led us to ask whether base pairing might be

[5]) Homo-DNA's $g/-g$ pairing conformation corresponds to the pairing conformation of RNA (and A-type conformation of DNA) as illustrated by the juxtaposition of the formulae below. *Herdewijn*'s closely related hexitol-NA [43] is a constitutional isomer of homo-DNA, it has a non-nucleosidic constitution and is, therefore, not to be considered a potentially natural nucleic acid alternative. Its importance lies in its capability to cross-pair with RNA (its nucleobase occupies an axial conformation [43]). *Herdewijn*'s observations on the diverging base-pairing capabilities of the two epimeric mono-hydroxylated HNA derivatives (the axial epimer cross-pairs with RNA [44], the equatorial epimer does not [45]) can equally be rationalized as being due to intrastrand steric hindrance in the latter [45]. Of special interest to the conformational analysis of oligonucleotide systems is *Wengel's* 'LNA' [48], the strongest *Watson–Crick* oligonucleotide base-pairing system encountered thus far. Its extraordinary pairing strength convincingly corroborates the relevance of the steric criteria that had been used for deriving the pairing conformation of homo-DNA (and, implicitly, also of A-type DNA) by qualitative conformational analysis [29][1].

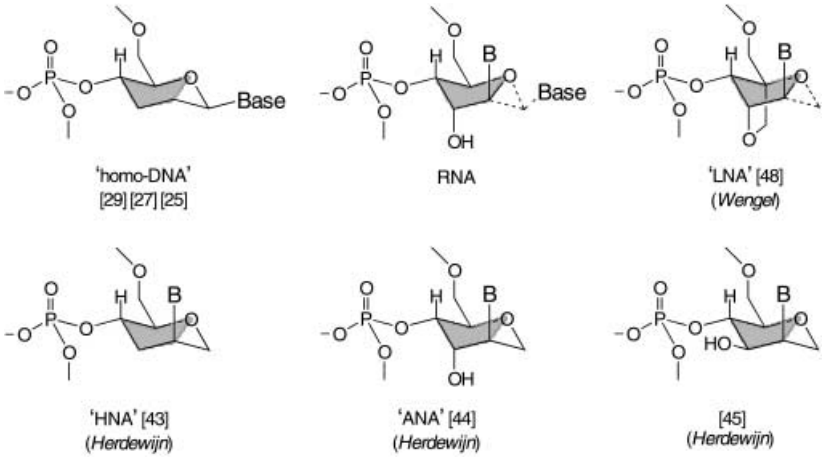

encountered in systems which, while still having their sugar unit in the *pyranose* form, would contain only *five* instead of six C-atoms. In such *pento*pyranosyl systems, the phosphodiester groups could not link, however, the pyranose units in the same way as they link the pentofuranosyl and the hexapyranosyl units in RNA and homo-DNA, respectively. According to a conjecture that, at the time, was believed to be valid[6]), any oligonucleotide system expected to possess the capability of informational base pairing should have in its backbone six covalent bonds per monomer unit, as is the case in the backbone of the natural nucleic acids (as well as of homo-DNA). Therefore, the backbone of a *pento*pyranosyl oligonucleotide system would have to link the pyranosyl units between the sugar atoms C(4′) and C(2′) (*Fig. 3*). Interestingly, such a (4′ → 2′)-positioning of the phosphodiester bridge in a pyranosyl isomer of RNA was highly reminiscent of an observation we had made earlier in a project relating to a problem in prebiotic chemistry: base-catalyzed aldomerization of glycolaldehyde phosphate under appropriate conditions in the presence of (0.5 equiv.) formaldehyde leads to (*rac*) ribopyranose-2,4-diphosphate as the most abundant component of a reaction mixture consisting of all possible diastereoisomeric (*rac*) tetrose-2,4-diphosphates, pentose-2,4-diphosphates, and hexose-2,4,6-triphosphates [30][7]).

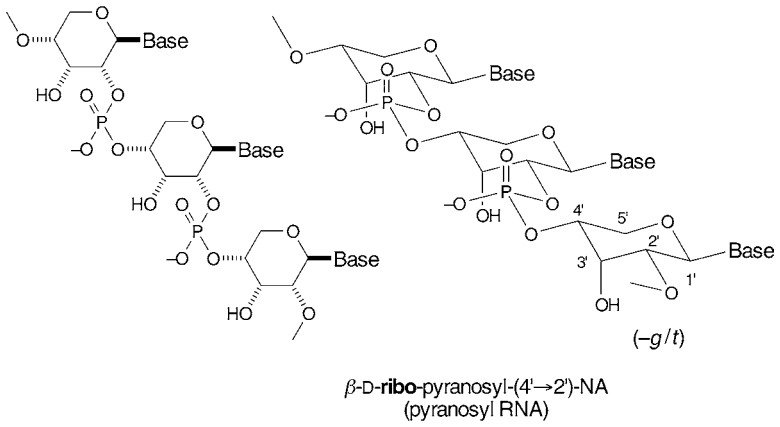

Fig. 3. *Constitutional, configurational, and conformational formulae representing the β-*D*-ribopyranosyl-(4′ → 2′)-oligonucleotide* (p-RNA) *system*

At the outset of our work on p-RNA stood a qualitative conformational analysis of the repeating unit of the β-ribopyranosyl-(4′ → 2′)-backbone. This analysis was delineated in pictorial detail in our first communication on p-RNA [1]; it showed that, within the ensemble of nine least strained (idealized) conformations, one, and only one, of them is conformationally repetitive and, therefore, a possible pairing

6) In later studies, it was found that this requirement is of limited validity only; see [10].

7) For a more detailed discussion of the relationship between these findings and the pentopyranosyl-(4′ → 2′)-type of oligonucleotide structure, see [22].

conformation[8]). Based on this criterion, the β-ribopyranosyl-(4′ → 2′)-oligonucleotide system was expected to be capable of base pairing since, in the homo-DNA series, a similar expectation that was reached by the same type of conformational reasoning had been vindicated by experiment [27]. Such experimental support for an expectation notwithstanding, the remarkable base-pairing properties of p-RNA came eventually nevertheless as a surprise: p-RNA was found to be a much stronger and, concerning the pairing mode, a more selective base-pairing system than the natural (furanosyl) RNA. We have reported on these properties and some of its consequences in our earlier communications [1–8] in sufficient detail so that we can concentrate in the present paper on describing mainly those aspects of p-RNA chemistry that refer to the synthesis, purification, and characterization of β-D-ribopyranosyl-mononucleotides and β-D-ribopyranosyl-(4′ → 2′)-oligonucleotides and deal with the properties of p-RNA oligonucleotides in the form of an overview.

2. Synthesis. – 2.1. *Preparation of the β-Ribopyranosyl-Nucleoside Derivatives Containing (Protected) Adenine (A), Guanine (G), 2,6-Diaminopurine (D), Isoguanine (isoG), Cytosine (C), and (Unprotected) Uracil (U), and Thymine (T) as Nucleobases.* Derivatives of β-D-ribopyranosyl nucleosides containing all five canonical nucleobases had already been described in the literature by various authors [49], however, not in the context of a synthesis of corresponding oligonucleotides. Our own efforts in this field include, in addition to β-D-ribopyranosyl nucleosides containing the five canonical nucleobases, the corresponding nucleosides of D and I. *Scheme 1* summarizes the synthesis of the seven β-D-ribopyranosyl nucleosides **3a** – **3g**, all of them – with the exception of the U and T derivatives – in a protected form suited for the construction of oligonucleotide sequences. In all cases, the nucleosidation methodology of *Vorbrüggen–Hilbert–Johnson* [50], previously successfully applied in the homo-DNA series [28], could be adopted without any difficulties by using an α/β-mixture of D-tetrabenzoyl-ribopyranose [51] as starting material[9]). As usual (see, *e.g.*, [28]), nucleosidation in the G series presented more problems and demanded extended exploratory experimentation. While benzoyl as NH_2-protection group in the A- and

---

[8]) See Scheme 1 in [1]. It seems worth pointing out that an analogously built hexopyranosyl-(4′ → 2′)-oligonucleotide system, *e.g.*, the β-allopyranosyl member depicted below, by the same reasoning, would not be expected to be a base-pairing system. The (repetitive) pairing conformation would suffer serious steric hindrance (see arrow) and, therefore, not become populated in competition with less strained (non-repetitive) conformations.

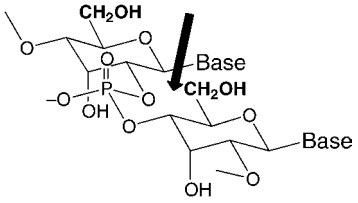

[9]) This starting material, prepared according to a procedure described in [51], contained according NMR spectroscopy *ca.* 70% of the β-pyranose and 20% of the α-pyranose form, and *ca.* 10% of furanose derivatives. In some of the nucleosidation experiments, crystalline and diastereoisomerically pure (but capriciously crystallizing) α-(2,3,4-tribenzoyl)-α-ribopyranosyl bromide [52][51] was used as starting material.

Scheme 1. *Preparation of the U, T, C, A, G, isoG, and D Nucleosides in the β-D-Ribopyranosyl Series*

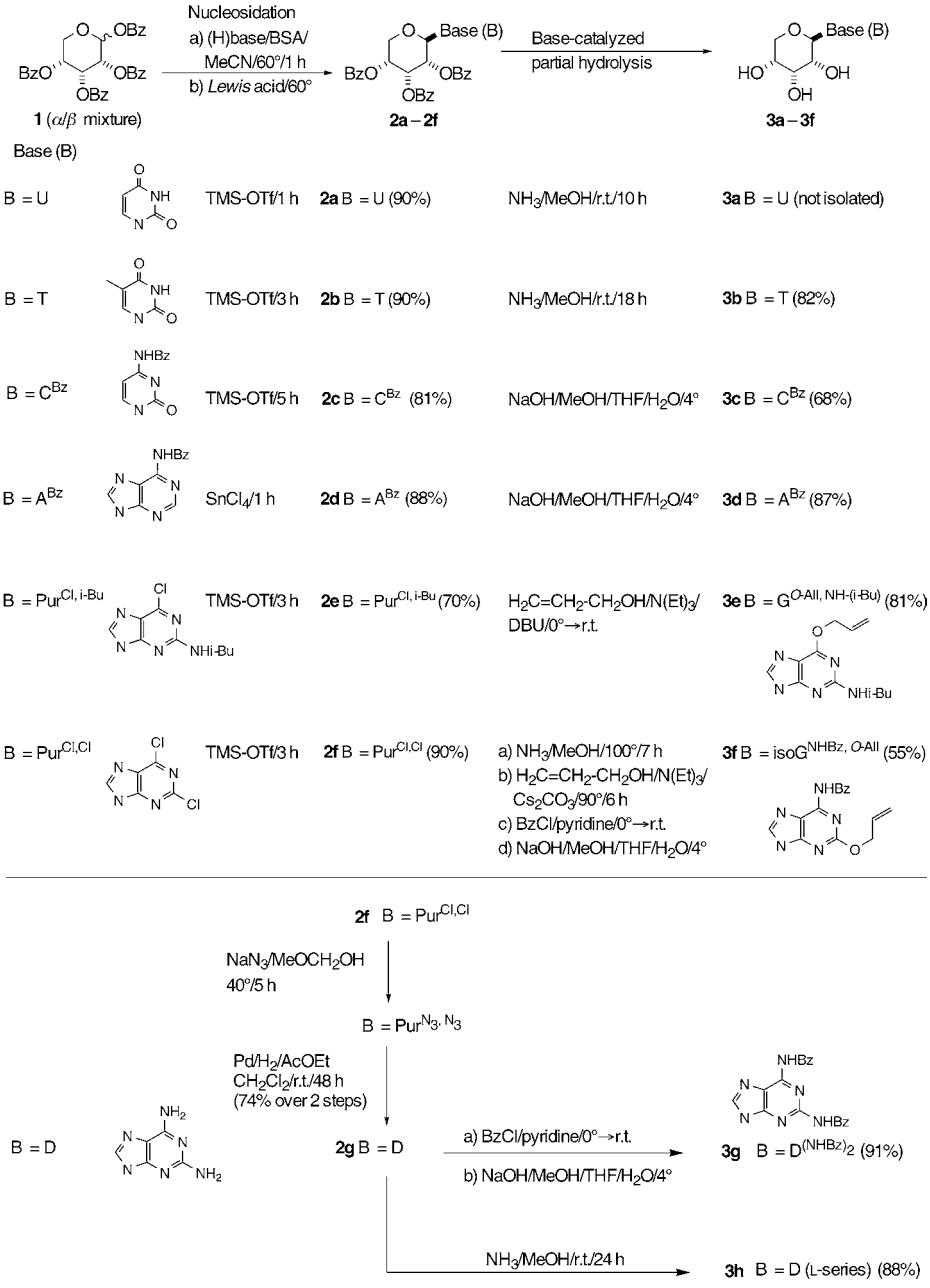

C-nucleosidation partner did not present any problems, exploratory experiments towards the synthesis of the guanosine member led to the choice of *O*-allyl/NH-isobutyryl protection in the nucleoside and of the 6-chloro-2-(isobutyrylamino)purine [53][54] (as against the N^2-isobutyryl-6-oxo derivative) as the nucleosidation partner. Originally, nucleosidation was explored by using N^2-isobutyryl guanine, but this procedure suffered from low yields, low N(9)/N(7)-selectivity, and difficult separations exacerbated by poor solubilities. Nucleosidation with 6-chloro-N^2-isobutyrylpurine proceeded with high N(9)-regioselectivity with only negligible amounts of (not isolated) N(7)-isomer formed. The replacement of the Cl-atom at C(6) by the allyloxy group (**2e** → **3e**) was most satisfactorily achieved by treatment with a concentrated (20% *v*/*v*) soln. of anhydrous Et_3N in dry allyl alcohol containing 1.5 mol-equiv. of DBU between 0° and room temperature for *ca.* 5 h. These conditions [55][56] concomitantly remove the three *O*-Bz groups of **2e** by alcoholysis, but leave the *N(2)*-isobutyryl protection untouched. The procedure was eventually preferred to that initially attempted employing anhydrous $Cs_2(CO_3)$ as a base in dry allyl alcohol. The isoguanine- and 2,6-diaminopurine-β-ribopyranosyl-nucleosides were derived, as in the homo-DNA series [25], from the 2,6-dichloropurine nucleoside, in both cases with benzoyl as the NH_2-protecting and allyl [55] as the carbonyl-protecting group. The somewhat tricky transformation of the 2,6-dichloropurine nucleoside **2f** to the 2,6-diaminopurine nucleoside **2g** *via* the (non-purified) 2,6-diazido derivative eventually proceeded satisfactorily under the conditions developed in the homo-DNA series [25].

All nucleosidations (**1** → **2a**–**2f**) gave the equatorial β-isomers as the exclusively isolated reaction products in (mostly) excellent yields. Assignment of their configuration at the anomeric center is based on the characteristic value of the ^{1}H-NMR coupling constants between the anomeric proton H–C(1′) (δ *ca.* 6 to 6.5 ppm) and the H-atom at C(2′), both occupying axial positions at the pyranose chairs; the observed range of these values in the nucleoside series **3a**–**3g** are consistently found in the range of 9.3 to 9.7 Hz (in various deuterated solvents).

Nucleosides of the L-ribopyranosyl series had been prepared in connection with our pairing studies with homochiral p-RNA strands of opposite sense of chirality [3]; they were made, for the nucleobases C, G, isoG, D, and T, by the same nucleosidation procedures as described for the D-series. L-Ribose was prepared by Mo^{IV}-catalyzed α-epimerization of L-arabinose according to the method described by *van Boom* and coworkers [57].

Scheme 2 summarizes the reaction sequence through which the nucleosides **3a**–**3g** containing their three OH groups in unprotected form were converted into their 3′-*O*Bz-4′-*O*DMT-protected derivatives **8a**–**8g** used as monomer units in the automated synthesis of p-RNA oligonucleotides[10]). The reaction sequence was originally worked out in the U and A series [1], later adapted to the nucleosides containing the other nucleobases [2], and, in the course of our work on the chemistry of p-RNA-oligonucleotides, optimized and simplified according to the demands of an efficient production of p-RNA monomers [4].

---

[10]) One of the early (unsuccessful) plans was to achieve a (4-methoxybenzyloxy)-protection of the 3′-OH function through partial reductive cleavage of a 3′,4′-(4-methoxybenzaldehyde) acetal derivative.

Scheme 2. *Preparation of the 3′-O-Benzoyl-4′-O-trityl Derivatives of U, T, C, A, G, isoG, and D Nucleosides in the β-D-Ribopyranosyl Series*

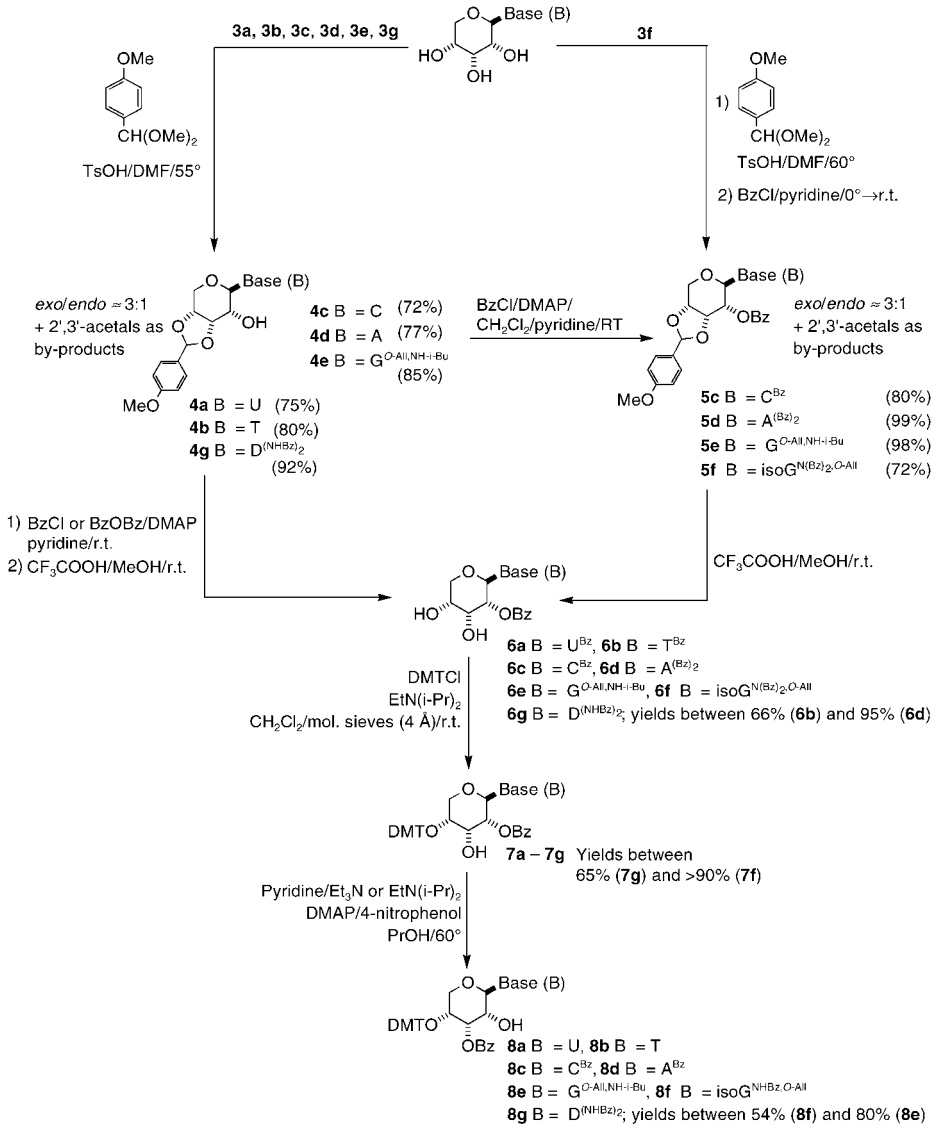

The efforts toward a synthesis of β-ribopyranosyl-(4′ → 2′)-oligonucleotides had to focus from the beginning on the problem of finding an adequate protection of the (axial) 3′-OH function in β-ribopyranosyl-nucleosides. Since this OH group is expected to be the sterically most hindered among the three OH functions, and since 'obvious' attempts in exploratory experiments to achieve regiodifferentiation through regioselectively removing hydrolytically the Bz groups from the (equatorial) positions 2′ and 4′

in a 2′,3′,4′-tribenzoyl-nucleoside derivative were unsuccessful, the protection problem presented itself for quite a while as the major hurdle to the development of a p-RNA synthesis[10]). Eventually, the hurdle was overcome by exploiting the observation[11]) that (unexpectedly) 2′-OBz-3′-OH-β-ribopyranosyl-adenine derivatives in basic media can undergo Bz migration from the equatorial 2′-position to the axial 3′-position. In exploratory experiments aiming at deprotonation of the free 3′-OH group of the easily accessible β-N^6,N^6-dibenzoyl-4′-ODMT-3′-OH-2′-OBz-ribopyranosyl-adenine derivative **7d** (see below and *Scheme 2*) to be followed by *O*-alkylation (*e.g.*, by 4-methoxybenzoyl chloride), it was found that deprotonation with NaH in THF, followed by addition of aq. NH_4Cl soln., affords the 3′-OBz-2′-OH derivative besides the 3′-OH-2′-OBz derivative in a ratio of *ca.* 5:1 and in moderate yield. This solved our protection problem in as far we then decided to aim, from now on, at using Bz as the protecting group of the axial 3′-OH function for the p-RNA-oligonucleotide synthesis. This choice was close at hand because of our earlier experience in the hexopyranosyl series where we had found that Bz could be successfully used as protecting group of axial sugar OH group in the synthesis of β-altropyranosyl-(6′ → 4′)-oligonucleotides [41][42].

The preparative conversion of the nucleosides **3a**–**3g** to their protected 4′-ODMT-3′-OBz-2′-OH derivatives is proceeding *via* a (2′ → 3′)-Bz migration **7** → **8** as the central and critical step. Acid-catalyzed acetalization of nucleosides **3a**–**3g** with 4-methoxybenzaldehyde dimethyl acetal affords – as mixtures of *endo*/*exo*-diastereoisomers in the ratio of *ca.* 3:1 – the 3′,4′-acetals **4a**–**4g** as the major products besides small amounts (ratio to major product *ca.* 1:5–1:6) of their 2′,3′-regioisomers (slightly more polar on TLC), which can be separated from the desired product by chromatography on silica gel[12]). In the exploratory phase of the investigation (working with the U, T, and A nucleosides), *exo*- and *endo*-diastereoisomers of **4** were separated by chromatography on silica gel for spectroscopic characterization and configurational assignments (*e.g.*, δ(CH) for *exo*-acetal of **4** 6.38 ppm, for *endo*-acetal 5.87 ppm, in $CDCl_3$ [58]). The yield of the acetalization step is highest when the reaction is terminated as soon as the starting trial has been consumed (TLC). Longer reaction times lead to acetal migration and mixed diacetal formations [58] (see *Exper. Part*). In the preparative routine, the mixtures of diastereoisomeric 4′,3′-acetals **4a**–**4g** were treated with 2.5 mol-equiv. BzCl in pyridine with 4-(dimethylamino)pyridine (DMAP) as catalyst at room temperature in order to benzoylate the 2′-OH group, the acetal groups were cleared by mild treatment with CF_3CO_2H in MeOH to give the 2′-OBz-3′,4′-dihydroxy nucleosides **6a**–**6g** and, finally, their (less hindered) 4′-OH groups were regioselectively protected as DMT derivatives **7a**–**7g**. Under the employed benzoylation conditions, the nucleobases of the U, T, A, and isoG nucleosides also undergo *N*-benzoylation of their imide NH and amide NH groups, respectively. Since such imide *N*-Bz and *N*,*N*-dibenzoyl groups are quite labile towards hydrolysis (and prone to Bz transfers), the benzoylation products in the U, T, and isoG series were routinely not isolated but subjected directly to the conditions of deacetalization and subsequent tritylation of the equatorial 4′-OH function. The latter reaction **6** → **7** proceeds with high regioselectivity in all seven nucleotide series.

---

[11]) Observation made by *S. W.*

[12]) 2′,3′-Regioisomers of **4a**–**4g** were recycled to triols **3a**–**3g** after acid-catalyzed deacetalization.

Extended optimization studies on the (2′ → 3′)-Bz migration **7** → **8** were carried out in the adenine (B = *N*,*N*-dibenzoyladenine) and uracil (B = *N*-Bz-uracil) series. They resulted in the development of a rather complex cocktail of agents (1 mol-equiv. DMAP, 3 equiv. Et_3N, 2 equiv. 4-nitrophenol, and 20 equiv. i-PrOH[13]) in 82 equiv. pyridine) that, at 60° during 24–28 h, produced with remarkable reliability (2′ → 3′)-Bz-migration products **8d** (B = *N*-monobenzoyladenine) and **8a** (B = uracil) in (*e.g.*) 67% yield (isolated). The equilibrium ratio between the components **7d** (as N^6-monobenzoyl derivative) and **8d** under these reaction conditions was estimated to lie on the side of the 3′-OBz derivatives by a factor of (at least) 1:10. Beyond the NMR-spectroscopic constitutional assignments given below, it was chemically shown that **7d** (B = *N*,*N*-dibenzoyl-adenine) and the *N*,*N*-dibenzoyl analogue of **8d** gave the same tetrabenzoyl derivative when *O*-benzoylated with BzCl in pyridine in the presence of DMAP, benzoylation of the free OH group of **7d** proceeding thereby much more slowly than that of the free OH group of the **8d** analogue.

The (**7** → **8**)-Bz-migration procedure developed in the N^6,N^6-dibenzoylated adenine and N^3-benzoylated-uracil series turned out to be comparably efficient in the G, isoG, and D series. Mixtures of 2′- and 3′-benzoates, when recovered as such in the course of the chromatographic isolation of pure 3′-benzoates, were recycled in the D-ribopyranosyl-guanine, the L-ribopyranosyl-thymine, and D-ribopyranosyl-cytosine series (yields up to 80%). In the C series, routine chromatographic separation of the migration product from the 2′-OBz-3′-OH derivative on silica gel met first with difficulties. This gave rise to a separation procedure that consisted in trimethylsilylation of the mixture's free OH groups (ratio C(2′)–OH to C(3′)–OH *ca.* 6:1) and subsequent regioselective desilylation of the 2′-*O*-silyloxy component by mild acid treatment, chromatographic separation of the 3′-OBz-2′-OH derivative **8c** from remaining silylated components (yield of **8c** 50%, after recycling up to 60%). Eventually, it was found that **8c** can be crystallized from the solution of a chromatographically purified mixture of **8c**/**7c** *in* Et_2O *containing ca.* 4% pentane and obtained thereby in pure form in 48% yield (see *Exper. Part*).

The constitutional assignments for the intermediates **6a**–**6g**, **7a**–**7g**, and **8a**–**8g** rest on the ^{1}H-NMR data of these intermediates; excerpts from such data are listed in *Table 2*. C-Atom C(1′) (anomeric center) in all derivatives is recognized by its chemical shift around 6 ppm and the (large) coupling constant (*ca.* 9.5 Hz) between its (axial) H-atom and H_{ax}–C(2′). The spectral identification of the H–C(3′), H–C(4′), and H_α–C(5′) and H_β–C(5′) centers in **3a**–**3g** is based on spin-coupling and NOE-correlation data. The position of the *O*-Bz group in **6a**–**6g, 7a**–**7g**, and **8a**–**8g** is corroborated by the chemical-shift pattern of H–C(3′), H–C(4′), and H–C(2′) in these derivatives.

A short comment on the Bz-migration step **7a**–**7g** → **8a**–**8g** seems appropriate, not necessarily with regard to the mechanistic and kinetic aspects of the reaction, but

---

[13]) i-PrOH serves the purpose of accepting the (activated) Bz group of the *N*-Bz-uracil nucleus and one of the Bz groups of the *N*,*N*-dibenzoyladenine nucleus; this precludes the formation of 2′,3′-dibenzoyl derivatives as by-products (only relevant for these two nucleosides). The presence of 4-nitrophenol has been found to be beneficial for both rate and product yield; its role is presumably that of a proton donator. In the cases of B = uracil and thymine, 3 equiv. of $EtN(i\text{-}Pr)_2$ was used instead of Et_3N.

Table 2. *Chemical Shifts* (δ/[ppm]) *of Non-Exchangeable Sugar H-Atoms of Synthetic Intermediates*

Entry		H–C(1′)	H–C(2′)	H–C(3′)	H–C(4′)	H_{ax}–C(5′)	H_{eq}–C(5′)	J(1′,2′) [Hz]
1	**2a** ($CDCl_3$)	6.48	5.52	6.31	5.54	4.23	4.34	9.6
2	**2b** ($CDCl_3$)	6.48	5.50	6.31	5.54	4.25	4.33	9.7
3	**2c** ($CDCl_3$)	6.76	5.56	6.34	5.60	4.29	4.37	9.6
4	**2d** ($CDCl_3$)	6.50	6.01	6.41	5.70	4.33–4.46	4.33–4.46	9.5
5	**2e** ($CDCl_3$)	6.44	5.93	6.38	5.68	4.34	4.41	9.3
6	**2f** ($CDCl_3$)	6.43	5.88	6.39	5.69	4.36	4.45	9.5
7	**2g** ($CDCl_3$)	6.21	6.04	6.42	5.67	4.35	4.38	9.4
8	**3a** (D_2O)	5.69	3.95	4.27	3.95	3.75	3.83	9.7
9	**3b** (CD_3OD)	5.75	3.71–3.80	4.17	3.71–3.80	3.71–3.80	3.71–3.80	9.3
10	**3c** (DMSO(D_6))	5.83	3.60–3.78	4.02	3.60–3.78	3.60–3.78	3.60–3.78	9.5
11	**3d** (CD_3OD)	5.92	4.37	4.26	3.90	3.80	3.90	9.4
12	**3e** (DMSO(D_6))	5.67	4.24	4.05	3.73	3.60	3.67	9.4
13	**3f** (CD_3OD)	5.80	4.35	4.24	3.70–3.90	3.70–3.90	3.70–3.90	9.8
14	**3g** (CD_3OD)	5.99	4.31	4.30	3.75–4.00	3.75–4.00	3.72–4.00	8.8
15	**3h** (D_2O)	5.48	4.24	4.22	3.95	3.74–3.76	3.74–3.76	9.4
16	**6a** (CD_3OD)	6.17	5.26	4.41	4.00	3.90	3.90	9.6
17	**6b** (CD_3OD)	6.18	5.30	4.42	4.03	3.90	3.90	9.6
18	**6c** (CD_3OD)	6.43	5.25	4.45	3.87–4.07	3.87–4.07	3.87–4.07	9.5
19	**6d** ($CDCl_3$)	6.28	5.52	4.54	4.08	3.85–3.97	3.85–3.97	9.5
20	**6e** ($CDCl_3$)	6.75	5.60	4.87	4.14	4.03	4.24	9.7
21	**6f** (CD_3OD)	6.19	5.60	4.47	4.08	3.91	4.00	9.4
22	**6g** (CD_3OD)	6.48	5.57	4.50	3.96	4.09	4.12	9.4
23	**7a** ($CDCl_3$)	6.20	4.88	3.91	3.97	3.27	3.91	9.4
24	**7b** ($CDCl_3$)	6.20	4.88	3.72	3.94	3.28	3.94	9.5
25	**7c** ($CDCl_3$)	6.46	4.84	3.76–3.79	3.84–3.88	3.25–3.28	3.84–3.88	9.0
26	**7d** ($CDCl_3$)	6.26	5.35	3.74	4.05	3.38	4.02	9.6
27	**7e** ($CDCl_3$)	6.13	5.38	3.86	4.02	3.28	3.98	9.6
28	**7f** ($CDCl_3$)	6.19	5.25	3.75	4.01	3.29	3.97	9.6
29	**7g** ($CDCl_3$)	5.89	5.73	4.44	4.00	2.49	3.61	9.2
30	**8a** ($CDCl_3$)	5.76	3.52	5.88	3.85	2.60	3.60	9.5
31	**8b** ($CDCl_3$)	5.90	3.52	5.96	3.88	2.59	3.61	9.5
32	**8c** ($CDCl_3$)	6.03	3.66–3.76	5.88	3.91–3.95	2.71	3.66–3.76	9.3
33	**8d** ($CDCl_3$)	5.81	4.39	5.92	4.04	2.79	3.79	9.2
34	**8e** ($CDCl_3$)	5.68	4.44	6.10	3.95	2.58	3.68	9.2
35	**8f** ($CDCl_3$)	5.71	4.29	5.92	4.00	2.74	3.72	9.3
36	**8g** ($CDCl_3$)	5.89	4.45	6.27	4.00	2.47	3.61	9.2

concerning the remarkably one-sided position of the thermodynamic equilibrium. Base-catalyzed migrations of acyl groups between *cis*-vicinal OH functionalities in six-membered ring systems are commonplace, not necessarily so, however, in cases of an acyl-group migrating from an equatorial to an axial position. Our interpretation, which involves the qualitative assessment of the contribution of both steric and stereoelectronic factors, leans toward considering the case as a nice example of the *gauche* effect [59] contributing to, if not dominating, the position of a reaction equilibrium: The violation of the *gauche* effect by the equatorial 2′-OH function (2′-O and 5′-O centers antiperiplanar to each other; *Fig. 4*) is expected to impose a deficit in conjugative $n \rightarrow \pi^*$ stabilization in the 2′-OBz group as compared to a BzO group whose OH function would not be antiperiplanar to another O center. Ester functions that are part of a *gauche*-effect-violating arrangement are expected to be more

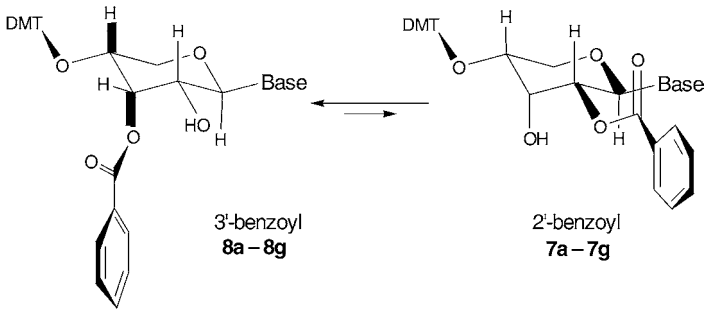

Fig. 4. *The (2′→3′)-Bz migration in β-*D*-ribopyranosyl-nucleosides.* Note the difference between the two isomers with reference to the '*gauche* effect'.

electrophilic (more prone to transesterification) than ester groups, which – *ceteris paribus* – obey the *gauche* effect in such a molecular environment. Thus, an ester function in a non-violating arrangement is the BzO group in the 3′-position (axial 3′-OBz antiperiplanar to H_{ax}–C(4)). Therefore, the *gauche* effect *per se* could drive the Bz migration from the 2′- to the 3′-position. In addition, the conjugative σ(C–H) → δ*(C–O) stabilization expected to be operative in 3′-C(OR)/4′-C(H) part of the molecule should be more pronounced when the 3′-OH is benzoylated than when it is a free OH group[14]). The preference of the 3′-OBz over the 2′-OBz position by such stereoelectronic factor seems clearcut.

Inspecting the (presumably) most stable conformations of the two BzO groups in **7a**–**7g** and **8a**–**8g**, for their steric constraints, the one imposed on the equatorial 2′-OBz group by the equatorial nucleobase may be more severe than that on the axial 3′-OBz group by the equatorial 4′-ODMT-group (with the O–trityl bond antiplanar to the C(3′)–C(4′) bond. Steric factors may, therefore, also contribute to the driving force of the (2′ → 3′)-Bz migration in these molecules.

Scheme 3 depicts the modifications of the nucleosides **8a**–**8g** into derivatives required for the automated solid-support synthesis. These modifications were performed according to procedures used in the homo-DNA series [28], but with the following change. The choice of the then used commercially available chloro(cyanoethoxy)(diisopropylamino)phosphine as phosphitylating agent had to be re-assessed because the 3′-*O*Bz protecting group in p-RNA oligonucleotides would have to be deprotected *after* the conversion of the phosphotriester linkages into the more stable phosphodiester linkages so as to avoid strand scission resulting from the *cis*-configuration of the (4′ → 2′)-phosphodiester linkages and free 3′-OH groups[15]). The

---

[14]) The argument echoes the qualitative rationalization of the *gauche* effect based on the $\sigma \rightarrow \sigma^*$ conjugation concept.

[15]) Deprotection under basic conditions would result in the concomitant deprotection of the 3′-OBz group leading to the free 3′-OH group, which, under the basic conditions, can attack the phosphotriester linkage leading to stand scission. Such a conclusion was also based on an observation in the case of the hexose-sugar-derived D-*β*-allopyranosyl-oligonucleotides, in which there is an all-*cis*-disposition of 2′-O, 3′-O, and 4′-O groups similar to the p-RNA case: when *β*-D-allopyranosyl-$(AC)_6$ was exposed to ethanolic NH_3, >20% decomposition was found to occur even at room temperature; at 50°, complete decomposition was observed within 6 h [41].

reagent allyloxy(chloro)(diisopropylamino)phosphine[16]) offered itself as an ideal replacement. The allyl group of *O*-allyl-phosphotriester-linked oligomers can be selectively removed under mild neutral conditions to afford the phosphodiester-linked oligomers [54][55]. Thus, phosphitylations of **8a**–**8g** were conducted with allyloxy-(chloro)(diisopropylamino)phosphine in CH_2Cl_2 with $EtN(i\text{-}Pr)_2$ as base to afford, without any complications, diastereoisomeric mixtures of phosphoramidites **9a**–**9g** in yields greater than 90%. Compounds **8a**–**8g** were also the starting materials for putting the starter units on the CPG solid support to be used in the automated oligomer synthesis. Based on our previous experience from the homo-DNA series [25][28], nucleosides **8a**–**8g** were coupled with bis(4-nitrophenyl) heptane-1,7-dioate [60] in the presence of DMAP in pyridine to afford the activated 2′*O*-(4-nitrophenyl)heptane-1,7-dioates **10a**–**10g** in yields ranging from average (66% for **10a**) to high (90% for **10d**). The activated 2′-*O*-ester derivatives **10a**–**10g** were immobilized on the CPG solid support[17]) by treatment with long-chain alkylamine–controlled pore glass (LCAA-CPG) in the presence of $EtN(i\text{-}Pr)_2$ in DMF/pyridine, and the derivatized solid supports were capped with excess Ac_2O in pyridine to afford **11a**–**11g**. The loadings of the **11a**–**11g** CPG solid supports were estimated by trityl-cation assay (treating *ca.* 2–3 mg of **11a**–**11g** with 70% aq. $HClO_4$/MeOH 1:1) and measuring the absorption at 498 nm (ε of the DMT cation 70000 $cm^{-1}\,l^{-1}\,mol^{-1}$).

2.2. *Synthesis of β-D-Ribopyranosyl-(4′→2′)-oligonucleotides* (p-RNAs). *Scheme 4* delineates the overall pathway followed in the automated solid-support synthesis of

Scheme 3. *Preparation of the 2′-*O*-Phosphoramidate and 2′-*O*-CPG Derivatives of U, T, C, A, G, isoG, and D Nucleosides in the β-D-Ribopyranosyl Series*

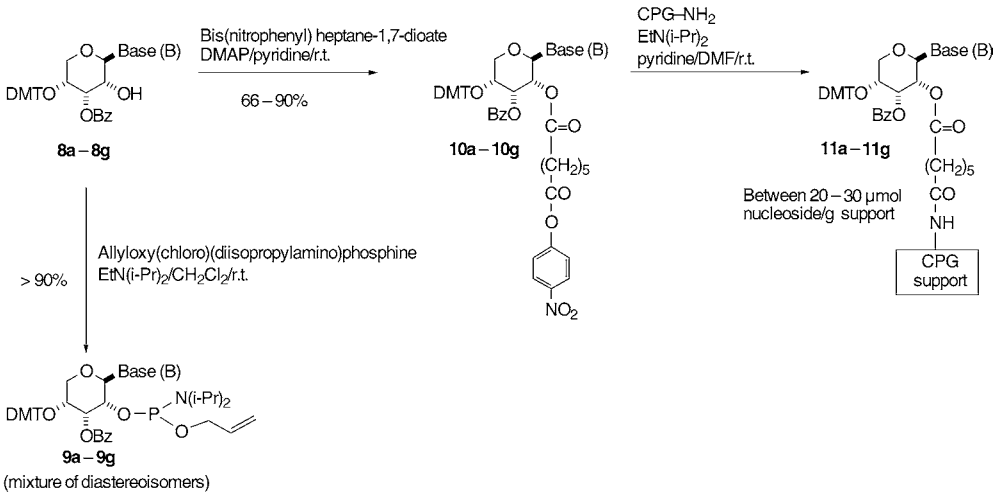

[16]) The concept of using the allyl group as a phosphodiester protecting group in oligonucleotide synthesis was first demonstrated by *Noyori* and co-workers [55]. They used the (allyloxy)[bis(diisopropylamino)]phosphine as the phosphitylating reagent.

[17]) *Via* the formation of an amide bond resulting from the attack of the NH_2–CPG onto the 4-nitrophenyl-activated esters **10a**–**10g**.

Scheme 4. *Overview of the Synthesis, Deprotection, Purification, and Isolation of β-D-Ribopyranosyl Oligonucleotides*

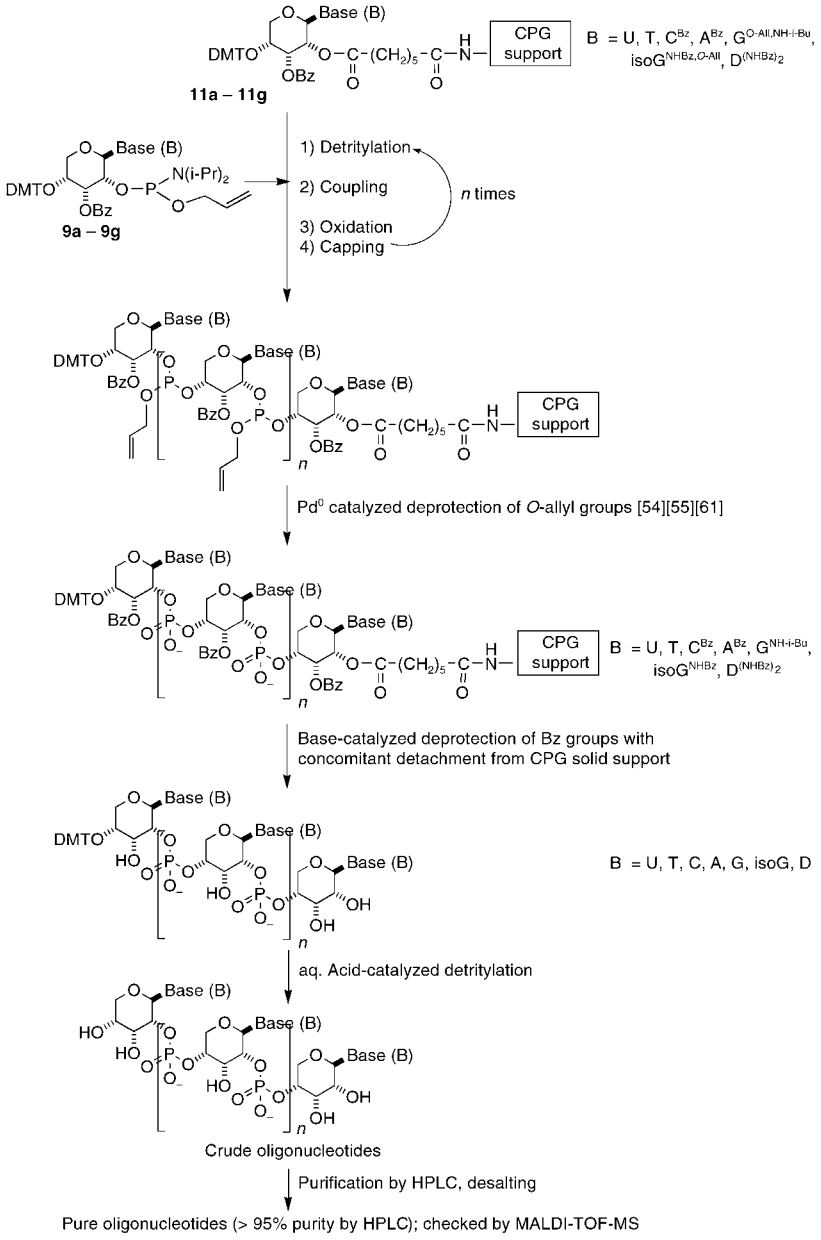

p-RNA oligonucleotides, and *Table 3* lists all the sequences synthesized over the course of this project. The syntheses were carried out on 1 – 10-μmol scale, initially on an automated DNA synthesizer *Gene Synthesizer Plus* (*Pharmacia*), with the phosphor-

Table 3. *HPLC and MS Data of p-RNA Oligonucleotides*

Entry	p-RNA	Deprotection[b])	Analytical HPLC		MALDI-TOF-MS[e])	
	β-D-pr-Oligonucleotide system[a])	*Methods*	Reverse phase[c]) gradient, t_R [min]	Ion Exchange[d]) gradient, t_R [min]	$[M-H]^-$ (obs.)	$[M-H]^-$ (calc.)
1	A_2	*A, F*	0 → 40% B in 30, 15.0		–	–
2	A_3	*A, F*	0 → 40% B in 30, 17.3		923.3	924.7
3	A_4-2′-phosphate	*B, D, F*		0 → 100% B in 30, 11.0	1335.3	1342.9
4	A_4-2′,3′-cyclophosphate			0 → 100% B in 30, 11.7	1317.8	1324.9
5	A_6	*B, F*		0 → 100% B in 30, 11.1	1913.8	1913.3
6	A_7	*A, F*	0 → 40% B in 30, 20.6	10 → 65% B in 30, 25.4[f])	2240.1	2241.5
7	A_8	*A, F*	0 → 40% B in 30, 21.0		2574.6	2570.7
8	A_{12}	*C, G*		0 → 100% B in 30, 19.3	3890.0	3888.5
9	$A_6T_2A_2T_6$	*B, F*		0 → 100% B in 30, 24.0	5127.9	5133.2
10	$A_4T_3ATAT_2AT_2A$	*B, D, F*		0 → 100% B in 30, 25.1	5101.5	5132.3
11	A_4T_4	*A, F*	0 → 40% B in 30, 20.3	0 → 100% B in 30, 17.0	2532.9	2535.7
12	A_4U_4	*A,E*	0 → 40% B in 30, 18.2	0 → 100% B in 30, 15.4	2480.4	2478.6
13	A_3TA_3T-2′-phosphate	*B, D, F*		0 → 100% B in 30, 18.0	2632.5	2632.7
14	A_2UAU_3A	*A, E*	0 → 40% B in 30, 18.5	0 → 100% B in 30, 16.4	–	–
15	AC_3GA_2	*B, F*		0 → 100% B in 30, 16.3	2187.3	2185.4
16	ACG_2-2′-phosphate	*B, D, F*		0 → 100% B in 30, 17.7	1343.6	1341.8
17	ACG_2-2′,3′-cyclophosphate			0 → 100% B in 30, 21.0	1326.3	1323.8
18	AG_4T	*B, F*		0 → 100% B in 30, 23.4	1967.2	1967.3
19	$AGCGT_4CGC$	*B, F*		0 → 100% B in 30, 24.9	3502.8	3499.2
20	$AGTG_3$	*C, G*		0 → 100% B in 30, 25.0	1967.0	1968.3
21	ATA_5TATCG-2′-phosphate	*B, D, F*		0 → 100% B in 30, 21.3	3934.8	3933.5
22	ATA_5TATCG-2′,3′-cyclophosphate			0 → 100% B in 30, 23.0	3917.4	3915.4
23	$(AT)_4$	*A, F*	0 → 40% B in 30, 19.9	0 → 100% B in 30, 17.5	2534.1	2535.7
24	$ATATG_2T_2AT$	*B, F*		0 → 100% B in 30, 23.0	3220.1	3223.1
25	ATCG-2′-phosphate	*B, D, F*		0 → 100% B in 30, 16.7	1315.9	1316.8
26	ATCG-2′,3′-cyclophosphate			0 → 100% B in 30, 19.2	1298.3	1298.8
27	AT-(L)C-G-2′-phosphate	*B, D, F*		0 → 100% B in 30, 16.6	1315.6	1316.8
28	AT-(L)C-G-2′,3′-cyclophosphate			0 → 100% B in 30, 19.1	1297.4	1298.8
29	ATC-(L)G-2′-phosphate	*B, D, F*		0 → 100% B in 30, 16.5	1318.3	1316.8
30	ATC-(L)G-2′,3′-cyclophosphate			0 → 100% B in 30, 19.1	1297.4	1298.8
31	AT-(L)C-(L)G-2′-phosphate	*B, D, F*		0 → 100% B in 30, 16.4	1318.3	1316.8
32	AT-(L)C-(L)G-2′,3′-cyclophosphate			0 → 100% B in 30, 19.0	1297.4	1298.8
33	A-(L)T-CG-2′-phosphate	*B, D, F*		0 → 100% B in 30, 16.7	1320.9	1316.8
34	A-(L)T-CG-2′,3′-cyclophosphate			0 → 100% B in 30, 19.1	1300.2	1298.8
35	A-(L)T-C-(L)G-2′-phosphate	*B, D, F*		0 → 100% B in 30, 16.3	1317.4	1316.8
36	A-(L)T-C-(L)G-2′,3′-cyclophosphate			0 → 100% B in 30, 19.2	1297.4	1298.8
37	A-(L)T-(L)C-G-2′-phosphate	*B, D, F*		0 → 100% B in 30, 16.3	1315.6	1316.8
38	A-(L)T-(L)C-G-2′,3′-cyclophosphate			0 → 100% B in 30, 19.2	1297.4	1298.8
39	A-(L)T-(L)C-(L)G-2′-phosphate	*B, D, F*		0 → 100% B in 30, 16.6	1319.1	1316.8
40	A-(L)T-(L)C-(L)G-2′,3′-cyclophosphate			0 → 100% B in 30, 19.2	1300.2	1298.8
41	ATCGATCG-2′-phosphate	*B, D, F*		0 → 100% B in 30, 21.2	2613.6	2616.6
42	ATCGATCG-2′,3′-cyclophosphate			0 → 100% B in 30, 24.3	2596.6	2598.6
43	ATCGATCGATCG-2′-phosphate	*B, D, F*		0 → 100% B in 30, 23.7	3919.6	3916.4
44	ATCGATCGATCG-2′,3′-cyclophosphate			0 → 100% B in 30, 26.5	3898.0	3898.4
45	ATGC-2′-phosphate	*B, D, F*		0 → 100% B in 30, 16.0	1318.2	1316.8
46	ATGC-2′,3′-cyclophosphate			0 → 100% B in 30, 17.9	1300.2	1298.9

Table 3 (cont.)

Entry	p-RNA	Deprotection[b])	Analytical HPLC		MALDI-TOF-MS[c])	
	β-D-pr-Oligonucleotide system[a])	*Methods*	Reverse phase[c]) gradient, t_R [min]	Ion Exchange[d]) gradient, t_R [min]	$[M-H]^-$ (obs.)	$[M-H]^-$ (calc.)
47	A-(L)T-(L)G-(L)C-2′-phosphate	*B, D, F*		0 → 100% B in 30, 16.2	1316.3	1316.8
48	A-(L)T-(L)G-(L)C-2′,3′-cyclophosphate			0 → 100% B in 30, 18.1	1300.2	1298.9
49	ATGCAT	*B, F*		0 → 100% B in 30, 17.6	1887.5	1887.2
50	ATGCATG	*B, F*		0 → 100% B in 30, 21.8	2234.5	2232.5
51	$AT_2AT_2AT_3A_4$	*A, F*	0 → 40% B in 30, 17.8		5147.6	5133.3
52	AT_2A-2′-phosphate	*B, D, F*		0 → 100% B in 30, 15.8	1316.0	1315.8
53	AT_2A-2′,3′-cyclophosphate			0 → 100% B in 30, 17.8	1298.0	1297.8
54	AT_2AT_2AT-2′-phosphate	*B, D, F*		0 → 100% B in 30, 20.4	2605.8	2606.6
55	AT_2AT_2AT-2′,3′-cyclophosphate			0 → 100% B in 30, 22.4	2593.2	2588.6
56	AT_2CAGCG	*C, G*		0 → 100% B in 30, 22.7	2537.0	2537.6
57	AT_3A_4-2′-phosphate	*B, F*		0 → 100% B in 30, 18.9	2623.3	2624.7
58	AT_3-2′-phosphate	*B, D, F*		0 → 100% B in 30, 16.8	1305.5	1306.8
59	AT_3-2′,3′-cyclophosphate			0 → 100% B in 30, 19.6	1288.5	1288.8
60	$(AU)_4$	*A, E*	0 → 40% B in 30, 18.2	0 → 100% B in 30, 15.4	2480.4	2478.6
61	AU_3AUA_2	*A, E*	0 → 40% B in 30, 18.6	0 → 100% B in 30, 16.5	–	–
62	$CACAC_3G_2CTC_2$	*C, G*		0 → 100% B in 30, 23.5	4049.0	4048.5
63	CATATA	*B, F*		0 → 100% B in 30, 15.7	1871.4	1870.2
64	C_2-2′-phosphate	*B, D, F*		0 → 100% B in 30, 6.5	628.1	627.4
65	C_2-2′,3′-cyclophosphate			0 → 100% B in 30, 6.5	611.0	609.4
66	3′,4′-cyclophosphate-C_3	*B, F*	0 → 40% B in 30, 10.4	0 → 100% B in 30, 9.5	918.1	915.6
67	$C_3ACTCG_2CTC_2$	*C, G*		0 → 100% B in 30, 23.4	4037.0	4039.5
68	C_4	*A, F*	0 → 40% B in 30, 11.5	0 → 100% B in 30, 8.8[f])	–	–
69	C_4-2′-phosphate	*B, F*	0 → 40% B in 30, 12.4	0 → 100% B in 30, 11.7	1239.7	1237.2
70	C_4-2′,3′-cyclophosphate		0 → 40% B in 30, 12.1	0 → 100% B in 30, 11.7	1220.1	1219.2
71	4′-phosphate-C_4	*B, F*	0 → 40% B in 30, 7.1	0 → 100% B in 30, 10.9	1238.2	1237.2
72	C_6	*B, F*	0 → 20% B in 20, 13.4	5 → 70% B in 30, 15.7[f])	1770.6	1768.14
73	C_8	*B, F*	0 → 30% B in 30, 14.4		2378.5	2379.5
74	C_8-2′-phosphate	*B, F*		0 → 100% B in 30, 15.5	2456.3	2457.3
75	C_8-2′,3′-cyclophosphate		0 → 40% B in 30, 13.9	0 → 100% B in 30, 16.6	2441.5	2439.3
76	4′-phosphate-C_8	*B, F*	0 → 40% B in 30, 13.9	0 → 100% B in 30, 15.3	–	–
77	C_3G-2′-phosphate	*B, D, F*		0 → 100% B in 30, 14.9	1278.2	1277.8
78	C_3G-2′,3′-cyclophosphate			0 → 100% B in 30, 17.0	1261.4	1259.8
79	C_3GC_3G	*B, F*		0 → 100% B in 30, 19.2	2460.9	2458.6
80	C_3G_3	*B, F*	0 → 40% B in 30, 20.6	10 → 100% B in 30, 15.1[f])	1889.6	1888.2
81	$C_3TC_3G_2CTC_2$	*B, F*		0 → 100% B in 30, 22.3	4027	4026.5
82	C_2TATA	*B, F*		0 → 100% B in 30, 16.2	1847.5	1847.2
83	CG-2′-phosphate	*B, D, F*		0 → 100% B in 30, 11.8	667.5	667.4
84	CGA_2T_2CG	*B, F*	0 → 30% B in 30, 18.5		2538.0	2538.0
85	CGAGCG	*C, G*		0 → 100% B in 30, 21.6	1915.0	1913.2
86	$CGCA_4GCG$	*B, F*		0 → 100% B in 30, 21.8	3204.0	3205.0
87	CGCG-2′-phosphate	*B, D, F*		0 → 100% B in 30, 17.2	1320.0	1317.8
88	CGCG-2′,3′-cyclophosphate			0 → 100% B in 30, 20.1	1301.9	1299.8
89	$(CG)_3$	*B, F*	0 → 40% B in 30, 17.5	10 → 100% B in 30, 14.8[f])	1889.6	1888.2
90	$CGCGT_4CGC$	*B, F*		0 → 100% B in 30, 23.8	3483.4	3474.2
91	$CGCTGA_2T$	*C, G*		0 → 100% B in 30, 22.2	2537.0	2537.6
92	$CGCT_2$-2′-phosphate	*B, D, F*		0 → 100% B in 30, 18.1	1614.7	1614.0
93	$CGCT_2$-2′,3′-cyclophosphate			0 → 100% B in 30, 20.6	1597.5	1596.0
94	(L)C-G_2-2′-phosphate	*B, D, F*		0 → 100% B in 30, 16.6	1316.4	1317.8
95	(L)C-G_2-2′,3′-cyclophosphate			0 → 100% B in 30, 18.6	1299.3	1299.8
96	CG_2C-2′-phosphate	*B, D, F*		0 → 100% B in 30, 16.9	1318.0	1317.8
97	CG_2C-2′,3′-cyclophosphate			0 → 100% B in 30, 18.8	1299.2	1299.8
98	CG_2-(L)C-2′-phosphate	*B, D, F*		0 → 100% B in 30, 16.9	1316.4	1317.8
99	CG_2-(L)C-2′,3′-cyclophosphate			0 → 100% B in 30, 18.7	1298.4	1299.8

Table 3 (cont.)

Entry	p-RNA	Deprotection[b])	Analytical HPLC		MALDI-TOF-MS[e])	
	β-D-pr-Oligonucleotide system[a])	*Methods*	Reverse phase[c]) gradient, t_R [min]	Ion Exchange[d]) gradient, t_R [min]	$[M-H]^-$ (obs.)	$[M-H]^-$ (calc.)
100	CG-(L)G-C-2′-phosphate	*B, D, F*		0 → 100% B in 30, 17.0	1316.4	1317.8
101	CG-(L)G-C-2′,3′-cyclo-phosphate			0 → 100% B in 30, 18.7	1298.4	1299.8
102	C-(L)G-GC-2′-phosphate	*B, D, F*		0 → 100% B in 30, 17.0	1315.5	1317.8
103	C-(L)G-GC-2′,3′-cyclo-phosphate			0 → 100% B in 30, 18.9	1297.5	1299.8
104	CG_3-2′-phosphate	*B, D, F*		0 → 100% B in 30, 19.2	1357.8	1357.8
105	CG_3-2′,3′-cyclophosphate			0 → 100% B in 30, 23.5	1340.6	1339.8
106	CG_3CG_3	*B, F*		0 → 100% B in 30, 25.9	2619.3	2618.6
107	CG_6C	*B, F*		0 → 100% B in 30, 25.4	2621.1	2618.6
108	CTC_3G_2CT	*B, F*		0 → 100% B in 30, 20.3	2806	2505.8
109	CT_2ATA	*B, F*		0 → 100% B in 30, 17.4	1861.7	1861.2
110	D_6	*B, F*	0 → 40% B in 20, 14.8	0 → 70% B in 30, 24.2	2003.6	2004.0
111	(L)D_6	*B, F*	0 → 40% B in 20, 15.1		2003.5	2004.0
112	D_8	*B, F*	0 → 40% B in 20, 15.6		2690.0	2691.0
113	(L)D_8	*B, F*	0 → 30% B in 20, 17.3		2869.6	2691.0
114	DTCG-2′-phosphate	*B, D, F*		0 → 100% B in 30, 17.1	1331.1	1331.8
115	DTCG-2′,3′-cyclophosphate			0 → 100% B in 30, 20.0	1314.0	1313.8
116	(L)D-TCG-2′-phosphate	*B, D, F*		0 → 100% B in 30, 17.0	1330.8	1331.8
117	(L)D-TCG-2′,3′-cyclophosphate			0 → 100% B in 30, 19.7	1315.5	1313.8
118	DTCGDTCG-2′-phosphate	*B, D, F*		0 → 100% B in 30, 22.1	2645.3	2646.6
119	DTCGDTCG-2′,3′-cyclo-phosphate			0 → 100% B in 30, 26.1	2630.9	2628.6
120	DTGC-2′-phosphate	*B, D, F*		0 → 100% B in 30, 16.7	1330.2	1331.8
121	DTGC-2′,3′-cyclophosphate			0 → 100% B in 30, 18.6	1314.9	1313.8
122	$GAGC_2$	*C, G*		0 → 100% B in 30, 17.8	1569.0	1568.0
123	$GAGC_2$-2′-phosphate	*C, G*		0 → 100% B in 30, 18.5	1649.0	1648.0
124	$GAGC_2$-2′,3′-cyclophosphate			0 → 100% B in 30, 20.8	1629.0	1629.9
125	$GAGC_2G$	*C, G*		0 → 100% B in 30, 20.9	1912.0	1913.2
126	$GAGC_2G$-2′-phosphate	*C, G*		0 → 100% B in 30, 21.6	1993.0	1993.2
127	$GAGC_2G$-2′,3′-cyclophosphate			0 → 100% B in 30, 24.7	1976.0	1975.2
128	$GAGC_2G_3TGTG$	*C, G*		0 → 100% B in 30, 29.4	3934.0	3934.5
129	$GAGC_2G_2TGTG$	*C, G*		0 → 100% B in 30, 28.6	3589.0	3589.3
130	$GAGC_2$-pI(G)	*C, G*		0 → 100% B in 30, 21.2	1913.0	1913.2
131	GATGCAT	*B, F*		0 → 100% B in 30, 21.3	2234.0	2232.5
132	GC-2′-phosphate	*B, D, F*		0 → 100% B in 30, 11.5	668.7	667.4
133	GC-2′,3′-cyclophosphate			0 → 100% B in 30, 13.2	649.8	649.4
134	GC_2-2′-phosphate	*B, D, F*		0 → 100% B in 30, 13.1	973.3	972.6
135	GC_2-2′,3′-cyclophosphate			0 → 100% B in 30, 14.3	955.4	954.6
136	GC_3-2′-phosphate	*B, D, F*		0 → 100% B in 30, 13.0	1276.1	1277.8
137	GC_3-2′,3′-cyclophosphate			0 → 100% B in 30, 15.3	1261.5	1259.2
138	(L)G-C_3-2′-phosphate	*B, D, F*		0 → 100% B in 30, 14.4	1277.0	1277.8
139	(L)G-C_3-2′,3′-cyclophosphate			0 → 100% B in 30, 15.4	1263.7	1259.8
140	G-(L)C-C_2-2′-phosphate	*B, D, F*		0 → 100% B in 30, 14.2	1275.2	1277.8
141	G-(L)C-C_2-2′,3′-cyclophosphate			0 → 100% B in 30, 15.2	1259.3	1259.8
142	GC-(L)C-C-2′-phosphate	*B, D, F*		0 → 100% B in 30, 14.1	1277.9	1277.8
143	GC-(L)C-C-2′,3′-cyclophosphate			0 → 100% B in 30, 15.8	1260.2	1259.8
144	GC_2-(L)C-2′-phosphate	*B, D, F*		0 → 100% B in 30, 14.2	1277.6	1277.8
145	GC_2-(L)C-2′,3′-cyclophosphate			0 → 100% B in 30, 15.9	1257.5	1259.8
146	(L)G-(L)C_3-2′-phosphate	*B, D, F*		0 → 100% B in 30, 15.0	1278.0	1277.8
147	(L)G-(L)C_3-2′,3′-cyclophosphate			0 → 100% B in 30, 16.0	1259.3	1259.8
148	GC_6G	*B, F*		0 → 100% B in 30, 19.6	2453.6	2458.6
149	GC_3GC_3	*B, F*		0 → 100% B in 30, 19.3	2457.6	2458.6
150	GC_3GC_3-2′,3′-cyclophosphate			0 → 100% B in 30, 20.7	2519.0	2520.5
151	GC_3GC_3-2′-phosphate	*B, D, F*		0 → 100% B in 30, 19.9	2538.3	2538.5
152	GC_3GC_3-3′-phosphate	*B, D, F*		0 → 100% B in 30, 20.3	2540.9	2538.5
153	$GC_3GC_3GC_3$	*B, F*		0 → 100% B in 30, 21.8	3718.8	3719.3
154	GC_2G-2′-phosphate	*B, D, F*		0 → 100% B in 30, 18.1	1318.7	1317.8

Table 3 (cont.)

Entry	p-RNA	Deprotection[b])	Analytical HPLC		MALDI-TOF-MS[e])	
	β-D-pr-Oligonucleotide system[a])	*Methods*	Reverse phase[c]) gradient, t_R [min]	Ion Exchange[d]) gradient, t_R [min]	$[M-H]^-$ (obs.)	$[M-H]^-$ (calc.)
155	GC_2G-2′,3′-cyclophosphate			0 → 100% B in 30, 19.9	1299.2	1299.8
156	(L)G-C_2G-2′-phosphate	*B, D, F*		0 → 100% B in 30, 17.3	1317.3	1317.8
157	(L)G-C_2G-2′,3′-cyclo-phosphate			0 → 100% B in 30, 20.1	1300.2	1299.8
158	G-(L)C-CG-2′-phosphate	*B, D, F*		0 → 100% B in 30, 17.0	1317.3	1317.8
159	G-(L)C-CG-2′,3′-cyclo-phosphate			0 → 100% B in 30, 19.7	1297.5	1299.8
160	GC-(L)C-G-2′-phosphate	*B, D, F*		0 → 100% B in 30, 16.9	1315.5	1317.8
161	GC-(L)C-G-2′,3′-cyclo-phosphate			0 → 100% B in 30, 19.7	1301.1	1299.8
162	GC_2-(L)G-2′-phosphate	*B, D, F*		0 → 100% B in 30, 17.2	1316.4	1317.8
163	GC_2-(L)G-2′,3′-cyclo-phosphate			0 → 100% B in 30, 19.8	1297.5	1299.8
164	$GC_2G_2C_2G$-2′-phosphate	*B, D, F*		0 → 100% B in 30, 23.0	2617.0	2618.6
165	$GC_2G_2C_2G$-2′,3′-cyclo-phosphate			0 → 100% B in 30, 25.8	2599.4	2600.6
166	$(GC)_3$	*B, F*	0 → 40% B in 30, 19.8	10 → 100% B in 30, 15.6[f])	1888.3	1888.2
167	GCG_2	*B, F*		0 → 100% B in 30, 18.8	1276.9	1277.8
168	GCG_2-2′-phosphate	*B, D, F*		0 → 100% B in 30, 20.9	1358.0	1357.8
169	GCG_2-2′,3′-cyclophosphate			0 → 100% B in 30, 23.5	1340.5	1339.8
170	GCGC-2′-phosphate	*B, D, F*		0 → 100% B in 30, 16.7	1320.9	1317.8
171	GCGC-2′,3′-cyclophosphate			0 → 100% B in 30, 18.8	1302.8	1299.8
172	$GCGT_2CGC$	*B, F*		0 → 100% B in 30, 23.3	2529.7	2529.6
173	$GCGT_3CGC$	*B, F*		0 → 100% B in 30, 23.9	2851.9	2849.8
174	$GCGT_4CGC$	*B, F*		0 → 100% B in 30, 24.4	3173.3	3170.0
175	$GCGT_4CGCA$	*B, F*		0 → 100% B in 30, 25.3	3500.0	3499.2
176	$GCGT_4CGC_2$	*B, F*		0 → 100% B in 30, 24.5	3473.3	3474.2
177	$GCGT_5CGC$	*B, F*		0 → 100% B in 30, 25.1	3489.1	3490.2
178	$GCGT_8CGCT$	*B, F*		0 → 100% B in 30, 26.8	4771.8	4771.8
179	$GCGT_2$-2′-phosphate	*B, D, F*		0 → 100% B in 30, 20.4	1655.8	1653.0
180	$GCGT_2$-2′,3′-cyclophosphate			0 → 100% B in 30, 23.6	1638.3	1636.0
181	GCTG-2′-phosphate	*B, D, F*		0 → 100% B in 30, 22.2	1333.6	1332.8
182	GCTG-2′,3′-cyclophosphate			0 → 100% B in 30, 18.7	1312.8	1314.8
183	GD_4C	*B, F*		0 → 100% B in 30, 17.2	1963.2	1965.3
184	G_2-2′-phosphate	*B, D, F*		0 → 100% B in 30, 15.7	708.1	707.4
185	G_2-2′,3′-cyclophosphate			0 → 100% B in 30, 19.5	–	–
186	$G_2A_2C_2G$	*C, G*		0 → 100% B in 30, 22.0	2243.0	2242.4
187	G_2AGC_2	*B, F*		0 → 100% B in 30, 20.7	1916	1916.3
188	G_2AGC_2-2′-phosphate	*C, G*		0 → 100% B in 30, 21.7	1992.0	1993.2
189	G_2AGC_2-2′,3′-cyclophosphate			0 → 100% B in 30, 23.6	1974.0	1975.2
190	G_2AGC_2G	*C, G*		0 → 100% B in 30, 23.2	2258.0	2258.4
191	G_3C-2′-phosphate	*B, D, F*		0 → 100% B in 30, 19.3	1357.4	1357.8
192	G_3C-2′,3′-cyclophosphate			0 → 100% B in 30, 20.7	1339.9	1339.8
193	G_3C_3	*B, F*	0 → 40% B in 30, 22.2	10 → 100% B in 30, 15.9[f])	1889.6	1888.2
194	G_3CG_3C	*B, F*	0 → 40% B in 30, 15.3	0 → 100% B in 30, 24.8	2617.5	2617.4
195	G_3CG_3C	*B, F*		0 → 100% B in 30, 25.8	–	–
196	$G_3CG_3CG_3C$	*B, F*		0 → 100% B in 30, 28.5	3960.1	3959.5
197	G_3I_3	*A, F*	0 → 40% B in 30, 15.7	0 → 60% B in 30, 21.2[f])	2010.0	2008.3
198	G_4-2′-phosphate	*B, F*		0 → 100% B in 30, 20.4	1398.7	1397.2
199	G_4-2′,3′-cyclophosphate	*B, F*	0 → 40% B in 30, 14.5	0 → 100% B in 30, 24.3	1220.9	1219.2
200	(L)G_4-2′-phosphate	*B, F*		0 → 100% B in 30, 20.4	1397.0	1397.2
201	4′-phosphate-G_4	*B, F*		0 → 100% B in 30, 20.7	1397.6	1397.2
202	G_5	*B, F*	0 → 40% B in 30, 17.2	10 → 100% B in 30, 10.2[f])	–	–
203	G_6	*B, F*	0 → 40% B in 30, 15.1	10 → 100% B in 30, 13.7[f])	2008.2	2008.3
204	(L)G_6	*B, F*	0 → 40% B in 30, 15.4	0 → 100% B in 30, 24.5	2008.7	2008.3
205	G_8	*B, F*	0 → 40% B in 30, 16.2	0 → 100% B in 30, 27.2	2698.4	2697.4
206	(L)G_8	*B, F*	0 → 40% B in 30, 16.1	0 → 100% B in 30, 27.2	2699.6	2697.4

Table 3 (cont.)

Entry	p-RNA	Deprotection[b])	Analytical HPLC		MALDI-TOF-MS[e])	
	β-D-pr-Oligonucleotide system[a])	*Methods*	Reverse phase[c]) gradient, t_R [min]	Ion Exchange[d]) gradient, t_R [min]	$[M-H]^-$ (obs.)	$[M-H]^-$ (calc.)
207	G_{10}	*A, F*	0 → 40% B in 30, 6.3		3390.7	3390.1
208	G_3TGTG	*C, G*		0 → 100% B in 30, 27.7	2305.0	2304.5
209	G_2TA_2	*B, F*		0 → 100% B in 30, 18.8	1605.3	1606.1
210	G_2TATA	*B, F*		0 → 100% B in 30, 20.8	1925.4	1926.3
211	G_2TG_3	*B, F*		0 → 100% B in 30, 26.0	1986	1984.3
212	G_2TGTG	*C, G*		0 → 100% B in 30, 26.2	1958.0	1959.3
213	GTACGTA	*B, F*		0 → 100% B in 30, 21.9	2234.0	2232.5
214	GTC_2-2′-phosphate	*B, D, F*		0 → 100% B in 30, 16.5	1295.7	1292.8
215	GTC_2-2′,3′-cyclophosphate			0 → 100% B in 30, 18.0	1276.9	1274.8
216	GTCG-2′-phosphate	*B, D, F*		0 → 100% B in 30, 18.8	1332.7	1332.8
217	GTCG-2′,3′-cyclophosphate			0 → 100% B in 30, 21.9	1313.7	1314.8
218	GT_2ATA	*B, F*		0 → 100% B in 30, 19.8	1901.4	1901.2
219	I_6	*A, F*	0 → 40% B in 30, 14.8		2008.8	2008.3
220	(L)I_6	*B, F*	0 → 100% B in 30, 10.3		2008.0	2008.3
221	I_8	*B, F*	0 → 18% B in 20, 17.7		2699.3	2698.7
223	(L)I_8	*B, F*	0 → 25% B in 20, 8.6		2700.1	2698.7
224	$(IG)_3$	*A, F*	0 → 40% B in 30, 15.8	0 → 60% B in 30, 18.3[f])	2009.0	2009.3
225	I_3G_3	*A, F*	0 → 40% B in 30, 14.7		2010.4	2008.3
226	TA_4TA_2	*C, G*		0 → 100% B in 30, 18.9	2555.0	2553.7
227	$TA_2TA_2TATA_3T_4$	*B, D, F*		0 → 100% B in 30, 23.6	5140.3	5132.3
228	TAC_2T_2CG-2′-phosphate	*B, D, F*		0 → 100% B in 30, 20.8	2564.7	2567.6
229	TAC_2T_2CG-2′,3′-cyclo-phosphate			0 → 100% B in 30, 23.4	2555.5	2549.6
230	$TAC_2T_2CG_2TA_2$	*B, F*		0 → 100% B in 30, 24.6	4160.7	4156.6
231	TACG-2′-phosphate	*B, D, F*		0 → 100% B in 30, 16.2	1316.3	1316.8
232	TACG-2′,3′-cyclophosphate			0 → 100% B in 30, 18.9	1300.2	1298.9
233	(L)T-ACG-2′-phosphate	*B, D, F*		0 → 100% B in 30, 16.1	1316.3	1316.8
234	(L)T-ACG-2′,3′-cyclophosphate			0 → 100% B in 30, 18.9	1299.3	1298.8
235	TAC-(L)G-2′-phosphate	*B, D, F*		0 → 100% B in 30, 16.4	1318.2	1316.2
236	TAC-(L)G- 2′,3′-cyclophosphate			0 → 100% B in 30, 18.9	1301.9	1298.8
237	TACGTA	*B, F*		0 → 100% B in 30, 18.2	1887.3	1887.2
238	TACGTAG	*B, F*		0 → 100% B in 30, 21.8	2233.8	2232.5
239	TAGC-2′-phosphate	*B, D, F*		0 → 100% B in 30, 15.6	1317.2	1316.8
240	TAGC-2′,3′-cyclophosphate			0 → 100% B in 30, 17.3	1300.2	1298.9
241	(L)T-AGC-2′-phosphate	*B, D, F*		0 → 100% B in 30, 15.7	1317.2	1316.8
242	(L)T-AGC-2′,3′-cyclophosphate			0 → 100% B in 30, 17.4	1299.3	1298.9
243	TAG_4TA	*B, F*		0 → 100% B in 30, 25.0	2622.6	2617.7
244	$TATA_2C$-2′-phosphate	*B, D, F*		0 → 100% B in 30, 16.4	1953.0	1950.2
245	$TATA_2C$-2′,3′-cyclophosphate			0 → 100% B in 30, 17.9	1934.3	1932.2
246	$TATA_2C_2ATATA$	*B, F*		0 → 100% B in 30, 21.0	3801.7	3803.4
247	$TATA_2G_2ATATA$	*B, F*		0 → 100% B in 30, 23.7	3887.6	3883.5
248	$TATAC_4TATA$	*B, F*		0 → 100% B in 30, 21.5	3758.1	3756.4
249	TATACC-2′-phosphate	*B, D, F*		0 → 100% B in 30, 16.9	1925.4	1926.2
250	TATACC-2′,3′-cyclophosphate			0 → 100% B in 30, 18.1	1910.8	1909.2
251	$TATAC_4TAT_2$	*B, F*		0 → 100% B in 30, 21.1	4088.4	4085.6
252	$TATAG_4TATA$	*B, F*		0 → 100% B in 30, 26.2	3916.6	3916.5
253	$TATAG_2$-2′-phosphate	*B, D, F*		0 → 100% B in 30, 20.6	2006.0	2006.2
254	$TATAG_2$-2′,3′-cyclophosphate			0 → 100% B in 30, 23.4	1988.2	1988.2
255	$TATAG_2T$-2′-phosphate	*B, D, F*		0 → 100% B in 30, 21.4	2327.1	2327.4
256	$TATAG_2T$-2′,3′-cyclophosphate			0 → 100% B in 30, 24.3	2311.1	2309.4
257	TATAT-2′-phosphate	*B, D, F*		0 → 100% B in 30, 17.0	1637.1	1636.0
258	TATAT-2′,3′-cyclophosphate			0 → 100% B in 30, 19.3	1621.0	1618.0
259	TATATC-2′-phosphate	*B, D, F*		0 → 100% B in 30, 17.7	1942.0	1941.2
260	TATATC-2′,3′-cyclophosphate			0 → 100% B in 30, 19.5	1924.5	1923.2
261	TATATG-2′-phosphate	*B, D, F*		0 → 100% B in 30, 19.9	1981.5	1981.2
262	TATATG-2′,3′-cyclophosphate			0 → 100% B in 30, 23.0	1962.7	1963.2
263	$TATATG_2T_2ATA$	*B, F*		0 → 100% B in 30, 24.7	3863.6	3865.5

Table 3 (cont.)

Entry	p-RNA	Deprotection[b])	Analytical HPLC		MALDI-TOF-MS[e])	
	β-D-p**r**-Oligonucleotide system[a])	*Methods*	Reverse phase[c]) gradient, t_R [min]	Ion Exchange[d]) gradient, t_R [min]	$[M-H]^-$ (obs.)	$[M-H]^-$ (calc.)
264	TAT_2	[g])	[g])	[g])	1567.3	1564.0
265	TAT_4A_2	*C, G*		0 → 100% B in 30, 21.8	2527.0	2526.6
266	T_2A_4TA	*C, G*		0 → 100% B in 30, 18.9	2544.7	2544.0
267	T_2CGC	*B, F*		0 → 100% B in 30, 17.4	1539.4	1534.0
268	T_2GCG	*B, F*		0 → 100% B in 30, 19.9	1572.4	1574.0
269	T_4A_4	*A, F*	0 → 40% B in 30, 20.7	0 → 100% B in 30, 18.4	2533.2	2535.7
270	$T_4A_3TA_2TA_2T$	*A, F*	0 → 40% B in 30, 17.5		5133.8	5133.3
271	**d**(T)-p**r**($T_4A_3TA_3TA_2T$)	*A, F*	0 → 40% B in 30, 17.9		5438.1	5437.3
272	TDCG-2′-phosphate	*B, D, F*		0 → 100% B in 30, 17.1	1331.6	1331.8
273	TDCG-2′,3′-cyclophosphate			0 → 100% B in 30, 19.9	1315.0	1313.8
274	TDGC-2′-phosphate	*B, D, F*		0 → 100% B in 30, 17.1	1331.7	1331.8
275	TDGC-2′,3′-cyclophosphate			0 → 100% B in 30, 19.3	1312.7	1313.8
276	T_8	*A, F*	0 → 40% B in 30, 19.6	0 → 100% B in 30, 14.0	2497.6	2498.4
278	T_{12}	*C, G*		0 → 100% B in 30, 26.5	3782.0	3780.4
279	UA_3UAU_2	*A, E*	0 → 40% B in 30, 18.6	0 → 100% B in 30, 16.2	–	–
280	$(UA)_4$	*A, E*	0 → 40% B in 30, 18.4	0 → 100% B in 30, 16.0	2481.4	2478.6
281	U_2	*A, E*	0 → 40% B in 30, 9.6	0 → 100% B in 30, 2.9	549.0	549.4
282	U_2AUA_3U	*A, E*	0 → 40% B in 30, 18.9	0 → 100% B in 30, 16.4	–	–
283	U_3	*A, E*	0 → 40% B in 30, 11.9	0 → 100% B in 30, 6.2	855.7	856.6
284	U_4A_4	*A, E*	0 → 40% B in 30, 19.0		2480.0	2478.6
285	U_7	*A, E*	0 → 40% B in 30, 18.9		2080.8	2081.2
286	U_8	*A, E*	0 → 40% B in 30, 15.7	0 → 100% B in 30, 13.4	2386.1	2386.4

[a]) All sequences refer to D-p-RNA (D-p**r**) unless indicated otherwise; (L) = L-p**r** = L-p-RNA; p**l** = D-pyranosyl-lyxoNA; **d**(T) = Thymidine. All cyclophosphate containing sequences were prepared from their respective 2′- or 3′- or 4′-phosphate precursor sequences by treatment with DEC · HCl. [b]) *Method A:* Allyl deprotection for 'Trityl-off' sequences: 360 µl (3.7 µmol) of $BuNH_2$, 20 mg (22 µmol) of (dibenzylideneacetone)$_3Pd^0$, 60 mg (225 µmol) of Ph_3P, 140 µl (3.7 µl) of HCO_2H in 4.5 ml of THF, 55°, 1.5 h; 4.5 ml of 0.1M aq. $NaCS_2NEt_2$. *Method B:* Allyl deprotection for 'Trityl-on' sequences: 20 mg (148 µmol) of $Et_2NH_2CO_3$ [54] in 0.75 ml of CH_2Cl_2 11.6 mg (10 µmol) of $(Ph_3P)_4Pd^0$,1.3 mg (5 µmol) of Ph_3P in 1.0 ml of CH_2Cl_2, room temperature, 2 h (12–24 h for isoG sequences); 3.5 ml of 0.1M aq. $NaCS_2NEt_2$. *Method C:* Allyl deprotection for 'Trityl-off' sequences: 460 µl (4.5 µmol) of Et_2NH_2, 177 mg (171 µmol) of (dibenzylideneacetone)$_3Pd^0$–$CHCl_3$ adduct [61], 432 mg (2.7 mmol) of Ph_3P, 360 µl (9.6 µmol) of HCO_2H in 6.5 ml of THF, 50°, 3–4 h; 4.5 ml of 0.1M aq. $NaCS_2NEt_2$. *Method D:* Detachment from CPG/acyl deprotection: sat. aq. NH_3/EtOH, 3:1, room temperature, 3–4 h. *Method E:* Detachment from CPG/acyl deprotection: 4.5 ml of 0.2M $MeONH_2 \cdot HCl$ in aq. conc. NH_3/EtOH, room temperature, 20 h. *Method F:* Detachment from CPG/acyl deprotection: 1.5 ml of 15–25% aq. $NH_2NH_2 \cdot H_2O$, 4°, 20–30 h (room temperature, 48 h for D-containing sequences). *Method G:* Detachment from CPG/acyl deprotection: 5 ml of 40% (*w*/*w*) aq. $MeNH_2$/conc. aq. NH_3 1:1, room temperature, 5–6 h. [c]) *Aquapore RP-300 C-8 Brownlee*, 220 × 4.6 mm, 7 µm, flow 1 ml/min. Mobile phase: eluant A: 0.1M Et_3N, 0.1M AcOH, H_2O, pH 7.0; eluant B: 0.1M Et_3N, 0.1M AcOH, H_2O/MeCN 1:4. [d]) *MONO-Q HR 5/5 Pharmacia*, 10 × 0.5 cm, flow 1 ml/min. Mobile phase: eluant A: 10 mM Na_2HPO_4, H_2O, pH 11.5; eluant B: 10 mM Na_2HPO_4, 1M NaCl, H_2O, pH 11.5. [e]) Matrix-assisted laser-desorption ionization time-of-flight mass spectroscopy; matrix: 3-hydropicolinic acid or α-cyanohydroxycinnamic acid or 2,4,6-trihydroxyacetophenone and ammonium citrate buffer. [f]) *Nucleogen-DEAE 60-7 Macherey-Nagel*, 125 × 4 mm, flow 1 ml/min eluant A: 10 mM Na_2HPO_4, H_2O/MeCN 1:4, pH 11.5; eluant B: 10 mM Na_2HPO_4, 1M NaCl, H_2O/MeCN 1:4, pH 11.5. [g]) From *Hoechst*, Zürich.

amidites **9a**–**9g** and the suitably derivatized CPG solid supports **11a**–**11g**, utilizing the protocols that were developed earlier for the homo-DNA-oligonucleotide synthesis and adapting them to the specific demands of the p-RNA synthesis [28]. The following were the conditions used: *a*) detritylation with 6% Cl_2CHCO_2H in $ClCH_2CH_2Cl$ for a period of 5–7 min, *b*) coupling for 45–60 min with 10% (*w*/*v*) soln. of phosphoramidites in MeCN (160–400 µl per coupling) in the presence of a mixture of 0.15M 5-(4-nitrophenyl)-1*H*-tetrazole and 0.35M 1*H*-tetrazole in MeCN (180–600 µl per coupling), *c*) capping for 1.5 min with 0.45M DMAP in MeCN plus a mixture of

collidine/Ac_2O/MeCN 3:2:5; and *d*) oxidation for 1 min with 0.01M I_2 in MeCN/collidine/H_2O 100:9:45. This procedure led to average coupling yields of > 99% (by trityl assay). Later in the study, the oligonucleotide sequences were also synthesized with *Expedite 8909 Gene Assembler* (*PE Biosystems*), with the following changes to the synthesis protocol: *a*) the use of 0.1M soln. of phosphoramidites **9a**–**9g** in MeCN, *b*) use of a 0.35M soln. of 2-(ethylsulfanyl)-1*H*-tetrazole in the coupling step, *c*) coupling time of 60 min, and *d*) the use of a 6% Cl_2CHCO_2H soln. in $ClCH_2CH_2Cl$ for detritylation over a 5-min period. Average coupling efficiencies were >98% (by tritylation assay). In both instances, the majority of the oligonucleotides were synthesized in the 'Trityl-on' mode, and, in the early phase of the investigation sequences, in the 'Trityl-off' mode[18]).

Prior to the detachment from the CPG solid support and deprotection of acyl groups, the p-RNA-oligonucleotide strands attached to the solid support were first treated with Pd^0 catalyst under the *Noyori* conditions [54][55] to remove the allyl groups, thus converting the labile phosphotriester linkage to the more stable phosphodiester linkage. In the early trials of the study, allyl deprotection was performed with the tris(dibenzylideneacetone)dipalladium(0) in a two-phase medium by using $BuNH_2$ and HCO_2H at 50° [55], a procedure which was cumbersome from an operational standpoint[19]). A more convenient approach was the modification developed by *Noyori* and co-workers [54] where $(Ph_3P)_3Pd^0$ and $Et_2NH \cdot HCO_3$ were used resulting in a more homogeneous reaction mixture leading to a complete reaction within 3–4 h at room temperature. In the case of G- and isoG-containing sequences, this treatment led to the simultaneous de-allylation of the allyl protecting groups on the purines as well. The Pd^0 catalyst was removed by reacting with 0.1M aq. $NaSC(S)NEt_2$ leaving the acyl-protected p-RNA-oligonucleotides on the solid support.

While detachment from the solid support could be achieved without complications under standard deprotection conditions (conc. aq. NH_3 in H_2O/EtOH 3:1, room temperature, 40 h), the acyl deprotection of p-RNA-oligonucleotides is more difficult because of the steric hindrance towards debenzylation in the axial 3′-OBz groups[20]). This can lead to partial acyl deprotection with substantial strand scission. The latter is a consequence of the all-*cis*-disposition of the 2′-O, 3′-O, and 4′-O groups that facilitates the formation of 2′,3′- or 3′,4′-cyclic phosphates (see below). However, treatment with 15–25% aq. $NH_2NH_2 \cdot H_2O$ at 4° over a period of 20–48 h resulted in the desired concomitant solid-support detachment and acyl-group deprotection with minimal strand scission. Attempts to remove NH_2NH_2 by evaporation on a rotavap resulted also in strand scission. However, it was observed that sequences still containing the end Tr

---

[18]) The terms 'Trityl-off' and 'Trityl-on' mode refer to whether the final 4′-*O*-DMT group is removed before or after taking the oligomer off the solid support. The sequences that were prepared in the 'Trityl-on' mode were conveniently handled in purification, when the base-deprotection step involved treatment with $NH_2NH_2 \cdot H_2O$ (see *Exper. Part*, *Sect. 4.3*).

[19]) This method was incompatible with oligonucleotides containing the end Tr group. Also the use of $BuNH_2$ has its drawbacks due to its high nucleophilicity [54].

[20]) In one case (p**r**-C_6), deprotection of the 3′-OBz groups under two different methods were tested: *a*) with 3.8M soln. of NH_4Cl in NH_3/EtOH 3:1, at room temperature for 28 h, which resulted in substantial strand scission without complete 3′-OBz deprotection; *b*) with 0.24M soln. of $MeONH_2 \cdot HCl$ in NH_3/EtOH 3:1, at room temperature for 28 h, which gave a smaller percentage of strand scission, but also greater percentage of incomplete deprotection of 3′-OBz as compared to *Method a*.

group could be best separated from NH_2NH_2 by passing through a *Sep Pak C18* (*Waters*) column. This became the reason for synthesizing and isolating p-RNA-oligonucleotide sequences with an end Tr group ('Trityl-on' mode). For D-containing sequences, the hydrazine deprotection had to be carried out at room temperature for at least 48 h to obtain fully deprotected oligomers[21]). In the case of U-containing sequences, not surprisingly, the NH_2NH_2 treatment fails due to the sensitivity of the pyrimidine ring towards the reactive nucleophile; this problem was overcome partially by the use of $MeONH_2$ in ethanolic NH_3 under carefully controlled conditions[22]). In contrast, the pyrimidine ring of thymine is sufficiently stable toward the hydrazinolytic conditions of deprotection. *Table 3* lists the specific deprotection methods applied to the various oligonucleotides synthesized.

Sequences without an end Tr group ('Trityl-off' mode) were directly taken to the next step of HPLC purification. Oligomers synthesized with the end Tr group ('Trityl-on' mode) were detritylated with 80% aq. HCO_2H at room temperature. Purification of the crude oligonucleotides was carried out by reverse-phase HPLC (*Spherisorb-S10X RP-C18*, 220 × 12 mm, with 0.1M aq. $Et_3NH \cdot AcOH$ as buffer) or ion-exchange HPLC (*Nucleogen DEAE 60-7* or *Mono Q HR 5/5*, with 10 mM Na_2HPO_4 as buffer) according to their preparative history. *Table 3* lists all synthesized p-RNA oligonucleotides with their specific purification protocol. In the initial stages of the project, the crude oligonucleotides containing the end Tr group were first purified by preparative reverse-phase HPLC, followed by detritylation (80% aq. HCO_2H, room temperature). Later, it was found that the initial reverse-phase purification could be bypassed and detritylation, followed by purification on ion-exchange HPLC, was efficient enough to provide oligonucleotides with purity of > 95%. For oligonucleotides containing a 2′- or 3′-phosphate or 2′,3′- or 3′,4′-cyclophosphate group (see below), ion-exchange HPLC was the purification method of choice.

The efficiency of the $(Ph_3P)_3Pd^0/Et_2NH \cdot HCO_3$/hydrazinolysis deprotection procedure employed as described above was fairly adequate for sequences of short lengths (*e.g.*, octamer or less), but, in some cases, the deprotection procedure gave unsatisfactory results, as typified by the HPLC traces in *Fig. 5*. This variation in yields depending on the sequences worsened when extended to longer sequences (*e.g.*, dodecamers), especially for mixed sequences (see, *e.g.*, *Fig. 6*).

Optimized Procedure for p-RNA-Oligonucleotide Deprotection. While the above mentioned synthesis methods were satisfactory, there was a need to improve the deprotection protocol, which would lead to increased efficiency of the purification process (by reducing the difficulties due to the occurrence of interfering peaks in the chromatogram). Towards this end, it was discovered that a 1:1 combination of 40% (*w*/*w*) aq. $MeNH_2$ in conc. aq. NH_3 at room temperature for 5–6 h could efficiently detach the oligonucleotides from the solid support and concomitantly remove the acyl protecting groups. Since NH_3 and $MeNH_2$ were easily removed by evaporation without any deleterious side effects, a side benefit was the riddance of the necessity of having to

---

[21]) The Bz group at the N^2-position of D is removed very slowly (compared to the N^6-Bz group).

[22]) The deprotection was monitored by HPLC and stopped at a stage judged to have the maximum amount of the fully deprotected sequence before degradation began to occur. The partially deprotected sequences were collected, combined, and subjected again to the deprotection reaction conditions. Such a tedious operation prompted us to replace U with T in our future studies.

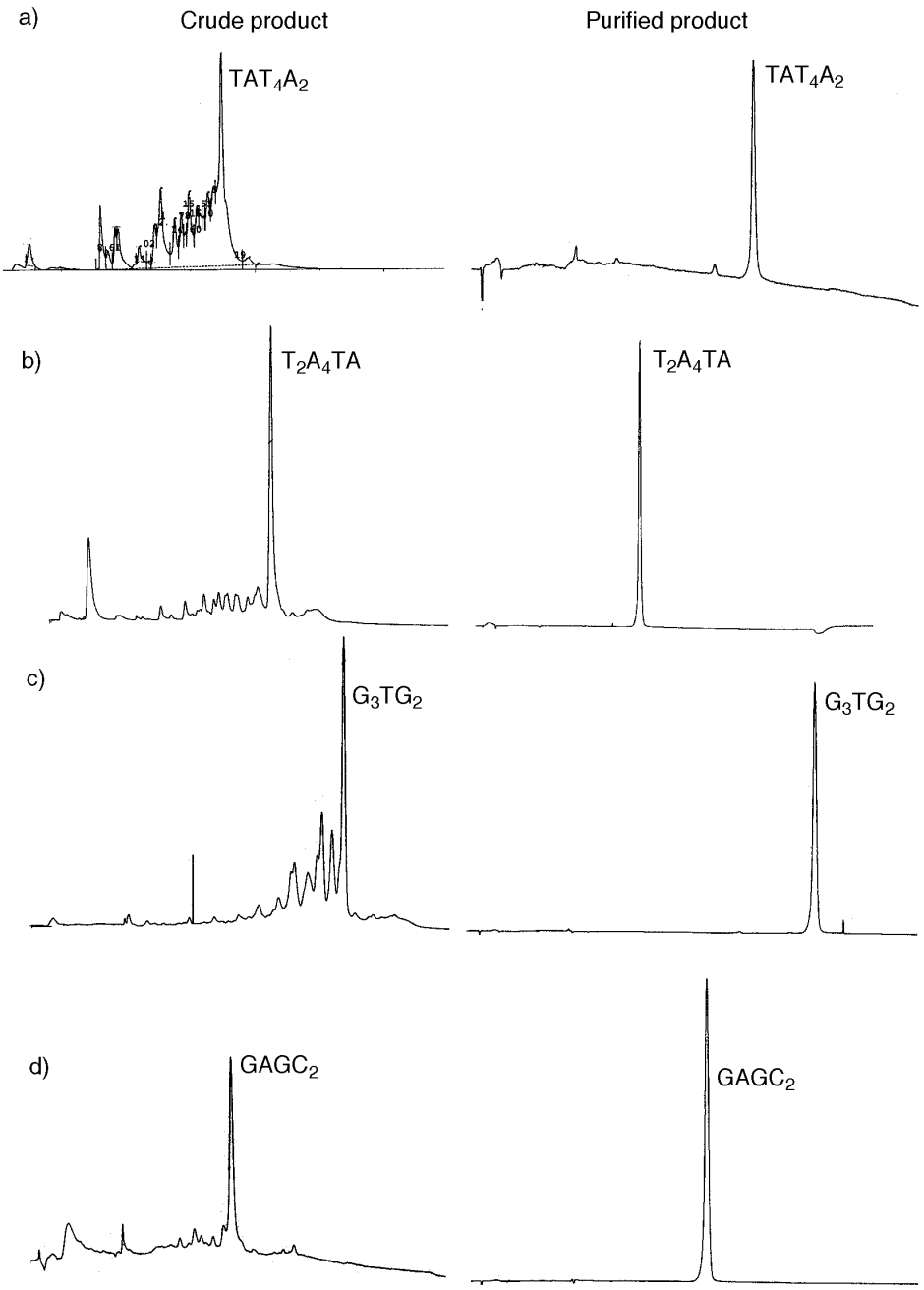

Fig. 5. *Ion-exchange HPLC traces* (*Mono-Q*) *of selected p-RNA-oligonucleotide sequences before and after purification.* The traces of the crude products document the wide variability in the efficiency of the deprotection protocol employed (deprotection of allyloxy groups by Pd^0 complex [55], followed by subsequent (concomitant) detachment from CPG and acyl group deprotection by hydrazinolysis). See also *Fig. 6,a.* For HPLC conditions, see *Exper. Part, Sect. 6.*

synthesize sequences with end Tr group ('Trityl-on') and thereby eliminating the need for an additional separation step (removal of NH_2NH_2 with the *Sep Pak C18* cartridge). The next improvement resulted from applying the procedure of *Noyori* and co-workers [61] for more efficient allyl deprotection[23]). Thus, the CPG solid support containing the oligonucleotide strand was treated with a homogenous soln. of the catalyst prepared from tris(dibenzylideneacetone)dipalladium(0)–$CHCl_3$ adduct, Ph_3P, Et_2NH_2, and HCO_2H in THF at 50° for 3–4 h[24]). After removal of the Pd catalyst by washing with 0.1M aq. $NaSC(S)NEt_2N$ soln., CPG containing the oligonucleotide sequence was subjected to 40% aq. $MeNH_2$/30% aq. NH_3 1:1, at room temperature for 5–6 h, which resulted in concomitant detachment and acyl-group deprotection. Concentration *in vacuo* and ion-exchange purification of the crude oligonucleotides (over a *Mono Q HR 5/5* column) afforded oligonucleotides with >95% purity with improved yields in the range of 2–10 fold (*Table 4*). *Fig. 6* demonstrates the effectiveness of this optimized deprotection method over the previously used hydrazine-based procedure for a 13-mer mixed sequence.

Table 4. *Comparison of the Efficiency of the Two Deprotection Methods for p-RNA Oligonucleotides*

Entry	p-RNA sequence	Deprotection *Method*[a])	O. D. 260 nm (yield %)
1	p**r**-GAGCC-2′-phosphate	*A*	7.5 (2.1)
2	p**r**-GAGCC-2′-phosphate	*B*	26.4 (8.0)
3	p**r**-CACACCCGGCTCC	*A*	7.1 (1.5)
4	p**r**-CACACCCGGCTCC	*B*	88.0 (15)
5	p**r**-GGAGCCG	*A*	21.1 (10)
6	p**r**-GGAACCG	*B*	88.7 (18)

[a]) *Method A:* 1. $Pd(PPh_3)_4$, PPh_3, $Et_2NH_2 \cdot HCO_3$ in CH_2Cl_2, 25°, 4.5 h; 2. NH_2NH_2/H_2O, 4°, 42 h; 3. HCO_2H/H_2O 4:1, 25°, 0.25 h. *Method B:* 1. Pd_2(dibenzylideneacetone)$_3$–$CHCl_3$ adduct, PPh_3, Et_2NH, HCO_2H in THF, 50°, 3.5 h; 2. $MeNH_2$/aq. NH_3 1:1, 25°, 5.5 h.

Synthesis of Phosphate and Cyclophosphate Derivatives of p-RNA Oligonucleotides. Studies on the capability of nonenzymatic template-directed ligation and replication necessitated the synthesis of the suitable 2′- or 4′-phosphate and 2′,3′- or 3′,4′-cyclophosphate derivatives of p-RNA oligonucleotides. The 4′-phosphate oligonucleotide derivatives were synthesized by the following procedure: after the final detritylation step on the synthesizer, the CPG-bound oligonucleotide was coupled with 0.1M (allyloxy)[bis(diisopropylamine)]phosphine [55] in MeCN in the presence of the activator, affording the 4′-*O*-phosphitylated oligonucleotide derivative. Subsequent capping and oxidation followed by the usual deprotection of the allyl groups under the *Noyori* conditions [54] resulted in the 4′-phosphorylated p-RNA oligonu-

---

[23]) Initiated by *M. S.* It was thought that there is incomplete allyl deprotection under the previously used *Noyori* conditions, which led to a greater percentage of strand scission in the subsequent acyl-deprotection step under basic conditions.

[24]) The progress of allyl deprotection could be monitored by HPLC after base-catalyzed release/deprotection step (Et_2NH/conc. aq. NH_3 treatment).

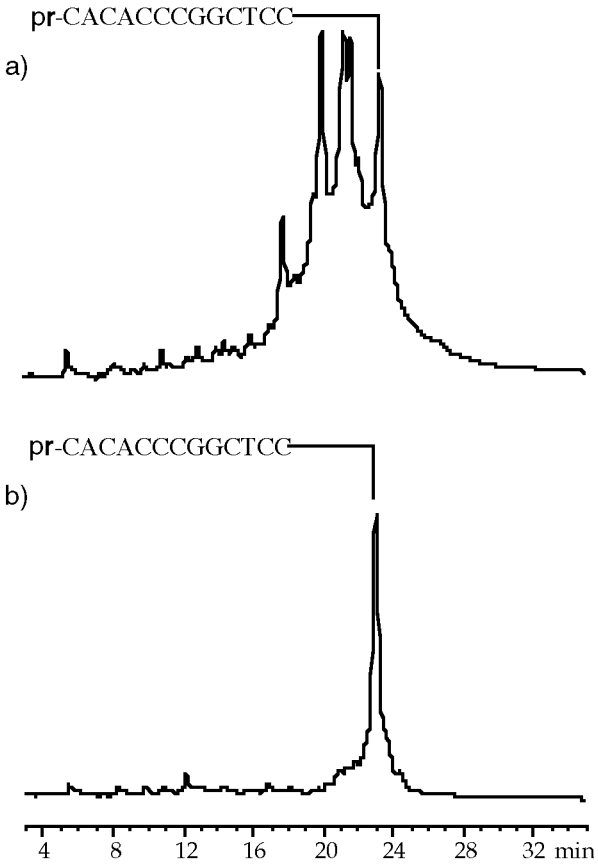

Fig. 6. *Ion-exchange HPLC traces* (*Mono Q*) *in the synthesis of the sequence p***r***-(CACACCCGGCTCC) documenting the efficiency of the optimized allyl and base deprotection procedure* B *over a previously used deprotection protocol* A. *a*) HPLC Trace resulting from the old deprotection protocol (1. $Pd(PPh_3)_4$, PPh_3, $Et_2NH_2 \cdot HCO_3$ in CH_2Cl_2, 25°, 4.5 h; 2. NH_2NH_2/H_2O, 4°, 42 h; 3. HCO_2H/H_2O 4:1, 25°, 0.25 h). *b*) HPLC Trace resulting from the optimized deprotection protocol (1. Pd_2(dibenzylideneacetone)$_3-CHCl_3$ adduct, PPh_3, Et_2NH, HCO_2H in THF, 50°, 3.5 h; 2. $MeNH_2$/aq. NH_3, 25°, 5.5 h). For HPLC conditions, see *Exper. Part. Sect. 6.*

cleotides (see *Exper. Part., Sect. 5.1*). Oligonucleotide-2′-phosphate (and 3′-phosphate) derivatives were synthesized by automated solid-support synthesis by using a universal solid support derivatized with a sulfone linker [62][25]). The 2′-end (or the

[25]) Initially CPG-derivatized with 2′-benzoyl-1′-benzyl-5′-(4,4′-dimethoxytrityl)-3′-succinyl-β-D-ribofuranoside was used; but this was later abandoned for the more convenient approach outlined above. We thank Dr. *H. Moser*, Dr. *R. Häner*, and Dr. *F. Natt* (*Novartis AG*, Basel) for a generous gift of the sulfone linker [62].

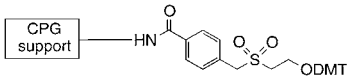

3′-end)[26]) of the starting nucleoside was coupled onto this solid support. Applying the *Noyori* protocol [54][55] removed the allyl groups; the base-deprotection procedure, while removing the acyl protecting groups, causes the simultaneous detachment of the oligonucleotide strand from the solid support (*via* the elimination of sulfone linker), yielding the p-RNA-oligonucleotide-2′- or 3′-phosphate to be subjected to HPLC-purification (see *Exper. Part., Sect. 5.2*).

p-RNA Oligonucleotides containing 3′,4′- and 2′,3′-cyclophosphate end groups were prepared by treating the corresponding 4′- or 2′-phosphate sequences (0.1 – 0.5 mM aq. soln.), with a large excess of *N*-[3-(dimethylamino)propyl]-*N*′-ethylcarbodiimide · hydrochloride (DEC · HCl; 0.5 – 1.0M aq. soln.) at room temperature for 3 – 4 h (*Scheme 5*). The reactions were monitored by ion-exchange HPLC and stopped when *ca.* 90% complete. The excess DEC · HCl was removed by desalting, and the cyclic phosphate group containing oligomers were isolated by ion-exchange HPLC. The cyclic phosphates are stable under the conditions of isolation and purification (see *Exper. Part., Sect. 5.3*).

Scheme 5. *Preparation of 2′,3′-Cyclophosphates of β-*D*-Ribopyranosyl Oligonucleotides from the Corresponding 2′-Phosphate Derivatized Oligonucleotides*

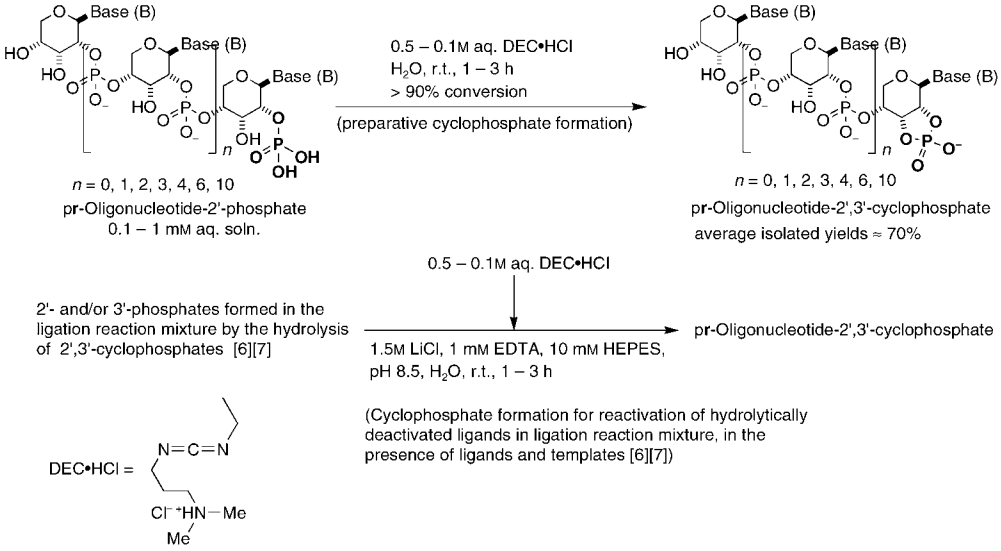

3. Properties of p-RNA Oligonucleotides. – As already mentioned in the *Introduction*, most results of our experimental studies on the structural and chemical properties of p-RNA oligonucleotides have been described in much detail in our preliminary communications [1 – 8], so that there is no need to fully reproduce and rediscuss these results here. Therefore, this chapter is restricted to an overview of the observations made in these many studies. However, some of the experiments on

[26]) The preparation of the p-RNA-mononucleoside 3′-phosphoramidites is described in [10].

p-RNA properties that have remained unpublished (or are only partially published) thus far are incorporated in this chapter in more detail.

3.1. *Structure.* A comprehensive NMR structure determination by *Jaun* and *Schlönvogt* and co-workers [4] of the duplex formed by the self-complementary p-RNA-octamer sequence p**r**(CGAATTCG), accompanied by a MD-based molecular modeling by *Wolf* and co-workers [4], has shown that this duplex has a left-handed (weakly) helical ladder structure held together in antiparallel strand orientation by canonical *Watson–Crick* base pairs with a large inclination of the (averaged) backbone axis relative to the (averaged) base-pair axes [1][8] and, as a consequence thereof, with a mode of base stacking that is purely *inter*strand (in sharp contrast to the pure *intra*strand stacking made of neighboring nucleobases in B-type DNA) (*Fig. 7*). The structure analysis confirmed in essence the conjectures on the p-RNA duplex structure suggested by a qualitative conformational analysis of a p-RNA single strand based on idealized conformations by using steric and stereoelectronic selection criteria [1]. *Fig. 8* recalls the two most pronounced deviations between the idealized and the experimental structure [4]; they occur in the torsion angles β and ε, and refer to the two bonds that connect the phosphodiester group to the ribopyranose positions C(4′) and C(2′). These deviations are interpreted to be the consequence of '*Newman* strain' [64], which is to be expected for any phosphodiester group bound to a secondary C-atom in an idealized (strictly staggered) conformation. Specifically in this case, the strain is due to the steric clash between the equatorial H-atom at C(5′) and the phosphodiester O-atom bound to C(2′) (partially relieved by the deviation of the torsion angle β from its idealized value of 180°), and to an analogous steric clash between the equatorial H-atom at C(3′) and one of the (negatively charged) phosphodiester O-atom of the C(2′)-bound phosphodiester group (relieved by the deviation of torsion angle ε from its idealized value $-60°$). The intra-phosphodiester torsion angles α (*ca.* $71°-77°$) and ζ ($-174°$ – $-177°$) [4] deviate only slightly from their idealized values; they reflect two well-behaved $-g/t$ phosphodiester conformations. The occurrence of *g*/*t* conformations in p-RNA duplexes documents that there can hardly be a significant difference in intrinsic stability of *g*/*g* and *g*/*t* phosphodiester conformations, as some earlier (theoretical) studies had been proposing [65], and as our original version of predicting the base-pairing potential of homo-DNA oligonucleotide systems by qualitative conformational analysis had assumed to exist [29][27]). Simulated annealing calculations of the structure of the p-RNA duplex derived from p**r**(CGAATTCG) based on the NMR data of [4] by *Schwalbe* and co-workers [66] corroborated the conclusions drawn by *Jaun* and *Schlönvogt* [4]. Complementary information on, and a further illustration of, such a quasi-linear type of oligonucleotide structure comes from a NMR structure analysis carried out by *Schwalbe et al.* [67] of a duplex derived from the partially self-complementary AATAT sequence in the series of *Quinkert*'s δ-peptide analogues of p-RNA [68].

3.2. *Base Pairing.* p-RNA-Oligonucleotide sequences containing the canonical nucleobases undergo base-pairing with strictly antiparallel strand orientation in the

---

[27]) However, the postulate that *t*/*t* phosphodiester conformations are 'forbidden conformations' formally deduced from the same type of stereoelectronic reasoning [29] seems to hold; no such conformation seems to have been observed in phosphodiester or oligonucleotide structures so far.

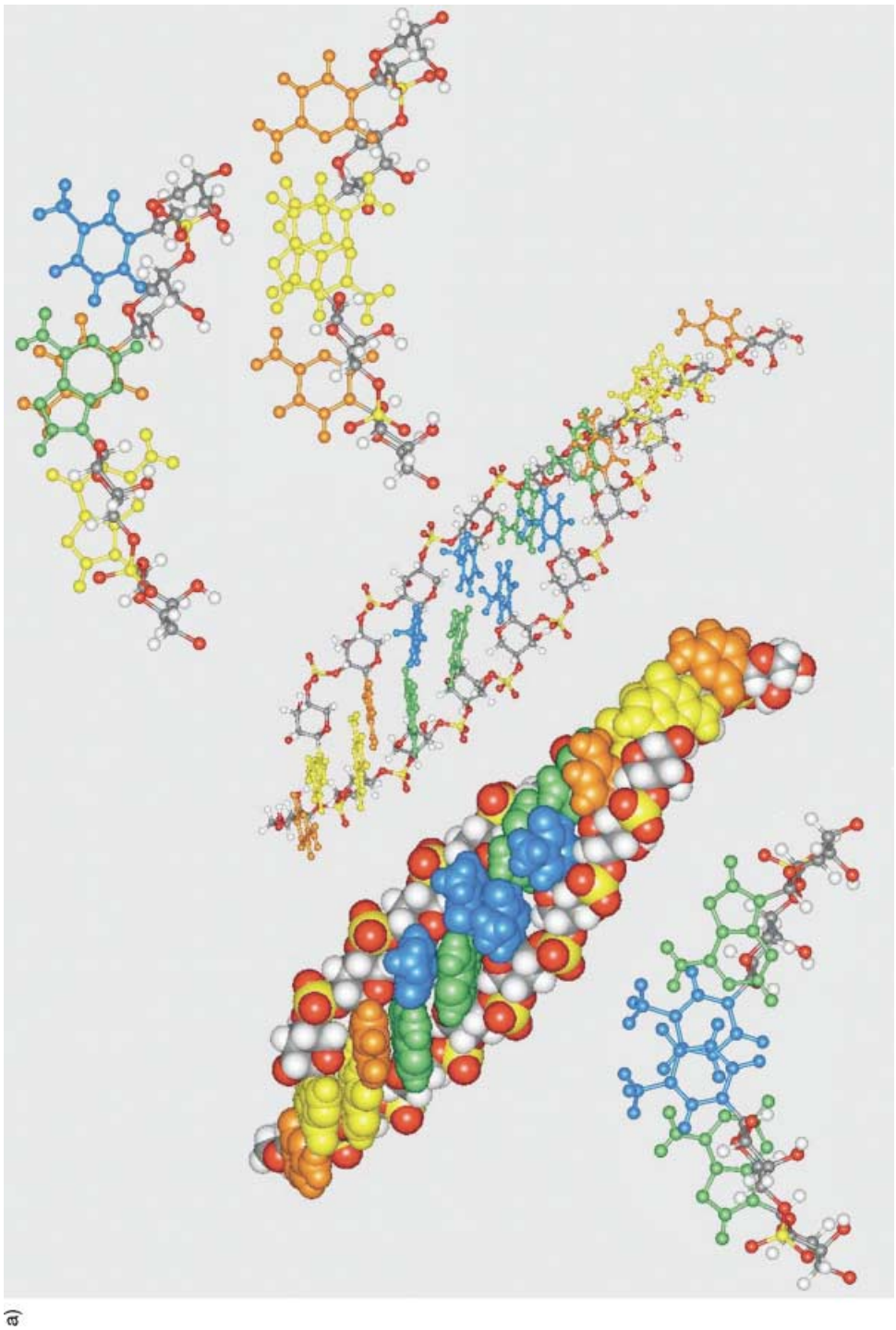

Fig. 7. *NMR Structure of p-RNA duplex derived from the self-complementary sequence p*-*(CGAATTCG)* [4]. *a*) Time-averaged and refined structure of octamer duplex derived from self-complementary p-RNA sequence 4′-CGAATTCG-2′, based on a 1000-ps MD calculation (*Amber*) by *R. M. Wolf* [39] and an NMR structure analysis by *Jaun et al.* [39]. Ball-and-stick representation as well as excerpts on upper right and lower left illustrate the interstrand base stacking characteristic to pentopyranosyl-(2′ → 4′)-oligonucleotide duplexes (purine-pyrimidine and purine-purine stacking: upper right, pyrimidine-pyrimidine 'non-stacking': lower left). Courtesy of Dr. *R. M. Wolf, Novartis Pharma AG*, Basel. *b*) Excerpt of duplex structure referred to in *a*), illustrating interstrand base stacking in side view (a former cover picture of *Helv. Chim. Acta*).

b)

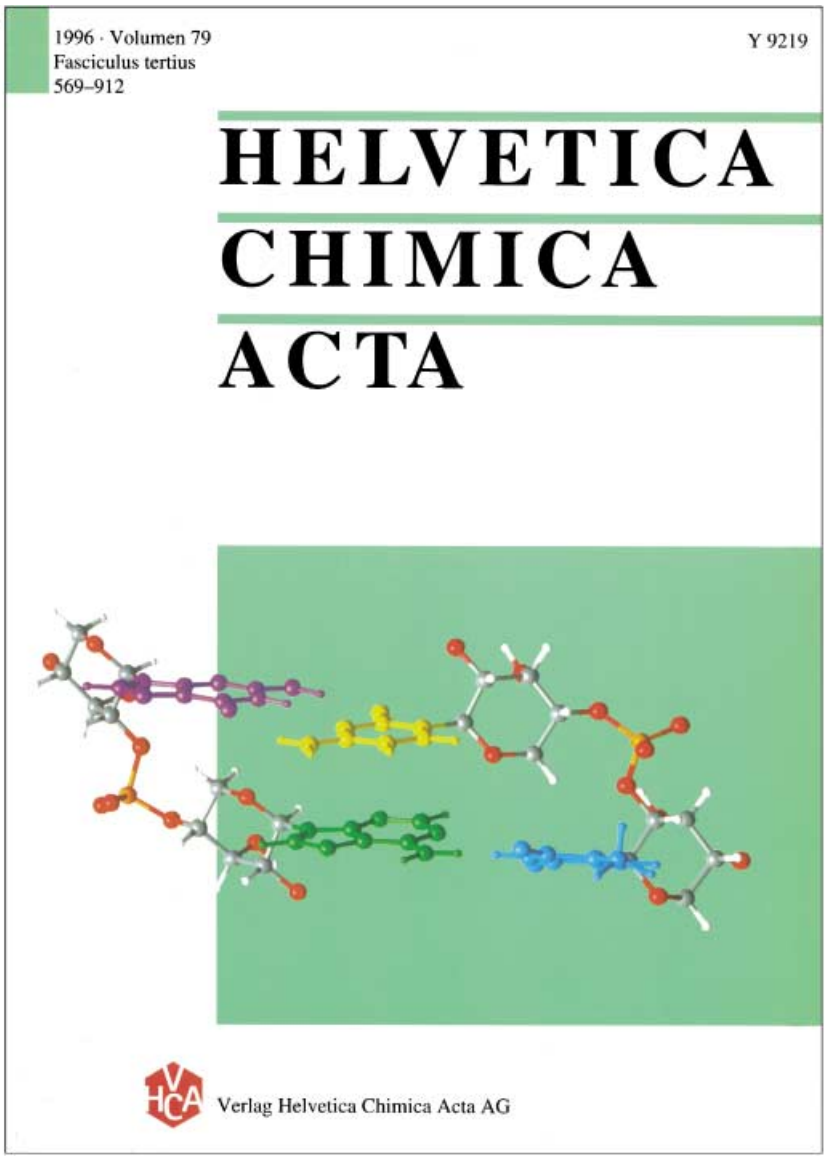

Fig. 7 (cont.)

canonical *Watson–Crick* pairing mode [1][2][4]. Their base-pairing strength is uniformly greater than that of corresponding RNA and DNA oligonucleotide sequences (*Tables 5* and *6*). This behavior is not specific to the ribopyranosyl oligonucleotide system, the entire family of pentopyranosyl-(4′→2′)-oligonucleotide systems shows *Watson–Crick* base pairing that is stronger than that of RNA and DNA

[17][9][11][12]. Superiority in base-pairing strength has been interpreted as being connected to a higher degree of conformational pre-organization of single strands toward their duplex conformations, as compared to the single strands of the ribofuranosyl-(5′→3′)-oligonucleotide system. This line of reasoning originated in the context of our previous studies on the chemistry of homo-DNA [35][27] and later turned out to serve as a fruitful lead in the search for modified oligonucleotide systems in anti-sense oligonucleotide chemistry [71–73] (see also *Footnote 5*). While no systematic experiments with p-RNA mismatch sequences that would allow us to compare base pairing fidelity of p-RNA with that of RNA have been carried out, it is clear from the information available that base pairing of p-RNA is more selective than that of natural RNA and DNA with respect to the pairing mode: neither the *Hoogsteen* nor the reverse-*Hoogsteen* pairing mode seem to be accessible to p-RNA sequences[28]) for efficient pairing. This is evidenced by the finding that, *e.g.*, homo-G sequences p**r**(G_n) ($n = 6-10$) do not show discernible self-pairing (*Entries 95* and *96* in *Table 5*), in pronounced contrast to such sequences in the natural series. This pairing-mode selectivity of p-RNA is also in sharp contrast to the behavior of homo-DNA, where self-pairing of homo-purine sequences such as ddGlc(A_n) and ddGlc(G_n) in the reverse-*Hoogsteen* mode with antiparallel strand orientation is a highly characteristic and well documented behavior [27].

The pyranosyl isomer of RNA is not capable of cross-pairing with natural RNA (or DNA), neither do p-RNA sequences cross-pair with complementary homo-DNA sequences (D-series). We have reasoned that such inability of a given oligonucleotide system to cross-communicate with another system goes parallel to a pronounced deviation of the two system's respective backbone inclinations (deviations from a quasi-orthogonal positioning of base-pair axes and backbone axis) [8][10]. While p-RNA and homo-DNA have strong and oppositely oriented backbone inclinations [8], the *Watson–Crick* B-type double-stranded DNA represents the prime example of a duplex structure in which the (averaged) backbone axis is essentially orthogonal to the (averaged) base-pair axis.

Pyranosyl-RNA sequences of the D-ribose series have been shown to undergo highly efficient cross-pairing with the three other members of the pentopyranosyl-(4′→2′)-oligonucleotide family that have been investigated in the course of our studies, namely, the β-D-xylo-, α-L-arabino-, and α-L-lyxopyranosyl systems [17][16]. All four members have in common that both their nucleobases and their 2′-phosphodiester attachment to the pyranosyl chairs are equatorial. They differ in the conformation of the 4′-phosphodiester attachment, this conformation being axial in the α-L-*lyxo*- and α-L-*arabino* series and equatorial in the β-D-*ribo*- and β-D-*xylo* series. The cross-pairing behavior of the four members indicates that their backbone inclinations can efficiently adapt to each other. That the backbone inclination of a system with axial 4′-phosphodiester conformation can be similar to that in the β-D-ribopyranosyl system (equatorial 4′-phosphodiester) has been shown by *Jaun* and *Ebert*'s recent NMR structure analysis of an α-L-arabinopyranosyl-octamer duplex [74][12]. A pathway by

---

[28]) Statements on a non-occurrence of base pairing in new oligonucleotide systems have to be taken as referring to sequence lengths that are covered by experiments. Base-pairing interactions may become discernible when sequences extend beyond a critical length.

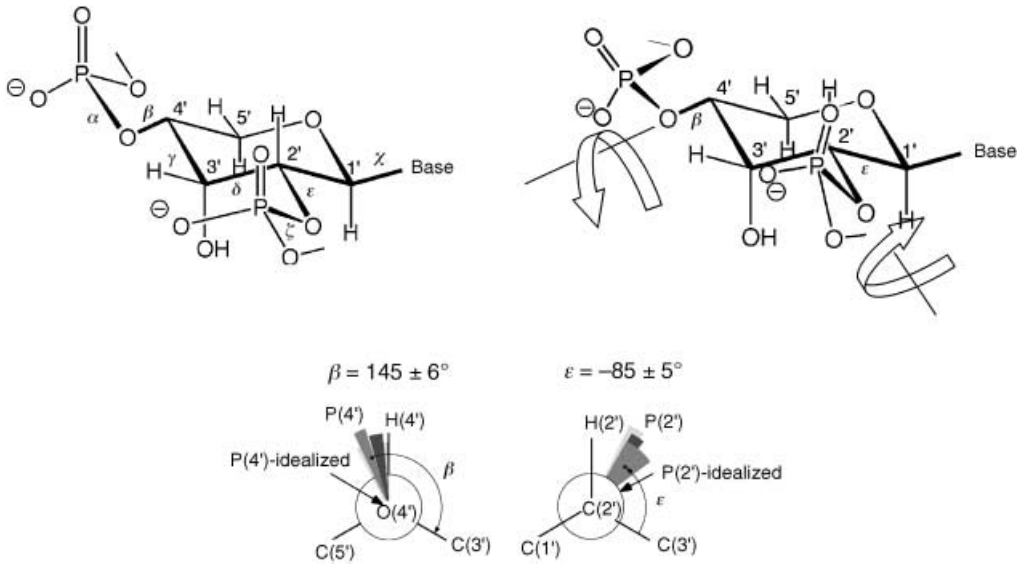

Fig. 8. *Comparison of idealized pairing conformation of repeating unit of p-RNA duplexes* (top left) *with conformation resulting from the NMR structure analysis of p-RNA duplex of* Fig. 7 [4]. The major deviations observed refer to torsional angles β and ε.

which backbone inclinations can efficiently adapt to each other is changing the nucleosidic torsion angles [16][8] (*Fig. 9*).

Oligonucleotide sequences in p-RNA are capable of forming hairpin structures with comparable ease as corresponding sequences in the natural series [5] (*Table 6*). It is not necessarily self-evident that this should be the case because the number of (formally) fully rotatable bonds per repetitive nucleotide unit in p-RNA is by one unit smaller than in the natural series, and a pyranose chair is assumed to be conformationally more rigid than the highly flexible furanose ring. An illustrative example of the propensity, as well as the limits, of p-RNA sequences to form hairpins is the behavior of the three sequences p**r**(GCG-T_n-CGC) ($n=2$, 3, 4): Whereas the sequence with $n=2$ in a standard range of concentrations ($c=3-150$ μM, 0.15M NaCl, 0.01M *Tris* buffer, pH 7) favors duplex over hairpin formation and, oppositely, the sequence with $n=4$ favors hairpin over duplex formation, the sequence with $n=3$ exists as hairpin at lower concentration, but leans toward forming the duplex at higher ones [5].

Hairpin-forming sequences of the p-RNA series have been used to demonstrate the specific contribution of interstrand nucleobase stacking to thermodynamic duplex stability [5][8]. In p-RNA, the presence of dangling bases at the 2′-end (downstream end) of hairpin- or duplex-strand sequences are found to consistently enhance both hairpin and duplex stability, while corresponding dangling bases located at the 4′-end (upstream end) have no such effect (*Figs. 10* and *11*). This sharp contrast clearly parallels the presence or absence of interstrand stacking of the dangling base at the 2′-end with the *Watson–Crick*-engaged nucleobase at the 4′-end of the complementary hairpin stem (or complementary duplex strand). A purine-purine interstrand stacking pair is found to stabilize a hairpin by *ca.* 2 kcal/mol, and a pyrimidine-purine stacking

Table 5. T_m *and Thermodynamic Data of Duplex Formation of p-RNA Oligonucleotides*

Entry	Oligonucleotide pairing System[a])	T_m [°C]	λ meas. [nm]	Thermodynamic data of duplex formation[c])		
		0.15M NaCl, *Tris*[b]) (5 + 5 μM)		ΔG°_{298} [kcal/mol]	$T\Delta S^\circ_{298}$ [kcal/mol]	ΔH° [kcal/mol]
1	$A_7 + U_7$	19	260			
2	$A_7 + U_8$	23	260			
3	$A_8 + U_7$	22	260			
4	$A_8 + U_8$	28 (30 + 30 μM)	260	− 8.0	− 42.1	− 50.1
5	$A_8 + T_8$	40	260	− 10.5	− 51.7	− 62.2
		47 (50 + 50 μM)	260			
		45.5 [d])	260			
6	$A_8 + G_8$	20.4	280			
7	$A_{12} + T_{12}$	60.8 [e])	260	− 15.4 [e])	− 53.6 [e])	− 69.0 [e])
		67.6 [d])[e])	260			
8	$C_6 + G_6$	61 (3.5 + 3.5 μM)	275	− 13.5	− 40.8	− 54.3
9	$C_6 + (L)G_6$	< 0	275			
10	$C_8 + G_8$	82 (2.5 + 2.5 μM)	275			
11	$C_8 + (L)G_8$	≈ 15	275			
12	$C_6 + I_6$	< 0	292			
13	$C_6 + (L)I_6$	29	292	− 7.6	− 26.6	− 34.2
14	$C_8 + I_8$	< 0	292			
15	$C_8 + (L)I_8$	49	292	− 10.7	− 31.3	− 42.0
16	$D_8 + G_8$	21.5	280			
17	$D_8 + T_8$	50	245	− 12.0	− 45.5	− 57.5
18	$(L)D_8 + T_8$	≈ 0	245			
		8 (25 + 25 μM)	245	− 4.8	− 27.0	− 31.8
		12 (25 + 25 μM) [d])	245			
19	$G_6 + I_6$	34	300			
20	$(L)G_6 + I_6$	≪ 0	300			
21	$G_8 + I_8$	56.5	300	− 12.5	− 37.7	− 50.2
22	$(L)G_8 + I_8$	≪ 0	300			
23	$G_8 + (L)G_8$	31/16 [f]) (50 + 50 μM)	252			
		51/25 [f]) (50 + 50 μM) [d])	252			
24	$I_6 + (L)I_6$	20 (25 + 25 μM)	298			
		23 (45 + 45 μM)	298			
25	$I_8 + (L)I_8$	34 (50 + 50 μM)	298	− 7.1	− 20.9	− 28.0
26	$A_4T_3ATAT_2AT_2A + TA_2TA_2TATA_3T_4$	48 (0.9 + 0.9 μM)	260			
27	$AT_2AT_2ATAT_3A_4 + T_4A_3TATA_2TA_2T$	65	260			
		60 (0.9 + 0.9 μM)	260			
28	$AT_2AT_2ATAT_3A_4 + TA_2TA_2TATA_3T_4$	—	260			
29	$AT_2CAGCG + CGCTGA_2T$	61.4 [e])	260	− 13.9 [e])	− 43.6 [e])	− 57.5 [e])
		67.6 [d])[e])	260			
30	$A_2UAU_3A + UA_3UAU_2$	≈ 17	260			
31	$AU_3AUA_2 + U_2AUA_3U$	≈ 20	260			
32	$CACAC_3G_2CTC_2 + GAGC_2$	38.0 (3.5 + 3.5 μM) [e])	260			
33	$CACAC_3G_2CTC_2 + GAGC_2G$	58.3 (3.5 + 3.5 μM) [e])	260			
34	$CACAC_3G_2CTC_2 + G_2TGTG$	49.9 (3.5 + 3.5 μM) [e])	260			
35	$CACAC_3G_2CTC_2 + G_2TGTG + GAGC_2$	45.5 (3.5 + 3.5 + 3.5 μM) [e])	260			
36	$CACAC_3G_2CTC_2 + G_2TGTG + GAGC_2G$	56.9 (3.5 + 3.5 + 3.5 μM) [e])	260			
37	$CACAC_3G_2CTC_2 + GAGC_2G_3TGTG$	> 90 (3.5 + 3.5 μM) [e])	260			
38	$CACAC_3G_2CTC_2 + GAGC_2G_2CTGTG$	81.5 (3.5 + 3.5 μM) [e])	260			
39	$C_3AC_3G_2CTC_2 + GAGC_2$	35.9 (3.5 + 3.5 μM)	260			
		38.0 (3.5 + 3.5 μM) [e])	260			
40	$C_3AC_3G_2CTC_2 + GAGC_2G$	59.0 (3.5 + 3.5 μM) [e])	260			
41	$C_3AC_3G_2CTC_2 + G_2AGC_2$	46.4 (3.5 + 3.5 μM)	260			
42	$C_3AC_3G_2CTC_2 + G_2GT_3$	56.9 (3.5 + 3.5 μM)	260			
43	$C_3AC_3G_2CTC_2 + G_2AGC_2 + G_2TG_3$	50.9 (3.5 + 3.5 + 3.5 μM)	260			
44	$C_3AC_3G_2CTC_2 + GAGC_2 + G_2TG_3$	53.8 (3.5 + 3.5 + 3.5 μM) [e])	260			

Table 5 (cont.)

Entry	Oligonucleotide pairing System[a])	T_m [°C]	λ meas. [nm]	Thermodynamic data of duplex formation[c])		
		0.15M NaCl, *Tris*[b]) (5 + 5 μM)		ΔG°_{298} [kcal/mol]	$T\Delta S^\circ_{298}$ [kcal/mol]	ΔH° [kcal/mol]
45	$C_3AC_3G_2CTC_2 + GAGC_2G + G_2TG_3$	57.2 (2.9 + 2.9 + 2.9 μM) [e])	260			
46	$C_3ACTCG_2CTC_2 + GAGC_2$	30.5 (3.5 + 3.5 μM) [e])	260			
47	$C_3ACTCG_2CTC_2 + AGTG_3$	49.6 (3.5 + 3.5 μM) [e])	260			
48	$C_3ACTCG_2CTC_2 + AGTG_3 + GAGC_2$	40.1 (3.5 + 3.5 + 3.5 μM) [e])	260			
49	$G_3CG_3C + GC_3GC_3$	76.4 (3.4 + 3.4 μM)	280			
		57.6 [g])	280			
50	$CG_3CG_3 + C_3GC_3G$	82.3	280			
51	$CG_6C + GC_6G$	79.1	280			
52	$G_3CG_3CG_3C + GC_3GC_3GC_3$	> 95	280			
53	G_3C-2′,3′-cyclophosphate + GC_3-2′,3′-cyclophosphate	18.2 (7.3 + 7.3 μM)	280			
54	$GCGT_4CGC + GD_4C$	66.4 (1.8 + 1.8 μM)	250			
55	$GCGT_8CGC + A_8$	38.2, 67.1 [h]) (2.5 + 2.5 μM)	250			
		37.4 (1 + 2.5 μM)	250			
56	$GCGT_8CGC + D_6$	31.4, 65.8 [h]) (2.0 + 2.0 μM)	250			
57	$TAC_2T_2CG_3TA_2 + AC_3GA_2$	63.3	250			
58	$TATA_2C_2ATATA + TATATG_2T_2ATA$	68.5	250	− 18.4	− 66.9	− 85.3
59	$TATAC_4TATA + TATAG_4TATA$	79.1	250	− 21.5	− 76.9	− 98.4
		73.5 (0.9 + 0.9 μM)	250			
60	$TATAC_4TATA$ + 4′-phosphate-G_4	46.5 (3.5 + 2.5 μM)	250			
61	$TATAC_4TATA + AG_4T$	51.0 (2 + 2 μM)	250			
62	$TATAC_4TATA + TAG_4TA$	61.5 (2.4 + 2.4 μM)	250			
63	$TATAG_2$-2′,3′-cyclophosphate + C_2TATA	32.0 (1.1 + 1.1 μM)	250			
64	$T_2A_4TA + TAT_4A_2$	38.8 [e])	260	− 9.8 [e])	− 39.8 [e])	− 49.6 [e])
		45.9 [d])	260			
	Self-pairing sequences					
65	A_8	– (no self-pairing)	260			
66	A_{12}	< 5 [d])[e])	260			
		25 (100 μM) [d])[e])	260			
67	A_5T_5	43	260	− 10.8	− 61.1	− 71.9
68	A_4T_4	27	260	− 7.3	− 40.8	− 48.1
		36 (50 + 50 μM)	260			
69	A_4U_4	14	260	− 5.2	− 37.3	− 42.5
		21 [d])[e])	260	− 6.2 [d])[e])	− 38.1 [d])[e])	− 44.3 [d])[e])
		23 (50 + 50 μM)	260			
		30 (50 + 50 μM) [d])[e])	260			
70	$(AT)_3A$	38	260	− 9.1	− 45.1	− 54.2
71	$(AT)_4$	38	260	− 9.2	− 49.5	− 58.7
		46 (50 + 50 μM)	260			
72	ATGCAT	29.0	250	− 7.3	− 28.7	− 36.0
73	ATGCATG	51.0	250	− 10.3	− 42.8	− 53.1
74	AT_2CAGCG	5.8 [d])[e])	260			
75	ATCGATCG-2′-phosphate	49.5	260			
76	ATCGATCGATCG-2′-phosphate	80.2	260			
77	$(AU)_4$	24	260	− 6.6	− 44.5	− 51.1
		33 (50 + 50 μM)	260			
		30 [d])	260			
78	C_3G_3	68	272	− 13.0	− 35.5	− 48.5
79	CGA_2T_2CG	60	259	− 12.6	− 42.3	− 54.9
80	CGAGCG	40.3 [d])[e])	280			
81	$(CG)_3$	65	272	− 12.5	− 35.4	− 47.9
82	$CGCTGA_2T$	29.5 [d])[e])	260			
83	CG_6C	38.9	280			
84	$GAGC_2G$	9.9 [d])[e])	260			
85	GATGCAT	28.0	250	− 7.1	− 29.5	− 36.6

Table 5 (cont.)

Entry	Oligonucleotide pairing System[a])	T_m [°C]	λ meas. [nm]	Thermodynamic data of duplex formation[c])		
		0.15M NaCl, *Tris*[b]) (5 + 5 μM)		ΔG°_{298} [kcal/mol]	$T\Delta S^\circ_{298}$ [kcal/mol]	ΔH° [kcal/mol]
86	GC_6G	< 0	280			
87	$GC_3GC_3GC_3$	32.7 (5 μM)	280			
88	$GC_2G_2C_2G$-2′-phosphate	74.2	260			
89	$(GC)_3$	62	272	− 11.3	− 29.2	− 40.5
90	$GCGT_2CGC$	34.4 (3 μM)	250	− 9.0	− 41.9	− 50.9
		48.9 (150 μM)				
91	G_2AGC_2G	51.3 (6.9 μM) [e])	260	− 11.4 [e])	− 37.4 [e])	− 48.8 [e])
		58.0 [d])[e])	260			
92	$G_2A_2C_2G$	42.8 [d])[e])	260			
93	G_3C_3	58	272	− 10.8	− 30.4	− 41.3
94	$G_3CG_3CG_3C$	50.1 (5 μM)	280	− 11.9	− 48.3	− 60.2
95	GTACGTA	37.0	260	− 8.3	− 30.7	− 39.0
96	G_6	– (no self-pairing)	260			
97	G_{10}	– (no self-pairing)	260			
98	I_3G_3	29.0	260			
99	TA_4TA_2	13 [d])[e])	260			
100	$(TA)_4$	40	260	− 9.3	− 42.3	− 51.6
101	$(TA)_3T$	29	260	− 7.4	− 36.2	− 43.6
102	TAT_4A_2	22	260			
		13 [d])[e])	260			
103	TACGTA	39.0	260	− 8.7	− 32.2	− 40.9
104	TACGTAG	46.0	260	− 10.3	− 42.8	− 53.1
105	T_2A_4TA	15	260			
106	T_4A_4	40	260	− 9.8	− 50.1	− 59.9
		47 (50 + 50 μM)	260			
107	T_5A_5	54	260	− 12.8	− 54.8	− 67.6
108	$(UA)_4$	27	260	− 7.2	− 41.2	− 48.4
		35 (50 + 50 μM)	260			
		34 [d])	260			
109	U_4A_4	32	260	− 8.1	− 46.8	− 54.9
		40 (50 + 50 μM)	260			
	Hairpin Sequences [g])					
110	$A_6T_2A_2T_6$	63.0 (3 μM)	250	− 18.7	− 81.0	99.7
		69.0 (45 μM)	250			
111	$AGCGT_4CGC$	67.9 (3 μM)	250	− 4.5	− 31.1	− 35.6
		67 (80 μM)	250			
112	ATA_5TATCG-2′-phosphate	31.4 (3 μM)	250			
		20.5 (75 μM)	250			
113	$ATATG_2T_2AT$	14.8 (3 μM)	250			
		16 (85 μM)	250			
114	$CGCA_4GCG$	62.5 (4.5 μM)	250	− 4.4	− 35.4	− 39.8
		64.0 (98 μM)	250			
115	$GCGT_3CGC$	59.9 (3 μM)	275	− 3.5	− 30.4	− 33.9
		62.0 (178 μM)	275			
116	$GCGT_4CGC$	65.8 (3 μM)	250	− 4.3	− 31.6	− 35.9
		63.5 (150 μM)	250			
117	$GCGT_5CGC$	66.5 (4.3 μM)	250	− 4.0	− 28.7	− 32.7
		68.3 (163 μM)	250			
118	$GCGT_4CGCC$	76 (3 μM)	250	− 5.4	− 31.3	− 36.7
		77 (80 μM)	250			
119	$CGCGT_4CGC$	68 (3 μM)	250	− 4.4	− 30.5	− 34.9
		66 (80 μM)	250			
120	$GCGT_4CGCA$	81.4 (3 μM)	250	− 6.3	− 33.6	− 39.9
		80 (80μM)	250			
121	$GCGT_8CGCT$	66.7 (3.4 μM)	250			
		67.6 (97.6 μM)	250			

Table 5 (cont.)

Entry	Oligonucleotide pairing System[a])	T_m [°C]	λ meas. [nm]	Thermodynamic data of duplex formation[c])		
		0.15M NaCl, *Tris*[b]) (5 + 5 μM)		ΔG°_{298} [kcal/mol]	$T\Delta S^\circ_{298}$ [kcal/mol]	ΔH° [kcal/mol]
122	$TATA_2C_2ATATA$	48.0 (1.8 μM)	250	−2.2	−29.0	−31.2
		49.4 (84 μM)	250			
123	$TATATG_2T_2ATA$	47.4 (2 μM)	250	−2.1	−27.8	−29.9
		47.1 (86 μM)	250			
124	$TATAC_4TATA$	44.7 (7 μM)	265	−2.0	−29.8	−31.8
		45.4 (88 μM)	265			
125	$TATAG_4TATA$	49 (36.8 μM)	265, 270	−2.5	−31.6	−34.1
		46 (80 μM)	265, 270			
126	$TATAC_4TATA_2$	55 (3 μM)	250			
		56 (80 μM)	250			
127	$TAC_2T_2CG_3TA_2$	72.3 (3 μM)	250	−5.8	−37.1	−42.9
		72.7 (88 μM)	250			
128	TAG_4TA	– (3 μM)	250			

[a]) All studies refer to the β-D-p-RNA-oligonucleotide system. [b]) T_m Measurements were made in *Tris* buffer: 10 mM aq. *Tris* · HCl, pH 7.0 in the presence of 0.15M NaCl. The total oligonucleotide concentration is *ca.* 10 μM, unless stated otherwise. Estimated error of T_m determination ±0.5°. –: T_m not observed. [c]) Thermodynamic data of duplexes from plots of T_m^{-1} vs. ln *c* [69]; experimental error estimated in ΔH values ±5%. Thermodynamic data of hairpins determined according to the α/T method or differentiation of the melting-curve method ([69], pp. 1603–1610). [d]) Measured in the presence of 1.0M NaCl. [e]) Measured in phosphate buffer: 10 mM aq. NaH_2PO_4, pH, 7.0. [f]) T_m values of heating and cooling curves, respectively. [g]) Measured in absence of salts. [h]) T_m values of duplex and hairpin, respectively.

pair by *ca.* 1 kcal/mol (*Fig. 11*), while two pyrimidines in (formal) stacking positions do not give rise to discernible stabilization.

This kind of reasoning on the influence of interstrand base stacking on hairpin and duplex stability has been successfully applied to interpret consistent regularities observed in p-RNA (as well as in the other members of the pentopyranosyl-(4′ → 2′)-oligonucleotide family) on the dependence of duplex stability on base sequence. In the case of p-RNA sequences with alternating purine and pyrimidine bases, it is found that p**r**(pyrimidine−purine)$_n$ strands form more stable duplexes than corresponding p**r**(purine−pyrimidine)$_n$ strands and, in the case of alternating block sequences, p**r**[(pyrimidine)$_n$−(purine)$_n$] strands give rise to more stable duplexes than corresponding p**r**[(purine)$_n$−(pyrimidine)$_n$] strands [8][29]). Strong support for the postulate that these regularities reflect corresponding regularities in interstrand base stacking come from observations in the homo-DNA series. There, the backbone inclination has the opposite orientation [8][26], and the regularities just mentioned are in fact inverted. This is to be expected if the relationship delineated above between backbone inclination, interstrand base stacking, and sequence dependence of duplex stabilities are assumed to hold [8] (*Figs. 12* and *13*). Our observation that opposite orientation of backbone inclination in p-RNA and homo-DNA correlate with opposite directionality

[29]) The regularities are more pronounced for sequences in which sequence blocks rather than single bases are alternating. In sequences of the latter type, the stability differences tend to disappear when the alternating bases are G and C. In comparing p-RNA with homo-DNA, the stability differences are more pronounced in the former (corroborating the notion that the scalar value of the backbone inclination in p-RNA is greater than that in homo-DNA).

Table 6. T_m *and Thermodynamic Data for Selected Sequences in the p-RNA* (excerpted from *Table 4*), *DNA, RNA, and 2′,5′-RNA Oligonucleotides*

Entry	Duplex	Oligonucleotide pairing system [a])	T_m [°C]	Thermodynamic data of duplex formation [c])		
			0.15M NaCl, *Tris.* [b]) ($c \approx 10$ μM)	$\Delta G°_{298}$ [kcal/mol]	$T\Delta S°_{298}$ [kcal/mol]	$\Delta H°$ [kcal/mol]
1	$A_8 + T_8$	p-RNA	40	−10.5	−51.7	−62.2
		RNA	11.0	−6.0	−30.4	−36.4
			23 [d])[e])	−7.3 [d])[e])	−26.4 [d])[e])	−33.7 [d])[e])
		DNA	17.0 [d])			
2	$A_{12} + T_{12}$	p-RNA	60.8 [e])	−15.4 [e])	−53.6 [e])	−69.0 [e])
		RNA	34.9 [e])	−10.1 [e])	−66.3 [e])	−76.4 [e])
			53.5 (7 μM) [d])[e])			
		2′,5′-RNA	21.1 (7 μM) [d])[e])	−7.0 [d])[e])	−50.1 [d])[e])	−57.1 [d])[e])
		DNA	41.6 [d])[e])			
3	$A_4T_3ATAT_2AT_2A + TA_2TA_2TATA_3T_4$	p-RNA	48 (0.9 + 0.9 μM)			
		RNA	58.8 [d])[e])	−20.0 [d])[e])	−111.9 [d])[e])	−131.9 [d])[e])
		DNA	47.7 [d])[e])	−16.8 [d])[e])	−112.4 [d])[e])	−129.2 [d])[e])
4	$AT_2AT_2ATAT_3A_4 + T_4A_3TATA_2TA_2T$	p-RNA	65			
			60 (0.9 + 0.9 μM)			
		RNA	57.0 [d])[e])	−21.8 [d])[e])	−124.1 [d])[e])	−145.9 [d])[e])
		DNA	43.3	−13.5 [d])[e])	−85.5 [d])[e])	−99.0 [d])[e])
			28.5 (1.1 + 1.1 μM)			
5	$AT_2CAGCG + CGCTGA_2T$	p-RNA	61.4 [e])	−13.9 [e])	−43.6 [e])	−57.5 [e])
		RNA	46.4 [e])	−11.3 [e])	−41.5 [e])	−52.8 [e])
			52.0 [d])[e])			
		2′,5′-RNA	16.3 [d])[e])	−6.4 [d])[e])	−30.1 [d])[e])	−36.5 [d])[e])
		DNA	36.3 [d])[e])	−9.2 [e])	−45.9 [e])	−55.1 [e])
6	$C_6 + G_6$	p-RNA	61 (3.5 + 3.5 μM)	−13.5	−40.8	−54.3
		DNA	62 (25 + 25 μM)	−7.1	−54.2	−61.3
7	$T_2A_4TA + TAT_4A_2$	p-RNA	38.8 [e])	−9.8 [e])	−39.8 [e])	−49.6 [e])
		RNA	12.1 [e])	−5.2 [e])	−48.3 [e])	−53.5 [e])
		DNA	7.2 [d])			
Self-Pairing Sequences						
8	A_4U_4	p-RNA	21 [d])[e])	−6.2 [d])[e])	−38.1 [d])[e])	−44.3 [d])[e])
			30 (100 μM) [d])			
		RNA [f])	≈5 [d])[e])[g])	−3.3 [d])[e])	−47.7 [d])[e])	−51.0 [d])[e])
			12 (100 μM) [d])			
9	A_4T_4	p-RNA	27	−7.3	−40.8	−48.1
		RNA	17.4 (13 μM) [d])	−5.6 [d])	−36.3 [d])	−41.9 [d])
		DNA	20.7 [d])[e])	−4.3 [e])	−59.6 [e])	−63.9 [e])
10	$(AT)_4$	p-RNA	38	−9.2	−49.5	−58.7
		DNA	7	−3.8	−44.2	−48.0
			10.4 [d])[e])	−6.1 [e])	−27.2 [e])	−33.3 [e])
11	ATGCAT	p-RNA	29.0	−7.3	−28.7	−36.0
		RNA	28.5 [d])	−7.3 [d])	−49.0 [d])	−56.3 [d])
		DNA	16.0 [d])[e])			
12	CGA_2T_2CG	p-RNA	60	−12.6	−42.3	−54.9
		DNA	30	−8.2	−46.2	−54.4
13	$(CG)_3$	p-RNA	65	−12.5	−35.4	−47.9
		DNA	52 (50 μM)	−10.8	−50.3	−61.5
14	$(GC)_3$	p-RNA	62	−11.3	−29.2	−40.5
		DNA	53 (39 μM)	−10.2	−43.5	−53.7
15	TACGTA	p-RNA	39.0	−8.7	−32.2	−40.9
		RNA	25.2 [d])	−6.7 [d])	−38.3 [d])	−45.0 [d])
		DNA	16.1 [d])[e])			
16	T_4A_4	p-RNA	40	−9.8	−50.1	−59.9
		RNA	14.6 [d])	−5.2 [d])	−40.9 [d])	−46.1 [d])

[a]) Oligonucleotide systems refer to the β-D-pyranosyl-RNA, DNA, RNA, and 2′,5′-linked RNA. [b]) T_m Measurements were made in aq. *Tris* buffer: 10 mM aq. *Tris*·HCl, pH 7.0 in the presence of 0.15M NaCl. The total oligonucleotide concentration is *ca.* 10 μM, unless stated otherwise. Estimated error of T_m determination ±0.5°. –: not observed. [c]) Thermodynamic data of duplexes from plots of T_m^{-1} vs. ln *c* [69]; experimental error estimated in ΔH values ±5%. [d]) Measured in the presence of 1.0M NaCl. [e]) Measured in phosphate buffer: 10 mM aq. NaH_2PO_4, pH, 7.0. [f]) Data taken from [70]. [g]) Extrapolated from thermodynamic data taken from [70].

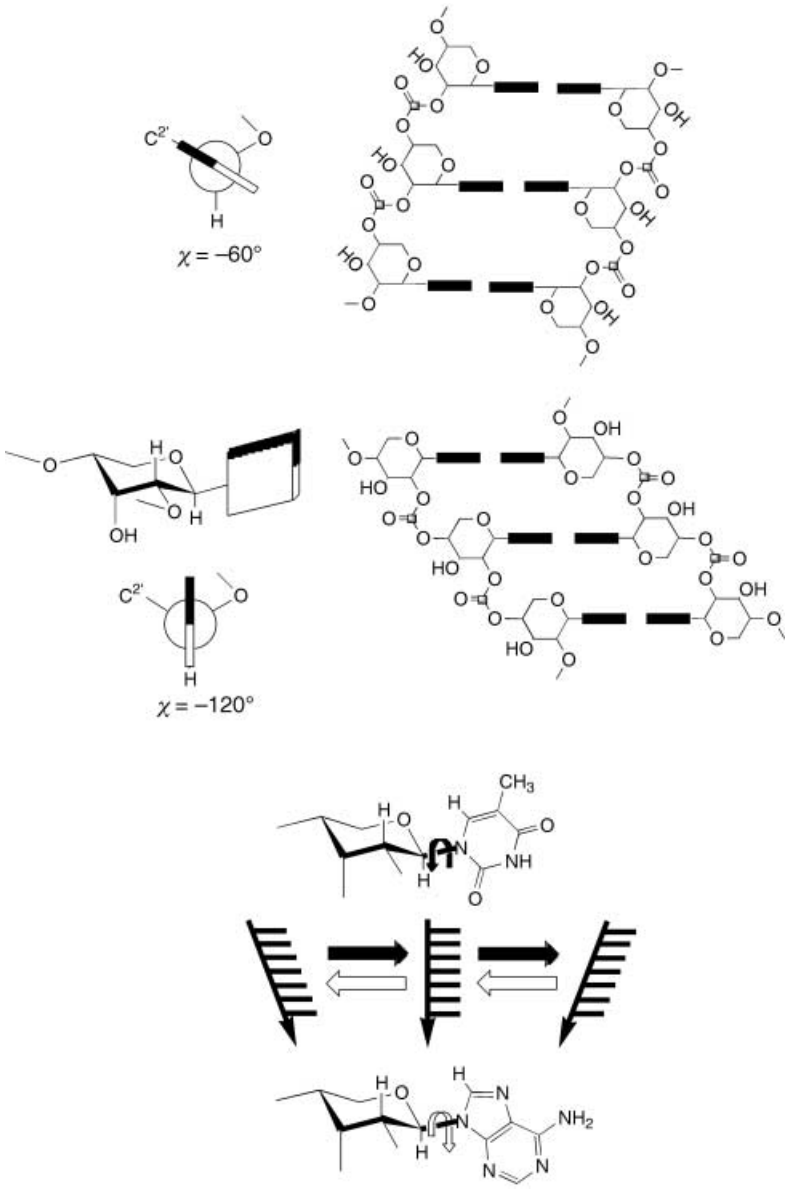

Fig. 9. *Tuning of backbone/basepair inclination* [8][4] *by changing nucleosidic torsion angle*

of duplex properties [8] points to the possibility to predict the orientation as well as the approximate scalar value of an oligonucleotide system's backbone inclination from an experimental screening of the sequence dependence of duplex stability.

We had already shown in the homo-DNA series that base pairing in the *Watson–Crick* mode can be extended from the canonical purine-pyrimidine nucleo-

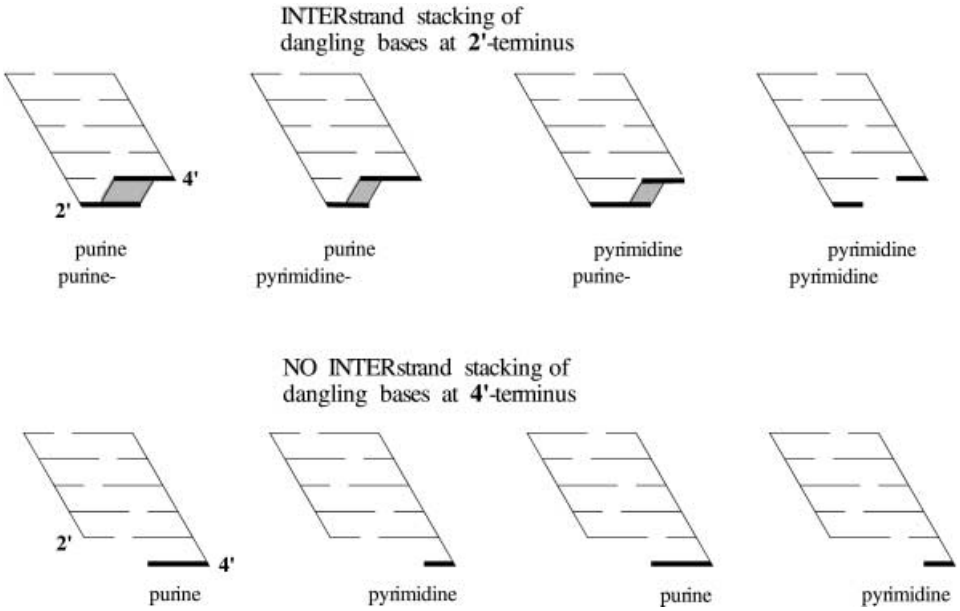

Fig. 10. *Orientation of backbone/base-pair inclination determines directionality of interstrand base stacking and, in turn, whether dangling bases at the upstream or downstream end stabilize duplexes.* In p-RNA, dangling bases at the downstream end (=2′-end) enhance duplex stability [8].

base combinations to purine-purine combinations involving the pairs G-isoG (analogous to the G-C pair) and D-xanthine (analogous to the A-U pair) [25]. The elongated dimension of such purine-purine pairs can be compatible within an all-purine duplex with the lateral flexibility of ladder-type oligonucleotide structures such as homo-DNA or p-RNA, but may not necessarily be so with the laterally constrained helical structures of RNA and DNA[30]). Not only homo-DNA, but also p-RNA, have been found to accommodate such all-purine-purine pairing (see *Fig. 14,a*, *e.g.,* D-p**r**(G_6)·D-p**r**($isoG_6$); *Table 6*). The strength of it in p-RNA is found to be lower than that of corresponding purine-pyrimidine pairing [2], quite in contrast to the homo-DNA series, where it had been observed to be stronger [25].

Watson–Crick pairing in the p-RNA series is highly enantioselective, as, for instance, the drastic difference in melting temperatures of the purine-pyrimidine duplexes D-p**r**(G_6)·D-p**r**(C_6) ($T_m = 61°$) and L-p**r**(G_6)·D-pr(C_6) (T_m (5μM) $\approx 0°$), or of the purine-purine duplexes D-p**r**(G_6)·D-pr($isoG_6$) ($T_m = 34°$) and L-p**r**(G_6)·D-p**r**-($isoG_6$) ($T_m \leq 0°$) demonstrate [2]. Further illustrations of base-pairing enantioselec-

---

[30]) An experimental resolution of the question as to whether the *Watson–Crick* double helix would be capable of accommodating an all-purine-purine pairing geometry would seem to be a highly desirable research project from both a structural as well as etiological point of view. ***Note added in proof:*** Experiments relevant to this question were recently published: H. Liu, J. Gao, S. R. Lynch, Y. D. Saito, L. Maynard, E. T. Kool, *Science* **2003**, *302*, 868.

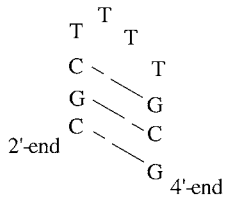

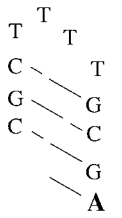

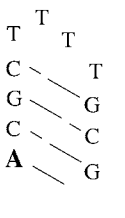

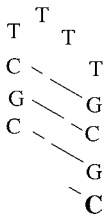

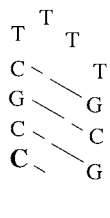

$T_{m\,(3\,\mu M)}$	66 ± 1°	68°	**81°**	68°	**76°**
$\Delta G^{298\,K}$	–4.3	–4.5	**–6.3**	–4.4	**–5.4**
ΔH	–35.9	–35.6	**–39.9**	–34.9	**–36.7**
$T\Delta S^{298\,K}$	–31.6	–31.1	**–33.6**	–30.5	**–31.3**

Fig. 11. *Stabilization of p-RNA hairpins by dangling bases at the 2′-end* (but not at the 4′-end). T_m Measurements in 0.15M NaCl, 0.01M aq. *Tris*, pH 7.0.

tivity were encountered in our studies on template-directed ligations in the p-RNA series and will be discussed below (see *Sect. 3.3*). Complementary p-RNA sequences consisting of canonical nucleobases and of homochiral backbones that have *opposite* sense of chirality show no (or only much weaker) duplex formation. In the context, we have also pursued the question whether base pairing between homochiral p-RNA strands of opposite sense of chirality may exist when other than the canonical base-pair combinations are considered [3] (*Fig. 14*, *b* and *c*). In predicting nucleobase combinations that could possibly give rise to duplex formation by such 'heterochiral' base pairing, one must take into account a constraint that is expected to impose itself on strand orientation, namely, that strong backbone inclination in duplexes is incompatible with parallel strand orientation (see Fig. 16 in [25]). Given that, therefore, p-RNA duplexes derived from strands with opposite sense of chirality must have antiparallel strand orientation, and restricting (for steric reasons) nucleosidic conformations to *anti-anti*, a p-RNA duplex deriving from strands with opposite sense of chirality must be held together by either reverse-*Watson–Crick* or *Hoogsteen* base pairs (see Table 1 in [3]). *Fig. 14*, *b* and *c*, illustrate two such base-pairs; both are deemed to have been observed in the p-RNA series to hold together corresponding (homobasic and homochiral) p-RNA strands of opposite sense of chirality in reasonably stable pairing complexes (T_m values 34° (50 + 50 μM) for L-p**r**(isoG$_8$) · D-p**r**(isoG$_8$) and 49° (5 + 5 μM) for L-p**r**(isoG$_8$) · D-p**r**(C$_8$)). Corresponding homochiral strand pairs with the same sense of chirality do not show complex formation under similar conditions.

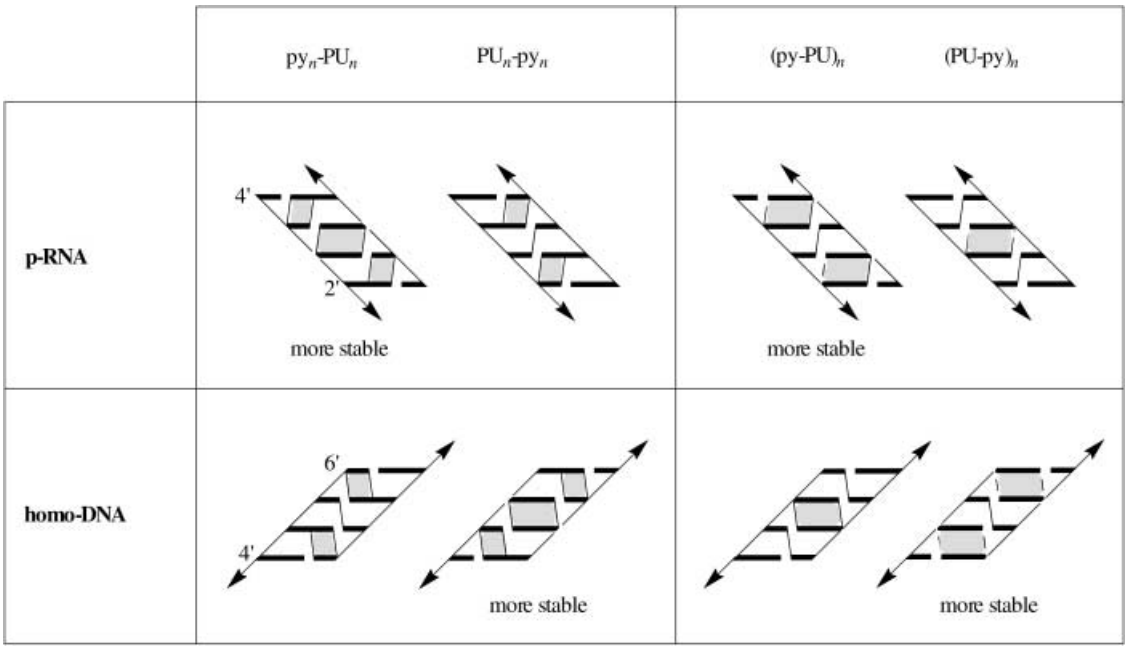

Fig. 12. *In duplexes of p-RNA sequences, pyrimidine → purine alternation is more stabilizing than purine → pyrimidine alternation, the reason being the orientation of p-RNA's backbone/base-pair inclination.* The orientation of homo-DNA's inclination is opposite, so is its duplex stabilization rule. [8]. PU = purine; py = pyrimidine.

Fig. 15 provides a glimpse on how the base pairing of two complementary p-RNA strands (as Et_3NH^+ salts) becomes gradually weakened when the aqueous medium is made to gradually contain increasing amounts of an organic solvent, specifically in this experiment, ethylene glycol. T_m Values drop from 74° (in pure H_2O) to 34° in a medium with ethyleneglycol to H_2O ratio (*v*/*v*) of 8:2; We have not done any systematic studies on the influence of organic solvents on base pairing behavior.

There are, in principle, three constitutionally different β-pyranosyl-isomers of RNA (with equatorial position of the nucleobase) possible, differing in the positioning of the phosphodiester function ($4' \rightarrow 2'$, $4' \rightarrow 3'$, and $3' \rightarrow 2'$). Only one of them, the ($4' \rightarrow 2'$)-isomer, contains six bonds within the constitutionally repeating unit, as RNA does. In the context of studying the regioselectivity of template-directed ligations of the ($4' \rightarrow 2'$)-pyranosyl isomer (see *Sect. 3.3* below), we had synthesized oligonucleotide sequences of the isomeric ($4' \rightarrow 3'$)-p-RNA series [10]. As expected [1], these sequences did not show the capability of base pairing [10][31]).

---

[31]) In remarkable contrast, however, to comparable sequences in the α-L-lyxopyranosyl-($4' \rightarrow 3'$)-oligonucleotide series [10].

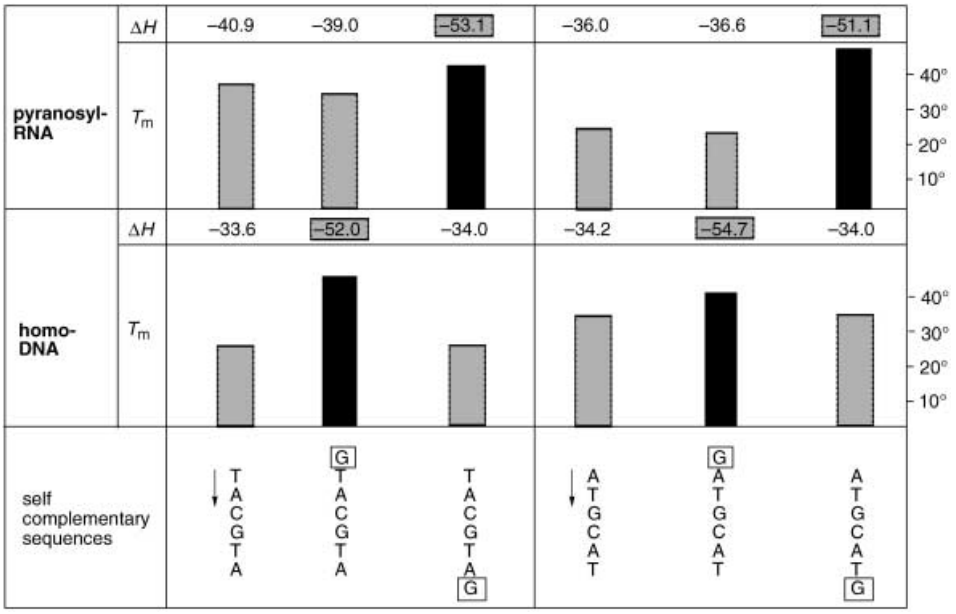

Fig. 13. *Comparison of p-RNA and homo-DNA*. The comparison refers to T_m- and ΔH-values of duplexes derived from the self-complementary sequences TACGTA (pyrimidine → purine alternation) to be compared to ATGCAT (purine → pyrimidine alternation), GTACGTA to be compared to GATGCAT (dangling G at upstream end), and TACGTAG to be compared to ATGCATG (dangling G at downstream end). Note the consistently opposite trends in the two oligonucleotide systems [8]. T_m Measurement in 0.15M NaCl, 0.01M aq. *Tris*, pH 7.0.

3.3. *Replicative Template-Directed Ligation.* One of the defining chemical properties of an informational oligomer system is the capability of its individual molecular members to direct the transcription of a specific sequence of recognition elements into either an exact copy, or an exact complement of it, through sequence-specific catalysis of sequence-forming chemical steps. Pioneering work by *Orgel* and co-workers [75] on non-enzymic template-directed oligomerization of activated mononucleotides in the RNA-oligonucleotide series, and of *Naylor* and *Gilham* [76], and others [77] on template-directed non-enzymic ligation of oligomer sequences in the DNA series have demonstrated that the informational properties of the natural nucleic acids can be mimicked and explored – to a modest extent to be sure – on the chemical level without the assistance of enzymes. Exploring the informational properties must, therefore, be part of the project that studies nucleic acid alternatives in an etiological context. In our work on the chemistry of p-RNA, we have performed extensive studies on replicative template-controlled ligations of activated ribopyranosyl oligonucleotides, their regio- and chiroselectivity, their fidelity and sequence dependence, as well as their role in the self-assembly of p-RNA duplexes by self-templating oligomerizations of hemi-self-complementary activated p-RNA tetramer sequences. Since these investigations have been extensively described in our previous publications [2][6][7], we give here only a short summary of their results; an exception is made with regard to our (unpublished)

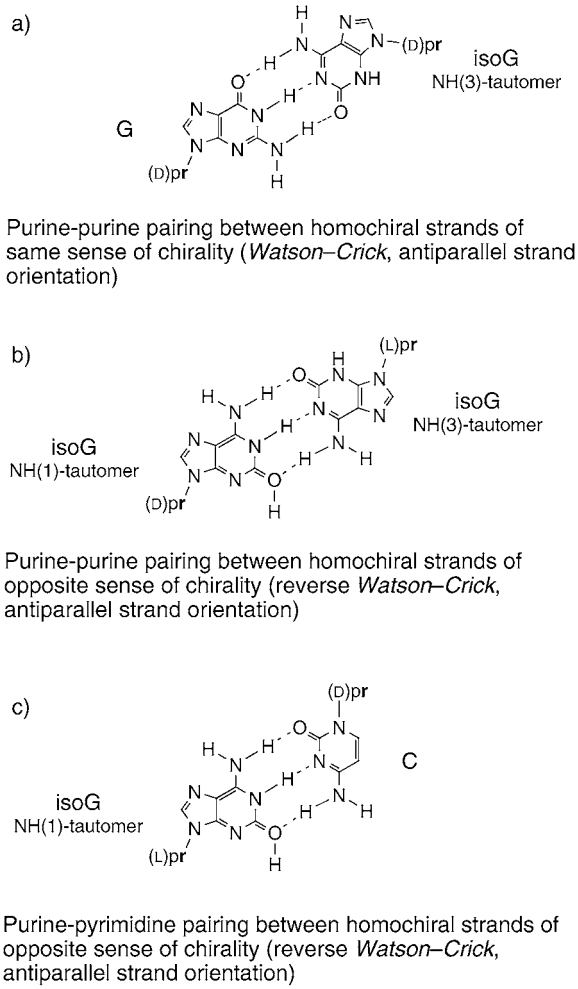

Fig. 14. *Novel purine-purine and purine-pyrimidine base pairings in p-RNA* (for details, see [3])

experiments on the ligative replication of hairpin-forming template sequences; a rather detailed description of them is given in *Sect. 3.3.1.*

Table 7 gives an overview of a selection of documented template-controlled ligation reactions we have carried out in the p-RNA series[32]). With the exception of early exploratory experiments (transcription of p**r**(G_8) into p**r**(C_8)-2′-phosphate and of p**r**(C_8) into p**r**(G_8)-2′-phosphate; *Entries 1* and *2*, *Table 7*), where an *in situ* activation of the ligand's 2′-phosphate end group by DEC · HCl (H_2O-soluble carbodiimide [78], see *Scheme 5*) was used to induce phosphodiester formation on the template, the standard procedure in all other ligation experiments consisted in converting the 2′-phosphate

[32]) *Table 7* does not include the (numerous) experiments carried out on self-templating oligomerizations published in [7].

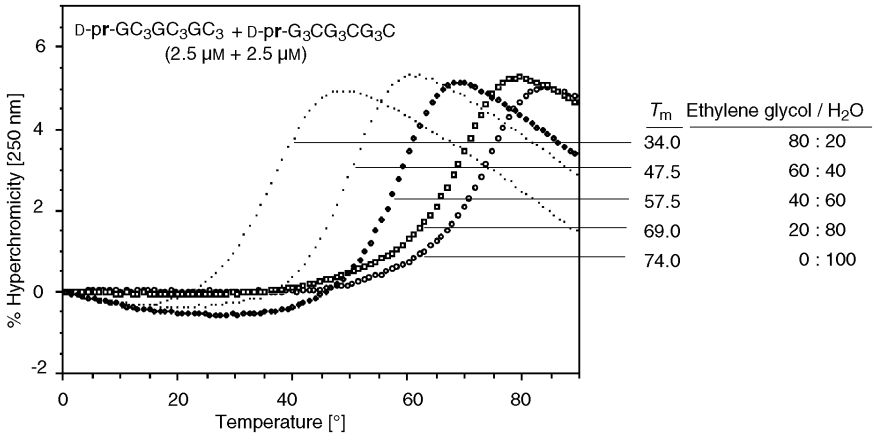

Fig. 15. *Dependence of the thermal stability of a p-RNA-dodecamer duplex from the composition of an ethyleneglycol/H_2O solvent mixture* (the T_m values measured in saltless, bufferless solvent mixtures). For comparison: the T_m value in aqueous 1.5M LiCl is over 90°.

end group of the ligand to be activated to the 2′,3′-cyclophosphate group first, and then to use these reasonably stable and easily isolable ligand-2′,3′-cyclophosphates as the activated partners in the ligation experiments (for preparation, see *Chapt. 2.2*, *Scheme 5*). In this way, the ligations can be run as template-induced trans-esterification reactions ('isomerizations') in environments that are devoid of aggressive activation reagents and their potentially affiliated side reactions. These 2′,3′-cyclophosphate end groups of p-RNA sequences embody a very mild and proper form of phosphate activation that proved remarkably apt to induce smooth and clean phosphodiester formation in the presence, but (rigorously) not in the absence, of templates. There was only one type of side reaction observed to efficiently compete with ligation, namely, hydrolytic deactivation of the 2′,3′-cyclophosphate group by ring opening to produce a mixture of corresponding 2′- and 3′-phosphates. This deactivation reaction is the yield-limiting factor in the template-induced ligation of p-RNA-ligand-2′,3′-cyclophosphates. The rate ratio between ligative phosphodiester formation and hydrolysis was found to markedly depend of – constitutional factors apart – the nature and the concentration of salt(s) present in the reaction medium. A (somewhat) systematic search in a representative ligation series (p**r**(GCCC)-2′,3′-cyclophosphate on the template p**r**(GGGCGGG), (*Entry 3* in *Table 7*) for a medium that would lead to an optimal ligation/deactivation ratio brought us to using aqueous 1.5M LiCl solutions producing a ligation/deactivation ratio of *ca.* 3:1 and ligation yields of 57% under the conditions 100 mM HEPES buffer, pH 8.5; *c*(template) = 150 μM; 3 mol-equiv. of ligand, reaction time 1 week (room temperature; see Table 1 in [6]). Expectedly, the primary products of such template-induced ligations (duplexes between template sequences and complementary ligated ligand sequences) do not dissociate into the partner sequences under ligation conditions. Monitoring the reaction course and product analysis can reliably be done, however, by HPLC of the reaction mixture under denaturing conditions at pH 11.5 (for details, see [6], p. 1941 ff.).

Table 7. *Template Assisted Ligative-Replication with Pyranosyl-RNA (p**r**)-Sequences*

Entry	*Ligation System* $^{4'}$Temp—late$^{2'}$ + $^{4'}$Ligand$^{2'}$ + $^{4'}$Ligand$^{2'}$	*Conditions*[a])	Conc. [μM] template + ligand	Time [weeks]	Yield [%][b])	Ligation product(s) [c])
1	$^{4'}$GGGG—GGGG$^{2'}$ + $_{P}{}^{2'}$CCCC$^{4'}$ + $_{P}{}^{2'}$CCCC$^{4'}$	*A*	150 + 450	36 h	25	$(C)_8{}^{2'}{}_P + (C)_8{}^{2'}{}_{CP}$
					12	$(C)_{12}{}^{2'}{}_P + (C)_{12}{}^{2'}{}_{CP}$
2	$^{4'}$CCCC—CCCC$^{2'}$ + $_{P}{}^{2'}$GGGG$^{4'}$ + $_{P}{}^{2'}$GGGG$^{4'}$	*A*	150 + 450	36 h	20	$(G)_8{}^{2'}{}_P + (G)_8{}^{2'}{}_{CP}$
					3	$(G)_{12}{}^{2'}{}_P + (G)_{12}{}^{2'}{}_{CP}$
3	$^{4'}$GGGC—GGGC$^{2'}$ + $_{CP}{}^{2'}$CCCG$^{4'}$ + $_{CP}{}^{2'}$CCCG$^{4'}$	*B*	150 + 450	4	45	$GC_3GC_3{}^{2'}{}_{CP} + GC_3GC_3{}^{2'}{}_P + GC_3GC_3{}^{3'}{}_P$
		C		10	48	
		D		4	48	
		E		1	57	
		E	150 μM + 4.5 mM	1	68	
4	$^{4'}$GCCC—GCCC$^{2'}$ + $_{CP}{}^{2'}$CGGG$^{4'}$ + $_{CP}{}^{2'}$CGGG$^{4'}$	*B*	150 + 450	4	34	$G_3CG_3C^{2'}{}_{CP} + G_3CG_3C^{2'}{}_P + G_3CG_3C^{3'}{}_P$
5	$^{4'}$CGGG—CGGG$^{2'}$ + $_{CP}{}^{2'}$GCCC$^{4'}$ + $_{CP}{}^{2'}$GCCC$^{4'}$	*B*	150 + 450	4	28	$C_3GC_3G^{2'}{}_{CP} + C_3GC_3G^{2'}{}_P + C_3GC_3G^{3'}{}_P$
6	$^{4'}$CCCG—CCCG$^{2'}$ + $_{CP}{}^{2'}$GGGC$^{4'}$ + $_{CP}{}^{2'}$GGGC$^{4'}$	*B*	150 + 450	4	17	$CG_3CG_3{}^{2'}{}_{CP} + CG_3CG_3{}^{2'}{}_P + CG_3CG_3{}^{3'}{}_P$
7	$^{4'}$CGGG—GGGC$^{2'}$ + $_{CP}{}^{2'}$GCCC$^{4'}$ + $_{CP}{}^{2'}$CCCG$^{4'}$	*B*	150 + 225 + 225	4	40	$GC_6G^{2'}{}_{CP} + GC_6G^{2'}{}_P + GC_6G^{3'}{}_P$
8	$^{4'}$GCCC—CCCG$^{2'}$ + $_{CP}{}^{2'}$CGGG$^{4'}$ + $_{CP}{}^{2'}$GGGC$^{4'}$	*B*	150 + 225 + 225	4	22	$CG_6C^{2'}{}_{CP} + CG_6C^{2'}{}_P + CG_6C^{3'}{}_P$
9	$^{4'}$GGGC—GGGC—GGGC$^{2'}$ + $_{CP}{}^{2'}$CCCG$^{4'}$ + $_{CP}{}^{2'}$CCCG$^{4'}$ + $_{CP}{}^{2'}$CCCG$^{4'}$	*E*	0.15 mM 1.35 mM	2	28	$GC_3GC_3{}^{2'}{}_{CP} + GC_3GC_3{}^{2'}{}_P + GC_3GC_3{}^{3'}{}_P$
					56	$GC_3GC_3GC_3{}^{2'}{}_{CP} + GC_3GC_3GC_3{}^{2'}{}_P + GC_3GC_3GC_3{}^{3'}{}_P$
10	$^{4'}$GCCC—GCCC—GCCC$^{2'}$ + $_{CP}{}^{2'}$CGGG$^{4'}$ + $_{CP}{}^{2'}$CGGG$^{4'}$ + $_{CP}{}^{2'}$CGGG$^{4'}$	*E*	0.15 mM 1.35 mM	2	36	$G_3CG_3C^{2'}{}_{CP} + G_3CG_3C^{2'}{}_P + G_3CG_3C^{3'}{}_P$
					32	$G_3CG_3CG_3C^{2'}{}_{CP} + G_3CG_3CG_3C^{2'}{}_P + G_3CG_3CG_3C^{3'}{}_P$
11	$^{4'}$GGGCGGGC—GG—GC$^{2'}$ + $_{CP}{}^{2'}$CCCGCCCG$^{4'}$ + $_{CP}{}^{2'}$CC$^{4'}$	*F*	0.15 mM 0.15 mM + 1.8 mM	24	58	$C_2GC_3GC_3{}^{2'}{}_{CP} + C_2GC_3GC_3{}^{2'}{}_P + C_2GC_3GC_3{}^{3'}{}_P$
12	$^{4'}$GCCCGCCC—GC—CC$^{2'}$ + $_{CP}{}^{2'}$CGGGCGGG$^{4'}$ + $_{CP}{}^{2'}$CG$^{4'}$	*F*	0.15 mM 0.15 mM + 0.9 mM	24	33	$GCG_3CG_3C^{2'}{}_{CP} + GCG_3CG_3C^{2'}{}_P + GCG_3CG_3C^{3'}{}_P$
13	$^{4'}$AAAT—AAAT$^{2'}$ + $_{CP}{}^{2'}$TTTA$^{4'}$ + $_{CP}{}^{2'}$TTTA$^{4'}$	*F*	150 + 450	12	25	$AT_3AT_3{}^{2'}{}_{CP} + AT_3AT_3{}^{2'}{}_P + AT_3AT_3{}^{3'}{}_P$
14	$^{4'}$TTTTAAAT—ATAATAAT$^{2'}$ + $_{P}{}^{2'}$AAAATTTA$^{4'}$ + $_{CP}{}^{2'}$TATTATTA$^{4'}$	*G*	0.15 mM + 0.15 mM + 0.15 mM	4	52 [d])	$AT_2AT_2ATAT_3A_4{}^{2'}{}_P$
Hairpin-Forming Sequences as Templates						
15	$^{4'}$TATAGG—GGTATA$^{2'}$ + $^{2'}$ATATCC$^{4'}$ + $_{CP}{}^{2'}$CCATAT$^{4'}$	*D*	0.15 mM + 0.3 mM + 0.3 mM	3	81	$TATAC_4TATA^{2'}$
16	$^{4'}$TATACC—CCTATA$^{2'}$ + $^{2'}$ATATGG$^{4'}$ + $_{CP}{}^{2'}$GGATAT$^{4'}$	*H*	0.15 mM + 0.3 mM + 0.3 mM	3	80	$TATAG_4TATA^{2'}$
17	$^{4'}$TAGG—GGTA$^{2'}$ + $^{2'}$ATATCC$^{4'}$ + $_{CP}{}^{2'}$CCATAT$^{4'}$	*H*	0.075 mM + 0.3 mM + 0.3 mM	16	71	$TATAC_4TATA^{2'}$
18	$^{4'}$ACC—CGAA$^{2'}$ + $^{2'}$AATGG$^{4'}$ + $_{CP}{}^{2'}$GCATAT$^{4'}$	*D*	0.1 mM + 0.45 mM + 0.3 mM	4	58	$TACCTTCGGGTAA^{2'}$
19	$^{4'}$AGG—GGT$^{2'}$ + $^{2'}$ATATCC$^{4'}$ + $_{CP}{}^{2'}$CCATAT$^{4'}$	*D*	0.075 mM + 0.3 mM + 0.3 mM	5	5	$TATAC_4TATA^{2'}$
20	$^{4'}$CC—CG$^{2'}$ + $^{2'}$AATGG$^{4'}$ + $_{CP}{}^{2'}$GCTTCCAT$^{4'}$	*D*	0.1 mM + 0.45 mM + 0.3 mM	4	0	
21	$^{4'}$GG—GG$^{2'}$ + $^{2'}$TATACC$^{4'}$ + $_{CP}{}^{2'}$CCATAT$^{4'}$	*H*	0.6 mM + 0.3 mM + 0.3 mM	11	0	
22	$^{4'}$TATAAC—CATATA$^{2'}$ + $^{2'}$ATATTG$^{4'}$ + $_{CP}{}^{2'}$GTATAT$^{4'}$	*D*	0.15 mM + 0.3 mM + 0.3 mM	3	75	$TATATGGTTATA^{2'}$
23	$^{4'}$TATATG—GTTATA$^{2'}$ + $^{2'}$ATATTC$^{4'}$ + $_{CP}{}^{2'}$CAATAT$^{4'}$	*D*	0.15 mM + 0.3 mM + 0.3 mM	3	80	$TATAACCATATA^{2'}$

Table 7 (cont.)

Entry	*Ligation System* $^{4'}$Temp—late$^{2'}$ + $^{4'}$Ligand$^{2'}$ + $^{4'}$Ligand$^{2'}$	*Conditions*[a])	Conc. [μM] template + ligand	Time [weeks]	Yield [%][b])	Ligation product(s) [c])
24	$^{4'}$CGCAA—AAGCG$^{2'}$ + $^{2'}$GCGTT$^{4'}$ + $_{CP}{}^{2'}$TTCGC$^{4'}$	*D*	0.6 mM + 0.3 mM + 0.3 mM	3	65	$CGCT_4GCG$
25	$^{4'}$AA—AA$^{2'}{}_{P}$ + $^{2'}$GCGTT$^{4'}$ + $_{CP}{}^{2'}$TTCGC$^{4'}$	*H*	0.038 mM + 0.3 mM + 0.3 mM	3	0	
26	$^{4'}$GDD—DDC$^{2'}$ + $^{2'}$GCGTT$^{4'}$ + $_{CP}{}^{2'}$TTCGC$^{4'}$	*D*	0.1 mM + 0.3 mM + 0.3 mM	8 months	61	$CGCT_4GCG$
27	$^{4'}$GCGTTTT—TTTTCGCT$^{2'}$ + $_{CP}{}^{2'}$AAAA$^{4'}$ + $_{CP}{}^{2'}$AAAA$^{4'}$	*I*	0.15 mM + 0.45 mM	10	20	$(A_8)^{2'}{}_{CP}$ + $(A_8)^{2'}{}_{P}$
Ligative Replication with Monomer Incorporation						
28	$^{4'}$CACACC—C—GGCTCC$^{2'}$ + $^{2'}$GTGTGG$^{4'}$ + G + $_{CP}{}^{2'}$CCGAG$^{4'}$	*I*	0.2 mM + 0.2 + 12 + 0.2 mM	22	28 21	$^{4'}$GAGCC – G$^{2'}$ $^{4'}$GAGCC – GGTGTG$^{2'}$ (side product)
29	$^{4'}$CCCACC—C—GGCTCC$^{2'}$ + $^{2'}$GGGTGG$^{4'}$ + G + $_{CP}{}^{2'}$CCGAG$^{4'}$	*I*	0.2 mM + 0.2 + 12 + 0.2 mM	22	30 17	$^{4'}$GAGCC – G$^{2'}$ $^{4'}$GAGCC – AGTGGG$^{2'}$ (side product)
30	$^{4'}$CCCACT—C—GGCTCC$^{2'}$ + $^{2'}$GGGTGA$^{4'}$ + G + $_{CP}{}^{2'}$CCGAG$^{4'}$	*I*	0.2 mM + 0.2 + 12 + 0.2 mM	22	34 < 2	$^{4'}$GAGCC – G$^{2'}$ $^{4'}$GAGCC – AGTGGG$^{2'}$ (side product)

[a]) *Conditions: A:* 0.1M aq. HEPES, 1.5M NaCl, 0.125M $MgCl_2$, excess EDC·HCl, pH 6.3, 40°. *B:* 0.1M aq. HEPES, 1.0M NaCl, 0.25M $MgCl_2$, pH 8.0, room temperature. *C:* 0.1M aq. HEPES, 1.0M NaCl, 5 mM EDTA, pH 8.0, room temperature. *D:* 0.1M aq. HEPES, 1.0M LiCl, 1 mM EDTA, pH 8.0, room temperature. *E:* 0.1M aq. HEPES, 1.5M LiCl, 1 mM EDTA, pH 8.5, room temperature. *F:* Same as *E* but conducted at 4°. *G:* Same as *D* but conducted at 10°. *H:* Same as D but conducted at 4°. *I:* Same as *E* but conducted at 4°. [b]) Determined by ion-exchange HPLC based on the template concentration. [c]) Identified by MALDI-TOF-MS analysis and in some cases by ion-exchange HPLC co-injection with authentic sample. [d]) Yield determined after conversion to the corresponding 2′,3′-cyclophosphate with DEC·HCl.

The decision to use 2′,3′-cyclophosphates as activated ligands had not been reached by straightforward reasoning at the outset of our ligation studies. As a matter of fact, our first ligation attempts had focussed on the idea of achieving phosphodiester formation starting from the (more easily accessible) ligand-4′-phosphates and ligand-3′,4′-cyclophosphates. Working with p**r**(G_8 or C_8) as templates, and p**r**(C_4 or G_4)-4′-phosphates and the corresponding 3′,4′-cyclophosphates as ligands, in no combination and under no conditions did we observe template-induced ligative phosphodiester formation, although in some of the experiments the formation of the expected ternary complexes could be clearly inferred from observation. However, an experiment with the 2′-phosphate of p**r**(C_4) (instead of its 4′-phosphate) and EDC under otherwise similar conditions[33]) revealed the occurrence of ligation (7% yield), an observation that had the significance of a breakthrough[34]). It induced an extended search for optimal ligation conditions with 2′,3′-cyclophosphates as activated ligands.

The contrasting behavior of 3′,4′- and 2′,3′-cyclophosphates in template-directed ligations (*Fig. 16*) can be (retrospectively) satisfactorily rationalized as a consequence of p-RNA's characteristic backbone inclination, which, in a ternary ligation complex,

---

[33]) 50 μM template, 4 mol-equiv. ligand, 1.0M NaCl, 150 mM $MgCl_2$; 0.1M EDC; 0.2M HEPES, pH 7.5, room temperature 1 week. Identification of ligation product pr(C_8) by HPLC (coinjection) after treatment with alkaline phosphatase.

[34]) Experiment by *S. P.*

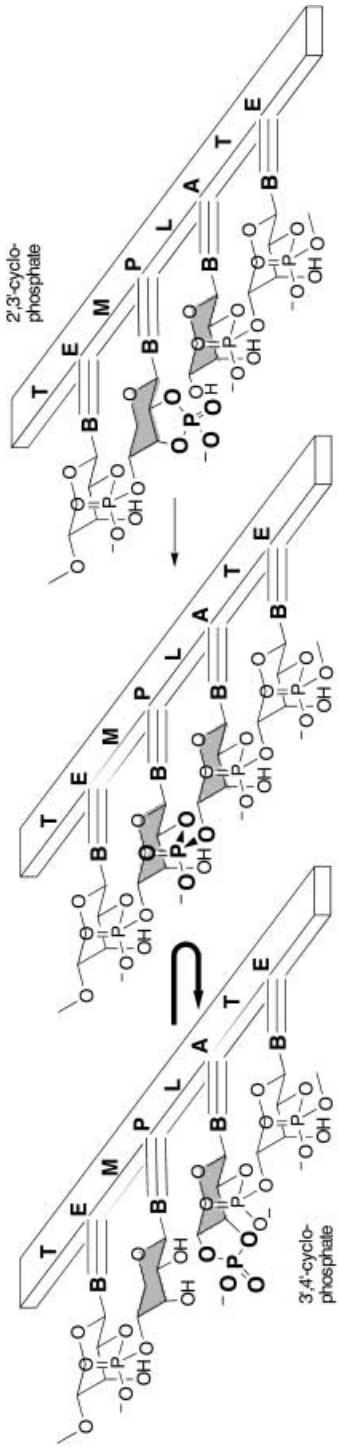

Fig. 16. *2',3'-Cyclophosphate derivatives of p-RNA ligands do undergo template-directed ligation, whereas 3',4'-cyclophosphate derivatives do not*

orients the 4′-OH of the downstream ligand (as the nucleophile of the ligation step) at the backside of the 3′- (but not the 2′)-cyclophosphate P–O-bond, so that an in-line S_N2 reaction at the P-center selectively engages the 3′-O-atom of the cyclophosphate group as leaving group to form regioselectively a (4′ → 2′)- (and not a (4′ → 3′))-phosphodiester group by the transesterification process (see *Fig. 17*)[35]). A corresponding optimal pre-organization of reaction centers for an S_N2-type 3′,4′-cyclophosphate → (4′ → 2′)-phosphodiester transesterification seems not to be accessible to a ternary complex.

An important aspect of the behavior of p-RNA in template-directed reactions is the system's refusal to undergo purine-purine self-pairing in the *Hoogsteen* or reverse-*Hoogsteen* mode (no self-pairing of, *e.g.*, the p**r**(G_8) sequence, when serving as a template). According to *Orgel* and co-workers [79], such self-pairing can be a major handicap of a purine-rich template sequence in the RNA series with regard to their capability to sustain replicative cycles by template-induced oligomerizations, although recent work of *Göbel* and co-workers. [80] has shown how to circumvent the difficulty through an appropriate choice of test and reaction conditions. The crucial test in comparing RNA with p-RNA in this regard, however, has not really been made, because 2′,3′-cyclophosphate groups are much less activated and, therefore, intrinsically less reactive phosphorylation agents than *Orgel*'s imidazolyl-phosphate groups [75]. This is presumably one of the reasons why the ligation reactions we observed in the p-RNA series require – in spite of proceeding very cleanly – relatively very long reaction times, and why, therefore, p-RNA templates in contrast to RNA templates have not been observed to induce oligomerization of mono-nucleotides (in their respective form of activation).

The ligation experiments listed in *Entries 1–14* of *Table 7* explored first the stepwise realization of replicative cycles of p**r** octamers involving non-selfcomplementary and non-hemiselfcomplementary[36]) G,C-containing p**r** tetramers as ligands (*Entries 1–8*, *Table 7*), the replicative ligations of such tetramers to corresponding p**r** dodecamer sequences (*Entries 9–12*, *Table 7*) and, finally, the question concerning the behavior of template and ligand sequences that contain as nucleobases A and T only (*Entries 13* and *14*, *Table 7*). Execution, results, and their interpretation have been fully covered in [2] (*Entries 1–4*) and [3] (*Entries 5–14*).

Template-directed ligations in the p-RNA series proceed *regioselectively* in the sense that the formation of the alternative cyclophosphate ring-opening mode to give a (4′ → 3′)-phosphodiester junction (see *Fig. 16*) is not observed. This has been rigorously checked by detailed characterization and identification of ligation products, including a comparison of them with authentic (synthetic) (4′ → 3′)-isomers for the transcription of p**r**(GGGCGGGC) into p**r**(GCCCGCCC)-2′,3′-cyclophosphate, and of the latter sequence (as the 2′-OH derivative; see *Entries 3* and *4* in *Table 7*) into the 2′,3′-cyclophosphate of the former (see Chapt. 4 in [6]). In this context, we have done the very same transcription experiments in the RNA series by subjecting the corresponding **r**- (instead of p**r**)-tetramer-2′,3′-cyclophosphates in the presence of the corresponding **r** templates to the same reaction conditions. Through proceeding somewhat slower and

---

[35]) We are indebted to Dr. *Romain Wolf* (see [4]) for this picture.

[36]) See *Sect. 3.3.3*.

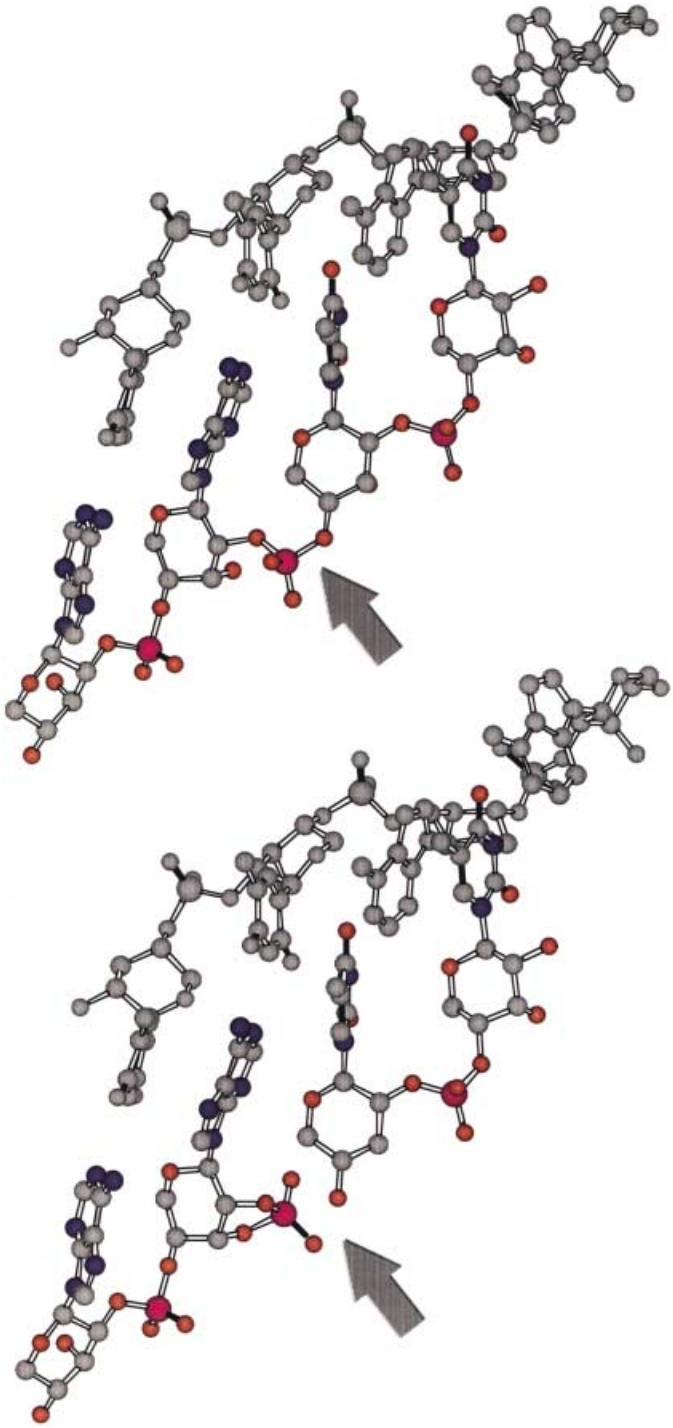

Fig. 17. *Modeling of a ternary pre-ligation complex of the p-RNA series* (courtesy of Dr. *R. Wolf*, formerly *Ciba-Geigy*, now *Novartis AG*, Basel)

in somewhat lower yields than in the p-RNA series, the ligation is equally regioselective, but produces exclusively its (5′ → 2′)-isomer of the natural (5′ → 3′)-phosphodiester junction (see Chapt. 10 in [6][37])). Remarkably, the template-directed ligation of 2′,3′-cyclophosphate ligands in the p-RNA series is regioselective and replicative, while in the RNA series the same reaction is regioselective, but non-replicative[38]) (*Scheme 6*).

Scheme 6. *Comparing the Course of the Template Mediated Ligation of the 2′,3′-Cyclophosphate Derivative of the Same Tetramer Sequence in the p-RNA* (top) *and RNA* (bottom) *Series.* Note that the outcome of the two ligations is different.

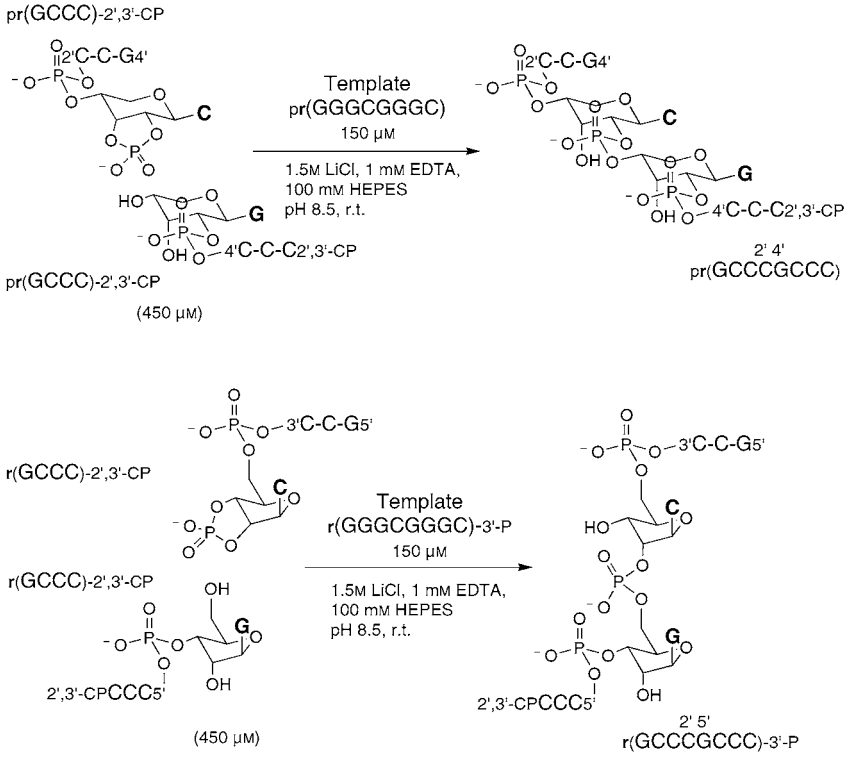

Expectedly, template-controlled ligations of the type documented in *Table 7* proceed mostly with high *chiroselectivity*[39]). This has amply been demonstrated for the template-ligand combination p**r**(GGGCGGGC) + p**r**(GCCC)-2′,3′-cp (*Entry 3* in *Table 7*). Successive replacements of D-ribopyranosyl units in the activated ligand by corresponding enantiomeric units hampers the ligation reaction to an extent that

---

[37]) The preferred formation of (5′ → 2′)-phosphodiester junctions from ring opening of 2′,3′-cyclophosphates in the RNA series has previously been observed by *Orgel* and co-workers [81] and *Usher* and *Hale* [82].

[38]) It would clearly be of interest to know whether template-directed ligations of 2′,3′-cyclophosphates would also occur in the (5′ → 2′)-RNA series (all phosphodiester junctions in template and ligands 5′ → 2′), and, if they do, whether they would be regioselective and replicative.

[39]) For the term 'chiroselectivity', see Footnote 17 in [6].

product formation has not been discernable anymore, except in the case of the replacement of the unit positioned at the activated ligand's 4′-end; in this case the ligation rate dropped to *ca.* 10% of the normal rate (see Fig. 15 in [6]).

The questions referring to the *sequence dependence of relative ligation rates* and to *ligation fidelity* do not necessarily have simple answers from the observations made in the series of octamer/tetramer G,C-model systems (see Fig. 16 in [6]). There are marked differences in relative ligation rates, depending on the G,C-sequence pattern within the tetramer ligand, differences that seem to parallel differences in the stabilities of the corresponding ternary pre-ligation complexes, which, in turn, are conjectured to correspond to the differences in their interstrand-base-stacking patterns (see Chapt. 9 in [6]). For judging the sequence fidelity of template-controlled ligations in the p-RNA series, the G,C-model systems chosen are in retrospect equally not necessarily the best ones. This is because, first, rigorous non-complementarity between stretches of base sequences occurs statistically in a two-base system much more rarely than in a four-base system, and, second, mismatches are more efficiently overpowered by matching G,C pairs than with (weaker) A,T pairs. While observed ligation yields reflected mismatches in corresponding ternary pre-ligation complexes more or less according to expectations (Fig. 16 in [6]), (formally) forbidden ligations were encountered that proceeded quite efficiently *via* a reading-frame shift. *Fig. 18* shows an example and illustrates a rationalization of its occurrence by pointing to the possibility of the stabilization of a frame-shifted ternary pre-ligation complex by favorable interstrand base stacking.

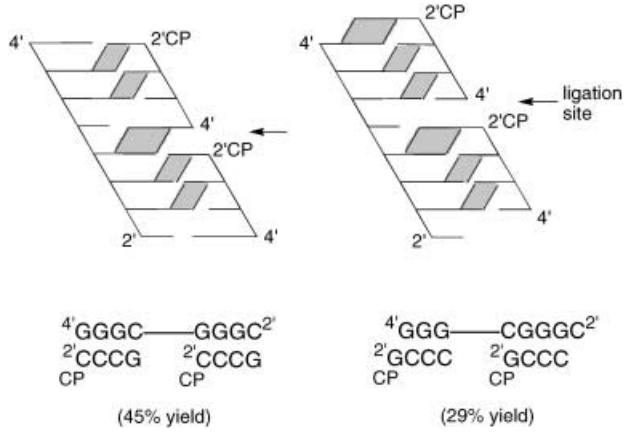

Fig. 18. *Reading-frame shift in template controlled ligation.* The template sequence p**r**(GGGCGGGC) mediates the ligation of the complementary p**r**(GCCC)-2′,3′-cp (cp = cyclophosphate) as well as that of the non-complementary p**r**(CCCG)-2′,3′-cp. In the latter case, the necessary frame shift in the ternary pre-ligation complex is stabilized by superior interstrand base stacking.

Relative ligation rates are expected to be slower if octamer/tetramer model systems of the type discussed above contain A in place of G and T in place of C. Attempts to transcribe the sequence p**r**(AAATAAAT) with the activated ligand p**r**(ATTT)-2′,3′-cp to p**r**(ATTTATTT)-2′cp (p) (*Entry 13*, *Table 7*) illustrates the point. At room temperature, the reaction does hardly proceed at all, yet it does so (not unexpectedly)

at 4°, but much more slowly than the corresponding G/C analog (*Entry 3*, *Table 7*). At lower temperature, the ligation step proper will be slower, but the concentration of a ternary pre-ligation complex can be critically higher, and, since the yield-limiting hydrolytic deactivation of the activated ligand will also be slowed down, the overall ligation may, in spite of requiring a long reaction time, produce clean products. Two experiments that impressively illustrate this point are the elongations of octamer primers on dodecamer templates in the G,C-only series with pr(CC or GC)-dimer-2′,3′-cyclophosphates at 4° with tenfold excess of ligands under otherwise standard conditions (*Entries 11* and *12* in *Table 7*). Such experiments kept on showing very clean HPLC traces in the template-primer-product region with growing product peaks over a very long time, at least as long we choose to observe it (up to half a year; see Figs. 21 and 22 in [6]).

3.3.1. *Replicative Ligations Involving Hairpin-Forming Sequences (A Search for 'Ligases')*[40]). Template-controlled ligations such as those discussed above are 'catalytic' processes that *de facto* stop after one turnover due to efficient product inhibition: product and template strands are glued together by the same type of bonds that are responsible for the formation of the ternary pre-ligation complex, yet by about twice as many of them. Catalysis of the transcription of oligonucleotide sequences would require at least a partial reversibility of duplex formation between template and product strands under ligation conditions[41]). The problems associated with attempts to achieve this by heating-cooling cycles for such (relatively very) short oligonucleotide sequences are numerous; the sharp increase in the efficiency of deactivation by cyclophosphate hydrolysis with rising temperature being one of them. In this context, we undertook a study of the behavior of template sequences that can form hairpins, and explored the possibility to derive from them sequences that might have the potential to show turnover as 'ligases'.

Figs. 19 and *20* depict and document two complementary template-ligation reactions whose dodecamer template sequences can form relatively stable hairpins. Both ligations proceed under (more or less) standard conditions (1.0M LiCl, 1 mM EDTA, 100 mM HEPES buffer, pH 8.0, room temperature, ligands to template ratio 2 : 2 : 1, c(template) = 0.15 mM) exceptionally cleanly and produce the (same) template-ligation product duplex in yields that may be essentially quantitative. Since the ligations are (relatively) fast, only minor amounts of the two (hydrolytically deactivated 2′- and 3′-phosphates of the activated ligand) are observed as by-products. In the absence of template, there is no ligation at all under the same conditions.

Fig. 21 illustrates an experiment in which the C-containing dodecamer template p**r**(TATACCCTATA) was shown to mediate the ligation of its complementary (G-containing) hexamer ligands efficiently in spite of the co-presence of the two corresponding C-contaning hexamer ligands (ratio 1 : 4 : 4 : 4 : 4, c(template) = 0.075 mM). This shows that the ligation is not, or only slightly, inhibited by the duplex formation taking place between complementary hexamer ligands ($T_m = 32°$, $c = 1.1 + 1.1$ μM; *Entry 63*, *Table 5*). In other words, the complementary ligation processes of

---

[40]) The material described in this *Sect.* had not been dealt with in previous communications.

[41]) For a state-of-the-art report on the self-replication of oligonucleotide system, see *e.g.*, *Sievers* and *v. Kiedrowski* [83].

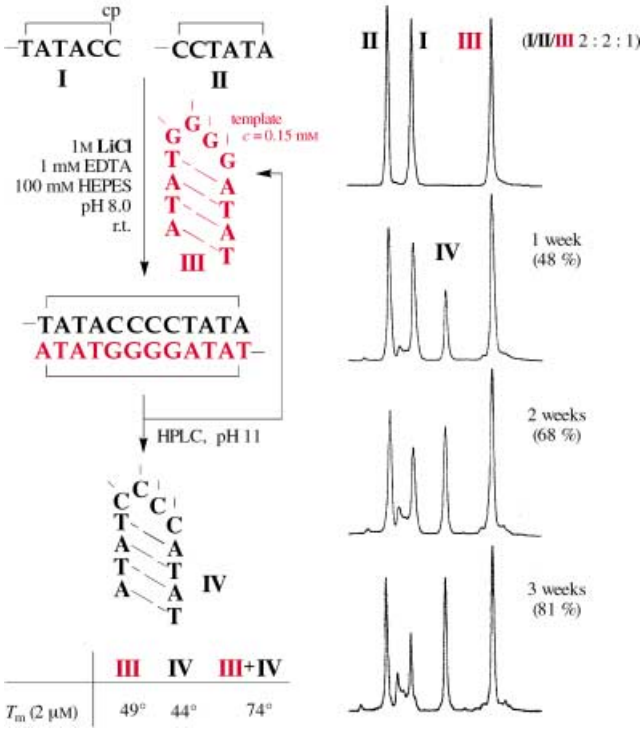

Fig. 19. *Ligation of the ligand* p**r**(*TATAC*$_2$)*-2′,3′-cp and* p**r**(*C*$_2$*TATA*) *mediated by the hairpin sequence* p**r**(*TATAG*$_4$*TATA*) (= **III**, *Entry 125* in *Table 5*) *as template to afford hairpin-forming product sequence* p**r**(*TATAC*$_4$*TATA*) (= **IV**, *Entry 124* in *Table 5*)

Figs. 20 and *21* can proceed in the same medium without appreciably interfering with each other. Exploratory testing of whether ligation yields could be pushed beyond 100% (which would indicate traces of turnover) by increasing the molar template/ligands ratio for the ligation of *Fig. 20* produced yields that could not be forced to go beyond a value of *ca.* 150% (with eightfold excess of ligand pair) making clear that (at least in the mM and μM concentration range) product inhibition cannot be overruled in this series by stabilizing template and product single strands through hairpin formation. The thermodynamic data of the corresponding single-strand $\rightleftharpoons$ hairpin formations ($T_m = 49°$ and 44, $c = 2$ μM; $\Delta G^{25°} = -2.5$ and -2.0 kcal/mol for G- and C-dodecamers, *Entries 125* and *124* in *Table 5*) as compared to the template-product duplexation ($T_m = 74°$, c = 2 μM, $\Delta G^{25°} = -21.5$ kcal/mol, *Entry 59* in *Table 5*) quantitate this finding[42]).

The observations presented in *Figs. 20–23* have been complemented by experiments with a replicative ligation cycle that differs from the first by having the loop sequences of the templates changed from GGGG (4′ → 2′ direction) to TGGT, and from CCCC to ACCA, respectively, with the four ligand sequences changed

[42]) Regrettably, the thermodynamic data for the two ligand-ligand duplexes have not been determined.

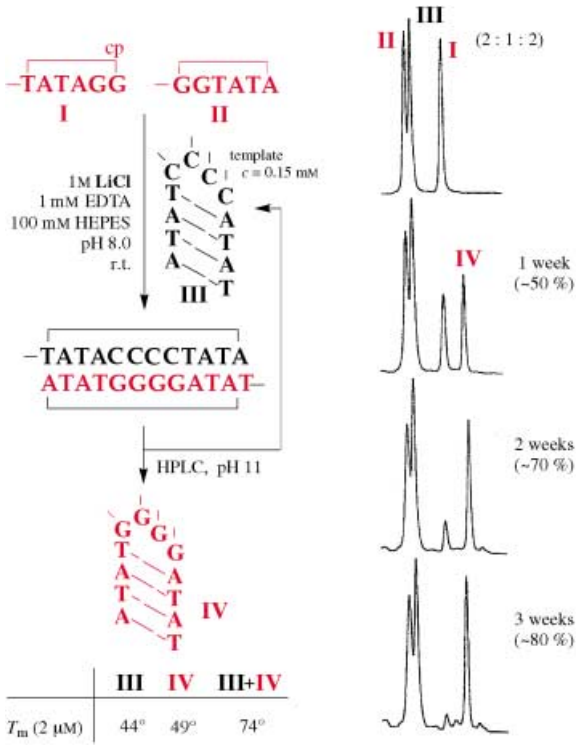

Fig. 20. *Use of the product sequence of ligation of* Fig. 19 *as template for the ligation of the ligands* p**r**(*TATAG*$_2$)-*2′,3′-cp and* p**r**(*G*$_2$*TATA*) *to afford the product sequence* p**r**(*TATAG*$_4$*TATA*), *which is the hairpin-forming template in ligation of* Fig. 19

correspondingly. The diminution of the thermodynamic stability of the template-product duplex in this cycle to $\Delta G^{25^\circ} = -18.4$ kcal/mol (*Entry 58* in *Table 5*) with the ΔG values for the hairpin transitions essentially unchanged ($\Delta G^{25^\circ} = -2.2$ and -2.1 kcal/mol; *Entries 122* and *123* in *Table 5*) was found, not surprisingly, to be insufficient for promoting the ligation (still proceeding in high yield) to one that shows signs of turnover.

Exploratory experiments were also carried out with template sequences that were shortened at their ends, instead of changed in their central region. After shortening the G-containing dodecamer template of *Fig. 19* to the octamer sequence p**r**(TAGGGGTA), ligation still occurred smoothly (61% yield in 3 weeks; template/ligand ratio 1:4:4, room temperature; *Entry 17* in *Table 7*), but not so anymore when shortening went as far as to the hexamer sequence p**r**(AGGGGT) (< 5% yield in 5 weeks at 4°; *Entry 19* in *Table 7*). No ligation was detectable with p**r**(GGGG) as the template[43]).

---

[43]) T_m Values of the duplexes between these shortened template strands and the ligation-product strand are between 46° and 63° (*Entries 60–62* in *Table 4*). This shows that already p**r**(G_4) ($T_m = 46^\circ$, $c = 7\mu M$) is able to break the hairpin structure of p**r**($TATAC_4TATA$) ($T_m = 44^\circ$; note that the ΔG values of duplexation and not the T_m values are relevant).

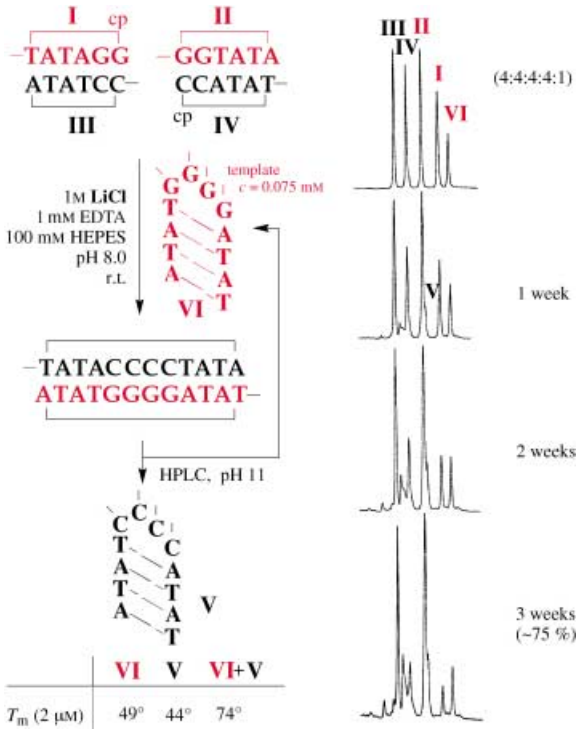

Fig. 21. *The hairpin sequence* p**r**(*TATAG$_4$TATA*) *acts as a template for the ligation of the ligands* p**r**(*TATAC$_2$*)-*2′,3′-cp* (**IV**) *and* p**r**(*C$_2$TATA*) (**III**) *in the presence of the complementary ligands* p**r**(*TATAG$_2$*)-*2′,3′-cp (I) and* p**r**(*G$_2$TATA*) (**II**)

Attempts to observe the formation of the product dodecamer p**r**(TATAG$_4$TATA) by inducing ligation of the ligand pair p**r**(TATACC)-2′,3′-cp and p**r**(CCTATA) with either p**r**(AG$_4$T) or p**r**(TAG$_4$TA) as (shortened) templates in the co-presence of complementary ligand pair p**r**(TATAGG)-2′,3′-cp and p**r**(GGTATA) failed. If, in such a setup, the shortened templates could have acted as ligases to form traces of p**r**(TATAC$_4$TATA), and if the resulting product-(shortened)template duplexes would at least partly dissociate, the free product sequence would (efficiently) initiate the formation of its complement, the observation of which would amount to observing a ligation with turnover, namely the one of p**r**(TATACC)-2′,3′-cp and p**r**(CCTATA) by the shortened template(s). The negative results of this (and the complementary) experiment may be mostly due to the resistance of the duplexes between the complementary ligand pairs to be broken up by the shortened templates.

A reasonable next step in the search of a 'ligase' was to investigate ligand/template combinations in which the relative strengths of the H-bonding within the stem of the product hairpin, and that between hairpin loop and template would be shifted toward dominance of the former. *Fig. 22* shows such an example: while no ligation was observed in the presence of the potential template p**r**(AAAA)-2′-p at 4°, the elongated

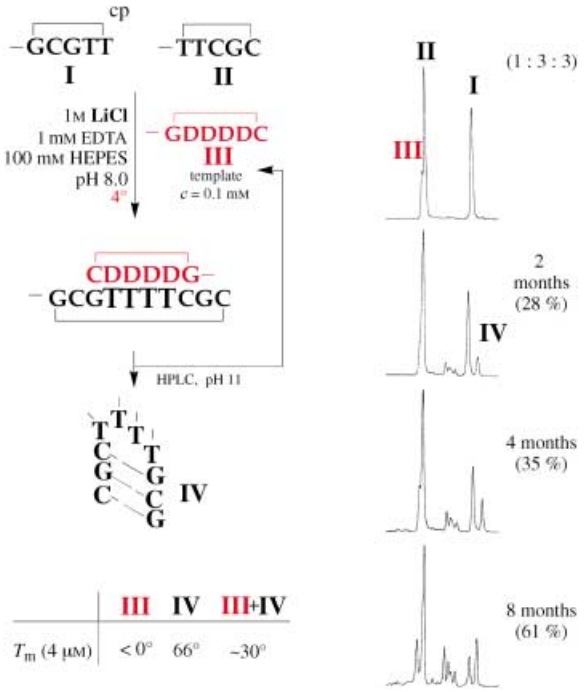

Fig. 22. *The hexamer p***r***(GD*$_4$*C)* (D = 2,6-diaminopurine) *acts as a template for the ligation of the ligands p***r***(GCGT*$_2$*)-2′,3′-cp and p***r***(T*$_2$*CGC) to afford the product sequence p***r***(GCGT*$_4$*CGC) (Entry 116* in *Table 5)*. Note that the reaction is extremely slow, but nevertheless clean.

sequence p**r**(GDDDC) (reinforced by A → D replacement) led to ligation at 4°. While proceeding very cleanly, the reaction did so only very slowly, reaching a plateau yield of 61% in 8 months, being limited by the hydrolytic deactivation of the activated ligand (*Entry 26* in *Table 7*). Ligation rates that involve linking thymidines seem to be slower, as the ligation of *Entry 27* in *Table 7* indicates[44]).

Finally, a glimpse of the behavior of a combination of sequences in which none of the sequence symmetries of the previous examples are present, and where, therefore, neither the template nor the ligand sequences have an opportunity for self-pairing is given in *Fig. 23* (*Entry 20* in *Table 7*). Here again, the 'hoped-for' template sequence p**r**(CCCG)-2′-p was found to be inactive, while the elongated sequence p**r**(ACCC-GAA) induced a clean ligation to the expected dodecamer. It might appear that a systematic exploration of this system by studying the shortened template sequences

---

[44]) This ligation has also been tested for whether or to what extent it would proceed in the non-aqueous solvents formamide, *N*-methylformamide, trifluoroethanol, and ethylene glycol. All tests were negative. In a 1:1 mixture of the standard aqueous ligation medium and ethylene glycol, ligation to a minor extent was observed (see pairing behavior of the complementary sequences p**r**($GC_3GC_3GC_3$) and p**r**($G_3CG_3CG_3C$) in ethylene glycol/H_2O mixtures; *Fig. 15*, *Sect. 3.2*).

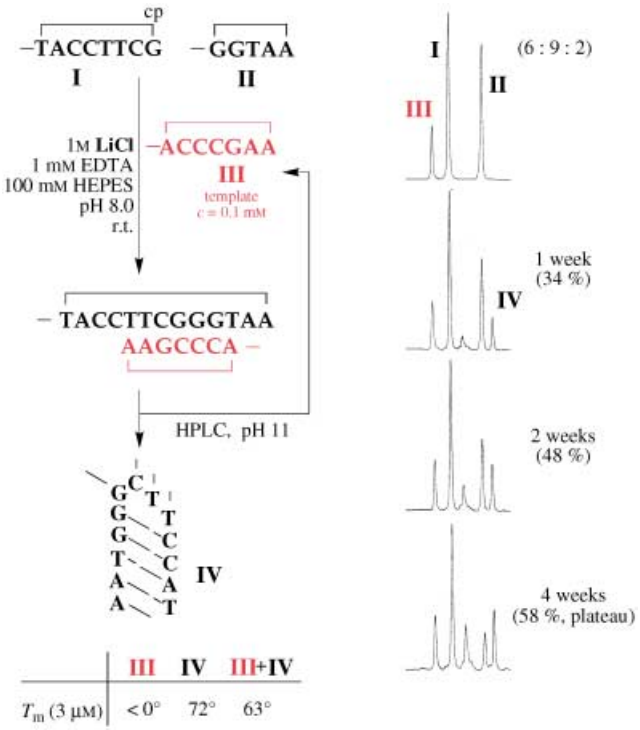

Fig. 23. *Formation of a tridecamer product sequence containing all four canonical bases by ligation of an octamer ligand with a pentamer ligand mediated by a heptamer template*

p**r**(ACCCGA), p**r(**ACCCG), or p**r**(CCCGA) under a broad range of conditions might lead to the observation of a ligase activity. However, these studies had not been carried out.

Some of the experiments listed in *Table 7* that were not explicitly mentioned so far are worthy of comment. In a context not to be further discussed here, we were checking the possibility of inserting a monomeric pyranosyl-guanosine unit into a central single-unit gap of a ternary complex *vis-à-vis* an unpaired C. The constitution of the system around the insertion site was carefully chosen: the G base of the monomer in the quartenary complex should enjoy optimal G/G interstrand stacking, and both base pairs flanking the insertion site should be strong G/C pairs (*Fig. 24*). Conditions were found (*Entry 28* in *Table 7*) under which the desired elongation of the activated upstream ligand sequence by p**r**(G) proved possible (in contrast to earlier unsuccessful attempts to elongate a primer of a binary complex). However, the (very slowly proceeding) elongation was accompanied by a side reaction that revealed itself to be the 'over-the-gap' ligation of the two ligand sequences, exposing an unexpected degree of plasticity in the system with respect to the reactivity of its ligands within the ternary complex. While increasing the strength of the pairing interaction between downstream ligand and templates by exchanging its T/A into a G/C pair did alone not appreciably suppress the side reaction (*Entry 29* in *Table 7*), additional replacement of the (strong)

G/C base pair at the downstream side of the gap by a (weaker) A/T pair had the desired effect (*Entry 30* in *Table 7*): the elongation yield was (modestly) improved and the 'over-the-gap' ligation had essentially disappeared (for T_m values of ternary complexes, see *Entries 35*, *44,* and *48* in *Table 5*).

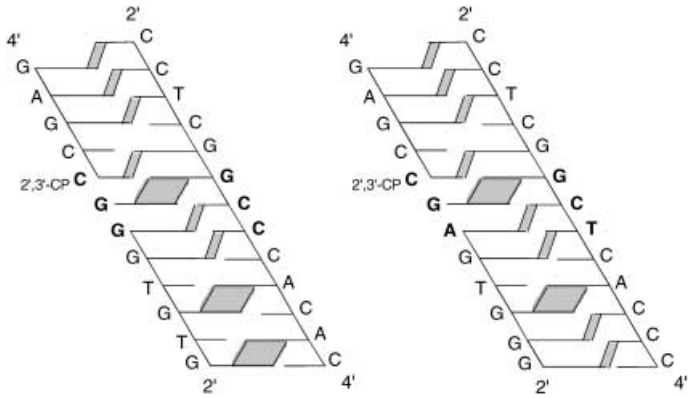

Fig. 24. *Elongation of the upstream ligand-2′,3′-cp by a p***r***(G) unit within a ternary complex containing a tridecamer template and a single-gap position between the upstream heptamer ligand and the downstream hexamer ligand.* In the example on the left an 'over-the-gap' ligation to the undecamer sequence p**r**(GAGCCGGTGTG) is observed as a side reaction. No such side reaction takes place in the example on the right.

Our extended explorations on template-directed ligations in the p-RNA series amply demonstrate a great potential for informational oligonucleotide chemistry in this system, but above all, they also show that the central problem, namely, that of overcoming product inhibition in this system, is bound to be very difficult, at least within the concentration range, which is high enough that reactions can be monitored by such conventional analytical methods we were using (template concentrations that would be lower by many orders of magnitude while ligand concentration remaining high would be promising). The main cause for the failure to see turnover under our conditions is seen in the disparity between the system's duplex stabilities and ligation rates; these rates are much too slow relative to the stability of the duplexes, at these concentrations the latter being a consequence of high base-pairing strength, and the former a consequence of the 'softness' of 2′,3′-cyclophosphates in their role as activated phosphates. There must also be structural shortcomings in the juxtapositioning of the reaction centers for the ligation step proper. Although such shortcomings are not discernible in model considerations, they have to exist, otherwise the relative efficiency of hydrolytic deactivation of the cyclophosphates under ligation conditions would not be understandable. Competition between 'hydrolysis' and (ligative) 'alcoholysis' is probably at the center of the problem, and it is there that the enzymes in the natural systems exert their power most impressively.

3.3.2. *Self-Templating Oligomerization of Hemi-Selfcomplementary Tetramer-2′,3′-cyclophosphates.* A remarkable and appealing potential of template-directed ligation of p-RNA-oligonucleotide strands is the propensity of certain sequences, when activated as the 2′,3′-cyclophosphates, to act not only as a ligand but at the same time also as

template. This amounts to self-templating the oligomerization of an activated ligand monomer to a ligand oligomer within a growing duplex held together by the continuously growing ligand oligomer strands. Prerequisite of such a (exothermic) process would be (antiparallel) hemi-selfcomplementarity of the activated ligand's base sequence. Such processes would constitute examples of autocatalyzed molecular *growth* (as against molecular replication), and, as such, would not be dependent on a system's ability to achieve turnover in template-controlled ligations. We have performed extensive studies on p-RNA's capacity to undergo such self-templated oligomerizations, by using hemi-selfcomplementary 2′,3′-cyclophosphates of tetramer sequences such as p**r**(ATCG), p**r**(DTCG), p**r**(GCCG), p**r**(CGGC) *etc.* as activated ligands (*Scheme 7*). The results of these studies have been extensively described in [7] and are, therefore, only summarized here.

Under the reaction conditions chosen (c(tetramer) = 2.5 mM in 1.5M LiCl, pH 8.5, 0.1M aq. HEPES at 4°), oligomerizations such as the one depicted in *Scheme 7* proceed

Scheme 7. *Self-Templating Oligomerization of Hemi-Selfcomplimentary p***r***-(Tetramer)-2′,3′-cyclophosphates*

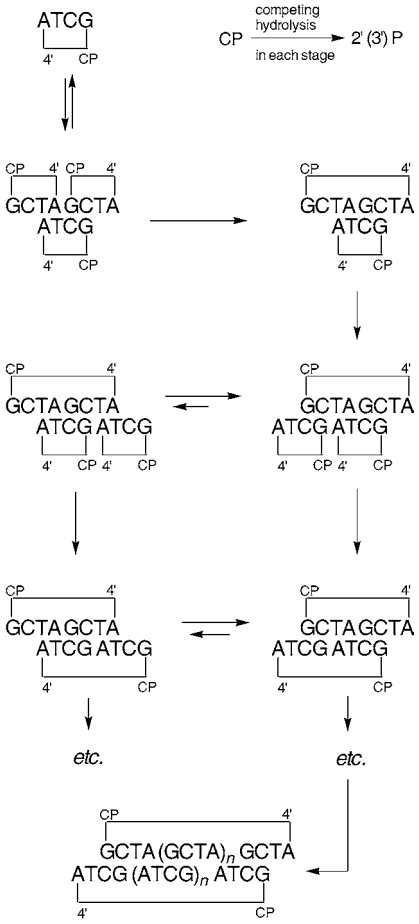

slowly (within weeks) but consistently and cleanly, and produce a steadily growing mixture of oligomers in the form of their 2′,3′-cyclophosphates, 2′-phosphates, and (presumably) 3′-phosphates, the growth-limiting factor being, as expected, the hydrolytic deactivation of 2′,3′-cyclophosphate groups. Reactivation of the system and thereby pushing the ensemble of oligomers to higher members is possible by treatment of the oligomerization mixture by excess DEC·HCl (see *Scheme 5*). Oligomers p**r**$(ATCG)_n$ up to the 36-mer have been tentatively identified by HPLC comparison with the products of analogous self-driven oligomerizations of the octamer and dodecamer 2′,3′-cyclophosphates. As *Fig. 25* demonstrates, the reaction is highly chiroselective in the sense that it does not proceed anymore to any discernible extent when the second ribopyranosyl unit of the activated monomer is an L-(instead of D-) ribosyl unit. Moreover, the oligomerization of the all-D-tetramer is not inhibited by the presence of equal amounts of its DLDD-diastereoisomer.

Fig. 26 illustrates this chiroselectivity for all seven possible heterochiral diastereoisomers of p**r**(ATCG)-2′,3′-cyclophosphate in terms of total yields of higher oligmers observed under identical reaction conditions after 2 weeks reaction time. Only one of the diastereoisomer shows appreciable oligomerization: it is the diastereoisomer in which the reversal of the sense of chirality resides in the ribopyranosyl unit at the 4′-end. In contrast to all others, this diastereoisomer produces oligomers, but about ten times more slowly than the homochiral standard. The phenomenon is not unique to the tetramer sequence p**r**(ATCG), about the same degree in leakage of chiroselectivity has been observed with the tetramer p**r**(GCCG)-2′,3′-cyclophosphate (*Fig. 27*).

Relative rates in self-templating oligomerization of p**r**-tetramer-2′,3′-cyclophosphates depend on base sequence, the trend of decreasing rate being p**r**(PUpypyPU) ≫ p**r**(PUpyPUpy) > p**r**(pyPUPUpy) ≥ p**r**(pyPUpyPU) (see Fig. 4 in [7]). Not unexpectedly, these differences in rate go parallel with the occurrence or non-occurrence of efficient interstrand base stacking between the nucleobases at the ligation sites (nucleobases of both 2′-ends), as well as between the two bases at the two neighboring positions (Fig. 4 in [7]).

In principle, not just one given tetramer base sequence may drive itself to higher oligomers, but different tetramer sequences may collaborate and act cooperatively both as templates and ligands. *Scheme 8* depicts two different variants of how two different, yet mutually semi-complementary, tetramer sequences can cooperatively co-oligomerize. In the first variant, both sequences are hemi-selfcomplementary, as well as mutually hemi-complementary. They will afford, when co-oligomerizing stochastically, a complex library of different (duplexed) oligomer sequences. The second example involves two tetramer sequences that are hemi-complementary not to themselves, but to each other, and this in such a way that their co-oligomerization leads to two single sequence-repeating oligomer strands rather than to a library of different sequences. The first variant involving the two tetramer sequences p**r**(DTGC)- and p**r**(GCCG)-2′,3′-cyclophosphates[45]) has been tested experimentally and observed to form, shortly

---

[45]) The sequence p**r**(DTGC) was chosen in preference to p**r**(ATGC) because the former (expectedly) oligomerizes somewhat faster than the latter, the rate being about the same as that of p**r**(GCCG) (see Table 1 in [7]).

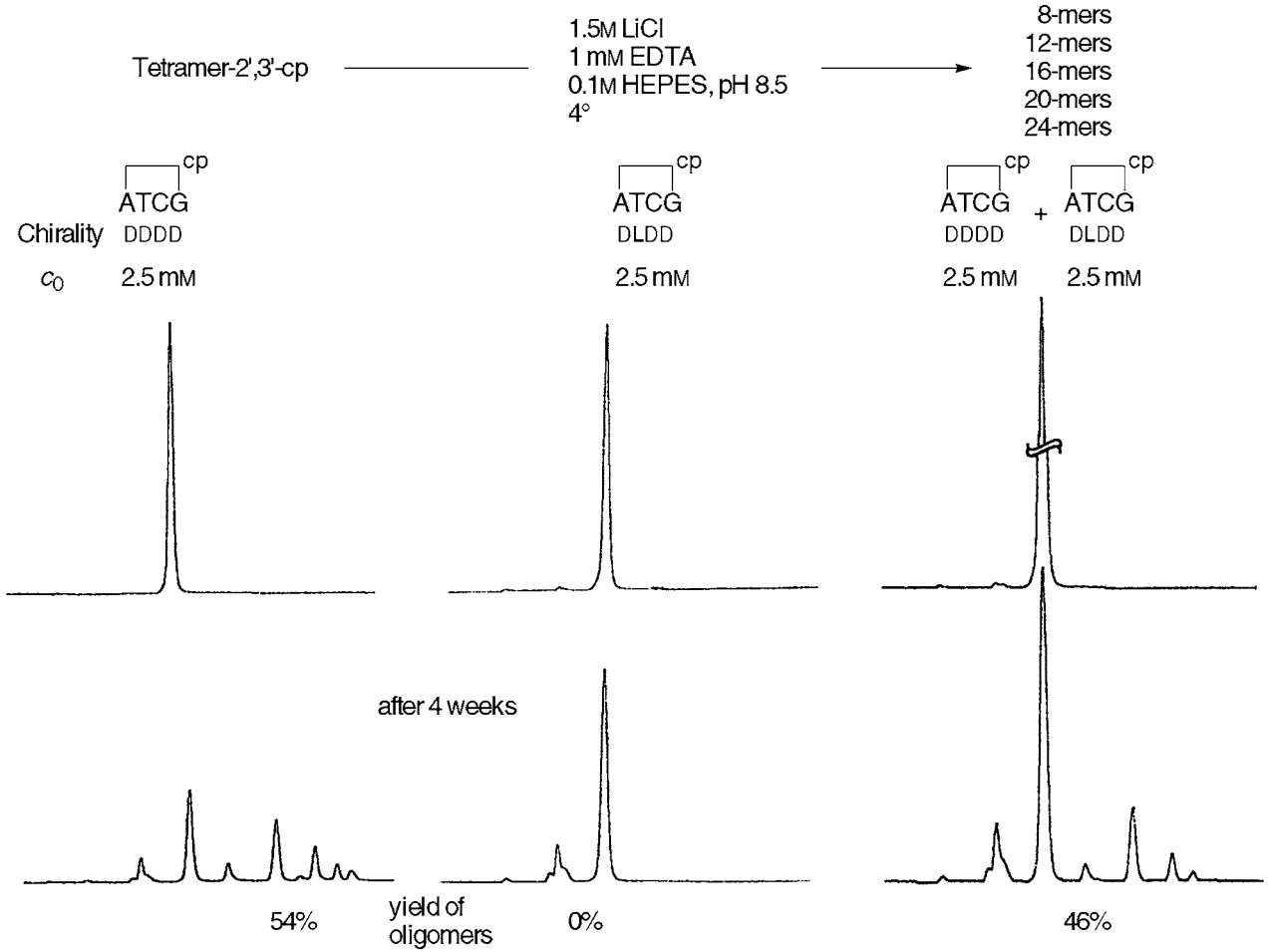

Fig. 25. *Chiroselectivity of ligative oligomerization of* p**r**(ATCG)-2′,3′-cp. No oligomers are formed in the experiment starting from the heterochiral diastereoisomer p**r**(A(L)TCG)-2′,3′-cp. Note that the presence of this diastereoisomer does not (or only weakly) inhibit the oligomerization of the homochiral diastereoisomer.

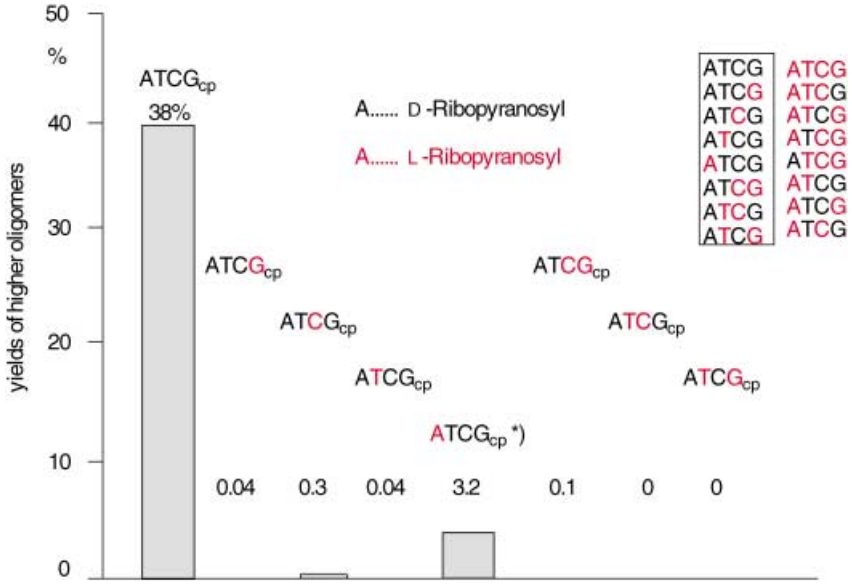

Fig. 26. *Chiroselectivity of ligative oligomerization of p***r***-(tetramer)-2′,3′-cp*. Yields (in%) of higher oligomers after 2 weeks reaction time ($c = 2.5$ mM in 1.5M LiCl, pH 8.5, 4°) for all 8 diastereoisomers of the sequence p**r**(ATCG)-2′,3′-cp. Note the partial loss of chiroselectivity in the case of the diastereoisomer in which the unit at the 4′-end has its chirality inverted. (* denotes that experiment has been carried out in the enantio series).

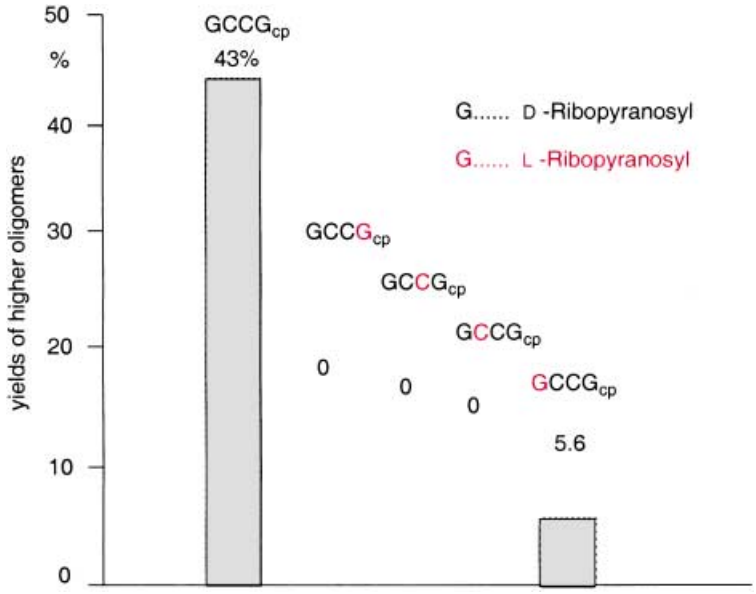

Fig. 27. *Chiroselectivity of ligative oligomerization of p***r***(tetramer)-2′,3′-cp*. Comparison of the homo-chiral p**r**(GCCG)-2′,3′-cp with four of its diastereoisomers. Yields (in %) of higher oligomers after 2 weeks reaction time ($c = 2.5$ mM in 1.5M LiCl, pH 8.5, 4°). Note the similarity in chiroselectivity leakage in this and the p**r**(ATCG) series.

Scheme 8. *Two Different Types of Cooperative Co-oligomerization between Hemi-Selfcomplimentary p***r***-(Tetramer)-2′,3′-cyclophosphates: One* (top) *Leading to a Library of Sequences, and the Other* (bottom) *Leading to a Single Type of Sequence-Repeat Oligomer*

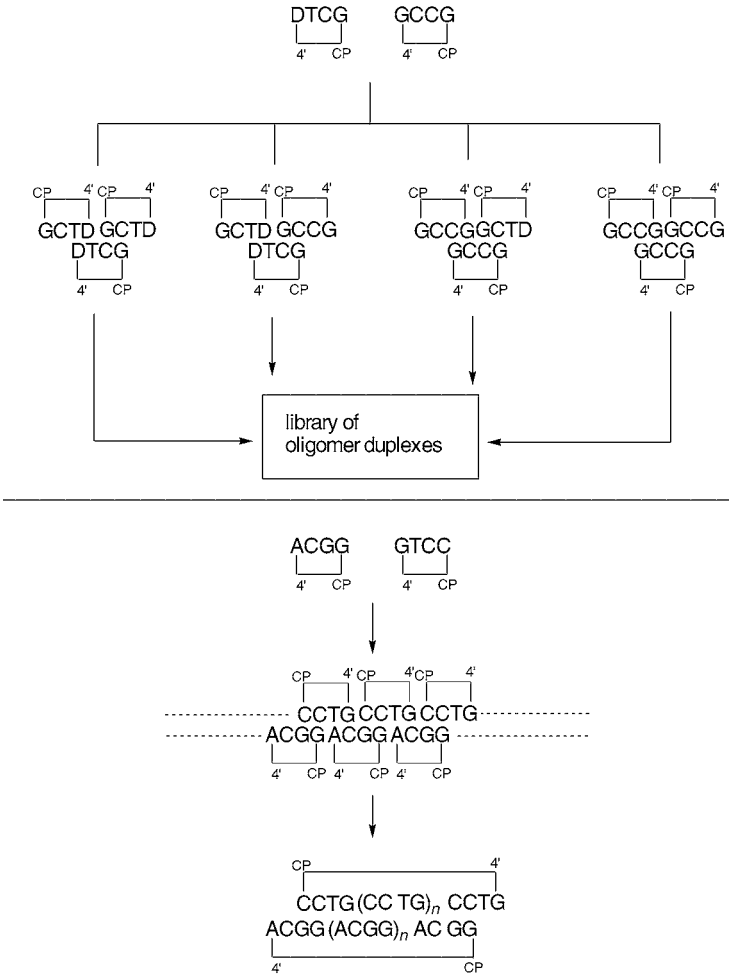

after the start of the reaction, a mixture of dimers that, according to HPLC, contained the four isomers expected of a starting random co-oligomerization (see Fig. 5 in [7]).

Cooperative co-oligomerization of ensembles of judiciously selected activated tetramer sequences to form libraries of base sequences in steadily growing duplexes would appear to be – at least in principle – a powerful way for the constitutional self-assembly of libraries of p-RNA sequences. The statement can be illustrated by (formal) extrapolations ignoring – for the sake of the argument – intrinsic differences in ligation rate of different hemi-complementary tetramer sequences as well as rate retardations due to non-productive complexation between tetramer sequences. The sequence diversity of product libraries formed by co-oligomerization of cooperating tetramer sequences can, in principle, become very large. *Fig. 28* lists, as an examples, 16 sequences

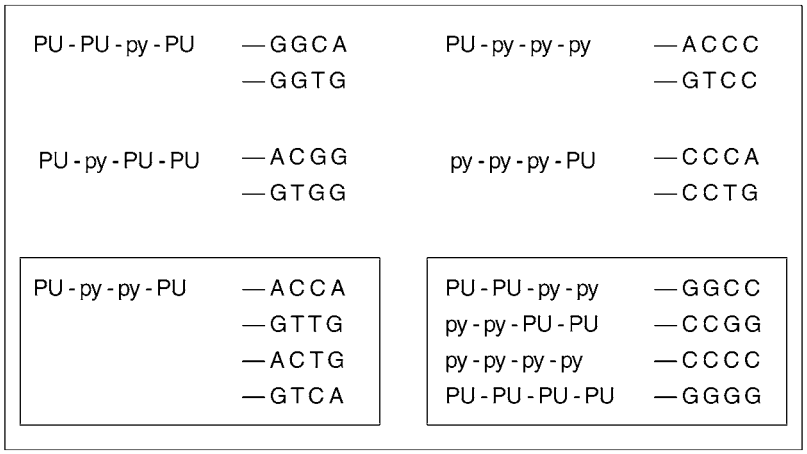

Fig. 28. *Example of a closed co-oligomerization set consisting of 16 tetramer sequences.* Potential ligative co-oligomerization of libraries of tetramer-2′,3′-cyclophosphates. The figure depicts a closed co-oligomerization set of 16 tetramers (for any ligative combination between any of the 16 sequences, there is a corresponding template-tetramer contained in the set). The framed quartets of tetramers also represent closed sets. PU = purine; py = pyrimidine.

that together would represent a closed co-oligomerization set in the sense that, for any ligative combination between any of these 16 sequences, there is the required template tetramer available within the set. The same holds for the two framed quartets of tetramer sequences[46]). If a co-oligomerization, *e.g.*, of the A-, T-, C-, and G-containing quartet of tetramers would proceed at random to form 40-mers, their (formal) sequence diversity would amount to already 10^6 possible sequences[47]). If, in such extrapolations, one took into account the experimentally demonstrated potential of the oligomerizations to proceed chiroselectively (see above), and if one were to consider starting the co-oligomerization from a racemic mixture of all eight diastereoisomers of each one of the four tetramer sequences, one would have to conclude that equal amounts of (mostly) D- and (mostly) L-libraries were formed that would consist of sequences that are largely homochiral. It seems unfortunate that the technical demands for analyzing the outcome of such experiments would go far beyond what realistically seems feasible at present. For a remarkable conclusion to be drawn from this kind of reasoning see the chapter '*Concerning the Problem of Biomolecular Homochirality*' in [7]. For the relative stability of p-RNA sequences against hydrolytic phosphodiester cleavage, see Fig. 9 in [90].

---

46) Out of the set of 16 sequences only two are self-complementary, and only four form (fully) complementary and, therefore, non-oligomerizing pairs (they happen to be the GC sequences of one of the framed sets of four).

47) Extrapolating what had been reasoned with respect to the set of 16 tetramer sequences to the ensemble of all possible tetramer sequences (=64), one would conclude that the (formally) accessible diversity of product sequences among 40-mers would be 1.6×10^{18} and among 100-mers 1.4×10^{45}.

4. Concluding Remarks. – The work on the chemistry of p-RNA establishes the remarkable existence of an informational oligonucleotide system isomeric to natural RNA, composed of the very same chemical building blocks as RNA, and possessing chemical properties that could have made it a candidate in Nature's evolutionary choice of the molecular basis of genetic function. The task of commenting on the originally posed etiological question 'Why did nature choose the furanose and not the pyranose form of RNA' would certainly be much easier, had the pyranosyl isomer of RNA turned out to lack such properties, as it was the case with hexopyranosyl-$(6' \rightarrow 4')$-oligonucleotide systems derived from natural hexose sugars. To observe functional incompetence in potential RNA alternatives on the chemical level is presumably the only kind of outcome in a research project of the type we are pursuing that can lead to solid conclusions regarding the origin of the natural nucleic acids. In all other cases, especially one such as p-RNA, where competence as an informational system on the chemical level turns out to be comparable, if not 'superior', to that of the natural system, conclusions on a system's etiological role in the origin of RNA are much more difficult.

Such caution notwithstanding, p-RNA, together with the other members of the family of diastereoisomeric pentopyranosyl-$(4' \rightarrow 2')$-oligonucleotide systems, makes us recognize that informational *Watson–Crick* base pairing is by no means a property unique to the natural system. This capability is widespread among potentially natural nucleic acid alternatives from RNA's structural neighborhood. It is at least with respect to this biologically fundamental chemical property that Nature's evolutionary selection of RNA appears as if it had been the choice out of a 'library' of structurally closely related candidate systems. Whether such a choice would have been driven predominantly by functional or by generational criteria persists as a major uncertainty, irrespective of whether RNA originated in a prebiological or biological environment.

A few comments on some of the chemical properties of p-RNA in comparison to those of RNA are appropriate, including cautious attempts to extrapolate properties observed on the chemical level to functional potential on the biological level. A major difference between pyranosyl- and furanosyl-RNA is assumed to reside in backbone flexibility. Although a number of observations on hairpin formation in the p-RNA series did not indicate the existence of any handicap of the system with respect to the ease of formation or the stability of hairpins, there is far too little experimental information available in order to delineate the consequences of the expected pronounced difference in backbone flexibility between the two systems, except that it is presumably co-responsible for the observed difference in base pairing strengths. In addition to the intrinsically higher flexibility of furanose *vs.* pyranose rings, the backbone of p-RNA contains two C,C bonds that are rotationally constrained by being part of the sugar ring, as against only one such bond in the backbone of RNA. Assessing the consequences of such a 'simple' constitutional difference for the potential diversity of molecular shapes of long oligonucleotide sequences and, in turn, for the diversity in their chemical phenotype on a biological level is beyond reach, not to mention the virtual impossibility of having an idea about what such a 'small' constitutional difference might mean for the evolvability of an emerging biological system that would have had to operate with either one or the other of the two nucleic acid isomers. This

reminds us forcibly of the limitations to the quest of exploring a chemical etiology of nucleic acid structure once we encounter alternative systems that are capable of acting as informational systems with efficiencies comparable to that of the natural systems on the chemical level.

Nevertheless, from both a chemical and biological point of view, one would intuitively tend to consider backbone flexibility as a critically important asset to the natural system. The importance of knowing the properties of nucleic acid alternatives such as p-RNA may be seen in that such knowledge offers reference points for our recognition of assets of RNA that (supposedly) make it 'the superior system'. Such points of reference were not available before. This is especially significant with respect to a property that may well be the most important functional parameter of the natural system, namely, RNA's specific base-pairing strength. The base-pairing properties of p-RNA and the other members of the pentopyranosyl-oligonucleotide family make it clear that Nature did not select RNA as a result of pursuing a strategy of maximizing base-pairing strength. High base-pairing strength in an informational oligomer system can be either advantageous or detrimental, depending on purpose. It can be advantageous, *e.g.*, for the self-assembly of oligonucleotide sequences by self-templating the growth of smaller oligomers to higher oligomers, as the experimental example of the self-templating oligomerization of hemi-complementary tetramer-2′,3′-cyclophosphates in the p-RNA series illustrates (see *Sect. 3.3.2*). It is not less obvious, however, that it can seriously hamper a system's capability to undergo autocatalytic self-replication with turnover, as again experiments carried out in the p-RNA series may be considered to illustrate (see *Sect. 3.3.1*). Difficulties in overcoming product inhibition in experiments that aim at demonstrating nonenzymatic replication of oligonucleotide sequences are by no means specific to the p-RNA system; this can be learned, *e.g.*, from the pioneering work of *Sievers* and *von Kiedrowski* [83] on oligonucleotide replication in the natural series, even though these workers were able to define experimental conditions under which certain (modified) oligonucleotide sequences of the natural (DNA) series can and do undergo replication with turnover[48]).

In view of the (presumably) enormous complexity of the interplay between all the various structural and chemical factors that co-determine the potential of a given oligonucleotide system to undergo autocatalytic self-replication, there is far too little factual knowledge on the chemical behavior of p-RNA in comparison to RNA that would allow intuitively appealing statements such as '*Pyranosyl-RNA is too strong a pairing system that it could have become Nature's genetic system*' to be accorded more than the status of 'coffee-break hypotheses'.

Any discussion in depth referring to the question of a possible role of nucleic acid alternative in the origin of RNA would have to go beyond the question of function and consider the generational aspect of the problem. In our very first communication on p-RNA [1], we pointed at the end of the paper to '*three aspects of potential biological relevance*' of which we thought that they encourage a comprehensive investigation of

---

[48]) For recent work on the problem of nonenzymatic replication of oligonucleotides and of peptides, see, *e.g.*, [84] and [85], respectively; for the state-of-the-art in the field of *in vitro* evolution of ribozymes with RNA-polymerase or RNA-ligase activity, see, *e.g.*, [86].

the chemical properties of p-RNA, namely, the system's (presumed) linear ladder structure and its base-pairing strengths that both might relate – in comparison to RNA – to a higher potential for constitutional self-assembly; second, the absence of purine-purine *Hoogsteen* pairing that would facilitate template-directed transcription of purine-rich sequences, and, third, the existence of a hypothetical chemical pathway for the metamorphosis of p-RNA into RNA with retention of sequence information. We stated that '*It will depend from the outcome of such investigations whether the letter 'p' in 'p-RNA' will adopt another connotation*'. In retrospect, after ten years of systematic studies on the chemistry of p-RNA and other potentially natural nucleic acid alternatives, we have learned enough to know that no other connotations such as 'pre' or 'proto' are supposed to be associated with the letter 'p' in 'p-RNA'. Of the conceptual shortcomings on which those '*three aspects of potential biological relevance*' were based, the one concerning the p-RNA → RNA metamorphosis happens to touch upon a point of more general interest and is perhaps most easily rectified: even if there were a realistic mechanistic pathway for such a transformation (we do no longer consider this to be the case), retention of sequence information in such a p-RNA → RNA conversion would be essentially pointless from an evolutionary point of view. The reason is that retention of genetic information (base sequence) would not be accompanied by retention of phenetic information (molecular shape), which would mean that any evolutionary achievement residing in the sequence-determined chemical phenotype of the ancestor system would be lost in the transformation; the successor system would have to evolve *de novo* again [87].

In spite of, for instance, the remarkably successful experimental demonstration of the capability of p-RNA duplexes to self-assemble chiroselectively by self-templating growth consuming hemi-selfcomplementary tetramer-2′,3′-cyclophosphates (see *Sect. 3.3.2*), we value in retrospect such findings more from a chemical than an etiological point of view in the sense that we interpret the results of these experiments not so much as demonstrations of the relative simplicity of the chemical processes and reactands involved, but rather as one of a still staggering generational complexity of these systems relative to what a true constitutional self-assembly under natural conditions of oligonucleotide sequences (including their activated monomers!) were to demand from a geochemical environment[49]). The work makes us appreciate that the question as to what is apparent and what is real generational simplicity in such a context can be approached only by way of further comparisons. What will be needed are as many potentially natural and structurally diverging informational oligomer systems as possible; from their comparison with each other, we may recognize the limits of structural and generational simplicity that are still compatible with the potential of an oligomer to function as an informational system under natural conditions. It may well turn out that, at those limits, the molecules look quite different from oligonucleotides.

---

[49]) This is also our view regarding the remarkably successful experiments on the mineral-assisted assembly of ribofuranosyl-(5′ → 3′ and 5′ → 2′) oligonucleotide sequences from activated mononucleotide-5′-phosphates; see [88] (and also [89]).

The work at the ETH laboratory was supported by the 'Schulleitung' of ETH, by (the former) *Ciba-Geigy AG*, and subsequently by *Novartis AG*, Basel. The work at *TSRI* was supported by the *Skaggs Foundation*. *A. H., R. M.*, and *M. S.* thank the *Österreichische Fonds zur Förderung der Wissentschaftlichen Forschung*, Wien, for *Schrödinger* fellowships.

A. E. would like to express his personal thanks to Prof. Dr. *R. Hütter* (former Vice President for Research, ETH) and Prof. Dr. *R. Lerner* (President of *TSRI*) for their generous support. He also expresses his appreciation to Prof. *D. Arigoni* without whose initiative and administrative help in 1992 the (post retirement) work on p-RNA described in this paper could not have been started. Finally, he would like to thank Prof. *A. Vasella* for the administrative hospitality he continually enjoys in the *Vasella* research group since 1996.

Experimental Part

General. Solvents for extraction: ACS grade. Solvents for reaction: reagent grade. Reagents: unless otherwise noted, from *Acros*, *Fluka,* or *Aldrich*, highest quality available. Chloro(2-cyanoethoxy)(diisopropylamino)phosphine (97%) was purchased from *Chem-Impex Inc.*, Wood Dale, IL, USA. TLC: silica-gel *60* F_{254} aluminum plates, (*Whatman*, type *Al Sil G/UV*, 250 μm layer); visualization by UV absorption and/or *A*) by *dipping* in a soln. anisaldehyde/H_2SO_4/AcOH/EtOH 5:5:1:18 or *B*) $CeSO_4$ (3 mM)/ammonium molybdate (250 mM) in aq. H_2SO_4 (10%); followed by heating. Flash column chromatography (CC) was performed on silica gel *60* (0.40–0.63 mm, 230–440 mesh, *EM Science*) at low pressure (max. 2 bar). In case of acid-sensitive compounds, the silica gel was pre-treated with solvents containing *ca.* 0.5% Et_3N. M.p. (uncorrected): *MEL-TEMP II* (*Laboratory Devices Inc.*, USA). NMR: ^1H: δ values in ppm (TMS as internal standard); *J* [Hz], assignments of ^1H resonances were, in some cases, based on 2D experiments ($^1H,^1H$-COSY); ^{13}C: δ values in ppm (TMS as internal standard); *J* [Hz]; assignments and multiplicities were based on 2D experiments ($^1H,^{13}C$-COSY); ^{31}P: δ values in ppm (85% H_3PO_4 as external standard). FAB-MS (pos., matrix-soln.): *m/z* (intensity in %); performed in the positive-ion mode, with 3-nitrobenzyl alcohol (3-NBA) as matrix, on a *VG ZAB-VSE* double-focusing high-resolution (HR) mass spectrometer equipped with a Cs ion gun or on a *KRATOS AEI MS-5* mass spectrometer. Matrix-assisted laser-desorption-ionization time-of-flight mass spectrometry (MALDI-TOF-MS)[50])) was performed on a *Voyager-Elite* mass spectrometer (*Perseptive Biosystems*) with delayed extraction with THAP or DHB as the matrix with ammonium citrate added to the sample. Oligonucleotides were synthesized on an *Expedite 8909 Nucleic Acid Synthesis System* (*Perseptive Biosystems*) or on a *Pharmacia Gene Synthesizer Plus.* HPLC: Reverse-phase HPLC was performed with a *Pharmacia-LKB-2249* gradient pump, *ABI-Kratos Spectraflow 757* UV/VIS detector, and a *Hewlett-Packard 3396A* analog integrator or *W&W 600* recorder. Reverse-phase columns: *a*) Anal.: *Aquapore RP-300 C-8* (*Brownlee*), 220 × 4.6 mm, 7 μm, flow 1 ml/min; buffer A: 0.1M Et_3N, 0.1M AcOH, H_2O, pH 7.0; buffer B: 0.1M Et_3N, 0.1M AcOH, H_2O/MeCN 1:4; *b*) prep.: *Spherisorb-S10X* RP-*C18*, 10 μ, 300 Å (packed by Dr. *J. Schreiber*, ETH Zürich), 220 × 12 mm, flow 3–5 ml/min; buffer *A:* 0.1M Et_3N, 0.1M AcOH, H_2O, pH 7.0; buffer *B:* 0.1M Et_3N, 0.1M AcOH, H_2O/MeCN 1:4. Ion exchange (IE) HPLC was performed on *A*) *Pharmacia GP-250 Gradient Programmer* equipped with two *Pharmacia P-500* pumps, *ABI-Kratos Spectraflow 757* UV/VIS detector and a *Hewlett-Packard 3396A* analog integrator or *B*) *Pharmacia Äkta Purifier (900)* controlled by *UNICORN* system. Columns*: a*) *Mono Q HR 5/5* (*Pharmacia*) or SAX 1000-8 (*Macherey & Nagel*); buffer *A:* 10 mM Na_2HPO_4 in H_2O, pH 11.5; buffer *B:* 10 mM Na_2HPO_4 in H_2O, 1M NaCl, pH 11.5; *b*) *Nucleogen-DEAE 60–7* (*Macherey & Nagel*), 125 × 4 mm, flow 1 ml/min; buffer *A:* 10 mM Na_2HPO_4, H_2O/MeCN 1:4, pH 11.5; buffer *B:* 10 mM Na_2HPO_4, 1M NaCl, H_2O/MeCN 1:4, pH 11.5. UV Spectra were recorded on a *Cary 1 C* (*Varian*) or on a *Perkin-Elmer Lambda-2* or on a *Kontron UVIKON 860* spectrophotometer. Concentrations of oligonucleotide solns. were calculated from the UV absorbance of the solns. at 260 nm (pH 7) at *ca.* 80° with the following molar extinction coefficients [6]: $\varepsilon(pr(A)) = 15000$, $\varepsilon(pr(D)) = 10000$ (at 279 nm), $\varepsilon(pr(I)) = 11600$ (at 290 nm), $\varepsilon(pr(C)) = 7600$, $\varepsilon(pr(G)) = 11700$, $\varepsilon(pr(T)) = 10000$, $\varepsilon(pr(U)) = 10000$. Abbreviations: BSA = bis(trimethylsilyl)acetamide, CPG = 'controlled pore glass', DMAP: 4-(dimethylamino)pyridine, DMT = 4,4′-dimethoxytrityl, DEC·HCl = *N*-[3-(dimethylamino)propyl]-*N*′-ethylcarbodiimide hydrochloride, LCAA-CPG: long-chain aminoalkyl-CPG (500 Å);

---

[50]) We acknowledge the help of Dr. *U. Pieles* and Dr. *H. Moser* (former *Ciba*, Basel) in the determination of some of the spectra in their laboratory; for the methodology and accuracy of the method in the field of oligonucleotides, see [63].

TMS-OTf = trimethylsilyl trifluoromethanesulfonate, THAP = 2,4,6-trihydroxyacetophenone, UF H_2O = ultrafiltered H_2O. Nucleosides in the L-ribopyranosyl series were prepared for the nucleobases C, G, isoG, D, and T by the same procedures described for the D-ribopyranosyl series.

1. ***General Procedure for the Preparation of the Nucleosides* 3a–3g, (*Scheme 1*).** A suspension of **1** (α/β mixture) [51] and the nucleobase in MeCN was heated to 60°, and BSA was added. After 1 h (clear soln.), the *Lewis* acid was added at once, and the mixture was kept at 60° until TLC analysis showed complete reaction. The mixture was cooled and poured into a stirred mixture of 500 ml of AcOEt and 500 ml of sat. aq. $NaHCO_3$ in H_2O. The aq. phase was washed twice with AcOEt, the combined org. phases were dried ($MgSO_4$), evaporated, and filtered on silica gel.

*1-(2′,3′,4′-Tri-*O*-benzoyl-β-*D*-ribopyranosyl)uracil* (**2a**). From 28.3 g (50 mmol) of **1**, 5.6 g (50 mmol) of uracil, 20.3 g (100 mmol) of BSA, and 27.6 g (150 mmol) of TMS-OTf in 250 ml of MeCN (1 h). Filtration on 250 g of SiO_2 (AcOEt/hexanes 1:1), followed by crystallization (MeCl/MeOH), gave 25.0 g (90%) of **2a**. Colorless crystals. M.p. 217–219°. TLC (AcOEt/hexanes 3:2): R_f 0.45. ^{1}H-NMR (300 MHz, $CDCl_3$): 8.79 (br. *s*, NH); 8.15 (*m*, 2 H); 8.12–7.82 (*m*, 4 H); 7.69–7.64 (*m*, 1 H); 7.57–7.47 (*m*, 5 H); 7.39–7.27 (*m*, 4 H); 6.48 (*d*, *J* = 9.6, H–C(1′)); 6.31 (br. *t*, *J* = 2.6, H–C(3′)); 5.81 (*d*, *J* = 8.2, H–C(5)); 5.54 (*ddd*, *J* = 2.2, 5.7, 10.9, H–C(4′)); 5.52 (*dd*, *J* = 2.9, 9.7, H–C(2′)); 4.34 (*ddd*, *J* = 0.8, 4.9, 11.0, H_{eq}–C(5′)); 4.23 (*t*, *J* = 11.0, H_{ax}–C(5′)). ^{13}C-NMR (75 MHz, $CDCl_3$): 165.4 (*s*); 165.1 (*s*); 164.8 (*s*); 162.5 (*s*, C(4)); 150.3 (*s*, C(2); 139.0 (*d*, C(6)); 133.8 (*d*); 133.7 (*d*); 133.6 (*d*); 130.0 (*d*); 129.8 (*d*); 129.2 (*d*); 128.9 (*d*); 128.7 (*d*); 128.6 (*d*); 128.5 (*d*); 128.0 (*d*); 103.6 (*d*, C(5)); 78.7 (*d*, C(1′)); 69.2 (*d*); 68.2 (*d*); 66.7 (*d*); 64.3 (*t*, C(5′)). FAB-MS (pos.): 1113 (16, $[2M+H]^+$), 557 (20, $[M+H]^+$), 446 (28), 445 (92), 105 (100), 77 (43).

*1-(2′,3′,4′-Tri-*O*-benzoyl-β-*D*-ribopyranosyl)thymine* (**2b**). From 35.0 g (62 mmol) of **1**, 7.8 g (62 mmol) of thymine, 26.4 g (130 mmol) of BSA, and 41.2 g (185 mmol) of TMS-OTf in 310 ml of MeCN (3 h). Filtration on 250 g SiO_2 (AcOEt/hexanes 1:1) gave 31.3 g (90%) of **2b**. Colorless foam. TLC (AcOEt/hexanes 2:1): R_f 0.65. ^{1}H-NMR (300 MHz, $CDCl_3$): 8.56 (br. *s*, NH); 8.12 (*m*, 2 H); 7.90–7.82 (*m*, 4 H); 7.69–7.63 (*m*, 1 H); 7.56–7.50 (*m*, 5 H); 7.48–7.27 (*m*, 4 H); 6,48 (*d*, *J* = 9.7, H–C(1′)); 6.31 (br. *t*, *J* = 2.4, H–C(3′)); 5.54 (*ddd*, *J* = 2.8, 5.7, 10.6, H–C(4′)); 5,50 (*dd*, *J* = 2.9, 9.6, H–C(2′)); 4,33 (*dd*, *J* = 5.6, 11.2, H_{eq}–C(5′)); 4.25 (*t*, *J* = 10,9, H_{ax}–C(5′)); 1.95 (*s*, Me–C(5)). ^{13}C-NMR (75 MHz, $CDCl_3$): 165.8 (*s*); 165.5 (*s*); 165.2 (*s*); 163.7 (*s*, C(4)); 150,8 (*s*, C(2); 134.9 (*d*, C(6)); 133.8 (*d*); 134.2 (*d*); 134.1 (*d*); 134.0 (*d*); 130.3 (*d*); 130.2 (*d*); 129.6 (*d*); 129.2 (*d*); 129.1 (*d*); 128.9 (*d*); 128.8 (*d*); 128.7 (*d*); 128.5 (*d*); 112.5 (*s*, C(5)); 78.8 (*d*, C(1′)); 69.5 (*d*); 68.5 (*d*); 67.0 (*d*); 64.5 (*t*, C(5′)); 12.7 (*q*, Me). FAB-MS (pos.): 571 (20, $[M+H]^+$), 446 (17), 445 (53), 105 (100), 77 (26).

*N^4-Benzoyl-1-(2′,3′,4′-tri-*O*-benzoyl-β-*D*-ribopyranosyl)cytosine* (**2c**). From 26.0 g (46 mmol) of **1**, 10.0 g (46 mmol) of *N*^{4}-benzoylcytosine, 28 g (115 mmol) of BSA, and 27 ml (138 mmol) of TMS-OTf in 70 ml of MeCN (5 h). Filtration on SiO_2 (AcOEt/hexanes 1:1) gave, 24.5 g (81%) of **2c**. Colorless foam. TLC (AcOEt/hexanes 1:1): R_f 0.40. ^{1}H-NMR (400 MHz, $CDCl_3$): 4.29 (*dd*, *J* = 11, 11, H–C(5′)); 4.37 (*dd*, *J* = 11, 5, H–C(5′)); 5.56 (*dd*, *J* = 2.9, 9.6, H–C(2′)); 5.6 (*ddd*, *J* = 2.8, 5.8, 10.7, H–C(4′)); 6.34 (*dd*, *J* = 2.5, 2.5, H–C(3′)); 6.76 (*d*, *J* = 9.6, H–C(1′)); 7.28–7.67 (*m*, 12 arom. H, H–C(5)); 7.85–7.86 (m, 6 arom. H); 7.95 (*d*, *J* = 7.5, H–C(6)); 8.14–8.17 (*m*, 2 arom. H); 8.36 (br. *s*, NH). ^{13}C-NMR (100 MHz, $CDCl_3$): 64.38 (*t*, C(5′)); 66.85, 69.24, 69.31 (3*d*, C(2′), C(3′), C(4′)); 79.56 (*d*, C(1′)); 97.64 (br. *d*, C(5)); 127.6, 128.23, 128.47, 128.5, 128.77, 129.0, 129.24, 129.83, 129.92, 130.07, 133.24, 133.58, 133.67, 133.71 (*d*,*s*, arom. C); 144.16 (br. *d*, C(6)); 154.6 (br. *s*, C(2)); 162.34 (br. *s*, C(4)); 164.94, 165.08, 165.51 (3*s*, CO). FAB-MS (pos.): 1319.2 (13, $[2M+H]^+$), 661 (31, $[M+2H]^+$), 660 (63, $[M+H]^+$), 446 (19), 445 (52), 216 (25), 105 (100), 77 (33).

*N^6-Benzoyl-9-(2′,3′,4′-tri-*O*-benzoyl-β-*D*-ribopyranosyl)adenine* (**2d**). From 17.0 g (30 mmol) of **1**, 6.0 g (25 mmol) of *N*^{6}-benzoyladenine, 12.6 ml (52 mmol) of BSA, and 10.5 ml (89 mmol) of $SnCl_4$ in 120 ml of MeCN (1 h). Filtration on SiO_2 (AcOEt/hexanes 1:1) gave 15.0 g (88%) of **2d**. Colorless foam. TLC (AcOEt/hexanes 7:3): R_f 0.23. ^{1}H-NMR (300 MHz, $CDCl_3$): 4.33–4.46 (*m*, 2 H–C(5′)); 5.70 (*ddd*, *J* = 10.3, 5.9, 2.7, H–C(4′)); 6.01 (*dd*, *J* = 9.5, 2.9, H–C(2′)); 6.41 (*dd*, *J* = 2.7, 2.7, H–C(3′)); 6.50 (*d*, *J* = 9.5, H–C(1′)); 7.15–8.20 (*m*, 20 arom. H); 8.33 (*s*, H–C(8)); 8.81 (*s*, H–C(2)); 9.06 (br. *s*, NH). ^{13}C-NMR (75 MHz, $CDCl_3$): 64.4 (*t*, C(5′)); 66.8, 69.1, 69.2 (3*d*, C(4′,3′,2′)); 79.1 (*d*, C(1′)); 122.6 (*d*, C(5)): 127.8, 128.0, 128.4, 128.5, 128.8, 128.9, 129.3, 129.8, 129.9, 132.8, 133.6, 133.8 (12*d*, arom. C); 140.7 (*d*, C(8)); 149.7 (*s*, C(4)); 152.0 (*s*, C(6)); 153.2 (*d*, C(2)); 164.4, 164.5, 165.0, 165.3 (4*s*, C=O). FAB-MS (pos., 3-NBA): 684.2 (83, $[M+H]^+$), 445.1 (100), 240.1 (74).

*6-Chloro-*N^2*-isobutyrylpurine*. A mixture of 5 g (29.5 mmol) of 2-amino-6-chloropurine, 13.2 ml (79.6 mmol) of isobutyric anhydride, and 40 ml of dry *N*,*N*-dimethylacetamide (dried over 3-Å molecular sieves) was heated with stirring to 140°. During heating, all the solid material dissolved, and the color changed from pale yellow to brown; heating was continued for 2–4 h and was stopped before the color changed to dark

brown[51]). The soln. was cooled, diluted with CH_2Cl_2, and carefully extracted with sat. aq. $NaHCO_3$ soln to remove isobutyric acid. The org. layer was washed thoroughly with large amounts of H_2O to remove *N,N*-dimethylacetamide[52]). The soln. was concentrated *in vacuo*, and the resulting mushy yellow solid was suspended in 100 ml of 50% aq. EtOH and refluxed for 2 h to give a homogenous soln. and was adsorbed on 20 g of SiO_2. CC (5% MeOH in CH_2Cl_2) gave further material for a total yield of 4.7 g (67%). A small sample was recrytallized from EtOH/MeOH for characterization purposes. Pale yellow needles: M.p. > 320°. TLC (7% MeOH in CH_2Cl_2): R_f 0.36. ^{1}H-NMR (200 MHz, $CDCl_3$): 1.36 (*d*, *J* = 6.9, 2 Me); 2.70 (br. *sept.*, CH of isobutyryl); 8.39 (br. *s*, H–C(9)); 8.59 (*s*, H–C(8)); 13.53 (br. *s*, NH). ^{13}C-NMR (75 MHz, $CDCl_3$): 19.3 (2*q*, Me); 35.6 (*d*, CH of isobutyryl); 128.1 (*s*, C(5)); 145.5 (*s*, C(8)); 150.3, 151.9, 153.2 (3*s*, C(6), C(2), C(4)); 176.5 (*s*, CO). FAB-MS (pos., 3-NOBA): 241.9 (49, $[M+{}^{37}Cl+H]^+$), 239.9 (100, $[M+{}^{35}Cl+H]^+$), 169.9 (25), 135.9 (73), 120.0 (23), 106.9 (38), 95.0 (22), 88.9 (33), 76.9 (37), 68.9 (29), 54.8 (34).

*6-Chloro-*N^2*-isobutyryl-9-(2′,3′,4′-tri-*O*-benzoyl-β-*D*-ribopyranosyl)purine* (**2e**). From 32.8 g (57.8 mmol) of **1**, 12.6 g (52.6 mmol) of 6-chloro-*N*^{2}-isobutyrylpurine, 32.1 ml (131.4 mmol) of BSA, and 28.6 ml (157.7 mmol) of TMS-OTf in 135 ml of MeCN (3 h). Filtration on SiO_2 (AcOEt/hexanes 1:1) gave 25.0 g (70%) of **2e**. Colorless foam. TLC (AcOEt/hexanes 1:1): R_f 0.34. ^{1}H-NMR (500 MHz, $CDCl_3$): 1.28 (*d*, *J* = 6.9, Me); 1.29 (*d*, *J* = 6.9, Me); 3.06 (br. *m*, CH of isobutyryl); 4.34 (*t*, *J* = 10.9, H'_{ax}–C(5)); 4.41 (*ddd*, *J* = 0.8, 5.6, 11.2, H'_{eq}–C(5)); 5.68 (*ddd*, *J* = 2.8, 5.6, 10.6, *H*–C(4′)); 5.93 (*dd*, *J* = 2.9, 9.3, H–C(2′)); 6.38 (br. *t*, *J* = 2.5, H–C(3′)); 6.44 (*d*, *J* = 9.3, H–C(1′); 7.21 (*t*, *J* = 7.9, 2 arom. H); 7.38 (*t*, *J* = 7.8, 2 arom. H); 7.43 (*t*, *J* = 7.5, arom. H); 7.55 (*t*, *J* = 7.5, arom. H); 7.62 (*t*, *J* = 7.7, 2 arom. H); 7.69 (*d*, *J* = 8.4, 2 arom. H); 7.70 (*t*, *J* = 7.4, arom. H); 7.91 (2 H, *d*, *J* = 8.4, arom. H); 8.05 (*s*, NH); 8.22 (*d*, *J* = 8.3, 2 arom. H); 8.28 (*s*, H–C(8)). ^{13}C-NMR (125 MHz, $CDCl_3$): 19.2, 19.3 (2*q*, Me); 35.8 (*d*, CH of isobutyryl); 64.4 (*t*, C(5′)); 66.7 (*d*, C(4′)); 69.1 (*d*, C(2′)); 69.3 (*d*, C(3′)); 79.7 (*d*, C(1′)); 127.9 (*s*, C(5)); 127.9 (*s*, C_{ipso} of Bz); 128.3 (*d*, C_m of Bz); 128.5 (*d*, 2 C_m of Bz); 128.8 (*s*, C_{ipso} of Bz); 129.0 (*d*, C_m of Bz); 129.3 (*s*, C_{ipso} of Bz); 129.8 (*d*, C_o of Bz); 129.9 (*d*, C_o of Bz); 130.0 (*d*, C_o of Bz); 133.6, 133.7, 133.8 (3*d*, C_p of Bz); 142.2 (*d*, C(8)); 151.6, 152.3, 152.7 (3*s*, C(6), C(2), C(4)); 164.4, 165.1, 165.4 (3*s*, C=O of Bz); 175.5 (*s*, C=O). MS: 686.3 (19, $[M+{}^{37}Cl+H]^+$), 684.2 (61, $[M+{}^{35}Cl+H]^+$), 445.1 (61), 240.1 (17), 201.1 (19), 136.0 (31), 105.0 (100), 76.9 (28), 68.9 (17), 54.9 (20).

*2,6-Dichloro-9-(2′,3′,4′-tri-*O*-benzoyl-β-*D*-ribopyranosyl)purine* (**2f**). To a soln. of 25.5 g (0.045 mol) of **1** and 7.8 g (0.041 mol) of 2,6-dichloropurine in 150 ml of MeCN was added 18.0 ml (0.074 mol) BSA, and the mixture was stirred at 60° for 0.5 h. To the clear soln. was added 14.5 ml (0.08 mol) TMS-OTf, and the soln. was heated for 3 h at 70°. The mixture was cooled to 25°, neutralized with 10 g (0.12 mol) of $NaHCO_3$, diluted with 200 ml of AcOEt and washed with 300 ml of sat. aq. $NaHCO_3$ soln. The aq. phase was extracted with 2 × 200 ml of AcOEt. The combined org. phases were washed with sat. aq. NaCl soln., dried (Na_2SO_4), and concentrated *in vacuo*. The residue was purified by CC (SiO_2; 20–50% AcOEt in hexane) to afford 23.6 g (90.3%) of **2f**. TLC (50% AcOEt in hexanes): R_f 0.41. ^{1}H-NMR (400 MHz, $CDCl_3$): 4.36 (*dd*, *J* = 11.0, 11.0, H_α–C(5′)); 4.45 (*ddd*, *J* = 12.0, 5.6, 0.9, H_β–C(5′)); 5.69 (*m*, H–C(4′)); 5.88 (*dd*, *J* = 9.5, 2.9, H–C(2′)); 6.39 (*dd*, *J* = 2.7, 2.7, H–C(3′)); 6.43 (*d*, *J* = 9.5, H–C(1′)); 7.25–8.19 (*m*, 15, arom. H); 8.44 (*s*, H–C(8)); *ca.* 5% of furanose derivative is seen in the spectrum. ^{13}C-NMR (100 MHz, $CDCl_3$): 64.5 (*t*, C(5′)); 66.6, 69.0, 69.4 (3*d*, C(2′), C(3′), C(4′)); 79.6 (*d*, C(1′)); 127.7 (*s*); 128.4, 128.5, 128.5, 128.7, 128.8; 128.9 (*d*); 129.2, 129.6, 129.7; 129.8, 129.9, 129.9, 130.1, 130.2 (5*d*, arom. C); 130.7 (*s*, C(5)); 133.6, 133.7, 133.9 (3*d*, arom. C); 143.5 (*d*, C(8)); 152.2, 153.0, 153.6 (3*s*, C(2), C(4), C(6)); 164.4, 165.0, 165.4 (3*s*, C=O). FAB-MS (pos., 3-NBA): 1267.3 (1, $[2M+H^+]$), 633.1 (4, $[M+H^+]$), 445.2 (67), 201.1 (25), 105.0 (100)

---

[51]) Sufficient heating was necessary to completely diacylate the purine (*N*^{9}- followed by *N*^{2}-position). TLC is not able to distinguish among these products. Diagnostic data for *6-chloro-*N^9*-isobutyrylpurine:* TLC (7% MeOH in CH_2Cl_2): R_f 0.73. ^{1}H-NMR (200 MHz, $CDCl_3$): 1.33 (*d*, *J* = 6.8, 2 Me); 4.14 (*sept.*, *J* = 6.8, CH of isobutyryl); 5.30 (br. *s*, NH_2); 8.48 (*s*, H–C(8)). ^{13}C-NMR (75 MHz, $CDCl_3$): 18.2 (2*q*, Me); 34.2 (*d*, CH of isobutyryl); 126.0 (*s*, C(5)); 140.1 (*s*, C(8)); 150.3, 151.9, 152.0 (2*s*, C(6), C(4)); 159.4 (*s*, C(2)); 174.7 (*s*, CO). Diagnostic data for *6-chloro-*N^2,N^9*-isobutyrylpurine:* TLC (7% MeOH in CH_2Cl_2): R_f 0.65. ^{1}H-NMR (200 MHz, $CDCl_3$): 1.36 (*d*, *J* = 7.0, 2 Me of *N*^{9}-isobutyryl); 1.36 (*d*, *J* = 7.0, 2 Me of *N*^{7}-isobutyryl); 2.92 (*sept.*, *J* = 6.8, CH of *N*^{2}-isobutyryl); 4.29 (*sept.*, *J* = 6.8, CH of *N*^{9}-isobutyryl); 8.16 (br. *s*, N^{2}H); 8.70 (*s*, H–C(8)). ^{13}C-NMR (75 MHz, $CDCl_3$): 18.7, 19.4 (4*q*, Me); 35.0, 36.3 (2*d*, CH of isobutyryl); 129.6 (*s*, C(5)); 143.2 (*s*, C(8)); 151.4, 152.5, 153.3 (3*s*, C(6), C(2), C(4)); 175.2, 175.8 (2*s*, CO).

[52]) Complete removal of *N,N*-dimethylacetamide is necessary; otherwise complete hydrolysis (instead of partial hydrolysis) to give the starting material occurs.

*2,6-Diamino-9-(2′,3′,4′-tri-*O*-benzoyl-β-*D*-ribopyranosyl)purine* (**2g**). To a soln. of 10.0 g (15.8 mmol) of **2f** in 200 ml of 2-methoxyethanol was added 10.1 g (158 mmol) of NaN_3, and the mixture was stirred at 40° for 5 h. The mixture was poured into 250 ml of AcOEt and washed with 50 ml of sat. aq. $NaHCO_3$. The org. layer was washed with 4×200 ml of H_2O. The combined aq. layers were extracted with 2×100 ml of AcOEt. The combined org. layers were dried (Na_2SO_4) and concentrated *in vacuo*. The residue was taken to the next step without any further purification. A small portion of this residue was purified by recrystallization from benzene/AcOEt for characterization purposes.

*Data for 2,6-Diazo-9-(2′,3′,4′-tri-*O*-benzoyl-β-*D*-ribopyranosyl)purine:* TLC (SiO_2; AcOEt/hexanes 2:1): R_f 0.31. IR ($CHCl_3$): 2163*s*, 2133*s*. ^{1}H-NMR (400 MHz, $CDCl_3$): 4.32 (*dd*, appears as *t*, $J = 11.0$, $H_{ax}-C(5')$); 4.43 (*dd*, $J = 11.0$, 4.9, $H_{eq}-C(5')$); 5.65 (*ddd*, $J = 10.7$, 4.9, 2.8, H–C(4′)); 5.89 (*dd*, $J = 9.5$, 2.9, H–C(2′)); 6.37 (*dd*, appears as *t*, $J = 2.9$, 2.8, H–C(3′)); 6.38 (*d*, $J = 9.5$, H–C(1′)); 7.2–8.19 (m, 15 arom. H); 8.19 (*s*, H–C(8)). ^{13}C-NMR (100 MHz, $CDCl_3$): 64.40 (*t*, C(5′)); 66.70 (*d*, C(4′)); 69.09, 69.16 (*d*, C(2′), C(3′)); 79.19 (*d*, C(1′)); 121.17 (*s*, C(5)); 127.92–133.85 (*d*, *s*, arom. C); 141.14 (*d*, C(8)); 153.88, 154.20, 156.42 (*s*, C(2), C(4), C(6)); 164.30, 165.02, 165.29 (*s*, C=O). FAB-MS (pos., 3-NBA): 1293 (2.4, $[2M+H]^+$), 647 (21, $[M+H]^+$), 445 (61), 201 (25), 154 (27), 105 (100), 77 (47).

The residue from the above reaction containing *2,6-diazo-9-(2′,3′,4′-tri-*O*-benzoyl-β-*D*-ribopyranosyl)purine* was dissolved in 100 ml of AcOEt and 80 ml of CH_2Cl_2, and added to a suspension of 4.2 g (3.95 mmol) of Pd(C) in 150 ml of AcOEt (pre-equilibrated with H_2). The mixture was stirred for 48 h at r.t. under H_2, the reaction was quenched with 50 g of SiO_2, and the mixture was concentrated *in vacuo*. The adsorped residue was purified by CC (200 g of SiO_2; eluted with AcOEt/hexanes 7:1 (with 1 → 10% MeOH)) to afford 6.9 g (74% over 2 steps) of **2g**. TLC (SiO_2; AcOEt/hexanes 3:2 (with 1% MeOH)): R_f 0.10. ^{1}H-NMR (400 MHz, $CDCl_3$): 4.35 (*dd*, $J = 12.2$, 10.4, $H_{ax}-C(5')$); 4.38 (*dd*, $J = 12.2$, 4.7, $H_{eq}-C(5')$); 5.67 (*ddd*, $J = 10.5$, 4.7, 2.8, H–C(4′)); 6.04 (*dd*, $J = 9.4$, 2.9, H–C(2′)); 4.81, 5.46 (br. *s*, 2, NH_2); 6.21 (*d*, $J = 9.4$, H–C(1′)); 6.42 (*t*, $J = 2.8$, H–C(3′)); 7.2–8.20 (*m*, 16, arom. H, H–C(8)). ^{13}C-NMR (100 MHz, $CDCl_3$): 64.09 (*t*, C(5′)); 66.89 (*d*, C(4′)); 68.76 (*d*, C(2′)); 69.19 (*d*, C(3′)); 78.84 (*d*, C(1′)); 114.33 (*s*, C(5)); 128.32–133.68 (*d*, *s*, arom. C); 135.89 (*d*, C(8)); 152.32, 155.89, 160.13 (*s*, C(2), C(4), C(6)); 164.63, 165.05, 165.33 (*s*, C=O). FAB-MS (pos., 3-NBA): 1189 (4.4, $[2M+H]^+$), 595 (75, $[M+H]^+$), 445 (30); 255 (10), 201 (27), 154 (26), 151 (58), 105 (100).

*1-(β-*D*-Ribopyranosyl)uracil* (**3a**). A soln. of 24.6 g (44.2 mmol) of **2a** in 250 ml of MeOH sat. with NH_3 was kept at r.t. for 10 h and was then evaporated. The residue was dissolved in 350 ml of H_2O and extracted with 4×300 ml of CH_2Cl_2. The aq. phase was evaporated, and the residue was dried *in vacuo* to afford 11.0 g of **3a**, containing 5% benzoic acid. This crude mixture was taken to the next step without further purification. TLC (CH_2Cl_2/MeOH 9:1): R_f 0.10. ^{1}H-NMR (300 MHz, D_2O): 7.70 (*d*, $J = 8.2$, H–C(6)); 5.88 (*d*, $J = 8.2$, H–C(5)); 5.69 (*d*, $J = 9.7$, H–C(1′)); 4.27 (br. *t*, $J = 2.5$, H–C(3′)); 3.95 (*m*, H–C(4′), H–C(2′)); 3.83 (*ddd*, $J = 0.8$, 5.4, 10.7, $H_{eq}-C(5')$); 3.75 (*t*, $J = 10.9$, $H_{ax}-C(5')$). ^{13}C-NMR (75 MHz, D_2O): 168.7 (*s*, C(4)); 154.8 (*s*, C(2)); 144.6 (*d*, C(6)); 105.6 (*d*, C(5)); 83.2 (*d*, C(1′)); 73.5 (*d*); 70.5 (*d*); 68.6 (*d*), 67.6 (*t*, C(5′)). FAB-MS (pos.): 489 (32, $[2M+H]^+$), 245 (100, $[M+H]^+$), 155 (20), 154 (65), 138 (24), 137 (50), 136 (54), 122 (44), 113 (72), 107 (25), 89 (28), 77 (37).

*1-(β-*D*-Ribopyranosyl)thymine* (**3b**). A soln. of 31.0 g (54.3 mmol) of **2b** in 210 ml of sat. methanolic NH_3 was kept at r.t. for 18 h and was then evaporated. The residue was dissolved in 350 ml of H_2O and extracted with 4×300 ml of CH_2Cl_2. The aq. phase was evaporated, and the residue was dissolved in 150 ml of MeOH, treated with 100 ml of Et_2O, and stored 14 h at 4° to afford 11.5 g (82%) of **3b**. Off-white powder. TLC (CH_2Cl_2/MeOH 9:1): R_f 0.10. ^{1}H-NMR (300 MHz, CD_3OD + 2 drops of (D_6)DMSO): 7.50 (*s*, H–C(6)); 5.75 (*d*, $J = 9.3$, H–C(1′)); 4.17 (br. *t*, $J = 2.3$, H–C(3′)); 3.80–3.71 (*m*, H–C(4′), H–C(2′), $H_{eq}-C(5')$, $H_{ax}-C(5')$); 1.89 (*s*, Me–C(5)). ^{13}C-NMR (75 MHz, CD_3OD + 2 drops of (D_6)DMSO): 166.1 (*s*, C(4)); 153.1 (*s*, C(2)); 138.3 (*d*, C(6)); 111.7 (*s*, C(5)); 81.5 (*d*, C(1′)); 73.0 (*d*); 69.8 (*d*); 68.2 (*d*), 66.8 (*t*, C(5′)); 12.6 (*q*, *Me*–C(5)). FAB-MS (pos.): 259 (17, $[M+H]^+$), 155 (55), 154 (100), 139 (37), 138 (69), 137 (91), 136 (92), 120 (23), 107 (39), 91 (26), 90 (22), 89 (31), 77 (33), 55 (25).

N^4*-Benzoyl-1-(β-*D*-ribopyranosyl)cytosine* (**3c**). To an ice-cooled soln. of 24.0 g (36.4 mmol) of **2c** in 150 ml of THF/MeOH/H_2O 6:3:1 were added 80 ml of 1N aq. NaOH soln. in THF/MeOH/H_2O 6:3:1 during 20 min. After stirring for 30 min, the mixture was neutralized with 1% aq. HCl soln., 20 g of SiO_2 was added, and the mixture was evaporated to dryness. CC (SiO_2; CH_2Cl_2/MeOH 7–16%) afforded 8.6 g (68%) of **3c**. White solid. TLC (CH_2Cl_2/MeOH 17:3): R_f 0.30. ^{1}H-NMR (400 MHz, (D_6)DMSO): 3.6–3.78 (*m*, 2 H–C(5′), H–C(4′), H–C(2′)); 4.02 (*d*, $J = 2.7$, H–C(3′)); 4.86 (*d*, $J = 6.4$, OH); 5.08–5.1 (*m*, 2 OH); 5.83 (*d*, $J = 9.5$, H–C(1′)); 7.32 (br. *s*, H–C(5)); 7.5–7.65 (m, 3 arom. H); 8.02 (*dd*, $J = 7.2$, 5.3, 2 arom. H); 8.14 (*d*, $J = 7.2$, H–C(6)); 11.28 (br. *s*, NH). ^{13}C-NMR (100 MHz, (D_6)DMSO): 65.33 (*t*, C(5′)); 66.46, 68.35, 71.28 (3*d*, C(2′), C(3′), C(4′)); 80.56 (*d*, C(1′)); 96.4 (*d*, C(5)); 128.34, 128.38, 32.65 (arom. C); 146.19 (br. *d*, C(6)); 155.01 (br. *s*,

C(2)); 162.84 (br. *s*, C(4)); 167.31 (br. *s*, CO). FAB-MS: 348 (5, $[M+1]^+$), 241 (79), 207 (29), 165 (29), 149 (100), 117 (46).

N^6-*Benzoyl-1-(β-*D*-ribopyranosyl)adenine* (**3d**). To an ice-cooled soln. of 15.0 g (22 mmol) of **2d** in 1000 ml of THF/MeOH/H_2O 5:4:1 was added 100 ml of 2N aq. NaOH soln. in THF/MeOH/H_2O 5:4:1 at once. After stirring for 20 min, the mixture was treated with 20 g (37 mmol) of solid NH_4Cl and evaporated. The residue was dissolved in MeOH, 20 g of SiO_2 was added, and the mixture was evaporated to dryness. CC (SiO_2, CH_2Cl_2/MeOH 1–20%) afforded 7.1 g (87%) of **3d**. White solid. TLC (CH_2Cl_2/MeOH 9:1): R_f 0.16. ^{1}H-NMR (300 MHz, CD_3OD): 3.77–3.98 (*m*, H–C(4′), 2 H–C(5′)); 4.26 (br. *s*, H–C(3′)); 4.37 (*dd*, *J* = 9.4, 2.8, H–C(2′)); 5.92 (*d*, *J* = 9.4, H–C(1′)); 7.55 (*dd*, *J* = 7, 7, 2 arom. H); 7.65 (*t*, *J* = 7.3, arom. H); 8.08 (*d*, *J* = 7.05, arom. H); 8.57, 8.71 (2*s*, 2 H). ^{1}H-NMR (300 MHz, (D_6)DMSO): 3.60–3.83 (*m*, H–C(4′), 2 H–C(5′)); 4.10 (br. *s*, H–C(3′)); 3.32 (br. *d*, *J* = 9.0, H–C(2′)); 4.97, 5.25 (2 br. *s*, 3 OH); 5.81 (*d*, *J* = 9.5, H–C(1′)); 7.50–7.70 (*m*, 3 arom. H); 8.06 (*d*, *J* = 7.1, 2 arom. H); 8.67, 8.76 (2*s*, H–C(2), H–C(8)); 11.19 (br. *s*, NH). ^{13}C-NMR (75 MHz, (D_6)DMSO): 65.1 (*t*, C(5)); 66.5, 68.1, 71.1 (3*d*, C(2′), C(3′), C(4′)); 79.9 (*d*, C(1′)); 125.4 (*s*, C(5)); 128.4, 132.4 (2*d*, arom. C); 133.3 (*s*, arom. C); 143.4 (*d*, C(8)); 150.1 (*d*, C(4)); 151.5 (*d*, C(2)); 152.7 (*s*, C(6)); 165.6 (*s*, C=O). FAB-MS (pos., 3-NBA): 372.1 (58, $[M+H]^+$), 240.1 (48), 136.0 (100), 107.0 (41).

*2-Amino-*N^2*-isobutyryl-6-[(prop-2-enyl)oxy]-9-(β-*D*-ribopyranosyl)purine* (**3e**). To an ice-cold, stirred soln. of 13.3 g (19.4 mmol) of **2e** in 45 ml of dry allyl alcohol was added 110 ml of an ice-cold 20% (*v*/*v*) soln. of anh. Et_3N in dry allyl alcohol (prepared from 22 ml of liquid Et_3N and 88 ml of allyl alcohol). After 5 min, 4.35 ml (29.2 mmol, 1.5 eq) of DBU was added. The soln. was stirred for 1.75 h at 0° and then for 3 h at r.t. After concentration, the resulting oil was triturated with Et_2O, which caused a gummy precipitate to form. The Et_2O was removed, and the precipitate was washed twice with fresh Et_2O. The precipitate was dissolved in MeOH and adsorbed on SiO_2. CC (SiO_2; 5–15% MeOH in CH_2Cl_2) gave 6.2 g (81%) of **3e**. White glassy foam[53]). TLC (CH_2Cl_2/MeOH 9:1): R_f 0.22. ^{1}H-NMR (500 MHz, (D_6)DMSO): 1.10 (*d*, *J* = 6.8, Me); 1.10 (*d*, *J* = 6.8, Me); 2.89 (*sept.*, *J* = 6.8, CH of isobutyryl); 3.60 (*dd*, *J* = 5.2, 10.2, H_{eq}–(C5′)); 3.67 (*t*, *J* = 10.4, H_{ax}–C(5′)); 3.73 (br. *m*, H–C(4′)); 4.05 (br *s*, H–C(3′)); 4.24 (*ddd*, *J* = 2.5, 6.6, 9.1, H–C(2′)); 4.92 (br *d*, *J* = 5.4, OH); 5.07 (*d*, *J* = 5.6, CH_2O (allyl)); 5.12 (*m*, 2 OH); 5.30 (*ddt*, *J* = 1.1, 1.8, 10.4, 1 H, $=CH_2$ (allyl) (*E*)); 5.47 (*dq*, *J* = 1.6, 17.2, 1 H, $=CH_2$ (allyl) (*Z*)); 5.67 (*d*, *J* = 9.4, H–C(1′)); 6.18 (*ddt*, *J* = 5.8, 10.4, 17.2, =CH (allyl)); 8.40 (*s*, H–C(8)); 10.39 (*s*, N^{2}H). ^{13}C-NMR (125 MHz, (D_6)DMSO)): 19.2, 19.3 (2*q*, 2 Me); 34.3 (*d*, CH of isobutyryl); 65.0 (*t*, C(5′)); 66.5 (*d*, C(4′)); 66.9 (*t*, allyl CH_2O); 68.1 (*d*, C(2′)); 71.1 (*d*, C(3′)); 79.6 (*d*, C(1′)); 116.9 (*s*, C(5)); 118.7 (*t*, allyl = CH_2); 132.9 (*d*, allyl = CH); 141.5 (*d*, C(8)); 152.0, 153.5 (2*s*, C(2), C(4)); 159.4 (*s*, C(6)); 174.9 (*s*, C=O). MS: 394.1 (100, $[M+H]^+$), 262.1 (87), 192.1 (38), 136.0 (43), 107.0 (22), 88.9 (20), 76.9 (21), 68.9 (16), 54.8 (16).

*6-Amino-*N^6*-benzoyl-2-[(prop-2-enyl)oxy]-9-(β-*D*-ribopyranosyl)purine* (**3f**). A soln. of 5.0 g (7.9 mmol) of **2f** in 40 ml of sat. methanolic NH_3 soln. (*ca.* 30%) was heated in an autoclave at 100° for 7 h. The mixture was cooled to 25°, concentrated *in vacuo*, and co-evaporated with 2 × 100 ml MeOH. The residue was adsorbed on SiO_2 (with MeOH) and purified by CC (SiO_2; 5–20% MeOH in CH_2Cl_2) to give 1.95 g (82.6%) of *6-amino-2-chloro-9-(β-*D*-ribopyranosyl)purine*. R_f (20% MeOH in CH_2Cl_2) 0.24 . ^{1}H-NMR (400 MHz, CD_3OD): 3.78 (*dd*, *J* = 9.9, 4.8, H_β–C(5′)); 3.82–3.95 (m, H_α–C(5′), H–C(4′)); 4.23 (m, H–C(3′), H–C(2′)); 5.72 (*d*, *J* = 9.0, H–C(1′)); 8.23 (*s*, H–C(8)). ^{13}C-NMR (100 MHz, CD_3OD): 66.7 (*t*, C(5′)); 68.2, 70.3, 72.8 (3*d*, C(2′), C(3′), C(4′)); 82.1 (*d*, C(1′)); 119.1 (*s*, C(5)); 141.8 (*d*, C(8)); 152.5, 155.5, 158.1 (3*s*, C(2), C(4), C(6)). FAB-MS (pos., 3-NBA): 302.0 (100, $[M+H^+]$), 170 (43).

In a 100-ml round-bottomed flask was placed 3.0 g (9.96 mmol) of *6-amino-2-chloro-9-(β-*D*-ribopyranosyl)purine*, 6.5 g (20 mmol) of Cs_2CO_3, 35 ml of allyl alcohol, and 3-Å molecular sieves were added, and the mixture was heated under reflux at 90° with stirring for 6 h. The mixture was concentrated *in vacuo*, and the residue was co-evaporated with two 25 ml portions of pyridine. The brownish residue was suspended in 50 ml of pyridine, cooled to 0° (ice bath), and 11.6 ml (99.6 mmol) of BzCl was added dropwise. The mixture was stirred at 0°, allowed to warm to r.t. overnight and poured into 200 ml of ice-cold sat. aq. $NaHCO_3$ soln. The mixture was extracted with 2 × 200 ml of CH_2Cl_2, the combined org. layers were dried (Na_2SO_4) and concentrated *in vacuo*. The residue was co-evaporated with 2 × 50 ml of toluene, and the dark brown residue was dissolved in 100 ml of THF/MeOH/H_2O 5:4:1 and cooled to 0° (ice bath). To this mixture was added 63 ml (126 mmol) of a 2M aq. NaOH soln. dropwise, and the mixture was stirred vigorously for 30 min. Then, 8.8 g (151 mmol) of solid NH_4Cl was added, and the mixture was stirred for an additional 10 min. The mixture was concentrated *in vacuo*, and the residue was adsorbed on 20 g of silica gel and purified by CC (40 g SiO_2; CH_2Cl_2 (1 → 10% MeOH)) to

---

[53]) Contains traces of DBU · HCl, which could not be be removed with aq. washings due to the high water solubility of **3e**.

afford 1.12 g (55%) of **3f**. Pale yellow powder. TLC (SiO_2; AcOEt/MeOH/H_2O 90:9:1): R_f 0.47. ^{1}H-NMR (300 MHz, CD_3OD): 3.7–3.9 (*m*, H–C(5′), H–C(4′)); 4.24 (br. *d*, *J* = 2.7, H–C(3′)); 4.35 (*dd*, *J* = 9.8, 2.7, H–C(2′)); 4.92 (*dt*, *J* = 5.6, 1.5, CH_2(allyl)); 5.25 (*dm*, *J* = 10.5, CH_2=); 5.45 (*dm*, *J* = 17, CH_2=); 5.80 (*d*, *J* = 9.8, H–C(1′)); 6.11 (*m*, =CH); 7.35–8.10 (*m*, 5 arom. H); 8.32 (*s*, H–C(8)). ^{13}C-NMR (100 MHz, CD_3OD): 66.71 (*t*, C(5′)); 68.23 (*d*, C(2′)); 69.77 (*t*, C(allyl)); 70.16 (*d*, C(4′)); 72.85 (*d*, C(3′)); 82.17 (*d*, C(1′)); 118.33 (*t*, C(allyl)); 121.13 (*s*, C(5)); 129.30–135.02 (*d* + *s*, arom. C, C(allyl)); 143.26 (*d*, C(8)); 152.19, 156.02, 162.48 (*s*, C(2), C(4), C(6)); 168.30 (*s*, C=O). FAB-MS (pos., 3-NBA): 450 (30, $[M+Na]^+$), 428 (82, $[M+H]^+$), 296 (73), 154 (54), 105 (100).

2,6-Diamino-N^2,N^6*-dibenzoyl-9-(β-*D*-ribopyranosyl)purine* (**3g**). To a soln. of 6.9 g (11.6 mmol) of **2g** in 100 ml of pyridine cooled to 0° (ice bath) was added 9.8 g (69.7 mmol) of BzCl dropwise, the mixture was stirred at 0° for 2 h and allowed to warm to r.t. overnight. The mixture was poured into 200 ml of ice-cold sat. aq. $NaHCO_3$ soln. and extracted with 3 × 200 ml of CH_2Cl_2. The combined org. phases were dried (Na_2SO_4) and concentrated *in vacuo*. The residue was dissolved in 100 ml of THF/MeOH/H_2O 5:4:1, cooled to 0° (ice bath), 47 ml (94 mmol) of 2M aq. NaOH was added, and the mixture was stirred for 35 min. Then, 5.9 g (111 mmol) of solid NH_4Cl was added, and the mixture was stirred for an additional 5 min. The mixture was concentrated *in vacuo*, and the residue was adsorbed on 50 g of SiO_2 and purified by CC (100 g SiO_2; CH_2Cl_2 (with 1 → 10% MeOH)) to afford 5.2 g (91%) of **3g**. TLC ($CHCl_3$/MeOH 10:1): R_f 0.37. ^{1}H-NMR (300 MHz, CD_3OD): 3.75–4.0 (*m*, 2 H–C(5′), H-(4′)); 4.30 (br. *s*, H–C(3′)); 4.31 (*dd*, *J* = 8.8, 2.8, H–C(2′)); 5.99 (*d*, *J* = 8.8, H–C(1′)), 7.3–8.20 (*m*, 10 arom. H); 8.4 (*s*, H–C(8)). ^{13}C-NMR (75 MHz, CD_3OD) 66.69 (*t*, C(5′)); 68.21 (*d*, C(2′)); 71.15 (*d*, C(4′)); 72.84 (*d*, C(3′)); 82.09 (*d*, C(1′)); 120.4 (*s*, C(5)); 129.02–135.43 (*d* + *s*, arom. C); 143.63 (*d*, C(8)); 150.94, 154.01, 154.57 (*s*, C(2), C(4), C(6)); 167.72 (*s*, C=O). FAB-MS (pos., 3-NBA): 981 (4, $[2M+H]^+$), 513 (6, $[M+Na]^+$), 491 (77, $[M+H]^+$), 359 (82), 255 (7), 105 (100).

*2,6-Diamino-9-(β-*L*-ribopyranosyl)purine* (**3h**). In a 50-ml round-bottomed flask was placed 200 mg (0.34 mmol) of L-**2g** and treated with sat. methanolic NH_3 soln. for 24 h. The mixture was concentrated *in vacuo*, and the residue was purified by CC (25 g of SiO_2; CH_2Cl_2/MeOH, 10:1 → 2:1) to afford 86 mg (88%) of **3h**. Crystallization from H_2O afforded 64 mg (65%) of **3 h**. M.p. 169–171°. TLC (SiO_2; AcOEt/hexanes 1:2 (with 1% MeOH)): R_f 0.42. ^{1}H-NMR (300 MHz, D_2O): 3.74, 3.76 (br. *m*, 2, H–C(5′)); 3.95 (*ddd*, *J* = 11.4, 6.4, 2.7, H–C(4′)); 4.22 (*t*, *J* = 2.7, H–C(3′)); 4.24 (*dd*, *J* = 9.4, 2.7, H–C(2′)); 5.48 (*d*, *J* = 9.4, H–C(1′)); 7.89 (*s*, H–C(8)). ^{13}C-NMR (100 MHz, D_2O): 67.41 (*t*, C(5′)); 68.69 (*d*, C(4′)); 70.61 (*d*, C(2′)); 73.44 (*d*, C(3′)); 82.56 (*d*, C(1′)); 115.54 (*s*, C(5)); 140.72(*d*, C(8)); 154.13, 159.03, 163 (3*s*, C(2), C(4), C(6)). FAB-MS (pos., 3-NBA): 283 (40, $[M+H]^+$).

2. ***General Procedure for the Preparation of the Nucleosides*** **4a–4g** (***Scheme 2***). A soln. of the base-protected nucleoside **3a–3g**, anisaldehyde dimethylacetal, and TsOH·H_2O in DMF was heated at 55° under vacuum (30 mbar) until no starting material could be detected. After cooling, the mixtures were treated with 50 ml of sat. $NaHCO_3$ soln. and diluted with 750 ml of CH_2Cl_2. The org. phase was washed with H_2O, dried ($MgSO_4$), and evaporated. The residue was purified by CC on SiO_2.

*1-{3′,4′-*O*-[(4-Methoxyphenyl)methylidene]-β-*D*-ribopyranosyl}uracil* (**4a**). From 10.5 g (44 mmol) of **3a** (crude product, containing 5% BzOH), 19.5 g (107 mmol) of *p*-anisaldehyde dimethylacetal, and 800 mg (4.5 mmol) of TsOH·H_2O in 250 ml of DMF (60 min). CC (450 g SiO_2; CH_2Cl_2 → CH_2Cl_2/MeOH 85:15) afforded 11.9 g (75%) of **4a** (*endo/exo* isomers 3:1). Colorless foam. A small part of this mixture was separated by CC for characterization purposes.

Data of endo-**4a**: TLC (CH_2Cl_2/MeOH 9:1): R_f 0.40. ^{1}H-NMR (300 MHz, CD_3OD): 7.64 (*d*, *J* = 8.1, H–C(6); 7.51 (*m*, 2 H); 6.94 (*m*, 2 H); 5.81 (*s*, ArCH); 5.71 (*d*, *J* = 9.5, H–C(1′)); 5.68 (*d*, *J* = 8.1, H–C(5)); 4.64 (*dd*, *J* = 3.2, 7.6 H–C(2)); 4.47 (*m*, H–C(4′), H–C(3′)); 4.24 (*dd*, *J* = 2.8, 12.9, H–C(5′)); 3.85 (*dd*, *J* = 3.0, 12.9, H–C(5′)); 3.80 (*s*, 3 H). ^{13}C-NMR (75 MHz, CD_3OD): 166.3 (*s*, C(4)); 162,3 (*s*); 152.8 (*s*, C(2)); 144.9 (*d*, C(6)); 130.2 (*s*); 129.7 (*d*); 114.8 (*d*); 105.6 (*d*); 102.7 (*d*, C(5)); 85.9 (*d*, C(1′)); 77.5 (*d*); 75.5 (*d*); 67.0 (*t*, C(5′)), 66.3 (*d*); 55.8 (*q*). FAB-MS (pos.): 363 (87, $[M+H]^+$), 361 (32), 205 (41), 154 (27), 137 (100), 136 (40), 135 (53), 121 (28), 113 (41), 77 (31).

Data of exo-**4a**: TLC (CH_2Cl_2/MeOH 9:1): R_f 0.45. ^{1}H-NMR (300 MHz, CD_3OD + 5 drops of (D_6)DMSO): 7.68 (*d*, *J* = 8.1, H–C(6); 7.51 (*m*, 2 H); 7.43 (*m*, 2 H); 6.99 (*s*, 1 H); 5.71 (*d*, *J* = 8,0, H–C(5)); 5.69 (*d*, *J* = 9.5, H–C(1′)); 4.66 (*m*, H–C(2′), H–C(4′)); 4.35 (*dd*, *J* = 6.6, 9.5, H–C(3′)); 4.27 (*dd*, *J* = 4.1, 12.8, H–C(5′)); 3.86 (*dd*, *J* = 4.5, 12.8, H–C(5′)); 3.82 (*s*, 3 H). ^{13}C-NMR (75 MHz, CD_3OD + 5 drops of (D_6)DMSO): 165.8 (*s*, C(4)); 161.9 (*s*); 152.8 (*s*, C(2)); 144.1 (*d*, C(6)); 132.7 (*s*); 129.2 (*d*); 115.0 (*d*); 105.9 (*d*); 103.1 (*d*, C(5)); 85.0 (*d*, C(1′)); 77.3 (*d*); 75.5 (*d*); 66.9 (*t*, C(5′)), 66.0 (*d*); 56.1 (*q*). FAB-MS (pos.): 363 (100, $[M+H]^+$), 361 (22), 252 (26), 155 (21), 154 (80), 152 (23), 138 (27), 137 (77), 136 (71), 135 (38), 113 (24), 107 (30), 91 (24), 90 (22), 89 (35), 78 (22), 77 (50), 63 (22).

*Mixture of 1-{3′,4′-*O*-[(4-Methoxyphenyl)methylidene]-β-*D*-ribopyranosyl}thymine and 1-{2′,3′-O-[(4-Methoxyphenyl)methylidene]-β-*D*-ribopyranosyl}thymine* (**4b**). From 11.0 g (43 mmol) of **3b**, 19.5 g (107 mmol) of *p*-anisaldehyde dimethylacetal, and 800 mg (4.5 mmol) of TsOH · H_2O in 250 ml of DMF (75 min). CC (450 g of SiO_2; $CH_2Cl_2 \rightarrow CH_2Cl_2$/MeOH 9:1) afforded 12.9 g (80%) of **4b** as a mixture of 60% 3′,4′-*endo*-, 25% 3′,4′-*exo*-, 10% 2′,3′-*endo*-, and 5% 2′,3′-*exo*-acetals (^{1}H-NMR). TLC (CH_2Cl_2/MeOH 9:1): R_f 0.50. ^{1}H-NMR (300 MHz, $CDCl_3$): 7.55–7.32 (*m*, 2 H); 7.09 (*s*, 0.85 H, H–C(6)(3′,4′-acetal)); 7.07 (0.15 H, H–C(6)(2′,3′-acetal)); 6.97–6.86 (*m*, 2 H); 6.37 (*s*, 0.05 H, H–C(2′,3′)(2′,3′-*exo*-acetal)); 6.33 (*s*, 0.25 H, H–C(3′,4′)(3′,4′-*exo*-acetal)); 5.92 (*s*, 0.10 H, H–C(2′,3′)(2′,3′-*endo*-acetal)); 5.84 (*s*, 0.60 H, H–C(3′,4′)(3′,4′-*endo*-acetal)); 5.79 (*d*, $J = 8.5$, 0.05 H, H–C(1′)(2′,3′-*exo*-acetal); 5.78 (*d*, $J = 8.1$, 0.10 H, H–C(1′)(2′,3′-*endo*-acetal); 5.44 (*d*, $J = 9.0$, 0.25 H, H–C(1′)(3′,4′-*exo*-acetal); 5.38 (*d*, $J = 8.8$, 0.60 H, H–C(1′)(3′,4′-*endo*-acetal); 4.79–4.30 (*m*, H–C(2′), H–C(3′), H–C(4′), H–C(5′)); 4.02–3.86 (*m*, H–C(5′)); 3.80 (3*s*, 3 H); 1,79 (*d*, $J = 0.9$, 0.15 H, Me–C(5)(2′,3′-acetal); 1.74 (*d*, $J = 0.9$, 0.85 H, Me-C(5)(3′,4′-acetal). ^{13}C-NMR (75 MHz, $CDCl_3$): 165.3, 164.8; 163.5, 162.6 (*s*, C(4)); 160.9, 160.8, 160.4, 160.3 (*s*); 151.3, 151.2, 150.7, 150.6 (*s*, C(2)); 140.8, 139.3, 135.7, 135.2 (*d*, C(6)); 133.2, 132.0, 130.4, 130.3 (*s*); 128.6, 128.5, 128.4, 127.5, 127.4 (*d*); 114.2, 114.0, 113.8 (*d*); 112.0, 111.9, 110.1, 109.4 (*s*, C(5)); 105.6, 104.5 (*d*); 88.6, 87.0, 83.1, 80.0 (*d*, C(1′)); 77.3, 77.2 (*d*); 75.9, 75.3, 75.2, 75.0 (*d*); 74.3, 74.0, 73.9 (*d*); 67.2, 67.1, 66.2, 66.1 (*t*, C(5′)), 65.6, 65.3, 65.0, 64.5 (*d*); 55.3 (*q*); 12.5, 12.3, 12.1 (*q*, *Me*–C(5)). FAB-MS (pos.): 377 (100, $[M + H]^+$), 375 (24), 251 (24), 205 (28), 154 (41), 138 (23), 137 (91), 136 (47), 135 (44), 127 (58), 122 (26), 121 (24), 115 (23), 77 (27), 69 (31).

N^4-*Benzoyl-1-{3′,4′-*O*-[(4-methoxyphenyl)methylidene]-β-*D*-ribopyranosyl}cytosine* (**4c**). From 8.5 g (24.5 mmol) of **3c**, 10.5 g (61.2 mmol) of *p*-anisaldehyde dimethylacetal, and 500 mg (2.6 mmol) of TsOH · H_2O in 250 ml of DMF (5 h). CC (SiO_2; $CH_2Cl_2 \rightarrow CH_2Cl_2$/MeOH 9:1) afforded 8.2 g (72%) of **4c** (*endo/exo* 3:1). Colorless foam[54]).

Data of exo-**4c**: TLC (CH_2Cl_2/MeOH 7:1): R_f 0.70. ^{1}H-NMR (400 MHz, (D_6)DMSO): 3.77 (*s*, MeO); 3.77–3.81 (*m*, H–C(5′)); 4.35 (*dd*, $J = 12.8$, 3.9, H–C(5′)); 4.44–4.48 (*m*, H–C(4′)*); 4.57 (*dd*, $J = 2.8$, 6.7, H–C(3′)*); 4.67–4.7 (*m*, H–C(2′)); 5.66 (*d*, $J = 9.3$, H–C(1′)); 5.69 (*d*, $J = 6.3$, OH); 6.24 (*s*, ArC*H*); 6.96 (*dd*, $J = 6.8$, 2.0, 2 arom. H); 7.31 (*d*, $J = 3.2$, H–C(5)); 7.39 (*dd*, $J = 6.8$, 1.9, 2 arom. H); 7.5–7.54 (m, 2 arom. H); 7.61–7.65 (*m*, 1 arom. H); 8.01 (*dd*, $J = 7.2$, 7.2, 2 arom. H); 8.19 (*d*, $J = 7.5$, H–C(6)); 11.32 (br. *s*, NH). ^{13}C-NMR (100 MHz, (D_6)DMSO): 55.04 (*q*, MeO); 64.33 (*d*, C(2′)*); 65.54 (*t*, C(5′)); 73.84, 75.43 (2*d*, C(3′), C(4′)*); 85.2 (*d*, C(1′)); 96.19 (*d*, C(5)); 103.61 (*d*, OCHO); 113.52 (*d*, arom. C); 127.68, 128.34, 128.38 (*d*, arom. C); 131.01 (*s*, arom. C); 132.64 (*d*, arom. C); 147.85 (*d*, C(6)); 154.84 (*s*, C(2)); 159.7 (*s*, arom. C); 163.07 (*s*, C(4)); 167.6 (*s*, CO). FAB-MS (pos.): 466 (85, $[M + H]^+$); 216 (79), 176 (74), 124 (62), 120 (71), 107 (100), 105 (76), 91 (71), 77 (91).

Data of endo-**4c**: TLC (CH_2Cl_2/MeOH 7:1): R_f 0.65.

Data of exo-**4c**/endo-**4c** isomer: ^{1}H-NMR (300 MHz, (D_6)DMSO): 3.76 (*s*, MeO (*endo*)); 3.79 (*s*, MeO (*exo*)); 3.77–3.88 (*m*, H–C(5′)); 4.35–4.7 (*m*, H–C(2′), H–C(3′), H–C(4′), H–C(5′)); 5.58 (*m*, H–C(1′), OH); 5.77 (*s*, ArC*H* (*endo*)); 6.22 (*s*, 2 ArC*H* (*exo*)); 6.83–6.95 (*m*, 2 arom. H); 7.28–7.61 (*m*, 5 arom. H, H–C(5)); 7.95–8.18 (*m*, 2 arom. H, H–C(6)).

N^6-*Benzoyl-9-{3′,4′-*O*-[(4-methoxyphenyl)methylidene]-β-*D*-ribopyranosyl}adenine* (**4d**). From 7.0 g (18.9 mmol) of **3d**, 7.7 ml (45.2 mmol) of *p*-anisaldehyde dimethylacetal, and 358 mg (1.9 mmol) of TsOH · H_2O in 170 ml of DMF (1 h). CC (SiO_2; $CH_2Cl_2 \rightarrow CH_2Cl_2$/MeOH 9:1) afforded 7.1 g (77%) of **4d** (*endo/exo* 3:1). Colorless foam. A small portion of this mixture was separated by CC for characterization purposes.

Data of endo-**4d**: TLC (CH_2Cl_2/MeOH 19:1) R_f 0.20. ^{1}H-NMR (300 MHz, $CDCl_3$): 3.79 (*s*, MeO); 3.99 (*d*, $J = 11.3$, H–C(5′)); 4.43 (*dd*, $J = 12.75$, 2.2, H–C(5′)); 4.53 (*d*, $J = 7.5$, H–C(3′)); 4.72 (*d*, $J = 7.53$, H–C(4′)); 4.92 (br. *s*, OH); 5.86 (*s*, ArC*H*); 5.90 (*s*, H–C(1′)); 6.93 (*d*, $J = 8.7$, 2, arom. H); 7.44 (*dd*, $J = 7.7$, 7.7, 2 arom. H); 7.54 (*m*, 3 arom. H); 7.89 (*s*, H–C(8)); 7.97 (*d*, $J = 7.5$, arom. H); 8.61 (*s*, H–C(2)); 9.12 (br. *s*, NH). ^{13}C-NMR (75 MHz, $CDCl_3$): 55.4 (*q*, MeO); 65.9 (*t*, C(5′)); 66.0, 73.8, 75.6 (3*d*, C(2′), C(3′), C(4′)); 84.3 (*d*, C(1′)); 104.6 (*d*, C(acetal)); 113.9 (*d*, arom. C); 123.1 (*s*, C(5)); 127.7, 127.9, 128.4, 128.6, 128.8 (arom. C); 132.9 (*d*, arom. C); 133.3 (*s*, arom. C); 142.9 (*d*, C(8)); 149.3 (*s*, C(4)); 151.2 (*s*, C(5)); 152.3 (*d*, C(2)); 160.9, 164.6 (2*s*, C=O, rotamer). FAB-MS (pos., 3-NBA): 490.1 (61, $[M + H]^+$), 240.1 (100), 105.0 (56).

Data of exo-**4d**/endo-**4d**: TLC (CH_2Cl_2/MeOH 19:1): R_f 0.20/0.26. ^{1}H-NMR (300 MHz, $CDCl_3$): diagnostic signals: 3.82 (*s*, Me); 4.80 (*d*, $J = 7.1$, H–C(2′)). ^{13}C-NMR (75 MHz, $CDCl_3$): 55.38 (*q*, MeO); 65.9, 66.6, 73.9,74.2, 74.8, 75.7 (6*d*, C(2′), C(3′), C(4′)); 66.1 (*t*, C(5′)); 84.0, 84,2 (2*d*, C(1′)); 104.6, 105.0 (2*d*, C(acetal)); 113.8, 113.9 (2*d*, arom. C); 122.8, 123.0 (2*s*, C(5)); 127.7, 127.9, 128.4, 128.8, 130.4 (arom. C); 132.9 (*d*, arom. C);

---

[54]) From this mixture, pure *exo*-isomer could be obtained by crystallization from CH_2Cl_2.

133.3 (*s*, arom. C); 142.8, 143.0 (2*d*, C(8)); 149.2 (*s*, C(4)); 151.2 (*s*, C(6)); 152.2 (*d*, C(2)); 160.4, 160.9, 164.6 (3*s*, C=O).

*2-Amino-*N^2*-isobutyryl-9-{3′,4′-*O*-[(4-methoxyphenyl)methylidene]-6-[(prop-2-enyl)oxy]-β-*D*-ribopyranosyl}purine* (**4e**). From 3.4 g (8.6 mmol) of **3e**, 3.7 ml (21.6 mmol) of *p*-anisaldehyde dimethylacetal, and 250 mg (1.3 mmol) of TsOH · H_2O in 45 ml of DMF (45 min). CC (SiO_2; $CH_2Cl_2 \rightarrow CH_2Cl_2$/MeOH 19:1) afforded 3.7 g (85%) of **4e** (*endo*/*exo* 3:1). Colorless foam[55]). TLC (CH_2Cl_2/MeOH 19:1): R_f 0.39. ^{1}H-NMR (400 MHz, $CDCl_3$): 1.28 (*d*, *J* = 6.8, Me of isobutyryl of *exo*); 1.29 (*d*, *J* = 6.9, Me of isobutyryl (*endo*)); 1.29 (*d*, *J* = 6.9, Me isobutyryl (*endo*)); 2.74 (*sept.*, *J* = 6.9, CH of isobutyryl); 3.81 (*s*, MeO (*endo*)); 3.82 (*s*, MeO (*exo*)); 4.01 (*d*, *J* = 12.0, H–C(5′) (*endo*)); 4.03 (*dd*, *J* = 2.0, 13.0, H–C(5′) (*exo*)); 4.47 (*dd*, *J* = 1.7, 13.1, H–C(5′)); 4.52 (*d*, *J* = 7.9, H–C(4′) (*endo*)); 4.62 (*dt*, *J* = 2.2, 7.4, H–C(4′) (*exo*)); 4.72 (*ddd*, *J* = 2.9, 6.0, 7.9, H–C(2′) (*exo*)); 4.80 (*m*, H–C(2′) (*endo*) H–C(3′)); 4.90 (*dd*, *J* = 6.2, 12.8, 1 H, CH_2O); 4.96 (*ddd*, *J* = 1.1, 5.5, 12.8, 1 H, CH_2O); 5.34 (*dd*, *J* = 1.2, 10.4, 1 H, $=CH_2$); 5.51 (*dm*, *J* = 17.2, 1 H, $=CH_2(Z)$); 5.79 (*d*, *J* = 7.9, H–C(1′) (*exo*)); 5.84 (*d*, *J* = 7.6, H–C(1′) (*endo*)); 5.87 (*s*, ArC*H* (*endo*)); 6.12 (*ddm*, *J* = 10.5, 17.2, =CH (allyl)); 6.38 (*s*, ArC*H* (*exo*)); 6.82 (*d*, *J* = 5.8, O*H* (*exo*)); 6.91 (*d*, *J* = 8.7, OH (*endo*), and H–C(3), H–C(5) of Ar); 7.43 (*d*, *J* = 8.8, H–C(2), H–C(6) of Ar (*exo*)); 7.54 (*d*, *J* = 8.7, H–C(2), H–C(6) of Ar (*endo*)); 7.85 (*s*, H–C(8) (*endo*)); 7.86 (*s*, H–C(8) (*exo*)); 8.15 (*s*, N^{2}H (*exo*)); 8.17 (*s*, N^{2}H (*endo*)). ^{13}C-NMR (100 MHz, $CDCl_3$): 19.3, 19.5 (2*q*, *Me* of isobutyryl); 36.7 (*d*, CH of isobutyryl); 55.3 (*q*, MeO); 65.5 (*t*, C(5′) (*endo*)); 65.8 (*d*, C(2′) (*endo*)); 65.9 (*t*, C(5′) (*exo*)); 66.4 (*d*, C(2′) (*exo*)); 67.8 (*t*, CH_2O); 74.0 (*d*, C(4′)* (*endo*)); 74.5 (*d*, C(3′) , C(4′) (*exo*)); 75.7 (*d*, C(3′) (*endo*)); 86.1 (*d*, C(1′) (*endo*)); 86.1 (*d*, *C*(1′) (*exo*)); 104.4 (*d*, Ar*C*H (*endo*)); 104.8 (*d*, Ar*C*H (*exo*)); 113.7 (*d*, C(3), C(5) of Ar (*exo*)); 113.7 (*d*, C(3), C(5) of Ar (*endo*)); 118.5 (*s*, C(5)); 119.1 (*t*, $=CH_2$ (allyl) (*exo*)); 119.2 (*t*, $=CH_2$ (allyl) (*endo*)); 127.6 (*d*, C(2), C(6) of Ar (*exo*)); 128.6 (*d*, C(2), C(6) (*endo*)); 128.7 (*s*, C_{ipso} of Ar (*endo*)); 130.8 (*s*, C_{ipso} of Ar (*exo*)); 132.0 (*d*, CH (allyl)); 141.4 (*d*, C(8) (*exo*)); 141.5 (*d*, C(8) (*endo*)); 151.3, 151.4 (2*s*, C(2), C(4)); 159.8 (*s*, C(6) (*endo*)); 159.9 (*s*, C(6) (*exo*)); 160.2 (*s*, C_{ipso} to MeO (*exo*)); 160.7 (*s*, C_{ipso} to MeO (*endo*)); 174.8 (*s*, C=O). FAB-MS (pos., 3-NBA): 512.3 (86, $[M+H]^+$), 290.1 (10), 262.1 (100), 192.1 (36), 152.1 (19), 136.0 (59), 135.0 (27), 121.0 (18), 107.0 (27), 88.9 (24), 76.9 (26), 68.9 (19), 54.8 (14).

*2,6-Diamino-*N^2,N^6*-dibenzoyl-9-{3′,4′-*O*-[(4-methoxyphenyl)methylidene]-β-*D*-ribopyranosyl}purine* (**4g**). To a 4.0 g (8.2 mmol) of **3g** in 20 ml of DMF was added 280 mg (1.6 mmol) of TsOH · H_2O, and 3.5 ml (20 mmol) of *p*-anisaldehyde dimethyl acetal. The mixture was connected to house vacuum (*via* cold trap), warmed to 60°, and stirred for 2.5 h. The mixture was treated with 100 mg of solid $NaHCO_3$, stirred for 15 min, partitioned between 150 ml of sat. aq. $NaHCO_3$ soln. and 200 ml of CH_2Cl_2. The aq. layer was extracted once with 100 ml CH_2Cl_2, the combined org. layers were dried (Na_2SO_4), concentrated *in vacuo*, and subjected to bulb-to-bulb distillation (50°, 0.01 mm Hg) to remove DMF. The residue was chromatographed (100 g of SiO_2; CH_2Cl_2 (with $0 \rightarrow 8\%$ MeOH)) to afford 4.57 g (92%) of **4g** as mixture of 1:3 diastereoisomers. TLC (SiO_2; $CHCl_3$/MeOH 10:1): R_f 0.54. ^{1}H-NMR (400 MHz, $CDCl_3$): 3.80, 3.82 (*s*, MeO); 3.92 (*dd*, *J* = 12.8, 1.6, H_{ax}–C(5′)); 4.30–4.71 (*m*, H_{eq}–C(5′), H–C(4′), H–C(3′)); 4.79 (*dd*, *J* = 8.3, 2.4, 1/3 H, H–C(2′)(*exo*)); 4.93 (*dd*, *J* = 8.3, 2.4, 1/3 H, H–C(2′)(*endo*)); 5.82 (*s*, 2/3 H (*endo*-acetal)); 5.85 (*d*, *J* = 8.3, 1/3 H –C(1′)(*exo*)); 5.89 (*d*, *J* = 8.3, 2/3 H, H–C(2′)(*endo*)); 6.31 (*s*, 1/3 H (*exo*-acetal)); 6.8–8.1 (*m*, 14 arom. H, H–C(8)); 9.5, 9.7 (br. *s*, 2 NH). ^{13}C-NMR (100 MHz, $CDCl_3$): 53.35 (*q*, MeO); 65.74, 65.91 (*t*, C(5′)); 66.23, 66.07 (*d*, C(4′)); 73.88 (*d*, C(2′)); 74.23, 75.04 (*d*, C(3′)); 84.39, 84.81 (*d*, C(1′)); 104.55, 104.83 (*d*, C(acetal)); 113.77, 113.84 (*d*, arom. C); 119.52 (*s*, C(5)); 127.47–133.81 (*d* + *s*, arom. C); 141.62, 141.92 (*d*, C(8)); 149.11–152.19 (*s*, C(2), C(4), C(6)); 164.97, 165.03 (*s*, C=O). FAB-MS (pos., 3-NBA): 1217 (2, $[2M+H]^+$), 609 (100, $[M+H]^+$).

2.1. *General Procedure for the Preparation of the Nucleosides* **5c**, **5d**, *and* **5e** (*Scheme 2*). A soln. of the nucleoside **4c** or **4d** or **4e** and DMAP was treated with BzCl. After completion of the reaction (as indicated by TLC), sat. aq. $NaHCO_3$ soln. was added, and the mixture was stirred for 30 min, then extracted with CH_2Cl_2. The org. phase was washed once with H_2O, dried ($MgSO_4$), concentrated *in vacuo*, co-evaporated twice with *ca.* 50 ml of toluene and purified by CC (SiO_2).

N^4*-Benzoyl-1-{2′-*O*-benzoyl-3′,4′-*O*-[(4-methoxyphenyl)methylidene]-β-*D*-ribopyranosyl}cytosine* (**5c**). From 3.2 g (6.88 mmol) of **4c**, 1.93 g of BzCl, and 200 mg of DMAP in 60 ml of CH_2Cl_2/pyridine 5:1 (90 min). CC (170 g of SiO_2; CH_2Cl_2/acetone $9:1 \rightarrow 7:3$) afforded 3.1 g (80%) of **5c**. Colorless foam (*endo*/*exo*, 3:1). TLC (CH_2Cl_2/MeOH 33:1): R_f 0.4 (*exo*-**5c**), 0.35 (*endo*-**5c**). ^{1}H-NMR (300 MHz, $CDCl_3$): *endo*-**5c**: 3.84 (*s*, MeO); 4.07 (*dd*, *J* = 12.7, 3.2, H–C(5′)); 4.6–4.65 (*m*, H–C(4′)); 4.69 (*dd*, *J* = 12.7, 3.2, H–C(5′)); 4.95 (*dd*,

---

[55]) Also isolated were varying amounts of the 2′,3′-acetal (3:2 *endo*/*exo* mixture of expimers, R_f (5% MeOH in CH_2Cl_2) 0.30), and the mixed 3′,4′- and 2′,Me-diacetals (R_f (5% MeOH in CH_2Cl_2) 0.65). These by-products were hydrolyzed under the conditions used to deprotect the acetals (*i.e.*, step **5** → **6**).

$J = 7.4, 3.0$, H–C(3′)); 5.87 (*s*, ArC*H*); 6.0 (*d*, $J = 9.3$, H–C(1′)); 6.13 (*dd*, $J = 9.3, 3.0$, H–C(2′)); 6.93–6.98 (*m*, 2 arom. H); 7.36–8.1 (*m*, 12 arom. H, H–C(5), H–C(6), 1 NH). ^{13}C-NMR (75 MHz, $CDCl_3$): 55.39 (*q*, MeO); 67.47 (*t*, C(5′)); 67.59, 73.68, 73.94 (3*d*, C(2′), C(3′), C(4′)); 85.39 (*d*, C(1′)); 97.24 (*d*, C(5)); 104.98 (*d*, OCHO); 114.04 (*d*, arom. C); 127.96, 128.32, 128.57 (3*d*, arom. C); 128.74 (*s*, arom. C); 130.07, 130.16 (2*d*, arom. C); 133.08 (*s*, arom. C); 133.21, 133.69 (2*d*, arom. C); 146.87 (*d*, C(6)); 154.6 (*s*, C(2)); 160.98 (*s*, arom. C); 162.93 (*s*, C(4)); 165.35 (*s*, CO). MS: 1140 (12, $[2M + 2\,H]^+$), 1139 (17, $[2M + 2\,H]^+$),), 571 (21), 570 (44, $[M + H]^+$), 569 (44, M^+), 355 (23), 217 (14), 216 (54), 187 (14), 121 (19), 107 (18), 106 (32), 105 (100), 89 (16), 77 (34).

Diagnostic signals for *exo*-**5c**: ^{1}H-NMR (300 MHz, $CDCl_3$): 3.79 (*s*, MeO); 4.03–4.16 (*m*, H–C(5′)); 4.55–4.68 (*m*, H–C(5′)); 4.77 (*dd*, $J = 10.7$, 5.3, H–C(4′)); 4.88 (*dd*, $J = 6.0$, 3.0, H–C(3′)); 5.84 (*dd*, $J = 9.4$, 3.1, H–C(2′)); 6.18 (*d*, $J = 9.4$, H–C(1′)); 6.38 (*s*, ArC*H*). ^{13}C-NMR (75 MHz, $CDCl_3$): 66.97 (*t*, C(5′)); 68.53, 73.33, 73.84 (3*d*, C(2′), C(3′), C(4′)); 83.46 (*d*, C(1′)).

N^6,N^6-*Dibenzoyl-9-[2′-*O*-benzoyl-3′,4′-*O*-[(4-methoxyphenyl)methylidene]-β-*D*-ribopyranosyl]adenine* (**5d**). From 5.7 g (11.7 mmol) of **4d**, 3.4 ml (29.1 mmol) of BzCl, and 140 mg DMAP (1.2 mmol) in 55 ml of CH_2Cl_2/pyridine 10:1 (16 h). CC (SiO_2; AcOEt/hexanes 4:6 → 6:4) afforded 8.1 g (99%) of **5d**. Colorless foam (*endo*/*exo* 3:1). TLC (AcOEt/hexanes 8:2): R_f 0.41. ^{1}H-NMR (300 MHz, $CDCl_3$): *endo*-**5d**: 3.83 (*s*, MeO); 4.14 (*dd*, $J = 13.2$, 1.7, H_α–C(5′)); 4.86 (*dd*, $J = 13.2$, 2.2, H_β–C(5′)); 4.98 (*dd*, $J = 7.9$, 2.7, H–C(3′)); 5.88 (*s*, ArC*H*); 6.27 (*d*, $J = 9.1$, H–C(1′)); 6.44 (*dd*, $J = 9.1$, 2.9, H–C(2′)); 6.85–8.00 (*m*, 19 arom. H); 8.14 (*s*, H–C(2)); 8.68 (*s*, H–C(8)). Diagnostic signals for *exo*-**5d**: 3.79 (*s*, MeO); 4.7 (*m*, H_β–C(5′)); 6.33 (*dd*, $J = 9.1$, 2.4, H–C(2′)); 8.18 (*s*, H–C(2)); 8.68 (*s*, H–C(8)). ^{13}C-NMR (75 MHz, $CDCl_3$): 55.4 (*q*, MeO); 66.9, 67.2 (*t*, C(5′)); 67.6, 68.3, 72.7, 73.5, 74.1, 74.6 (6*d*, C(2′), C(3′), C(4′)); 80.6 (*d*, C(1′)); 104.9, 105.6 (2*d*, C(acetal)); 113.9, 114.0 (*d*, arom. C); 127.7; 128.1; 128.4; 128.5; 128.6; 129.0; 129.2; 129.4; 129.7; 129.9; 130.0; 132.9; 133.3; 133.8; 134.0; 144.0; 144.4 (2*d*, C(8)); 152.2, 152.3 (2*d*, C(2), C(4)); 152.9, 153.0 (2*s*, C(6)); 160.6, 161.1, 165.1, 172.1 (4*s*, C=O). FAB-MS (pos., 3-NBA): 698.2 (24, $[M + H]^+$), 355.1 (10), 22.1 (10), 105 (100).

*2-Amino-*N^2*-isobutyryl-9-[2′-*O*-benzoyl-3′,4′-*O*-[(4-methoxyphenyl)methylidene]-β-*D*-ribopyranosyl]purine* (**5e**). From 3.2 g (11.7 mmol) of **4e**, 1.5 ml (12.5 mmol) of BzCl, and 140 mg (1.2 mmol) of DMAP in 55 ml of CH_2Cl_2/pyridine 10:1 (90 min). CC (SiO_2; CH_2Cl_2 → CH_2Cl_2/MeOH 96:4) afforded 3.8 g (98%) of **5e**. Pale yellow foam (*endo*/*exo* 3:1). TLC (CH_2Cl_2/MeOH 19:1): R_f 0.67. ^{1}H-NMR (400 MHz, $CDCl_3$): 1.29 (*d*, $J = 6.9$, Me of isobutyryl); 1.31 (*d*, $J = 6.9$, Me of isobutyryl); 3.01 (br. *m*, CH of isobutyryl); 3.80 (*s*, MeO (*exo*)); 3.84 (*s*, MeO (*endo*)); 4.15 (*dd*, $J = 1.5$, 13.3, H–C(5′) (*endo*)); 4.17 (*dd*, $J = 2.4$, 13.3, H–C(5′) (*exo*)); 4.76 (*d*, $J = 8.1$, H–C(4′) (*endo*)); 4.91 (*dt*, $J = 2.6$, 7.0, H–C(4′) (*exo*)); 4.98 (m, H–C(3′) (*exo*)); 4.99 (*dd*, $J = 2.7$, 8.2, H–C(3′) (*endo*)); 5.01 (*d*, $J = 5.8$, CH_2O (allyl)); 5.15 (*m*, H–C(5′) (*exo*)); 5.17 (br. *d*, $J = 12.2$, H–C(5′) (*endo*)) 5.27 (*dq*, $J = 1.2$, 10.5, CH_2 (allyl) (*E*)); 5.42 (*dq*, $J = 1.4$, 17.2, CH_2 (allyl) (*Z*)); 5.88 (*s*, ArC*H* (*endo*)); 6.09 (*ddt*, $J = 5.6$, 10.6, 17.2, CH (allyl)); 6.13 (*d*, $J = 9.1$, H–C(1′) (*exo*)); 6.16 (*d*, $J = 9.1$, H–C(1′) (*endo*)); 6.33 (*dd*, $J = 2.6$, 9.1, H–(2′) (*exo*)); 6.42 (*dd*, $J = 2.7$, 9.1, H–C(2′) (*endo*)); 6.45 (*s*, ArC*H* (*exo*)); 6.91 (*d*, $J = 8.7$, H–C(3), H–C(5) of Ar (*exo*)); 6.97 (*d*, $J = 8.7$, H–C(3), H–C(5) of Ar (*endo*)); 7.33 (*t*, $J = 7.9$, H_m of Bz); 7.41 (*d*, $J = 8.8$, H–C(2) of Ar (*exo*)); 7.50 (*t*, $J = 7.4$, H_p of Bz); 7.60 (*d*, $J = 8.7$, H–C(2) of Ar (*endo*)); 7.85 (*d*, $J = 8.3$, H_o of Bz); 7.87 (*s*, H–C(8) (*endo*)); 7.89 (*s*, H–C(8) (*exo*)); 7.96 (*s*, N^{2}H). ^{13}C-NMR (100 MHz, $CDCl_3$): 19.4, 19.4 (2*q*, Me of isobutyryl); 36.0 (*d*, CH of isobutyryl); 55.3 (*q*, MeO (*exo*)); 55.4 (*q*, MeO (*endo*); 66.8 (*t*, C(5′) (*endo*)); 67.4 (*t*, C(5′) (*exo*)); 67.7 (*d*, C(2′) (*endo*)); 67.9 (*t*, CH_2O (allyl)); 68.4 (*d*, C(2′) (*exo*)); 72.6 (*d*, C(3′) (*exo*)); 73.4 (*d*, C(3′) (*endo*)); 74.5 (*d*, C(4′)* (*endo*)); 75.0 (*d*, C(4′)* (*exo*)); 80.3 (*d*, C(1′) (*endo*)); 80.6 (*d*, C(1′) (*exo*)); 104.8 (*d*, Ar*C*H (*endo*)); 105.6 (*d*, Ar*C*H (*exo*)); 113.9 (*d*, C(3), C(5) of Ar (*exo*)); 114.0 (*d*, C(3), C(5) of Ar (*endo*)); 118.7 (*t*, CH_2 (allyl)); 119.0 (*s*, C(5) (*exo*)); 119.1 (*s*, C(5) (*endo*)); 127.8 (*d*, C(2), C(6), of Ar (*exo*)); 128.3 (*s*, C_{ipso} of Bz); 128.4 (*d*, C(2), C(6) of Ar (*endo*)); 128.5 (*d*, C_m of Bz (*exo*)); 128.5 (*s*, Ar*C*H (*endo*)); 128.7 (*d*, C_m of Bz (*endo*)); 129.8 (*d*, C_o of Bz); 130.2 (*s*, Ar*C*H (*exo*)); 132.1 (*d*, =CH (allyl)); 133.7 (*d*, C_p of Bz); 140.9 (*d*, C(8) (*exo*)); 141.1 (*d*, C(8) (*endo*)); 151.8 (*s*, C(2) (*endo*)); 151.9 (*s*, C(2) (*exo*)); 152.6 (*s*, C(4) (*endo*)); 152.7 (*s*, C(4) (*exo*)); 160.5 (*s*, C(6) or C_{ipso} to MeO (*exo*)); 160.7 (*s*, C(6) (*endo*)); 161.0 (*s*, C_{ipso} to MeO (*endo*)); 165.1 (*s*, C=O of Bz (*exo*)); 165.1 (*s*, C=O of Bz (*endo*)); 175.4 (*s*, C=O of isobutyryl). FAB-MS (pos., 3-NBA): 616.3 (45, $[M + H]^+$), 355.2 (16), 262.2 (42), 192.1 (18), 187.1 (13), 151.1 (44), 136.1 (27), 135.1 (25), 121.1 (17), 105.0 (100), 89.0 (14), 76.9 (26), 68.9 (10), 54.9 (10).

*6-Amino-*N^6,N^6*-dibenzoyl-9-[2′-*O*-benzoyl-3′,4′-*O*-[(4-methoxyphenyl)methylidene]-2-[(prop-2-enyl)oxy]-β-*D*-ribopyranosyl]purine* (**5f**). To a soln. of 3.1 g (7.26 mmol) of **3f** in 20 ml of DMF was added 2.6 g (2.5 ml, 14.5 mmol) of *p*-anisaldehyde dimethyl acetal and 125 mg (0.73 mmol) of TsOH, and the mixture was warmed to 60° for 2 h with stirring. The mixture was neutralized with solid $NaHCO_3$, then diluted with 150 ml of CH_2Cl_2, and washed with 100 ml of sat. aq. $NaHCO_3$. The org. layer was dried (Na_2SO_4), concentrated *in vacuo*, and DMF was removed under high vacuum. The residue was dissolved in 50 ml of pyridine, cooled to 0°, and 4.2 ml (36 mmol) of BzCl was added. After complete addition, the mixture was stirred overnight (at r.t) and poured

into 100 ml of sat. aq. $NaHCO_3$, and extracted with 2×150 ml of CH_2Cl_2. The combined org. extracts were dried ($MgSO_4$), concentrated *in vacuo*, and co-evaporated with toluene to remove pyridine. The residue was filtered (100 g SiO_2; hexanes/AcOEt, $10:1 \rightarrow 1:4$) to afford 3.92 g (72%) of **5f** as a diastereoisomer mixture (*ca.* 2:5 by ^{1}H-NMR). TLC (60% AcOEt in hexanes): R_f 0.49. ^{1}H-NMR (400 MHz, $CDCl_3$): diastereoisomer mixture: 3.80, 3.84 (2*s*, MeO); 4.11 (*dd*, $J = 13.1, 2.3$ H–C(5′)); 4.54 (*m*, 2 H (allyl)); 4.69 (*ddd*, $J = 7.8, 2.5, 2.5$, H–C(4′)); 4.77 (*dd*, $J = 13.1, 2.5$, H–C(5′)); 4.90 (*m*, H–C(3′)); 5.14 (*dm*, $J = 10.4$, C=CH_2); 5.23 (*dm*, $J = 17.2$, C=CH_2); 5.80 (*m*, C*H*=CH_2); 5.86, 6.41 (2*s*, ArC*H*); 6.18 (2*d*, $J = 9.1$, H–C(1′)); 6.85–8.12 (*m*, 19 arom. H); 7.94, 7.97 (2*s*, H–C(8)); not assigned signals: 4.20 (*m*, 0.25 H), 4.84 (*m*, 0.33 H), 5.68 (*m*, 0.33 H), 6.03 (*m*, 0.25 H). ^{13}C-NMR (100 MHz, $CDCl_3$): 55.4 (*q*, MeO); 66.9, 69.0 (2*t*, C(5′), C(allyl)); 67.6, 68.3, 72.7, 73.5, 73.9, 74.4 (6*d*, C(2′), C(3′), C(4′)); 79.9, 80.1 (2*d*, C(1′)); 104.9, 105.5 (2*d*, Ar*C*H); 113.9, 114.0 (2*d*, arom. C); 118.5 (*t*, C=*C*H_2); 123.5, 123.7 (2*d*, C(5)); 127.7, 127.9, 128.1, 128.5, 128.5, 128.6, 128.7, 128.8, 129.3, 129.4, 129.9, 130 (arom. C); 132.3, 133.0, 133.7 (3*d*, arom. C); 134.0 (*s*, arom. C); 142.8 (*d*, C(8)); 152.5, 154.9 (2*s*, C(2), C(4)); 160.5 (*s*, C(6)); 161.0, 165.1, 172.1 (3*s*, C=O). FAB-MS (pos., 3-NBA): 754.2 (82, $[M+H]^+$), 632.2 (15), 400.1 (15), 105.0 (100).

N^3-*Benzoyl-1-(2′*-O-*benzoyl-β*-D-*ribopyranosyl)uracil* (**6a**). A soln. of 11.5 g (31.7 mmol) of **4a** (mixture of diastereoisomers) and 400 mg of DMAP (3.3 mmol) in 150 ml of pyridine was cooled to 4° and treated with 11.0 g (78 mmol) of BzCl. After 16 h at r.t., the reaction was quenched with 50 ml of sat. aq. $NaHCO_3$ soln., the mixture was stirred for 30 min and diluted with 500 ml of CH_2Cl_2. The org. phase was washed with 100 ml of H_2O, dried ($MgSO_4$), evaporated, and co-evaporated 3 times with 50 ml toluene. The residue (crude **5a**) was dried, dissolved in 180 ml of MeOH/20 ml THF, and treated with 22 ml of CF_3COOH. After 1 h at r.t., the mixture was treated with 26 g (309 mmol) of solid $NaHCO_3$, concentrated to a volume of 20 ml, and 200 ml of CH_2Cl_2 was added. SiO_2 (50 g) was added, and the solvents were evaporated. CC (300 g SiO_2; $CH_2Cl_2 \rightarrow CH_2Cl_2$/MeOH 90:10) afforded 10.0 g (70%) of **6a**. Colorless foam. TLC (hexanes/AcOEt 1:2): R_f 0.20. ^{1}H-NMR (300 MHz, CD_3OD): 8.02 (*d*, $J = 7.0$, 2 H); 7.94 (*d*, $J = 8.3$, H–C(6)); 7.63–7.53 (m, 4 H); 7.41 (*t*, $J = 7.8$, 2 H); 7.19–7.15 (br. *s*, 2 H); 6.17 (*d*, $J = 9.6$, H–C(1′)); 5.87 (*d*, $J = 8.3$, H–C(5)); 5.26 (*dd*, $J = 2.7, 9.5$, H–C(2′)); 4.41 (br. *t*, $J = 2.3$, H–C(3′)); 4.00 (*ddd*, $J = 2.3, 5.8, 10.9$, H–C(4′)); 3.90 (*m*, 2 H–C(5′)). ^{13}C-NMR (75 MHz, CD_3OD): 169.7 (*s*); 166.8 (*s*); 163.7 (*s*, C(4)); 150.9 (*s*, C(2)); 142.9 (*d*, C(6)); 136.2 (*d*); 134.8 (*d*); 132.6 (*s*); 131.1 (*d*); 130.6 (*d*); 130.3 (*d*); 129.4 (*d*); 103.3 (*d*, C(5)); 79.9 (*d*, C(1′)); 73.0 (*d*); 70.6 (*d*); 67.6 (*d*), 67.1 (*t*, C(5′)). FAB-MS (pos.): 453 (48, $[M+H]^+$), 307 (28), 237 (51), 155 (35), 154 (100), 139 (23), 138 (43), 137 (84), 136 (77), 107 (30), 105 (98), 91 (22), 89 (25), 77 (34).

N^3-*Benzoyl-1-(2′*-O-*benzoyl-β*-D-*ribopyranosyl)thymine* (**6b**). A soln. of 10.0 g (26.6 mmol) of **4b** (mixture of diastereoisomers) and 330 mg of DMAP (2.7 mmol) in 130 ml of pyridine was cooled to 4° and treated with 9.3 g (66 mmol) of BzCl. After 16 h at r.t., the reaction was quenched with 50 ml of sat. aq. $NaHCO_3$ soln., and the mixutre was stirred for 30 min and diluted with 500 ml CH_2Cl_2. The org. phase was washed with 100 ml of H_2O, dried ($MgSO_4$), evaporated, and co-evaporated 3 times with 50 ml of toluene. The residue was dried, dissolved in 243 ml of MeOH/27 ml of THF, and treated with 27 ml of CF_3COOH. After 1 h at r.t., the mixture was treated with 30 g (357 mmol) of solid $NaHCO_3$, concentrated to 20 ml of volume, and 200 ml CH_2Cl_2 was added. SiO_2 (50 g) was added, and the solvents were evaporated. CC (350 g SiO_2; hexanes/AcOEt $1:1 \rightarrow 1:4$) afforded 8.1 g (66%) of **6b**. Colorless foam[56]). TLC (hexane/AcOEt 1:4): R_f 0.50. ^{1}H-NMR (300 MHz, CD_3OD): 8.02 (*m*, 2 H); 7.79 (*d*, $J = 1.2$, H–C(6)); 7.63–7.53 (*m*, 4 H); 7.41 (*t*, $J = 7.7$, 2 H) 7.19–7.15 (br. *s*, 2 H); 6.18 (*d*, $J = 9.6$, H–C(1′)); 5.30 (*dd*, $J = 2.6, 9.4$, H–C(2′)); 4.42 (br. *t*, $J = 2,5$, H–C(3′)); 4.03 (*ddd*, $J = 2.4, 5.4, 9.5$, H–C(4′)); 3.90 (m, 2 H–C(5′)); 1.90 (*d*, $J = 1.2$, Me–C(5)). ^{13}C-NMR (75 MHz, CD_3OD): 169.9 (*s*), 166.8 (*s*); 164.4 (*s*, C(4)); 151.0 (*s*, C(2)); 138.5 (*d*, C(6)); 136.2 (*d*); 134.8 (*d*); 132.6 (*s*); 131.1 (*d*); 130.6 (*d*); 130.3 (*d*); 129.8 (*d*); 129.4 (*d*); 112.2 (*s*, C(5)); 79.8 (*d*, C(1′)); 73.0 (*d*); 70.6 (*d*); 67.6 (*d*), 67.0 (*t*, C(5′)); 12.4 (*q*, *Me*–C(5)). FAB-MS (pos.): 467 (52, $[M+H]^+$), 237 (63), 219 (23), 154 (49), 137 (34), 136 (37), 105 (100), 77 (24).

2.2. *General Procedure for the Preparation of the Nucleosides* **6c**, **6d**, and **6e** (*Scheme 2*). A soln. of **5c** or **5d** or **5e** was treated with CF_3COOH. After completion of the reaction (TLC), solid $NaHCO_3$ was added, and the mixture was evaporated to *ca.* 50 ml and extracted $4 \times CH_2Cl_2$. The combined org. phases were dried ($MgSO_4$), concentrated, and the products were purified by CC (SiO_2).

N^4-*Benzoyl-1-(2′*-O-*benzoyl-β*-D-*ribopyranosyl)cytosine* (**6c**). From 8.4 g (15 mmol) of **5c** in MeOH/THF/CH_2Cl_2/CF_3COOH 4:2:2:1 (1 h, 4°). CC (SiO_2; $CH_2Cl_2 \rightarrow CH_2Cl_2$/MeOH 93:7) afforded 5.3 g (80%) of **6c**. White solid. TLC (CH_2Cl_2/MeOH 17:1): R_f 0.35. ^{1}H-NMR (300 MHz, CD_3OD): 3.87–4.07 (*m*, 2 H–C(5′), H–C(4′)); 4.45 (*dd*, $J = 2.5, 2.2$, H–C(3′)); 5.25 (*dd*, $J = 9.5, 2.6$, H–C(2′)); 6.43 (*d*, $J = 9.5$, H–C(1′)); 6.93–6.98 (*m*, 2 arom. H); 7.38–7.65 (*m*, 6 arom. H, H–C(5)); 7.87–8.03 (*m*, 4 arom. H); 8.24 (*d*, $J = 7.6$, H–C(6)).

---

[56]) Also isolated 1.3 g (11%) of 4′-*O*-benzoylated derivative. TLC (hexanes/AcOEt 1:4): R_f 0.4.

^{13}C-NMR (75 MHz, CD_3OD): 67.27 (*t*, C(5′)); 67.78, 70.7, 74.0 (3*d*, C(2′), C(3′), C(4′)); 80.38 (*d*, C(1′)); 99.2 (*d*, C(5)); 129.25, 129.61, 129.84, 130.65, 130.91, 131.03, 134.15, 134.66 (arom. C); 147.1 (*d*, C(6)); not assigned (C(2)); 165.1(*s*, C(4)); 166.77 (*s*, CO). FAB-MS (pos.): 453 (29, $[M+2\,H]^+$), 452 (97, $[M+H]^+$), 124 (47), 123 (35), 107 (88), 105 (74), 91 (56), 89 (74), 77 (100).

N^6,N^6-*Dibenzoyl-9-(2′-*O*-benzoyl-β-*D*-ribopyranosyl)adenine* (**6d**). From 11.0 g (15.8 mmol) of **5d** in MeOH/THF/CF_3COOH 10:2:1 (75 min, r.t.). CC (SiO_2; AcOEt/hexane 1:1 → 9:1) afforded 8.7 g (95%) of **6d**. White solid. TLC (AcOEt/hexane 4:1): R_f 0.40. ^{1}H-NMR (400 MHz, $CDCl_3$): 3.06, 3.61 (2 br. *s*, OH); 3.85–3.97 (*m*, 2 H–C(5′)); 4.08 (*m*, H–C(4′)); 4.54 (*dd*, *J* = 2.5, 2.5, H–C(3′)); 5.52 (*dd*, *J* = 9.5, 2.6, H–C(2′)); 6.28 (*d*, *J* = 9.5, H–C(1′)); 7.20 (*m*, 6 arom. H); 7.38 (*m*, 2 arom. H); 7.47 (*m*, arom. H); 7.73 (*m*, 6 arom. H); 8.26 (*s*, H–C(2)); 8.59 (*s*, H–C(8)). ^{13}C-NMR (75 MHz, $CDCl_3$): 66.2 (*t*, C(5′)); 66.2, 69.4, 71.6 (3*d*, C(2′), C(3′), C(4′)); 78.5 (*d*, C(1′)); 127.4 (*s*, C(5)); 128.3 (*s*, arom. C); 128.5, 128.6, 129.4, 129.7, 133.0, 133.8 (6*d*, arom. C); 143.1 (*d*, C(8)); 151.9 (*s*, C(4)); 152.4 (*d*, C(2)); 153.0 (*s*, C(6)); 164.8, 172.2 (2*s*, C=O). FAB-MS (pos., 3-NBA): 580.1 (49, $[M+H]^+$), 344.1 (13), 237.0 (21), 219.0 (19), 105.0 (100).

*2-Amino-9-(2-*O*-benzoyl-β-*D*-ribopyranosyl)-*N^2*-isobutyryl-6-[(prop-2-enyl)oxy]purine* (**6e**). From 3.75 g (6.11 mmol) of **5e** in MeOH/CF_3COOH 10:1 (90 min, r.t.). CC (SiO_2; CH_2Cl_2 → CH_2Cl_2/MeOH 94:6) afforded 2.6 g (85%) of **6e**. White foam. TLC (CH_2Cl_2/MeOH 9:1): R_f 0.55. ^{1}H-NMR (400 MHz, $CDCl_3$): 1.21 (*d*, *J* = 7.2, Me); 1.23 (*d*, *J* = 7.2, Me); 2.67 (br. *m*, CH of isobutyryl); 3.37 (*d*, *J* = 9.3, HO–C(4′)*); 4.03 (*dd*, *J* = 5.0, 10.3, H_{eq}–C(5′)); 4.14 (*m*, H–C(4′)); 4.24 (*t*, *J* = 10.6, H_{ax}–C(5′)); 4.87 (*d*, *J* = 5.7, H–C(3′), CH_2O (allyl)); 5.26 (*dq*, *J* = 1.2, 10.5, 1 H, CH_2 (allyl) (*E*)); 5.39 (*dq*, *J* = 1.5, 17.2, 1 H, CH_2 (allyl) (*Z*)); 5.60 (*dd*, *J* = 2.9, 9.7, H–C(2′)); 5.70 (br. *s*, HO–C(3′)*); 6.03 (*ddt*, *J* = 5.7, 10.5, 17.2, CH (allyl)); 6.75 (*d*, *J* = 9.7, H–C(1′)); 6.83 (*t*, *J* = 7.9, 2 H_m of Bz); 7.21 (*t*, *J* = 7.5, H_p of Bz); 7.58 (*d*, *J* = 8.4, 2 H_o of Bz); 7.78 (*s*, N^2H); 7.90 (*s*, H–C(8)). ^{13}C-NMR (100 MHz, $CDCl_3$): 19.3 (*q*, Me); 36.3 (*d*, CH of isobutyryl); 66.2 (*t*, C(5′)); 66.3 (*d*, C(4′)); 67.9 (*t*, CH_2O (allyl)); 68.5 (*d*, C(3′)); 71.3 (*d*, C(2′)); 77.7 (*d*, C(1′)); 118.4 (*s*, C(5)); 118.8 (*t*, $=CH_2$ (allyl)); 127.8 (*d*, C_m of Bz); 128.4 (*s*, C_{ipso} of Bz); 129.2 (*d*, C_o of Bz); 131.9 (*d*, =CH (allyl)); 133.2 (*d*, C_p of Bz); 139.3 (*d*, C(8)); 151.7, 153.1 (2*s*, C(2), C(4)); 160.3 (*s*, *C*(6)); 164.8 (*s*, C=O of Bz); 175.6 (*s*, C=O of isobutyryl). FAB-MS (pos.): 498.3 (55 $[M+H]^+$), 262.2 (39), 237.1 (21), 219.1 (20), 192.1 (13), 176.1 (14), 136.1 (77), 120.0 (24), 105.0 (52), 89.0 (33), 76.9 (35), 68.9 (15), 64.9 (18), 54.9 (18).

6-Amino-N^6,N^6*-dibenzoyl-9-(2′-*O*-benzoyl-β-*D*-ribopyranosyl)-6-[(prop-2-enyl)oxy]purine* (**6f**). A soln. of 3.93 g (5.2 mmol) of **5f** in 36 ml of MeOH and 2 ml of THF was treated with 6 ml of CF_3COOH, the mixture was kept at 25° for 3 h, and the reaction was monitored by TLC. The mixture was cooled to 0° and carefully neutralized with 2.2 g of solid $NaHCO_3$. The mixture was concentrated to *ca.* 10 ml and diluted with 100 ml of CH_2Cl_2, and washed with 30 ml of sat. aq. $NaHCO_3$ soln. The aq. phase was extracted with 3 × 70 ml of CH_2Cl_2 (aq. phase was monitored by TLC), the combined org. phases were dried (Na_2SO_4) and concentrated *in vacuo*. The residue was purified by CC (SiO_2; 1–8% MeOH in CH_2Cl_2) to afford 2.68 g (80.7%) of **6f**. TLC (5% MeOH in CH_2Cl_2): R_f 0.32. ^{1}H-NMR (300 MHz, CD_3OD): 3.91 (*dd*, *J* = 10.2, 5.2, H_β–C(5′)); 4.00 (*dd*, *J* = 10.3, 10.3, H_α–C(5′)); 4.08 (m, H–C(4′)); 4.47 (*dd*, *J* = 2.5, 2.5, H–C(3′)); 4.59 (*ddd*, *J* = 5.5, 1.5, 1.5, 2 H (allyl)); 5.12 (*dm*, *J* = 10.4, C=CH_2); 5.23 (*dm*, *J* = 17.2, C=CH_2); 5.60 (*dd*, *J* = 9.4, 2.5, H–C(2′)); 5.82 (*m*, C*H*=CH_2); 6.19 (*d*, *J* = 9.4, H–C(1′)); 7.10–7.19 (*m*, 15 arom. H); 8.43 (*s*, H–C(8)). ^{13}C-NMR (75 MHz, CD_3OD): 67.1, 69.9 (2*t*, C(5′), C(allyl)); 67.7, 70.4, 73.7 (3*d*, C(2′), C(3′), C(4′)); 80.1 (*d*, C(1′)); 118.4 (*t*, C=*C*H_2); 124.3 (*s*, C(5)); 129.6, 129.8, 130.4, 130.7, 133.8, 134.3, 134.7 (7*d*, arom. C, *C*=CH_2); 135.3 (*s*, arom. C); 144.9 (*d*, C(8)); 153.7, 156.4 (2*s*, C(2), C(4)); 162.2, 166.3, 173.5 (3*s*, C=O). FAB-MS (pos., 3-NBA): 636.2 (100, $[M+H]^+$), 514.2 (50), 400.1 (71), 278.1 (19), 237.1 (57), 219.1 (85).

2,6-Diamino-N^2,N^6*-dibenzoyl-9-(2′-*O*-benzoyl-β-*D*-ribopyranosyl)purine* (**6g**). To a soln. of 4.0 g (6.6 mmol) of **4g** in 30 ml of pyridine, cooled to 0°, were added 3.7 g (16.5 mmol) of BzOBz and 200 mg (1.6 mmol) of DMAP with stirring for 1.5 h. The mixture was poured into 200 ml of CH_2Cl_2, washed with 3 × 150 ml 20% aq. citric acid, 3 × 50 ml sat. aq. $NaHCO_3$ soln., dried (Na_2SO_4), and concentrated *in vacuo*. The residue was dissolved in 100 ml of MeOH and 10 ml of THF, cooled to 0° (ice bath), 15 ml of CF_3CO_2H was added, and the mixture was stirred at r.t. for 2.5 h. Then, 19.8 g (235 mmol) of solid $NaHCO_3$ was added slowly, and the mixture was stirred for 15 min. This mixture was adsorped on 30 g of SiO_2 and purified by CC (150 g of SiO_2; CH_2Cl_2 (0 → 5% MeOH)) to afford 2.97 g (76%) of **6g**. TLC (SiO_2; $CHCl_3$/MeOH 5:1): R_f 0.65. ^{1}H-NMR (400 MHz, CD_3OD): 3.96 (*dd*, *J* = 10.5, 4.1, H–C(4′)); 4.09 (*dd*, *J* = 10.7, 10.5, H_{ax}–C(5′)); 4.12 (*dd*, *J* = 10.7, 4.1, H_{eq}–C(5′)); 4.50 (*d*, *J* = 2.5, H–C(3′)); 5.57 (*dd*, *J* = 9.4, 2.5, H–C(2′)); 6.48 (*d*, *J* = 9.4, H–C(1′)); 7.2–8.2 (*m*, 15, arom. H); 8.52 (*s*, H–C(8)). ^{13}C-NMR (100 MHz, CD_3OD) 67.13 (*t*, C(5′)); 67.84 (*d*, C(4′)); 70.53 (*d*, C(3′)); 74.39 (*d*, C(2′)); 79.82 (*d*, C(1′)); 120.59 (*s*, C(5)); 129.07–134.03 (*d* + *s*, arom. C); 134.97, 135.67, 151.14 (*s*, C(2), C(4), C(6)); 166.45, 167.79, 170.00 (*s*, C=O). FAB-MS (pos., 3-NBA): 1189 (1, $[2M+H]^+$), 595 (7, $[M+H]^+$), 359 (15), 237 (4), 105 (52).

2.3. *General Procedure for the Preparation of the Nucleosides* **7a–7g** (*Scheme 2*). A mixture of **6a–6g**, DMT-Cl, and 4-Å molecular sieves was suspended in CH_2Cl_2, and immediately $EtN(i\text{-}Pr)_2$ was added. After completion of the reaction, aq. $NaHCO_3$ soln. was added, and the mixture was extracted with CH_2Cl_2. The org. phase was dried ($MgSO_4$), evaporated, and purified by CC (SiO_2).

N^3-*Benzoyl-1-{2′-*O*-benzoyl-4′-*O*-[bis(4-methoxyphenyl)(phenyl)methyl]-β-*D*-ribopyranosyl}uracil* (**7a**). From 10.0 g (22 mmol) of **6a**, 10.0 g (29.5 mmol) of 4,4′-DMT-Cl, 10 ml (59 mmol) of $EtN(i\text{-}Pr)_2$ and 5 g of molecular sieves in 80 ml of CH_2Cl_2 (1 h). CC (300 g SiO_2, hexanes/AcOEt 4:1 → 1:1 (+2% Et_3N)) afforded 14.7 g (86%) of **7a**. Yellow foam. TLC (AcOEt/hexane 1:1): R_f 0.50. ^{1}H-NMR (300 MHz, $CDCl_3$): 7.98 (2*d*, *J* = 8.3, 2 H); 7.63–7.23 (m, 16 H); 7.15–7.10 (br. *s*, 2 H); 6.87 (2*d*, *J* = 8.1, 4 H); 6.20 (*d*, *J* = 9.4, H–C(1′)); 5.77 (*d*, *J* = 8.3, H–C(5)); 4.88 (*dd*, *J* = 2.7, 9.6, H–C(2′)); 3.97 (*m*, 1 H); 3.91 (*m*, 2 H); 3.81 (*s*, 3 H); 3.80 (*s*, 3 H); 3.27 (*m*, 1 H); 2.55 (br. *s*, 1 H). ^{13}C-NMR (75 MHz, $CDCl_3$): 168.1 (*s*), 165.2 (*s*); 161.6 (*s*, C(4)); 159.0 (*s*); 149.2 (*s*, C(2)); 144.7 (*s*); 139.3 (*d*, C(6)); 135.6 (*s*); 134.8 (*d*); 133.8 (*d*); 133.6 (*s*); 131.1 (*s*); 130.2 (*d*); 130.1 (*d*); 130.0 (*d*); 128.9 (*d*); 128.7 (*d*); 128.2 (*d*); 127.9 (*d*); 127.6 (*s*); 127.5 (*s*); 127.4 (*d*); 113.6 (*d*); 102.9 (*d*, C(5)); 87.5 (*d*, C(1′)); 77.9 (*s*); 70.3 (*d*); 69.0 (*d*), 68.6 (*d*); 65.0 (*t*, C(5′)); 55.3 (*q*). FAB-MS (pos.): 754 (4, $[M+H]^+$), 304 (51), 303 (100), 105 (28).

N^3-*Benzoyl-1-{2′-*O*-benzoyl-4′-*O*-[bis(4-methoxyphenyl)(phenyl)methyl]-β-*D*-ribopyranosyl}thymine* (**7b**). From 8.0 g (17 mmol) of **6b**, 7.5 g (22 mmol) of DMT-Cl, 7.5 ml (44 mmol) of $EtN(i\text{-}Pr)_2$ and 5 g of molecular sieves in 70 ml of CH_2Cl_2 (1 h). The crude product (15.5 g yellow foam) was used in the next reaction without further purification. For characterization purposes, a small portion was purified by CC (SiO_2; hexanes/AcOEt 1:1 (+2% Et_3N)). TLC (AcOEt/hexane 2:1): R_f 0.75. ^{1}H-NMR (300 MHz, $CDCl_3$): 7.98 (*d*, *J* = 8.1, 2 H); 7.63–7.23 (*m*, 16 H); 7.15–7.10 (br. *s*, 2 H); 6.87 (*d*, *J* = 8.1, 4 H); 6.20 (*d*, *J* = 9.5, H–C(1′)); 4.88 (*dd*, *J* = 2.7, 9.5, H–C(2′)); 3.94 (*m*, 2 H); 3.82 (*s*, 6 H); 3.72 (br. *s*, H–C(3′)); 3.28 (*m*, H–C(5′)); 2.48 (*s*, 1 H); 1.92 (*s*, 3 H, Me–C(5)). FAB-MS (pos.): 768 (1, $[M+H]^+$), 304 (44), 303 (100), 105 (30).

N^4-*Benzoyl-1-{2′-*O*-benzoyl-4′-*O*-[bis(4-methoxyphenyl)(phenyl)methyl]-β-*D*-ribopyranosyl}cytosine* (**7c**). From 5.3 g (11.8 mmol) of **6c**, 6.0 g (17.7 mmol) of DMT-Cl, 4 ml (23.6 mmol) of $EtN(i\text{-}Pr)_2$, and 3 g of molecular sieves in 40 ml of CH_2Cl_2 (4 h). CC (300 g SiO_2; 0 → 12% acetone in CH_2Cl_2 (+2% Et_3N)) afforded 7.2 g (82%) of **7c**. Yellow solid. TLC (CH_2Cl_2/acetone 9:1): R_f 0.25. ^{1}H-NMR (300 MHz, $CDCl_3$): 3.25–3.28 (*m*, H–C(5′)); 3.76–3.79 (*m*, H–C(3′)); 3.8, 3.81 (2*s*, 2 MeO); 3.88–4 (*m*, H–C(4′), H–C(5′)); 4.84 (*dd*, *J* = 9.5, 2.7, H–C(2′)); 6.46 (*d*, *J* = 9.0, H–C(1′)); 6.87 (*dd*, *J* = 9, 0.9, 4 arom. H); 7.2–7.99 (*m*, 19 arom. H, H–C(5), H–C(6), NH). ^{13}C-NMR (75 MHz, $CDCl_3$): 55.32 (*q*, MeO); 65.12 (*t*, C-(5′)); 68.83, 69.0, 71.35 (3*d*, C(2′), C(3′), C(4′)); 78.66 (*d*, C(1′)); 87.5 (*s*, Ar_3C); 97.57 (*d*, C(5)); 113.4, 113.65 (2*d*, arom. C); 127.38, 127.62, 127.9, 128.21, 128.55, 128.89, 128.99, 130, 133.17, 133.53 (arom. C); 135.74 (*s*, arom. C); 143.99 (*d*, C(6)); 159.1 (*s*, arom. C, C(2)); 161.97 (*s*, C(4)); 165.25 (*s*, CO). FAB-MS (pos.): 1508 (8, $[2M+2H]^+$), 1507 (8, $[2M+H]^+$), 754 (27, $[M+H]^+$), 319 (20), 305 (27), 304 (80), 303 (99), 289 (25), 216 (53), 107 (21), 106 (22), 105 (100), 89 (21), 77 (40).

N^6,N^6-*Dibenzoyl-9-{2′-*O*-benzoyl-4′-*O*-[bis(4-methoxyphenyl)(phenyl)methyl]-β-*D*-ribopyranosyl}adenine* (**7d**). From 8.6 g (14.9 mmol) of **6d**, 7.1 g (20.8 mmol) of DMT-Cl, 6.6 ml (38.6 mmol) of $EtN(i\text{-}Pr)_2$, and 12 g of molecular sieves in 60 ml of CH_2Cl_2 (90 min). CC (SiO_2; hexanes/AcOEt 7:3 → 3:7 (+2% Et_3N)) afforded 10.5 g (80%) of **7d**. Yellow solid. TLC (AcOEt/hexane 1:1): R_f 0.29. ^{1}H-NMR (400 MHz, $CDCl_3$): 3.38 (*dd*, *J* = 10.6, 4.7, H_β–C(5′)); 3.74 (br. *t*, H–C(3′)); 3.80 (*s*, 2 MeO); 4.02 (*dd*, *J* = 10.5, 10.5, H_α–C(5′)); 4.05 (*m*, H–C(4′)); 5.35 (*dd*, *J* = 9.5, 2.3, H–C(2′)); 6.26 (*d*, *J* = 9.6, H–C(1′)); 6.87 (*d*, *J* = 8.4, 4 arom. H); 7.15–7.50 (*m*, 18 arom. H); 7.74 (*m*, 6 arom. H), 8.11 (*s*, H–C(2)); 8.60 (*s*, H–C(8)). ^{13}C-NMR (100 MHz, $CDCl_3$): 55.3 (*q*, MeO); 65.1 (*t*, C(5′)); 68.5, 68.7, 70.6 (3*d*, C(2′), C(3′), C(4′)); 78.3 (*d*, C(1′)); 87.5 (*s*, Ar_3C); 113.6 (*d*, arom. C); 127.3 (*s*, C(5)); 127.4, 127.8, 128.2, 128.4, 128.6 (5*d*, arom. C); 128.6, 128.7 (2*s*, arom. C); 129.3, 129.7, 129.9, 130.0, 132.8, 133.5 (6*d*, arom. C); 133.9, 135.5, 136.6 (3*s*, arom. C); 142.9 (*d*, C(8)); 144.7 (*s*, arom. C); 151.8 (*s*, C(4)); 152.4 (*d*, C(2)); 153.1 (*s*, C(6)); 164.6 (*s*, arom. C); 164.6, 172.1 (2*s*, C=O). FAB-MS (pos., 3-NBA): 882.3 (11, $[M+H]^+$), 399.2 (15), 303.1 (100), 105.0 (61).

*2-Amino-9-{2′-*O*-benzoyl-4′-*O*-[bis(4-methoxyphenyl)(phenyl)methyl]-β-*D*-ribopyranosyl}-*N^2-*isobutyryl-6-[(prop-2-enyl)oxy]purine* (**7e**). From 2.85 g (5.73 mmol) of **6e**, 2.9 g (8.6 mmol) of DMT-Cl, 1.95 ml (11.5 mmol) of $EtN(i\text{-}Pr)_2$, and 5 g of molecular sieves in 40 ml of CH_2Cl_2 (1 h). CC (SiO_2; CH_2Cl_2 → CH_2Cl_2/MeOH 96:4 (+2% Et_3N)) afforded 4.1 g (85%) of **7e**. Yellow solid. TLC (CH_2Cl_2/acetone 93:7): R_f 0.41. ^{1}H-NMR (500 MHz, $CDCl_3$): 1.23 (*d*, *J* = 7.0, Me of isobutyryl); 1.25 (*d*, *J* = 6.9, Me of isobutyryl); 2.77 (br. *s*, OH); 3.28 (*dd*, *J* = 4.3, 10.4, H_{eq}–C(5′)); 3.32 (br. *m*, CH of isobutyryl); 3.80 (*s*, 2 MeO); 3.86 (br. *s*, H–C(3′)); 3.98 (*t*, *J* = 10.4, H_{ax}–C(5′)); 4.02 (*ddd*, *J* = 2.3, 4.4, 10.5, *H*–C(4′)); 4.97 (*dt*, *J* = 1.4, 5.7, CH_2O (allyl)); 5.24 (*dq*, *J* = 1.3, 10.5, 1 H, $=CH_2$ (allyl) (*E*)); 5.38 (*dd*, *J* = 2.6, 9.6, H–C(2′)); 5.39 (*dq*, *J* = 1.5, 17.2, 1 H; $=CH_2$ (allyl) (*Z*)); 6.05 (*ddt*, *J* = 5.7, 10.5, 17.2, =CH (allyl)); 6.13 (*d*, *J* = 9.6, H–C(1′)); 6.87 (*d*, *J* = 9.0, 2 H_o to MeO); 6.87 (*d*,

$J = 9.0$, 2 H_o to MeO); 7.25 (t, $J = 7.3$, H_p of DMT); 7.27 (t, $J = 7.9$, 2 H_m of Bz); 7.32 (t, $J \approx 7.6$, 2 arom.H); 7.39 (d, $J = 9.0$, 2 H_m to MeO); 7.40 (d, $J = 9.0$, 2 H_m to MeO); 7.44 (t, $J = 7.5$, H_p of Bz); 7.49 (d, $J = 8.4$, 2 H_o of DMT (unsubst. Ph)); 7.76 (d, $J = 8.4$, 2 H_o of Bz); 7.87 (s, H–C(8)); 7.88 (s, N^2H). ^{13}C-NMR (125 MHz, $CDCl_3$): 19.2, 19.3 (2q, Me of isobutyryl); 34.9 (d, CH of isobutyryl); 55.3 (q, MeO); 64.9 (t, C(5′)); 67.9 (t, CH_2O (allyl)); 68.7, 68.8 (2d, C(3′), C(4′)); 70.5 (d, C(2′)); 78.3 (d, C(1′)); 87.5 (s, Ar_3CO of DMT); 113.6 (d, C_o to MeO); 113.6 (d, C_o to MeO); 117.9 (s, C(5)); 118.7 (t, CH_2 (allyl)); 127.4 (d, C_p of DMT); 127.8 (d, C_m of Bz); 128.2 (d, C_o of DMT); 128.3 (d, C_m of DMT); 128.8 (s, C_{ipso} of Bz); 129.7 (d, C_o of Bz); 129.9 (d, C_m to MeO); 132.1 (d, =CH (allyl)); 133.4 (d, C_p of Bz); 135.6 (s, C_{ipso} to Ar_3CO of DMT); 135.7 (s, C_{ipso} to Ar_3CO of DMT); 139.8 (d, C(8)); 144.8 (s, C_{ipso} of DMT); 152.1, 152.9 (2s, C(2), C(4)); 159.1 (s, C_{ipso} to MeO); 160.6 (s, C(6)); 164.6 (s, C=O of Bz); 177.0 (s, C=O of isobutyryl). MS: 800.4 (13, $[M+H]^+$), 303.1 (100), 262.1 (12), 165.1 (10), 136.0 (18), 115.0 (21), 105.0 (20), 90.9 (17), 86.9 (22), 76.9 (23), 72.9 (41), 54.8 (18).

6-Amino-N^6,N^6-*dibenzoyl-9-{2′*-O-*benzoyl-4′*-O-*[bis(4-methoxyphenyl)(phenyl)methyl]-β*-D-*ribopyranosyl}purine* (**7f**). A soln. of 2.29 g (3.6 mmol) of **6f** in 15 ml of CH_2Cl_2 was kept over 3.4 g of 3-Å molecular sieves for 2.5 h, and 1.34 g (4.0 mmol) of DMT-Cl and 1.5 ml (8.8 mmol) of EtN(i-Pr)$_2$ were added, and the mixture was stirred for 1.25 h at 25°. The reaction was quenched with 0.5 ml of MeOH, and the mixture was stirred for 10 min, diluted with 150 ml of CH_2Cl_2 and washed with 70 ml of sat. aq. mit $NaHCO_3$. The aq. phase was re-extracted with 2 × CH_2Cl_2. The combined org. phases were dried (Na_2SO_4), concentrated *in vacuo*, and purified by CC (SiO_2; 30–50% AcOEt in hexanes, 5% MeOH) to afford 3.37 g (99.7%) of **7f**[57]. TLC (30% AcOEt, 65% hexanes, 5% MeOH): R_f 0.14. ^{1}H-NMR (400 MHz, $CDCl_3$): 2.52 (s, OH); 3.29 (dd, $J = 10.2$, 4.1, H_β–C(5′)); 3.75 (m, H–C(3′)); 3.79 (s, 2, MeO); 3.97 (dd, $J = 10.4$, 10.4, H_α–C(5′)); 4.01 (m, H–C(4′)); 4.47 (br. d, $J = 5.7$, 2 H (allyl)); 5.10 (dm, $J = 10.4$, C=CH_2); 5.20 (dm, $J = 17.2$, C=CH_2); 5.25 (dd, $J = 9.6$, 2.0, H–C(2′)); 5.75 (m, CH=CH_2); 6.19 (d, $J = 9.6$, H–C(1′)); 6.86 (d, $J = 8.5$, 4 arom. H); 7.13–7.87 (m, 24 arom. H); 7.92 (s, H–C(8)). ^{13}C-NMR (100 MHz, $CDCl_3$): 55.3 (q, MeO); 64.9, 64.8 (2t, C(5′), C(allyl)); 68.6, 68.7, 70.6 (3d, C(2′), C(3′), C(4′)); 77.7 (d, C(1′)); 87.5 (s, Ar_3C); 113.6 (d, arom. C); 118.3 (t, C=CH_2); 122.8 (s, C(5)); 127.4; 127.8; 128.0; 128.2; 128.4; 128.5; 128.6; 128.7; 129.3; 129.8; 129.9; 132.4; 132.8; 133.4 (3d); 133.9, 135.6 (2s, arom. C); 141.4 (d, C(8)); 152.1, 155.3 (2s, C(2), C(4)); 159.1, 160.6 (2s, C=O, C(6)); 164.6, 172.0 (2s, C=O). FAB-MS (pos., 3-NBA): 938.3 (32, $[M+H]^+$), 400.1 (6), 303.1 (100).

2,6-Diamino-N^2,N^6-*dibenzoyl-9-{2′*-O-*benzoyl-4′*-O-*[bis(4-methoxyphenyl)(phenyl)methyl]-β*-D-*ribopyranosyl}purine* (**7g**). In a 10-ml round-bottomed flask was placed 1.0 g (1.7 mmol) of **6g**, 3-Å molecular sieves, and 1.25 g (3.8 mmol) of DMT-Cl under Ar. To this mixture was added 5.0 ml of CH_2Cl_2, followed by 0.63 g (5.1 mmol) of EtN(i-Pr)$_2$; the mixture was sonicated at r.t. for 5 min and shaken for 30 min. The mixture was treated with 0.5 g of DMT-Cl at intervals of 15 min. After three such additions, TLC analysis indicated disappearance of the starting material. The mixture was purified by CC (50 g SiO_2; AcOEt/hexanes 1:3 → 10:1) to afford 0.31 g of **6g** and 0.98 g (65%) of **7g**. TLC (SiO_2; AcOEt/hexanes 1:4 (with 2% MeOH)): R_f 0.54. ^{1}H-NMR (400 MHz, $CDCl_3$): 2.49 (dd, $J = 11.0$, 4.9, H_{ax}–C(5′)); 3.61 (dd, $J = 11.0$, 10.5, H_{eq}–C(5′)); 3.77 (s, 2 MeO); 4.0 (ddd, $J = 10.5$, 4.9, 2.7, H–C(4′)); 4.44 (br. s, H–C(3′)); 5.73 (d, $J = 9.2$, H–C(2′)); 5.89 (d, $J = 9.2$, H–C(1′)); 6.77–8.3 (m, 29 arom. H, H–C(8)); 9.25, 9.41 (br. s, 2 NH). ^{13}C-NMR (75 MHz, $CDCl_3$) 55.23 (q, MeO); 65.25 (t, C(5′)); 68.38 (d, C(4′)); 70.05 (d, C(3′)); 74.21 (d, C(2′)); 80.09 (d, C(1′)); 87.42 (s, C(trityl)); 113.63 (d, arom. C); 118.56 (s, C(5)); 127.48–133.53 ($d+s$, arom. C); 134.12, 136.10, 136.24 (s, C(2), C(4), C(6)); 141.69 (d, C(8)); 166.67, 167.24, 169.09 (s, C=O). FAB-MS (pos., 3-NBA): 1794 (1, $[2M+2H]^+$), 897 (21, $[M+H]^+$), 358 (35), 303 (100), 154 (25), 105 (45).

2.4. *General Procedure for the Preparation of the Nucleosides* **8a**–**8g** (*Scheme 2*). A mixture of the **8a**–**8g**, 4-nitrophenol, and DMAP in pyridine, PrOH, and EtN(i-Pr)$_2$ or Et_3N was stirred at 60° until no further change in the product composition could be observed. The mixture was evaporated and co-evaporated 2 × with toluene. The residue was dissolved in 200 ml of CH_2Cl_2, washed with 6 × 200 ml sat. aq. $NaHCO_3$ soln. and with 2 × 100 ml 20% aq. citric acid soln. The org. phase was dried ($MgSO_4$), evaporated, and purified by CC.

1-{3′-O-*Benzoyl-4′*-O-*[bis(4-methoxyphenyl)(phenyl)methyl]-β*-D-*ribopyranosyl}uracil* (**8a**). From 9 g (11.9 mmol) of **7a**, 3.22 g (24 mmol) of 4-nitrophenol, 1.55 g (12.4 mmol) of DMAP, in 120 ml of pyridine, 50 ml PrOH, and 6.2 ml (36 mmol) of EtN(i-Pr)$_2$ (70 h, 60°). Purification by CC (400 g SiO_2, hexanes/AcOEt 1:1 → 3:7 (+2.5% Et_3N)) afforded 5.2 g (67%) of **8a**. Colorless foam. TLC (AcOEt/hexanes 7:3): R_f 0.50. ^{1}H-NMR (300 MHz, $CDCl_3$): 8.17 (2d, $J = 7.0$, 2 H); 7.62–7.15 (m, 12 H); 7.05 (d, $J = 8.2$, H–C(6)); 6.71 (2d, $J = 8.9$, 4 H); 5.88 (br. s, H–C(3′)); 5.76 (d, $J = 9.5$, H–C(1′)); 5.40 (d, $J = 8.2$, H–C(5)); 3.85 (ddd, $J = 2.8$, 5.3, 11.0, H–C(4′)); 3.78 (s, 3 H); 3.77 (s, 3 H); 3.60 (t, $J = 8.0$, H_{ax}–C(5′)); 3.52 (dd, $J = 2.8$, 9.4, H–C(2′)); 2.60 (dd, $J =$

[57]) When the reaction is allowed to proceed for longer times, benzoate migration (2′ → 3′) is observed.

5.0, 11.1, H_{eq}–C(5′)). ^{13}C-NMR (75 MHz, $CDCl_3$): 166.5 (*s*), 162.8 (*s*, C(4)); 158.8 (*s*); 151.1 (*s*, C(2)); 144.9 (*s*); 139.2 (*d*, C(6)); 136.0 (*s*); 135.8 (*d*); 133.3 (*d*); 130.1 (*d*); 130.0 (*d*); 128.5 (*d*); 128.0 (*d*); 127.1 (*d*); 113.4 (*d*); 103.0 (*d*, C(5)); 87.3 (*s*); 80.9 (*d*, C(1′)); 74.0 (*d*), 69.4 (*d*); 67.9 (*d*); 65.8 (*t*, C(5′)); 55.3 (*q*). FAB-MS (pos.): 650 (2, $[M+H]^+$), 304 (33), 303 (100).

*1-{3′-*O*-Benzoyl-4′-*O*-[bis(4-methoxyphenyl)(phenyl)methyl]-β-*D*-ribopyranosyl}thymine* (**8b**). From 9.5 g (*ca.* 10.4 mmol) of **7b** (crude product), 2.9 g (21 mmol) of 4-nitrophenol, 1.27 g (10.4 mmol) of DMAP, in 110 ml of pyridine, 44 ml of PrOH, and 5.4 ml (31 mmol) of EtN(i-Pr)$_2$ (72 h, 60°). CC (400 g of SiO_2; hexanes/AcOEt 2:1 → 3:7 (+2.5% Et_3N)) afforded 3.9 g (56%) of **8b**. Colorless foam. TLC (AcOEt/hexanes 3:1): R_f 0.40. ^{1}H-NMR (300 MHz, $CDCl_3$): 8.17 (2*d*, *J* = 7,0, 2 H); 7.62–7.15 (*m*, 12 H); 6.87 (*d*, *J* = 1.2, H–C(6)); 6.79 (2*d*, *J* = 7,0, 4 H); 5.96 (br. *s*, H–C(3′)); 5.90 (*d*, *J* = 9,5, H–C(1′)); 4.50 (br. *s*, 1 H); 3.88 (*ddd*, *J* = 2.5, 5.2, 10.5, H–C(4′)); 3.79 (*s*, 3 H); 3,78 (*s*, 3 H); 3.61 (*t*, *J* = 11.2, H_{ax}–C(5′)); 3.52 (br. *m*, H–C(2′)); 2.59 (*dd*, *J* = 5.2, 11.5, H_{eq}–C(5′)). ^{13}C-NMR (75 MHz, $CDCl_3$): 166.3 (*s*); 163.3 (*s*, C(4)); 158.8 (*s*); 151.4 (*s*, C(2)); 145.0 (*s*); 136.1 (*d*, C(6)); 135.9 (*s*); 134.6 (*d*); 133.2 (*d*); 130.3 (*d*); 130.2 (*d*); 130.1 (*d*); 129.9 (*d*); 128.8 (*d*); 128.6 (*d*); 128.3 (*d*); 128.0 (*d*); 127.0 (*d*); 113,4 (*d*); 113.3 (*d*); 111.8 (*s*, C(5)); 87.3 (*s*); 80.7 (*d*, C(1′)); 74.1 (*d*), 69.5 (*d*); 68.1 (*d*); 65.8 (*t*, C(5′)); 55.2 (*q*); 11.9 (*q*, *Me*–C(5)). FAB-MS (pos.): 664 (4, $[M+H]^+$), 304 (73), 303 (100), 105 (45).

N^4*-Benzoyl-1-{3′-*O*-benzoyl-4′-*O*-[bis(4-methoxyphenyl)(phenyl)methyl]-β-*D*-ribopyranosyl}cytosine* (**8c**). From 1.0 g (1.3 mmol) of **7c**, 362 mg (2.6 mmol) of 4-nitrophenol, 195 mg (1.2 mmol) of DMAP, in 20 ml of pyridine, 4 ml of PrOH, and 0.55 ml (3.9 mmol) of Et_3N (72 h, 85°). CC (SiO_2; CH_2Cl_2 → CH_2Cl_2/acetone 12:88) afforded 978 mg of a 4:1 mixture **8c**/**7c**, which was dissolved in 5 ml of CH_2Cl_2 and 8.5 ml of Et_2O, from which, after 16 h at r.t., colorless crystals were collected to give 365 mg (48%) of **8c**. TLC (CH_2Cl_2/acetone 9:1): R_f 0.25. ^{1}H-NMR (400 MHz, $CDCl_3$): 2.71 (*dd*, *J* = 11.3, 4.8, H–C(5′)); 3.66–3.76 (*m*, H–C(2′), H–C(5′)); 3.76, 3.77 (2*s*, MeO); 3.91–3.95 (*m*, H–C(4′)); 5.88 (*s*, H–C(3′)); 6.03 (*d*, *J* = 9.3, H–C(1′)); 6.76–6.82 (*m*, 4 arom. H); 7.15–7.66 (*m*, 16 arom. H, H–C(5)); 7.7 (*d*, *J* = 7.6, H–C(6)); 7.87 (*d*, *J* = 7.5, 2 arom. H); 8.19–8.22 (*m*, 2 arom. H); 8.81 (*s*, NH). ^{13}C-NMR (100 MHz, $CDCl_3$): 55.24 (*q*, MeO); 66.05 (*t*, C(5′)); 67.86 (*d*, C(4′)); 71.39 (*d*, C(3′)); 73.97 (*d*, C(2′)); 82.29 (*d*, C(1′)); 87.36 (*s*, Ar_3C); 97.51 (*d*, C(5)); 113.33, 113.40 (2*d*, arom. C); 127.05, 127.66, 127.97, 128.01, 128.33, 128.63, 129.01, 129.99, 130.07, 130.12, 132.88, 133.24, 133.44 (arom. C); 135.86, 136.02 (2*s*, arom. C), 144.18 (*d*, C(6)); 144.91 (*s*, arom. C); 156.91 (*s*, C(2′)); 158.76 (*s*, arom. C); 162.26 (*s*, C(4)); 166.57 (s, CO). FAB-MS (pos., 3-NBA): 1508 (5, $[2M+2H]^+$), 755 (5, $[M+2H]^+$), 754 (11, $[M+H]^+$), 319 (1), 305 (18), 304 (72), 303 (100), 289 (16), 216 (50), 121 (16), 107 (24), 106 (20), 105 (74), 89 (24), 77 (42).

N^6*-Benzoyl-9-{3′-*O*-benzoyl-4′-*O*-[bis(4-methoxyphenyl)(phenyl)methyl]-β-*D*-ribopyranosyl}adenine* (**8d**). From 2.6 g (3 mmol) of **7d**, 820 mg (5.9 mmol) of 4-nitrophenol, 400 mg (3.2 mmol) of DMAP, in 20 ml of pyridine, 4 ml of PrOH, and 1.23 ml (8.9 mmol) of Et_3N (48 h, 60°). CC (400 g of SiO_2; hexanes/AcOEt 9:1 → 2:3) afforded 1.54 g (67%) of **8d**. Colorless foam. TLC (AcOEt/hexane 4:1): R_f 0.13. ^{1}H-NMR (300 MHz, $CDCl_3$): 2.79 (*dd*, *J* = 11.4, 5.1, H_β–C(5′)); 3.76, 3.77 (2*s*, 2 MeO); 3.79 (*m*, H_α–C(5′)); 4.04 (m, H–C(4′)); 4.39 (br. *m*, H–C(2′)); 4.63 (br. *s*, OH); 5.81 (*d*, *J* = 9.2, H–C(1′)); 5.92 (br. *s*, H–C(3′)); 6.80 (*m*, 4 arom. H); 7.13–7.70 (*m*, 15 arom. H); 7.94 (*d*, *J* = 7.3, 2 arom. H); 8.01 (*s*, H–C(2)); 8.25 (*m*, 2 arom. H); 8.60 (*s*, H–C(8)); 8.97 (br. *s*, NH). ^{13}C-NMR (75 MHz, $CDCl_3$): 55.3 (*q*, MeO); 65.7 (*t*, C(5′)); 67.8, 69.0, 73.9 (3*d*, C(2′), C(3′), C(4′)); 82.3 (*d*, C(1′)); 87.4 (*s*, Ar_3C); 113.4 (*d*, arom. C); 122.4 (*s*, C(5)); 127.1, 127.8, 128.0, 128.7, 128.8, 130.1, 130.1, 132.8, 133.5 (9*d*, arom. C); 133.6, 135.9, 136.0 (3*s*, arom. C); 141.8 (*d*, C(8)); 145.0 (*s*, arom. C); 149.2, 151.6 (2*s*, C(4), C(6)); 152.8 (*d*, C(2)); 158.8 (*s*, arom. C); 164.5, 166.9 (2*s*, C=O). FAB-MS (pos. 3-NBA): 778.2 (14, $[M+H]^+$), 303.1 (100), 240.1 (39), 154.0 (34), 136.0 (31), 105.0 (49).

*2-Amino-9-{3′-*O*-benzoyl-4′-*O*-[bis(4-methoxyphenyl)(phenyl)methyl]-β-*D*-ribopyranosyl}-*N^2*-isobutyryl-6-[(prop-2-enyl)oxy]purine* (**8e**). From 4.1 g (5.1 mmol) of **7e**, 1.43 g (10.3 mmol) of 4-nitrophenol, 0.63 g (5.1 mmol) of DMAP, in 50 ml of pyridine, 15.3 ml of PrOH, and 2.1 ml (15.4 mmol) of Et_3N (60 h, 60°). CC (SiO_2; CH_2Cl_2 → CH_2Cl_2/acetone 12:88) afforded 3.3 g (80%) of **8e**. White foam[58]). TLC (CH_2Cl_2/acetone 93:7): R_f 0.28. ^{1}H-NMR (400 MHz, $CDCl_3$): 1.21 (*d*, *J* = 7.0, Me of isobutyryl); 1.23 (*d*, *J* = 7.0, Me of isobutyryl); 2.58 (*dd*, *J* = 5.0, 11.0, H_{eq}–C(5′)); 2.86 (br. *m*, CH of isobutyryl); 3.68 (*t*, *J* = 10.9, H_{ax}–*C*(5′)); 3.76–3.78 (*s*, 2, MeO); 3.95 (*ddd*, *J* = 2.7, 5.3, 10.4, *H*–C(4′)); 4.44 (*dd*, *J* = 3.6, 8.4, H–C(2′)); 4.99 (*dt*, *J* = 1.2, 5.6, *CH*$_2$O (allyl)); 5.26 (*dq*, *J* = 1.2, 10.5, 1 H, CH_2 (allyl) (*E*)); 5.38 (br. *s*, OH); 5.41 (*dq*, *J* = 1.4, 17.2, 1 H, =CH_2 (allyl) (*Z*)); 5.68 (*d*, *J* = 9.2, H–C(1′)); 6.07 (*ddt*, *J* = 5.6, 10.4, 17.2, =CH (allyl)); 6.10 (br. *s*, H–C(3′)); 6.79 (*d*, *J* = 8.9, 2 H_o to MeO); 6.82 (*d*, *J* = 8.9, 2 H_o to MeO); 7.18 (*t*, *J* ≈ 7.3, H_p of DMT); 7.22 (*t*, *J* ≈ 7.6, 2 H_m of DMT (unsubst. Ph)); 7.35 (*d*, *J* = 8.9, 2 H_m to MeO); 7.42 (*d*, *J* = 8.9, 2 H_m to MeO); 7.45 (*d*, *J* ≈ 8.4, 2 H_o of DMT (unsubst. Ph)); 7.54 (*t*, *J* ≈ 7.6, 2 H_m of Bz); 7.64 (*t*, *J* = 7.4, H_p of Bz); 7.85 (*s*, N^2H); 7.89 (*s*, H–C(8)); 8.24 (*d*, *J* ≈

[58]) Also recovered 0.8 g (20%) of **7e** and a mixture of **7e**/**8e**.

7.8, 2 H_o of Bz). ^{13}C-NMR (100 MHz, $CDCl_3$): 19.2, 19.3 (2*q*, Me of isobutyryl); 36.0 (*d*, CH of isobutyryl); 55.2 (*q*, MeO); 65.1 (*t*, C(5′)); 67.9 (*t*, *C*H_2O (allyl)); 68.1 (*d*, C(4′)); 68.2 (*d*, C(2′)); 74.1 (*d*, C(3′)); 83.5 (*d*, C(1′)); 87.3 (*s*, Ar_3*C*O of DMT); 113.3 (*d*, C_o to MeO); 113.4 (*d*, C_o to MeO); 118.0 (*s*, C(5)); 118.7 (*t*, =CH_2 (allyl)); 127.0 (*d*, C_p of DMT (unsubst. Ph)); 128.0 (*d*, C_o of DMT (unsubst. Ph); 128.0 (*d*, C_m of DMT (unsubst. Ph)); 128.6 (*d*, C_m of Bz); 130.0 (*d*, C_o of Bz); 130.2 (*d*, C_m to MeO); 130.4 (*s*, C_{ipso} of Bz); 132.0 (*d*, =CH (allyl)); 133.2 (*d*, C_p of Bz); 136.0 (*s*, C_{ipso} to Ar_3CO); 136.1 (*s*, C_{ipso} to Ar_3CO); 141.4 (*d*, C(8)); 145.1 (*s*, C_{ipso} of DMT (unsubst. Ph)); 151.5, 152.0 (2*s*, C(2), C(4)); 158.8 (*s*, C_{ipso} to MeO); 160.6 (*s*, C(6)); 166.4 (*s*, C=O of Bz); 175.8 (*s*, C=O of isobutyryl). FAB-MS (pos. 3-NBA): 800.2 (3, $[M+H]^+$), 303.0 (100), 262.0 (14), 104.8 (16), 76.8 (14).

6-Amino-N^6*-benzoyl-9-[3′*-O*-benzoyl-4′*-O*-[bis(4-methoxyphenyl)(phenyl)methyl]-β-*D*-ribopyranosyl]purine* (**8f**). A soln. of 2.94 g (3.1 mmol) of **7f** in 30 ml of pyridine was stirred with 9.7 ml (0.13 mol) of PrOH, 1.33 ml (9.5 mmol) of Et_3N, 0.87 g (6.3 mmol) of 4-nitrophenol, and 422 mg (3.4 mmol) of DMAP for 24 h at 60°. The mixture was concentrated *in vacuo*, taken up in 150 ml of CH_2Cl_2, washed with 150 ml of sat. aq. $NaHCO_3$ soln., and the aq. phase was re-extracted 2 × with CH_2Cl_2. The combined org. phases were dried (Na_2SO_4), concentrated *in vacuo*, and the residue was co-evaporated 2 × with toluene. The residue was purified by CC (SiO_2; 1–5% MeOH in CH_2Cl_2) to afford 1.41 mg (54%) of **8f**. TLC (2% MeOH in CH_2Cl_2): R_f 0.13. ^{1}H-NMR (400 MHz, $CDCl_3$): 1.9 (br. *s*, OH); 2.74 (*dd*, *J* = 11.3, 5.1, H_β–C(5′)); 3.72 (*dd*, H_α–C(5′)); 3.76, 3.77 (2*s*, 2 MeO); 4.00 (*m*, H–C(4′)); 4.29 (*dd*, *J* = 9.3, 2.8, H–C(2′)); 4.80 (*ddd*, *J* = 5.8, 1.2, 1.2, 2 H (allyl)); 5.16 (*ddd*, *J* = 10.4, 2.5, 1.1, C=CH_2); 5.33 (*ddd*, *J* = 17.2, 3.0, 1.5, C=CH_2); 5.71 (*d*, *J* = 9.3, H–C(1′)); 5.92 (br. *s*, H–C(3′)); 5.98 (*m*, C*H*=CH_2); 6.80 (*m* 4 arom. H); 7.15–8.30 (*m*, 19 arom. H); 7.18 (*s*, H–C(8)); 8.87 (br. *s*, NH). ^{13}C-NMR (100 MHz, $CDCl_3$): 55.2 (*q*, MeO); 65.6, 69.0 (2*t*, C(5′), C(allyl)); 67.9, 68.9, 73.9 (3*d*, C(2′), C(3′), C(4′)); 81.8 (*d*, C(1′)); 87.3 (*s*, Ar_3C); 113.4, 113.4 (2*d*, arom. C); 115.8 (*d*, arom. C); 118.3 (*s*, C(5)); 118.4 (*t*, C=*C*H_2); 126.0, 127.1, 127.9, 128.0, 128.0, 128.7, 128.7, 130.0, 130.1, 130.1, 130.1, 132.6, 132.7, 133.5, 133.5 (15*d*, arom. C, *C*=CH_2); 135.8, 136.0 (2*s*, arom. C); 140.2 (*d*, C(8)); 144.9 (*s*, arom. C); 150.0, 153.8 (2*s*, C(2), C(4)); 158.8 (*s*, arom. C); 161.0 (*s*, C(6)); 164.7, 166.8 (2*s*, C=O). FAB-MS (pos., 3-NBA): 834.3 (44, $[M+H]^+$), 303.1 (100)

2,6-Diamino-N^2,N^6*-dibenzoyl-9-[2′*-O*-benzoyl-4′*-O*-[bis(4-methoxyphenyl)(phenyl)methyl]-β-*D*-ribopyranosyl]purine* (**8g**). To a soln. of 1.0 g (1.12 mmol) of **7g** in 10 ml of pyridine were added 2.8 g (47 mmol) of PrOH, 0.34 g (3.4 mmol) of Et_3N, 0.31 g (2.2 mmol) of 4-nitrophenol, 0.14 mg (3.1 mmol) of DMAP, and the soln. was stirred at 60° for 48 h. The mixture was poured into 100 ml of CH_2Cl_2, washed with 2 × 100 ml of sat. aq. $NaHCO_3$ soln., 2 × 100 ml of 20% aq. citric acid soln., 2 × 150 ml of sat. aq. $NaHCO_3$ soln., dried ($MgSO_4$), and concentrated *in vacuo*. The residue was chromatographed over 30 g of SiO_2 (AcOEt/hexanes 1:3 → 1:1, then with 1:1 (1 → 5% MeOH)) to afford 59.6 mg of **7g** and 0.60 g (60%) of **8g**. TLC (SiO_2; AcOEt/hexanes 1:4 (with 2% MeOH)): R_f 0.31. ^{1}H-NMR (400 MHz, $CDCl_3$): 2.47 (*dd*, *J* = 11.1, 5.0, H_{ax}–C(5′)); 3.61 (*dd*, *J* = 11.0, 10.8, H_{eq}–C(5′)); 3.77 (*s*, 2 MeO); 4.0 (*ddd*, *J* = 10.8, 5.0, 2.7, H–C(4′)); 4.45 (*m*, H–C(2′)); 5.89 (*d*, *J* = 9.2, H–C(1′)); 6.27 (br. *s*, H–C(3′)); 6.31 (*d*, *J* = 6.8, OH); 6.77–8.3 (*m*, 28 arom. H, H–C(8)); 9.18, 9.35 (br. *s*, 2 NH). ^{13}C-NMR (75 MHz, $CDCl_3$) 55.24 (*q*, MeO); 65.28 (*t*, C(5′)); 68.36 (*d*, C(4′)); 69.05 (*d*, C(2′)); 74.11 (*d*, C(3′)); 83.06 (*d*, C(1′)); 87.42 (*s*, Ar_3C); 113.63 (*d*, arom. C); 118.56 (*s*, C(5)); 127.48–133.53 (*d* + *s*, arom. C); 134.02, 136.09, 136.25 (*s*, C(2), C(4), C(6)); 141.67 (*d*, C(8)); 164.87, 165.20, 166.33 (*s*, C=O). FAB-MS (pos., 3-NBA): 1794 (1, $[2M+2H]^+$), 897 (18, $[M+H]^+$), 358 (21), 303 (100), 154 (30), 105 (51).

3. ***General Procedure for the Preparation of the Nucleosides* 9a–9g (*Scheme 3*)**. A soln. of **8a**–**8g** in CH_2Cl_2 was stirred at r.t. consecutively with EtN(i-Pr)$_2$ and (chloro)(diisopropylamino)[(prop-2-enyl)oxy]-phosphine until no starting material could be detected. The mixture was then concentrated and directly subjected to CC (SiO_2).

1-(-3′-O*-Benzoyl-2′*-O*-{(diisopropylamino)[prop-2-enyl)oxy]phosphino}-4′-O-[bis(4-methoxyphenyl)-(phenyl)methyl]-β-*D*-ribopyranosyl)uracil* (**9a**). From 2.2 g (3.4 mmol) of **8a**, 2.2 ml (13 mmol) of EtN(i-Pr)$_2$, and 0.95 ml (4.3 mmol) of (chloro)(diisopropylamino)[(prop-2-enyl)oxy]phosphine in 10 ml of CH_2Cl_2 for 1.5 h. CC (50 g SiO_2; hexanes/AcOEt 8:2 → 1:1 (+2% Et_3N)) afforded 2.55 g (90%) **9a**. Colorless foam (diastereoisomers 1:2). TLC (hexanes/AcOEt 1:1): R_f 0.50. ^{1}H-NMR (500 MHz, $CDCl_3$): 8.25–8.17 (br. *s* + *m*, 3 H); 7.70–7.33 (*m*, 9 arom. H); 7.25–7.13 (*m*, 4 arom. H); 6.80 (*m*, 4 arom. H); 6.21 (br. *s*, 0.66 H, H–C(3′)); 6.02 (br. *s*, 0.34 H, H–C(3′)); 5.97 (br. *s*, H–C(1′)); 5.95 (m, 0.66 H); 5.76 (*m*, 0.34 H); 5.69 (*d*, *J* = 8.1, 0.66 H, H–C(5)); 5.65 (*d*, *J* = 8.2, 0.34 H, H–C(5)); 5.40 (*m*, 0.66 H); 5.18 (*m*, 0.66 H); 5.13 (*m*, 0.34 H); 5.03 (*m*, 0.34 H); 4.08 (*m*, 0.66 H); 4.02–3.80 (*m*, 2.34 H); 3.78 (*s*, 1 H); 3.77 (*s*, 2 H); 3,.77 (*s*, 1 H); 3.76 (*s*, 2 H); 3.72 (br. *s*, 1 H); 3.62 (*t*, *J* = 11.0, 0.34 H, H_{ax}–C(5′)); 3.54 (*t*, *J* = 10.9, 0.66 H, H_{ax}–C(5′)); 3.40 (*m*, 1 H); 2,52 (*dd*, *J* = 5.2, 11.4, 0.34 H, H_{eq}–C(5′)); 2.33 (*dd*, *J* = 4.6, 11.3, 0.66 H, H_{eq}–C(5′)); 1.04 (*d*, *J* = 6.6, 2 H); 0.99 (*d*, *J* = 6.8, 6 H); 0.84 (*d*, *J* = 6.7, 4 H). ^{13}C-NMR (125 MHz, $CDCl_3$): 165.8 (*s*); 165.7 (*s*); 162.6 (*s*, C(4)); 162.5 (*s*, C(4)); 158.8

(4*s*); 150.3 (*s*, C(2)); 150.2 (*s*, C(2)); 145.1 (*s*); 145.0 (*s*); 139.5 (br. *s*, C(6)); 136.3 (*s*); 136.1 (*s*); 135.9 (*s*); 135.2 (*s*); 135.1 (*s*); 135.0 (*d*); 134.9 (*d*); 133.1 (*s*); 133.0 (*s*); 130.6 (*s*); 130.5 (*s*); 130.3 (*s*); 130.2 (*d*); 130.1 (2*d*); 129.8 (*d*); 128.6 (*d*); 128.5 (*d*); 128.1 (*d*); 128.0 (3*d*); 127.0 (2*d*); 116.2 (*t*); 115.5 (*t*); 113.4 (2*d*); 113.3 (2*d*); 106.6 (*d*); 102.6 (*d*, C(5)); 102.4 (*d*, C(5)); 87.4 (*d*); 87.3 (*d*); 80.0 (br. *d*); 73.6 (), 72.9 (*d*); 70.0 (br. *d*); 68.0 (*d*); 65.8 (*t*, C(5′)); 65.7 (*t*, C(5′)); 64.1 (*t*, *J*(C,P) = 14.1); 63.3 (*t*, J_P = 15,7); 55.2 (*d*); 55.3 (*d*); 43.0 (4*q*); 24.3 (6*q*). ^{31}P-NMR (162 MHz, $CDCl_3$): 150.0; 149.0 (br. *s*). FAB-MS (pos., 3-NBA): 838 (3, $[M+H]^+$), 304 (58), 303 (100), 188 (23), 105 (42).

*1-3′-*O*-Benzoyl-(2′-*O*-[(diisopropylamino)[(prop-2-enyl)oxy]phosphino]-4′-*O*-[bis(4-methoxyphenyl)-(phenyl)methyl]-β-*D*-ribopyranosyl)thymine* (**9b**). From 2.0 g (3.0 mmol) of **8b**, 2.0 ml (12 mmol) of EtN(i-Pr)$_2$, and 0.95 ml (4.3 mmol) of (chloro)(diisopropylamino)[(prop-2-enyl)oxy]phosphine in 15 ml of CH_2Cl_2 for 2 h. CC (50 g SiO_2; hexanes/AcOEt 8:2 → 1:1 (+2% Et_3N)) afforded 2.42 g (95%) of **9b**. Colorless foam (diastereoisomers 1:1). TLC (hexanes/AcOEt 1:1): R_f 0.65. ^{1}H-NMR (500 MHz, $CDCl_3$): 8.22 (br. *s*, NH); 8.21–8.19 (*m*, 2 H); 7.64–7.34 (*m*, 8 H); 7.26–7.18 (*m*, 4 H); 7.00 (*d*, *J* = 1.1, 0.5 H, H–C(6)); 6.97 (*d*, *J* = 1.1, 0.5 H, H–C(6)); 6.81 (*m*, 4 H); 6.21 (br. *s*, 0.5 H, H–C(3′)); 6.04 (br. *s*, 0.5 H, H–C(3′)); 5.97 (br. *s*, 1 H, H–C(1′)); 5.95 (*m*, 0.5 H); 5.73 (*m*, 0.5 H); 5.40 (*m*, 0.5 H); 5.18 (*m*, 0.5 H); 5.13 (*m*, 0.5 H); 5.01 (*m*, 0.5 H); 4.08 (*m*, 0.5 H); 4.02–3.81 (*m*, 2.5 H); 3.78 (2*s*, 3 H); 3.77 (2*s*, 3 H); 3.74 (br. *s*, 1 H); 3.62 (*t*, *J* = 11.1, 0.5 H, H_{ax}–C(5′)); 3.54 (*t*, *J* = 11.1, 0.5 H, H_{ax}–C(5′)); 3.40 (m, 1 H); 2.52 (*dd*, *J* = 4.7, 11.0, 0.5 H, H_{eq}–C(5′)); 2.32 (*dd*, *J* = 5.0, 11.2, 0.5 H, H_{eq}–C(5′)); 1.89 (*d*, *J* = 1.2, 1.5 H, Me–C(5)); 1.87 (*d*, *J* = 1.2, 1.5 H, Me–C(5)); 1.04 (*d*, *J* = 6.8, 3 H); 0.99 (*d*, *J* = 6.7, 6 H); 0.84 (*d*, *J* = 6.7, 3 H). ^{13}C-NMR (125 MHz, $CDCl_3$): 165.9 (*s*); 165.8 (*s*); 163.3 (*s*. C(4)); 163.2 (*s*, C(4)); 158.8 (2*s*); 150.5 (*s*, C(2)); 150.3 (*s*, C(2)); 145.1 (*s*); 145.0 (*s*); 136.3 (br. *s*, C(6)); 136.1 (*s*); 136.0 (*s*); 135.9 (*s*); 135.5 (*s*); 135.3 (*s*); 135.2 (*d*); 135.1 (*d*); 135.0 (*d*); 133.1 (*s*); 133.0 (2*s*); 130.7 (*s*); 130.5 (*s*); 130.2 (3*s*); 139.9 (*d*); 129.8 (*d*); 128.6 (*d*); 128.5 (2*d*); 128.1 (*d*); 128.0 (3*d*); 127.0 (2*d*); 115.6 (*t*); 115.4 (*t*); 113.4 (2*d*); 113.3 (*d*); 106,6 (*d*); 111.0 (*d*, C(5)); 110.6 (*d*, C(5)); 87.4 (*d*); 87.3 (*d*); 79.7 (br. *d*); 78.5 (br. *d*); 73.6 (*d*), 72.9 (*d*); 70,0 (br. *d*); 68.1 (*d*); 68.0 (*d*); 65,7 (*t*, C(5′)); 65.6 (*t*, C(5′)); 64.1 (*t*, *J*(C,P) = 14,0); 63.3 (*t*, *J*(C,P) = 16.2); 55.2 (*d*); 43,0 (4*q*); 24.3 (6*q*); 12.5 (*q*, *Me*–C(5)); 12.4 (*q*, *Me*–C(5)). ^{31}P-NMR (162 MHz, $CDCl_3$): 149.8 (0.5 P); 148.7 (br., 0.5 P). FAB-MS (pos., 3-NBA): 852 (13, $[M+H]^+$), 304 (64), 303 (100), 188 (54), 105 (72).

N^4*-Benzoyl-1-(3′-*O*-benzoyl-2′-*O*-[(diisopropylamino)[prop-2-enyl)oxy]phosphino]-4′-*O*-[bis(4-methoxyphenyl))(phenyl)methyl]-β-*D*-ribopyranosyl)cytosine* (**9c**). From 93 mg (0.12 mmol) of **8c**, 46 µl (0.27 mmol) of EtN(i-Pr)$_2$, and 34 µl (0.15 mmol) of (chloro)(diisopropylamino)[(prop-2-enyl)oxy]phosphine in 1 ml of CH_2Cl_2 for 60 min. CC (SiO_2; hexanes/AcOEt 6:4 → 3:7 (+2% Et_3N)) afforded 95 mg (81%) of **9c**. Colorless foam (diastereoisomers 1:1). TLC (CH_2Cl_2/acetone 9:1): R_f 0.55, 0.50. ^{1}H-NMR (400 MHz, $CDCl_3$): 0.83, 0.97, 1.0, 1.03 (4*d*, *J* = 6.8, 6.8, 6.9, 6.9, 12 H, *Me*$_2$CHN); 2.35 (*dd*, *J* = 11.4, 5.4, 0.5 H, H_β–C(5′)); 2.54 (*dd*, *J* = 11, 5.3, 0.5 H, H_β–C(5′)); 3.35–3.44 (*m*, 2 Me$_2$C*H*N); 3.57 (*dd*, *J* = 11, 0.5 H, H_α–C(5′)); 3.65 (*dd*, *J* = 11, 0.5 H, H_α–C(5′)); 3.77, 3.77, 3.78, 3.78 (4*s*, 2 MeO); 3.77–4.13 (*m*, H–C(2′), H–C(4′), CH_2O(allyl)); 4.95 (*d*, *J* = 10.1, 0.5 H, C=CH_2); 5.08 (*d*, *J* = 17, 0.5 H, C=CH_2); 5.18 (*dd*, *J* = 10.1, 1.6, 0.5 H, C=CH_2); 5.41 (*dd*, *J* = 17, 1.6, 0.5 H, C=CH_2); 5.68–5.78 (*m*, 0.5 H, CH=C); 5.91–6.0 (*m*, 0.5 H, CH=C); 6.07 (br. *s*, 0.5 H, H–C(3′)); 6.2–6.35 (*m*, H–C(1′)); 6.25 (br. *s*, 0.5 H, H–C(3′)); 6.78–6.84 (*m*, 4 arom. H); 7.16–7.65, 7.92 (*m* + *s*, 17 arom. H, H–C(5), H–C(6), NH); 8.21–8.26 (*m*, 2 arom. H). ^{13}C-NMR (100 MHz, $CDCl_3$): 24.14, 24.23, 24.31, 24.35, 24.38, 24.41, 24.46 (7 *q*, *Me*CHN); 42.88, 42.92, 43.01, 43.04 (4*d*, Me*C*HN); 55.22 (*q*, MeO); 63.32, 64.08 (2*dt*, *J*(C,P) = 16.3, *J*(C,P) = 16.2, *C*H$_2$O(allyl)); 65.85 (*t*, C(5′)); 68.12 (*d*, C(4′) oder C(3′)); 70.8 (br. *d*, C(2′)); 73.08, 73.69 (2*d*, C(3′) oder C(4′)); 80.0, 80.85 (2 br. *d*, C(1′)); 87.35, 87.38 (2*s*, Ar_3C); 96.95 (br. *d*, C(5)); 113.31, 113.39, 113.42 (3*d*, arom. C); 115.43, 115.8 (2*t*, CH=*C*H$_2$); 126.96, 126.99 (2*d*, arom. C); 127.72 (*s*, arom. C); 127.99, 128.06, 128.98, 129.9, 130.18, 130.22 (6*d*, arom. C); 130.49, 130.65 (2*s*, arom. C); 132.98, 133.06, 133.18, 135.17, 135.24, 135.31 (*d*, *C*H=CH$_2$, arom. C); 135.96, 136.06, 136.14, 136.3, (4*s*, arom. C); 144.54 (br. *d*, C(6)); 145.07, 145.12 (2*s*, arom. C); 158.72, 158.76 (2*s*, arom. C, C(2)); 162.2 (*s*, C(4)); 165.92, 165.97 (2*s*, CO). ^{31}P-NMR (121.5 MHz, $CDCl_3$): 148.8, 150.8. FAB-MS (pos., 3-NBA): 1899 (0.5, $[2M+H_2O]^+$), 1833 (0.5, $[2M+2H]^+$), 1882 (0.5, $[2M+H]^+$), 942 (2, $[M+2H]^+$), 941 (3, $[M+H]^+$), 840 (17), 304 (2), 303 (100, $[DMT]^+$), 188 (25).

N^6*-Benzoyl-1-(3′-*O*-benzoyl-2′-*O*-[(diisopropylamino)[prop-2-enyl)oxy]phosphino]-4′-*O*-[bis(4-methoxyhenyl)(phenyl)methyl]-β-*D*-ribopyranosyl)adenine* (**9d**). From 0.77 g (0.99 mmol) of **8d**, 0.5 ml (3 mmol) of EtN(i-Pr)$_2$, and 0.37 ml (1.2 mmol) of (chloro)(diisopropylamino)[(prop-2-enyl)oxy]phosphine in 3 ml of CH_2Cl_2 for 2 h. CC (50 g SiO_2; hexanes/AcOEt 6:4 → 3:7 (+2% Et_3N)) afforded 0.95 g (quant.) of **9d**. Colorless foam (diastereoisomers 1:1). TLC (AcOEt/hexane 7:3): R_f 0.49. ^{1}H-NMR (500 MHz, $CDCl_3$): 0.48, 0.87, 0.91, 0.94 (4*d*, *J* = 6.8, 4 Me); 2.49 (*dd*, *J* = 11.3, 4.3, 0.5 H, H_β–C(5′)); 2.69 (*dd*, *J* = 11.3, 4.5, 0.5 H, H_β–C(5′)); 3.19, 3.25 (2*m*, NC*H*CH$_2$); 3.58 (*m*, H(allyl)); 3.68 (*dd*, *J* = 11.2, 11.2, 0.5 H, H_α–C(5′)); 3.77 (*dd*, 0.5 H, H_α–C(5′)); 3.76, 3.76, 3.79 (3*s*, 2 MeO); 3.93, 4.05 (*m*, H(allyl)); 4.07 (*m*, H–C(4′)); 4.36 (*ddd*, *J* = 9.2, 9.2, 3.0, 0.5 H, H–C(2′)); 4.42 (*ddd*, *J* = 10, 10, 2.8, 0.5 H, H–C(2′)); 4.90 (*m*, 0.5 H, C=CH_2); 4.93 (*ddm*,

J = 17.0, 1.7, 0.5 H, C=CH_2); 5.39 (*ddm*, J = 17.2, 1.8, 0.5 H, C=CH_2); 5.55, 5.93 (2*m*, C*H*=CH_2); 5.96, 5.97 (2*d*, J = 9.1, H–C(1′)); 6.10, 6.28 (2 br. *s*, H–C(3′)); 6.70 (*m*, 4 arom. H); 7.25–8.00 (*m*, 15 arom. H); 8.08, 8.09 (2*s*, H–C(2)); 8.25 (*m*, 2 arom. H); 8.81, 8.82 (2*s*, H–C(8)); 8.99 (br. *s*, NH). ^{13}C-NMR (125 MHz, $CDCl_3$): 23.8, 23.9, 24.1, 24.2, 24.3, 24.4 (7*q*, Me); 42.7, 42.8, 42.9 (4*d*, *Me*$_2$CH); 55.2 (*q*, MeO); 63.5, 63.9 (2*td*, J(C,P) = 17.5, O*C*H$_2$CH=CH_2); 65.8 (*t*, C(5′)); 68.0, 72.8, 73.6 (4*d*); 69.9, 70.4 (*dd*, J(C,P) = 9.9, 14.1, C(2′)); 81.0 (*d*, C(1′)); 87.4 (2*s*, Ar$_3$*C*); 113.3, 113.4, 113.5 (4*d*, *C*H=CH_2); 115.5, 115.7 (2*t*, CH=*C*H$_2$); 122.7, (2*s*, C(5)); 127.0, (2*d*); 127.8, 128.0, 128.1, 128.4, 128.6, 128.6, 128.7, 128.8, 128.9, 129.8, 130.0, 130.2, 130.3, 130.4, 130.6, 130.7 132.7, 133.1, 133.1 (19*d*); 133.8 (2*s*); 134.9 (2*d*); 135.2, 135.3, 135.9, 136.0, 136.1, 136.3 (6*s*); 141.3, 141.7 (2*d*, (C(8)); 145.1, 145.1 (2*s*, arom. C); 149.3, 149.4, 152.1, 152.2 (4*s*, C(4), C(6)); 152.9, 153.0 (2*d*, C(2)); 158.8, 158.8 (2*s*, arom. C); 164.3, 165.7, 165.7 (3*s*, C=O). ^{31}P-NMR (97 MHz, $CDCl_3$): 150.4, 149.3. FAB-MS (pos., 3-NBA): 965.3 (2, $[M+H]^+$), 923.2 (2), 864.1 (2), 726.1 (2), 303.1 (100), 240.0 (6), 188.1 (21), 105.0 (43).

*2-Amino-*N^2*-9-(3′-*O*-benzoyl-2′-*O*-[(diisopropylamino)[(prop-2-enyl)oxy]phosphino]-4′-*O*-[bis(4-methoxyphenyl)(phenyl)methyl]-β-*D*-ribopyranosyl)-*N^2*-isobutyryl-6-[(prop-2-enyl)oxy]purine* (**9e**): From 2.3 g (2.9 mmol) of **8e**, 1.5 ml (9 mmol) of EtN(i-Pr)$_2$, and 1.5 ml (7 mmol) of (chloro)(diisopropylamino)[(prop-2-enyl)oxy]phosphine in 9 ml of CH_2Cl_2 for 2 h. CC (50 g SiO_2; hexanes/AcOEt 5 : 1 → 1 : 2 (+2% Et_3N)) afforded 2.5 g (90%) of **9e**. Colorless foam (diastereoisomers 1 : 1). TLC (hexane/AcOEt 3 : 2 containing 1% Et_3N): R_f 0.67. ^{1}H-NMR (500 MHz, $CDCl_3$): 0.52–0.95 (4*d*, J = 6.8, 4 *Me*$_2$CH); 1.15–1.21(4*d*, J = 6.8, Me of isobutyryl); 2.45 (*dd*, J = 4.4, 11.5, H$_{eq}$–C(5′)); 2.61 (*dd*, J = 4.7, 11.4, H$_{eq}$–C(5′)); 3.22 (*d* of *sept.*, J(H,H) = 6.8, J(P,H) = 10.3, 2 Me$_2$C*H*); 3.29 (*d* of *sept.*, J(H,H) = 6.8, J(P,H) = 10.3, 2 Me$_2$C*H*); 3.49 (br. *m*, CH of isobutyryl); 3.52–3.63 (*m*, CH$_2$O (POallyl)); 3.64 (*t*, J = 11.0, H$_{ax}$–C(5′)); 3.71 (*t*, J = 11.0, H$_{ax}$–C(5′)); 3.76 (*s*, 2 MeO); 3.77 (*s*, 2 MeO); 3.93 (*ddd*, J(H,H) = 4.6, 13.8, J(P,H) = 9.1, 1 H, CH$_2$O (POallyl)); 4.02 (*ddd*, J = 2.7, 5.3, 10.6, H–C(4′)); 4.03 (*m*, 1 H, CH$_2$O (POallyl)); 4.31 (br. *t*, J(H,H) ≈ J(P,H) ≈ 8.0, H–C(2′)); 4.42 (br. *t*, J(H,H) ≈ J(P,H) ≈ 10.2); 4.91 (*d*, J ≈ 10.1, =CH$_2$ (POallyl) (*E*)); 4.94 (*dq*, J = 1.6, 17.1, =CH$_2$ (POallyl) (*Z*)); 5.03 (2*d*, 4 H, J ≈ 5.5, OCH$_2$ (6-allylO)); 5.17 (*dq*, J = 1.5, 10.5, =CH$_2$ (POallyl) (*E*)); 5.26 (*d*, J = 10.5, 2 H, =CH$_2$ (6-allylO) (*E*)); 5.39 (*dq*, J = 1.8, 17.2, 1 H =CH$_2$ (6-allylO) (*Z*)); 5.41 (*dq*, J = 1.5, 17.2, 1 H, =CH$_2$ (6-allylO) (*Z*)); 5.43 (*dq*, J = 1.5, 17.2, 1 H, =CH$_2$ (6-allylO) (*Z*)); 5.53 (*ddt*, J = 5.4, 10.4, 17.1, =CH (POallyl)); 5.78 (*d*, J = 9.2, 2 H–C(1′)); 5.92 (*ddt*, J = 4.8, 10.5, 17.1, =CH (POallyl)); 6.09 (*ddt*, J = 5.6, 10.5, 17.2, =CH (6-allylO)); 6.10 (*ddt*, J = 5.6, 10.5, 17.2, =CH (6-allylO)); 6.13 (br. *s*, H–C(3′)); 6.28 (br. *s*, H–C(3′)); 6.79 (*d*, J = 9.0, 2 H$_o$ to MeO); 6.80 (*d*, J = 9.1, 2 H$_o$ to MeO); 6.82 (*d*, J = 9.0, 2 H$_o$ to MeO); 6.84 (*d*, J = 9.0, 2 H$_o$ to MeO); 7.18 (*t*, J = 7.2, H$_o$ of DMT); 7.18 (*t*, J ≈ 7.2, H$_p$ of DMT); 7.23 (*t*, J ≈ 7.3, 2 H$_m$ of DMT); 7.24 (*t*, J ≈ 7.3, 2 H$_m$ of DMT); 7.36 (*d*, J = 8.5, 2 H$_m$ to MeO); 7.38 (*d*, J = 8.7, 2 H$_m$ to MeO); 7.43 (*d*, J = 9.0, 2 H$_m$ to MeO); 7.46 (*d*, J = 9.0, 2 H$_m$ to MeO); 7.46 (*d*, J ≈ 8.3, 2 H$_o$ of DMT); 7.49 (*d*, J ≈ 8.4, 2 H$_o$ of DMT); 7.58 (*t*, J ≈ 7.6, 2 H$_m$ of Bz); 7.59 (*t*, J ≈ 7.5, 2 H$_m$ of Bz); 7.66 (*t*, J = 7.6, H$_p$ of Bz); 7.67 (*t*, J = 7.2, H$_p$ of Bz); 7.78 (*s*, N^{2}H); 7.80 (*s*, N^{2}H); 7.86 (*s*, H–C(8)); 7.88 (*s*, H–C(8)); 8.23 (*d*, J = 8.3, 2 H$_o$ of Bz); 8.26 (*d*, J = 8.3, 2 H$_o$ of Bz). ^{13}C-NMR (125 MHz, $CDCl_3$): 19.0, 19.1, 19.2, 19.3 (4*q*, Me of isobutyryl); 23.9, 23.9, 24.1, 24.1, 24.3, 24.3, 24.3, 24.4 (8*q*, *Me*$_2$CH); 34.3 (*d*, CH of isobutyryl); 42.7 (*dd*, J(P,C) = 11.7, Me$_2$*C*H); 42.8 (*dd*, J(P,C) = 12.0, 2 Me$_2$*C*H); 55.2 (*q*, MeO); 63.4 (*d*t, J(P,C) = 17.7, *C*H$_2$O (POallyl)); 63.9 (*dt*, J(P,C) = 17.4, CH$_2$O (POallyl)); 65.6, 65.7 (2*t*, C(5′)); 67.8 (*t*, CH$_2$O (6-allylO)); 68.1, 68.1 (2*d*, C(4′)); 69.7 (*dd*, J(P,C) = 14.4, C(2′)); 70.3 (*dd*, J(P,C) = 9.9, C(2′)); 72.9 (*dd*, J(P,C) = 2.2, C(3′)); 73.6 (*d*, C(3′)); 81.1 (*d*, *C*(1′)); 87.4 (2*s*, Ar$_3$*C*O); 113.3, 113.4, 113.5 (3*d*, C$_o$ to MeO); 115.4, 115.7 (2*t*, =CH$_2$ (POallyl)); 118.0, 118.0 (2*s*, *C*(5)); 118.5, 118.6 (2*t*, =CH$_2$ (6-allylO)); 127.0, 127.0 (2*d*, C$_p$ of DMT); 128.0, 128.0, 128.0, 128.1 (4*d*, C$_o$, C$_m$ of DMT); 128.6, 128.6 (2*d*, C$_m$ of Bz); 129.8 (*d*, C$_o$ of Bz); 130.1, 130.2, 130.2, 130.2 (4*d*, C$_m$ to MeO); 130.6, 130.8 (2*s*, C$_{ipso}$ of Bz); 132.2, 132.2 (2*d*, =CH (6-allylO)); 133.1, 133.1 (2*d*, C$_p$ of Bz); 134.9 (*dd*, J(P,C) = 7.1, =CH (POallyl)); 135.2 (*dd*, J(P,C) = 7.4, =CH (POallyl)); 135.9, 136.0, 136.1, 136.3 (4*s*, C$_{ipso}$ to Ar$_3$CO of DMT); 139.8, 140.3 (2*d*, C(8)); 145.0, 145.1 (2*s*, C$_{ipso}$ of DMT); 151.8, 151.9, 153.2, 153.3 (4*s*, C(2), C(4)); 158.8, 158.8 (2*s*, C$_{ipso}$ to MeO); 160.6, 160.6 (2*s*, C(6)); 165.7, 165.7 (2*s*, C=O of Bz); 177.4 (*s*, C=O of isobutyryl). ^{31}P-NMR (121 MHz, $CDCl_3$): 149.4; 150.5. MS: 987.6 (18, $[M+H]^+$), 303.1 (100), 273.1 (12), 262.1 (15), 188.1 (51), 146.1 (25), 136.0 (12), 121.0 (12), 105.0 (74), 80.9 (12), 76.9 (20).

*6-Amino-*N^6*-benzoyl-9-(3′-*O*-benzoyl-2′-*O*-[(diisopropylamino)[(prop-2-enyl)oxy]phosphino]-4′-*O*-[bis(4-methoxyphenyl)phenyl)methyl]-β-*D*-ribopyranosyl)purine* (**9f**). A soln. of 264 mg (0.32 mmol) of **8f** in 3 ml of CH_2Cl_2, 120 µl (0.38 mmol) of (chloro)(diisopropylamino)[(prop-2-enyl)oxy]phosphine, and 163 µl (0.95 mmol) of EtN(i-Pr)$_2$ was stirred at 0°. The mixture was allowed to warm to r.t. and stirred for 1.5 h at 25°. The reaction was quenched with 0.5 ml of MeOH, the mixture was concentrated *in vacuo*, and the residue was chromatographed (SiO_2; 30–60% AcOEt in hexanes, 1% Et_3N) to afford 306 mg (94.6%) of **9f** (diastereoisomer mixture *ca.* 1 : 1 (^{1}H-NMR)). TLC (40% AcOEt in hexanes): R_f 0.12. ^{1}H-NMR (500 MHz, $CDCl_3$): 0.49, 0.88, 0.91, 0.95 (4*d*, J = 6.8, 4 Me); 2.46 (*dd*, J = 11.5, 5.3, 0.5 H, H$_\beta$–C(5′)); 2.64 (*dd*, J = 10.8, 4.6, 0.5 H, H$_\beta$–C(5′)); 3.23 (*m*, 2 Me$_2$C*H*); 3.65 (m, POCH$_2$); 3.66 (*dd*, J = 11.2, 11.2, 0.5 H, H$_\alpha$–C(5′)); 3.73 (*dd*, J =

10.9, 10.9, 0.5 H, H_α–C(5′)); 3.77, 3.78 (2*s*, 2 MeO); 3.94 (m, 0.5 H, $POCH_2$); 4.04 (m, 1.5 H, $POCH_2$, H–C(4′)); 4.23, 4.32 (2*m*, H–C(2′)); 4.89 (*m*, 2 H, $COCH_2$); 4.92 (*m*, 0.5 H, H(olef.)); 4.96 (*dm*, $J = 17.5$, 0.5 H, C=CH_2); 5.16 (*dm*, $J = 10.5$, 0.5 H, C=CH_2); 5.21 (*m*, 2×0.5 H, H(olef.)); 5.49 (*m*, 1.5 H, H(olef.)); 5.59 (m, 0.5 H, H(olef.)); 5.91 (*m*, 1.5 H, H–C(1′), H(olef.)); 6.10 (*m*, 1.5 H, H(olef.)); 6.27 (br. *s*, 0.5 H, H–C(3′)); 6.80–8.30 (*m*, 24 H, arom. H, H–C(8)); 8.79 (br. *s*, NH). ^{13}C-NMR (125 MHz, $CDCl_3$): 23.8, 23.9, 24.1, 24.1, 24.3, 24.3, 24.3, 24.4 (8*q*, Me); 42.7, 42.8 (2*d*, Me_2CH); 55.2 (*q*, MeO); 63.4, 64.0 (2*dt*, J(C,P) = 17.5, $POCH_2$); 65.8, 65.8, 68.7, 68.7 (4*t*, C(5′), $COCH_2$); 68.0, 68.1, 69.9, 70.0, 70.7, 70.7, 72.9, 73.7 (8*d*, C(2′), C(3′), C(4′)); 80.4 (*d*, C(1′)); 87.4, 87.4 (2*s*, Ar_3C); 113.3, 113.4, 113.4, 113.5 (4*d*, $POCH_2CH$=CH_2); 115.4, 115.6 (2 *t*, C=CH_2); 118.2, 118.3 (2*s*, C(5)); 118.7 (*t*); 127.8, 128.0, 128.0, 128.1, 128.1, 128.5, 128.6, 128.8, 129.8, 129.8, 130.2, 130.2, 130.2, 130.3 (14*d*); 130.6, 130.8 (2*s*, arom. C); 132.6, 133.0, 133.0, 133.0, 133.1 (5*d*); 133.8, 133.8 (2*s*); 135.0, 135.1, 135.2, 135.3 (4*d*); 136.0, 136.1, 136.2, 136.3 (4*s*); 139.5, 140.1 (2*d*, C(8)); 145.1, 145.1 (2*s*); 150.1, 150.2, 154.3, 154.5 (4*s*, C(2), C(4)); 158.8, 158.8 (2*s*, arom. C); 161.1, 161.2, 164.3, 164.4, 165.6, 165.7 (6*s*, C=O). ^{31}P-NMR (97 MHz, $CDCl_3$): 150.5, 149.1. FAB-MS (pos., 3-NBA): 1021.4 (12, $[M+H]^+$), 920.3 (17), 303.1 (100), 188.1 (46).

2,6-Diamino-N^2,N^6*-dibenzoyl-9-(3′-*O*-benzoyl-2′-*O*-{(diisoproylamino)[(prop-2-enyl)oxy]phosphino]-4′-*O*-[bis(4-methoxyphenyl)(phenyl)methyl]-β-*D*-ribopyranosyl)purine* (**9g**). In a 10-ml round-bottomed flask was placed 0.5 g (0.56 mmol) of **8g** with 3-Å molecular sieves, dried under high vacuum for 14 h, followed by addition of 3.0 ml of CH_2Cl_2, 0.22 g (1.7 mmol) of EtN(i-Pr_2), and 0.19 g (0.84 mmol) of (chloro)(diisopropylamino)[(prop-2-enyl)oxy]phosphine under Ar. The mixture was stirred at r.t. for 1.5 h, diluted with 50 ml of CH_2Cl_2, and washed with 50 ml of sat. aq. $NaHCO_3$ soln. The aq. layer was extracted with 2×50 ml of CH_2Cl_2. The combined org. layers were dried ($MgSO_4$), concentrated *in vacuo*, and the residue was purified by CC (50 g of SiO_2; AcOEt/hexanes (containing 2% Et_3N), 1:10 → 5:1) to afford 0.50 g (83%) of **9g**. TLC (AcOEt/hexanes 3:2): R_f 0.68. ^{1}H-NMR (500 MHz, $CDCl_3$): 0.51, 0.86, 0.91, 0.94 (4*d*, $J = 6.7$, 2 Me_2CH); 2.49, 2.70 (*dd*, $J = 11.2$, 5.5, H_{eq}–C(5′)); 3.25–3.42 (*m*, 2 Me_2CH); 3.51–3.71 (*m* with *dd* at 3.7 ppm, doubled due to diastereoisomers, 2 H(allyl), H_{ax}–C(5′)); 3.76, 3.77 (*s*, 2 MeO); 3.8–4.08 (*m*, doubled due to diastereoisomers, 2 H(allyl), H–C(4′)); 4.2–4.3 (*dm*, $J = 9.2$, H–C(2′)); 4.89, 5.13 (*dd*, $J = 10.6$, 1.5, CH_2=); 4.96, 5.35 (*dd*, $J = 17.1$, 1.5, CH_2=); 5.56–5.91 (*m*, CH=); 6.01–6.10 (*d*, doubled due to diastereoisomers, $J = 9.2$, H–C(1′)); 6.05, 6.24 (br. *s*, H–C(3′)); 6.7–8.5 (*m*, 28, arom. H, H–C(8)); 9.1, 9.2 (br. *s*, 2 NH). ^{13}C-NMR (100 MHz, $CDCl_3$): 23.79, 23.88, 24.10, 24.16 (*q*, 2 Me_2CH); 42.75, 42.87 (*d*, Me_2CH); 55.21 (*q*, MeO); 63.57 (*t*, C(5′)); 64.14, 65.85 (*t*, C(allyl)); 68.05 (*d*, C(4′)); 72.96, 73.75 (2*d*, C(3′), C(2′)); 80.51 (*d*, C(1′)); 87.38, 87.42 (*s*, Ar_3C); 113.34, 113.44 (2*d*, arom. C); 115.38, 115.60 (*t*, C(allyl)); 119.87 (*s*, C(5)); 126.96–133.57 (*d* + *s*, arom. C); 134.80, 135.29, 135.36, 135.99, 136.15, 136.33 (6*s*, C(2), C(4), C(6), arom. C); 140.81 (*d*, C(8)); 145.15–158.78 (*s*, arom. C, C=O); 164.54, 165.93 (*s*, C=O). ^{31}P-NMR (162 MHz, $CDCl_3$): 149.2, 150.4. FAB-MS (pos., 3-NBA): 2168 (5, $[2M+2H]^+$), 1084 (519 $[M+H]^+$), 983 (3), 359 (26), 303 (100), 188 (55), 154 (42), 105 (67).

(Chloro)(diisopropylamino)[(prop-2-enyl)oxy]phosphine. To a mechanically stirred soln. of 88 ml (137.3 g, 1 mol) of PCl_3 in 250 ml of dry Et_2O, 81 ml (79.1 g, 1 mol) of dry pyridine was slowly added under Ar. The slightly turbid soln. was chilled with dry ice in acetone, and, over a period of 6 h, 61 ml (51.8 g, 0.89 mol) of allyl alcohol in 100 ml of dry Et_2O was added. During the addition, a white precipitate formed, and vigorous stirring was continued. After the complete addition, the mixture was allowed to warm to r.t., and stirring was continued for 16 h. The mixture was diluted with 100 ml of Et_2O, filtered under Ar, the precipitate was washed with $3 \times$ 100 ml Et_2O, and the combined filtrates were concentrated under reduced pressure to remove the bulk of the Et_2O. The residual liquid was subjected to fractional distillation at 1 Torr; a fraction with a b.p. of 28–30° was collected[59]) to afford 74 g (47%) of (dichloro)[(prop-2-enyl)oxy]phosphine[60]). This phosphine was dissolved in 400 ml of dry Et_2O, and, under vigorous stirring, a soln. of 130 ml (94.3 g, 0.93 mol) of (i-$Pr)_2$NH in 100 ml of dry Et_2O was added over a period of 3 h while maintaining a temp. of − 78° under N_2. After complete addition of the amine, the resulting thick suspension was stirred at r.t. for 16 h. The mixture was diluted with 200 ml of Et_2O, filtered under N_2, the precipitate was washed with 3×100 ml of Et_2O, and the combined filtrates were concentrated under reduced pressure to remove the bulk of the Et_2O. The remaining liquid was distilled under reduced pressure (55–60°, 50 mTorr) to give 69.3 g (66%) of (chloro)(diisopropylamino)[(prop-2-enyl)-oxy]phosphine as clear liquid (contaminated with *ca.* 6% of (diisopropylamino)[(prop-2-enyl)oxy]-*H*-phosphonate (^{1}H-NMR)). ^{1}H-NMR (600 MHz, $CDCl_3$): 1.25–1.29 (*m*, 4 Me); 3.79–3.85 (*m*, H–CN); 4.38

---

[59]) A second fraction with a b.p. of 48–50° was collected to afford 15 g (8%) of the (chloro){bis[(prop-2-enyl)oxy]}phosphine.

[60]) ^{1}H-NMR (300 MHz, $CDCl_3$): 4.72 (*ddt*, $J = 8.4$, 5.7, 1.4, OCH_2C); 5.31 (*dq*, $J = 10.3$, 1.2, 1 H, CH_2=C); 5.39 (*dq*, $J = 18.5$, 1.4, 1 H, CH_2=C); 5.95 (*ddt*, $J = 16.1$, 10.6, 5.6, CH=C).

(br. *s*, CH_2O); 5.22 (*d*, *J* = 10.5, 1 H, CH_2=C); 5.34 (*d*, *J* = 16.9, 1 H, CH_2=C); 5.98 (*ddt*, *J* = 16.4, 10.7, 5.4, CH=C). ^{13}C-NMR (150 MHz, $CDCl_3$): 24.2, 23.5 (2*m*, Me); 46.2 (*dd*, *J*(C,H) = 137, *J*(C,P) = 12.9, HC–N); 66.6 (*dt*, *J*(C,H) = 158, *J*(C,P) = 18.2, CH_2O); 118.3 (*t*, *J*(C,H) = 158, CH_2=C); 134.3 (*dd*, *J*(C,H) = 160, *J*(C,P) = 7.9, CH). ^{31}P-NMR (242 MHz, $CDCl_3$): 183.0.

3.1. *General Procedure for the Preparation of the Nucleosides* **10a**–**10g** (*Scheme 3*). A soln. of DMAP and bis(4-nitrophenyl) heptane-1,7-dioate (pimelate) [60] in pyridine was treated slowly with **8a**–**8g** in pyridine. The mixture was stirred overnight, treated with toluene, and evaporated. The residue was subjected to CC (SiO_2).

*1-(3′-*O*-Benzoyl-4′-*O*-[bis(4-methoxyphenyl)(phenyl)methyl]-2′-*O*-{6-[(4-nitrophenoxy)carbonyl]-β-*D*-ribopyranosyl)uracil* (**10a**). From 30 mg (0.25 mmol) of DMAP, 400 mg (1 mmol) of bis(4-nitrophenyl) heptane-1,7-dioate and 160 mg (0.25 mmol) of **8a** in 2 × 0.5 ml of pyridine. CC (2 g of SiO_2; hexanes/AcOEt 3 : 2 → 1 : 1) afforded 150 mg (66%) of **10a**. Light yellow foam. TLC (AcOEt/hexanes 3 : 2): R_f 0.55. ^{1}H-NMR (300 MHz, $CDCl_3$): 8.45 (br. *s*, NH); 8.23 (*m*, 4 H); 7.89 (*m*, 1 H); 7.66 (m, 2 H); 7.41–7.16 (*m*, 16 H); 6.81 (2*d*, *J* = 6.6, 4 H); 6.02 (*d*, *J* = 9.7, H–C(1′)); 6.01 (br. *s*, H–C(3′)); 5.69 (*d*, *J* = 8.2, H–C(5)); 4.91 (*dd*, *J* = 2.9, 9.5, H–C(2′)); 3.92 (*ddd*, *J* = 2.8, 5.4, 11.0, H–C(4′)); 3.79 (*s*, 3 H); 3.78 (*s*, 3 H); 3,75 (*t*, *J* = 9.8, H_{ax}–C(5′)); 2.76 (*dd*, *J* = 5.0, 11.2, H_{eq}–C(5′)); 2.53 (*m*, 2 H); 2.23 (*m*, 2 H); 1,64 (*m*, 2 H); 1.53 (*m*, 2 H); 1.32 (*m*, 2 H). ^{13}C-NMR (75 MHz, $CDCl_3$): 171.9 (*s*); 171.2 (*s*); 165.9 (*s*), 162.4 (*s*, C(4)); 158.9 (*s*); 155.4 (*s*); 150.1 (*s*, C(2)); 145.2 (*s*); 144.7 (*s*); 139.3 (*d*, C(6)); 135.7 (*d*); 135.5 (*d*); 133.6 (*s*); 130.0 (*d*); 129.9 (*d*); 129.8 (*d*); 128.8 (*d*); 128.1 (*d*); 127.9 (*d*); 127.2 (*d*); 126.2 (*d*); 125.2 (*d*); 122.5 (*d*); 115.6 (*d*); 113.5 (*d*); 113.4 (*d*); 103.1 (*d*, C(5)); 87.4 (*s*); 78.5 (*d*, C(1′)); 71.1 (*d*), 67.8 (*d*); 67.5 (*d*); 66.1 (*t*, C(5′)); 55.3 (*q*); 33.9 (*t*); 33.5 (*t*); 28.1 (*t*); 24.2 (*t*); 24.1 (*t*). FAB-MS (pos.): 913 (1, $[M+H]^+$), 304 (27), 303 (100).

*1-(3′-*O*-Benzoyl-4′-*O*-[bis(4-methoxyphenyl)(phenyl)methyl]-2′-*O*-{6-[(4-nitrophenoxy)carbonyl]hexanoyl}-β-*D*-ribopyranosyl)thymine* (**10b**). From 30 mg (0.25 mmol) of DMAP, 400 mg (1 mmol) of bis(4-nitrophenyl) heptane-1,7-dioate, and 166 mg (0.25 mmol) of **8b** in 2 × 0.5 ml of pyridine. CC (2 g of SiO_2; hexanes/AcOEt 3 : 2 → 1 : 1) afforded 198 mg (80%) of **10b**. Colorless foam. TLC (AcOEt/hexanes 5 : 4): R_f 0.55. ^{1}H-NMR (300 MHz, $CDCl_3$): 8.22 (br. *s* + *m*, 5 H); 7.67 (*m*, 1 H); 7.56 (*m*. 2 H); 7.41–7.17 (*m*, 16 H); 6.99 (*d*, *J* = 1.2, H–C(6)); 6.79 (m, 4 H); 6.02 (*d*, *J* = 9.7, H–C(1′)); 5.80 (br. *t*, *J* = 2.3, H–C(3′)); 4.91 (*dd*, *J* = 2.9, 9.7, H–C(2′)); 3.94 (*ddd*, *J* = 2.5, 5.4, 10.7, H–C(4′)); 3.78 (*s*, 3 H); 3.77 (*s*, 3 H); 3.72 (*t*, *J* = 10.9, H_{ax}–C(5′)); 2.76 (*dd*, *J* = 4.8, 11.5, H_{eq}–C(5′)); 2.52 (*m*, 2 H); 2.21 (*m*, 2 H); 1.86 (*d*, *J* = 1.2, Me); 1.64 (*m*, 2 H); 1.52 (*m*, 2 H); 1.31 (*m*, 2 H). ^{13}C-NMR (100 MHz, $CDCl_3$): 171.9 (*s*); 171.1 (*s*); 165.9 (*s*), 162.9 (*s*, C(4)); 158.9 (*s*); 155.5 (*s*); 150.2 (*s*, C(2)); 145.3 (*s*); 144.7 (*s*); 135.8 (*d*, C(6)); 135.6 (*d*); 134.7 (*d*); 133.6 (*s*); 130.1 (*d*); 129.9 (*d*); 129.8 (*d*); 128.8 (*d*); 128.3 (*d*); 128.0 (*d*); 127.9 (*d*); 127.2 (*d*); 125.2 (*d*); 122.5 (*d*); 113.5 (*d*); 113.4 (*d*); 113.4 (*d*); 111.6 (*s*, C(5)); 87.4 (*s*); 78.3 (*d*, C(1′)); 71.1 (*d*), 67.7 (*d*); 67.5 (*d*); 66.0 (*t*, C(5′)); 55.3 (*q*); 33.9 (*t*); 33.5 (*t*); 28.1 (*t*); 24.2 (*t*); 24.1 (*t*); 12.4 (*q*, *Me*–C(5)). FAB-MS (pos.): 928 (2, $[M+H]^+$), 304 (34), 303 (100).

N^4*-Benzoyl-1-(3′-*O*-benzoyl-4′-*O*-[bis(4-methoxyphenyl)(phenyl))methyl]-2′-*O*-{6-[(4-nitrophenoxy)carbonyl]hexanoyl}-β-*D*-ribopyranosyl)cytosine* (**10c**). From 19 mg (0.16 mmol) of DMAP, 450 mg (1.1 mmol) of bis(4-nitrophenyl) heptane-1,7-dioate, and 110 mg (0.25 mmol) of **8c** in 2 × 1 ml of pyridine. CC (SiO_2; CH_2Cl_2 → CH_2Cl_2/acetone 85 : 15) afforded 117 mg (80%) of **10c**. Colorless foam. TLC (CH_2Cl_2/Acetone 9 : 1): R_f 0.47. ^{1}H-NMR (500 MHz, CD_2Cl_2): 1.2–1.26 (*m*, CH_2); 1.44–1.62 (*m*, 2 CH_2); 2.13–2.21 (*m*, CH_2); 2.5 (*ddd*, *J* = 30.8, 16.45, 7.5, CH_2); 2.8 (*dd*, *J* = 11.5, 4.5, H–C(5′)); 3.77, 3.78 (2*s*, 2 MeO); 3.79 (*dd*, *J* = 11, 9.7, H–C(5′)); 3.99–4.02 (*m*, H–C(4′)); 4.95 (*dd*, *J* = 9.6, 2.9, H–C(2′)); 5.85 (*dd*, *J* = 2.2, 2.2, H–C(3′)); 6.26 (*d*, *J* = 9.5, H–C(1′)); 6.8–6.84 (*m*, 4 arom. H); 7.19–7.71 (*m*, 17 arom. H, H–C(5), H–C(6)); 7.87 (*d*, *J* = 7.9, 2 arom. H); 8.17–8.27 (*m*, 4 arom. H); 8.61 (br. *s*, NH). ^{13}C-NMR (125 MHz, CD_2Cl_2): 24.56, 24.58, 28.48, 33.94, 34.25 (5*t*); 55.67 (*q*, MeO); 66.52 (*t*, C(5′)); 68.05, 69.42, 71.7 (3*d*, C(2′), C(3′), C(4′)); 79.9 (*d*, C(1′)); 87.83 (*s*, Ar_3C); 97.8 (*d*, C(5)); 113.78, 113.85 (2*d*, arom. C); 116.06, 122.96 (2*d*, arom. C); 125.44, 126.43, 127.5, 128.09, 128.33, 129.19, 129.33, 130.3, 130.39, 130.5, 130.51, 133.6, 133.97 (arom. C); 136.09, 136.23 (2*s*, arom. C); 144.71 (*d*, C(6)); 145.49, 145.67 (2*s*, arom. C); 156.0 (2 arom. C, C(2′)); 159.45 (*s*, arom. C); 162.84 (*s*, C(4)); 166.25, 171.62, 172.32 (3*s*, CO).

N^6*-Benzoyl-9-(3′-*O*-benzoyl-4′-*O*-[bis(4-methoxyphenyl)(phenyl)methyl]-2′-*O*-{6-[(4-nitrophenoxy)carbonyl]hexanoyl}-β-*D*-ribopyranosyl)adenine* (**10d**). From 38 mg (0.31 mmol) of DMAP, 870 mg (2.26 mmol) of bis(4-nitrophenyl) heptane-1,7-dioate, and 240 mg (0.31 mmol) of **8d** in 2 × 1.5 ml pyridine. CC (2 g of SiO_2; hexanes/AcOEt 3 : 2 → 2 : 3) afforded 290 mg (90%) of **10d**. Colorless foam. TLC (AcOEt/hexanes 4 : 1): R_f 0.53. ^{1}H-NMR (300 MHz, $CDCl_3$): 1.00–1.56 (*m*, 3 CH_2); 2.00 (*m*, CH_2); 2.44 (*t*, *J* = 7.4, CH_2); 2.90 (*dd*, *J* = 11.1, 4.9 H_β–C(5′)); 3.77, 3.78 (2*s*, 2 MeO); 3.90 (*dd*, *J* = 11.1, 11.1, H_α–C(5′)); 4.13 (*m*, H–C(4′)); 5.49 (*dd*, *J* = 9.7, 2.9, H–C(2′)); 5.86 (br. *t*, H–C(3′)); 6.09 (*d*, *J* = 9.7, H–C(1′)); 6.81 (*m*, 4 arom. H); 7.10–7.68 (*m*, 17 arom. H); 7.96 (*d*, *J* = 7.3, 2 arom. H); 8.08 (*s*, H–C(2)); 8.13–8.29 (*m*, 4 arom. H); 8.78 (*s*, H–C(8)); 9.02 (br. *s*, NH).

^{13}C-NMR (75 MHz, $CDCl_3$): 24.0, 24.1, 27.9, 33.3, 33.9 (5*t*, CH_2); 55.3 (*q*, MeO); 66.2 (*t*, C(5′)); 67.4, 68.6, 71.0 (3*d*, C(2′), C(3′), C(4′)); 78.8 (*d*, C(1′)); 87.5 (*s*, Ar_3C); 113.5, 113.6 (2*d*, arom. C); 124.2 (*d*, arom. C); 122.7 (*s*, C(5)); 125.1, 125.3, 126.1, 127.2, 127.8, 128.0, 128.1, 128.2, 128.8, 128.9, 129.0, 129.9, 130.1, 132.8, 133.4, 133.6, 135, 6, 135.8 (18*d*, arom. C); 140.9 (*d*, C(8)); 144.8 (*d*, arom. C); 145.3 (*s*); 149.6, 152.0 (2*s*, C(4), C(6)); 153.1 (*d*, C(2)); 155.4 ; 159.0 (*s*, arom. C); 162.4, 164.4, 165.8, 171.4, 170.0 (5*s*, C=O). FAB-MS (pos., 3-NBA): 1041.5 (2, $[M+H]^+$), 461.1 (2), 401.0 (2), 303.1 (100), 240.1 (22), 136.0 (34), 105.0 (48).

*2-Amino-9-(3′-*O*-benzoyl-4′-*O*-[bis(4-methoxyphenyl)(phenyl)methyl]-2′-*O*-{6-[(4-nitrophenoxy)carbonyl]hexanoyl}-β-*D*-ribopyranosyl-*N^2*-isobutyryl-6-[(prop-2-enyl)oxy]purine* (**10e**): From 44 mg (0.36 mmol) of DMAP, 1 g (2.5 mmol) bis(4-nitrophenyl) heptane-1,7-dioate, and 290 mg (0.36 mmol) of **8e** in 2 × 3.5 ml pyridine. CC (2 g of SiO_2, $CH_2Cl_2 \rightarrow CH_2Cl_2$/acetone 9:1) afforded 360 mg (90%) of **10e**. Colorless foam. TLC (5% acetone in CH_2Cl_2): R_f 0.52. ^{1}H-NMR (400 MHz, $CDCl_3$): 1.13 (d, J = 7.5, CH_2 (pimelate)); 1.18 (*d*, J = 6.8, Me of isobutyryl); 1.21 (*d*, J = 6.8, Me of isobutyryl); 1.36 (*m*, CH_2 (pimelate)); 1.55 (*d*, $J \approx 7.2$, CH_2 (pimelate)); 1.98 (*dt*, J = 7.3, 15.9, 1 H, CH_2 (pimelate)); 2.08 (*dt*, J = 7.4, 15.8, 1 H, CH_2CO (pimelate)); 2.47 (*t*, J = 7.5, CH_2 (pimelate)); 2.88 (*dd*, J = 5.1, 11.2, H_{eq}–C(5′)); 3.34 (br. *m*, CH of isobutyryl); 3.77 (*s*, MeO); 3.78 (*s*, MeO); 3.87 (*t*, J = 11.0, H_{ax}–C(5′)); 4.10 (*ddd*, J = 2.8, 5.2, 10.5, H–C(4′)); 5.02 (*d*, J = 5.7, CH_2O (allyl)); 5.26 (*dm*, J = 1.2, 10.5, 1 H, $=CH_2$ (allyl) (*E*)); 5.42 (*dq*, J = 1.4, 17.2, 1 H, $=CH_2$ (allyl) (*Z*)); 5.49 (*dd*, J = 2.7, 9.7, H–C(2′)); 5.87 (br. *s*, H–C(3′)); 5.91 (*d*, J = 9.7, H–C(1′)); 6.08 (*ddt*, J = 5.7, 10.5, 17.2, =CH (allyl)); 6.80–6.83 (*d*, J = 9.2, 4 H_o to MeO); 7.22 (m, 2 H_m, H_p of DMT (unsubst. Ph)); 7.25 (*d*, J = 9.2, 2 H_m to NO_2); 7.33 (*d*, J = 8.9, 2 H_m to MeO); 7.37 (*d*, J = 8.9, 2 H_m to MeO); 7.42 (*d*, J = 7.5, 2 H_o of DMT (unsubst. Ph)); 7.61 (*t*, $J \approx 7.6$, 2 H_m of Bz); 7.71 (*t*, J = 7.4, H_p of Bz); 7.83 (*s*, H–C(8)); 7.86 (*s*, N^2H); 8.22 (*d*, J = 9.1, 2 H_o to NO_2); 8.26 (*d*, $J \approx 7.8$, 2 H_o of Bz). ^{13}C-NMR (100 MHz, $CDCl_3$): 19.1 (*q*, Me of isobutyryl); 24.0, 24.1 (2*t*, CH_2 (pimelate)); 27.9 (*t*, CH_2 (pimelate)); 33.3 (*t*, CH_2 (pimelate)); 33.7 (*t*, CH_2 (pimelate)); 34.8 (*d*, CH of isobutyryl); 55.2 (*q*, MeO); 66.0 (*t*, C(5′)); 67.4 (*d*, C(4′)); 68.0 (*t*, CH_2O (allyl)); 68.2 (*d*, C(2′)); 71.0 (*d*, C(3′)); 78.8 (*d*, C(1′)); 87.4 (*s*, Ar_3CO of DMT); 113.5 (*d*, C_o to MeO); 113.5 (*d*, C_o to MeO); 117.8 (*s*, C(5)); 118.9 (*t*, $=CH_2$ (allyl)); 122.5 (*d*, C_m to NO_2); 125.2 (*d*, C_o to NO_2); 127.2 (*d*, C_p of DMT (unsubst. Ph)); 127.9 (*d*, C_o of DMT (unsubst. Ph)); 128.1 (*d*, C_m of DMT (unsubst. Ph)); 128.8 (*d*, C_m of Bz); 129.9, 130.0 (2*d*, 2 C_o of Bz and 4 C_m to MeO (and C_{ipso} of Bz)); 132.0 (*d*, =CH (allyl)); 133.6 (*d*, C_p of Bz); 135.6 (*s*, C_{ipso} to Ar_3CO of DMT-PhOMe); 135.7 (*s*, C_{ipso} to Ar_3CO of DMT-PhOMe); 139.5 (*d*, C(8)); 144.8 (*s*, C_{ipso} of DMT (unsubst. Ph)); 145.2 (*s*, C_{ipso} to NO_2); 152.2, 152.9 (2*s*, C(2), C(4); 155.4 (*s*, C_p to NO_2); 158.9 (*s*, C_{ipso} to MeO); 160.7 (*s*, C(6)); 165.8 (*s*, C=O of Bz); 170.9 (*s*, C=O (pimelate)); 171.4 (*s*, C=O (pimelate)); 177.0 (*s*, C=O (isobutyryl)). MS: 1063.2 (11, $[M+H]^+$), 303.1 (100), 262.1 (16), 136.0 (21), 105.0 (33), 88.9 (10), 76.9 (16), 68.9 (10), 54.9 (9).

*6-Amino-*N^6*-benzoyl-9-(3′-*O*-benzoyl-4′-*O*-[bis(4-methoxyphenyl)(phenyl))methyl]-2′-*O*-{6-[(4-nitrophenoxy)carbonyl]hexanoyl}-β-*D*-ribopyranosyl-2-[(prop-2-enyl)oxy]purine* (**10f**). A soln. of 134 mg (0.16 mmol) of **8f** in in 2 ml of pyridine was treated with 453 mg (1.13 mmol) of bis(4-nitrophenyl) heptane-1,7-dioate and 20 mg (0.16 mmol) of DMAP. The mixture was stirred for 16 h at 25°, diluted with 50 ml of CH_2Cl_2, and washed with sat. aq. $NaHCO_3$ soln. The aq. phase was re-extracted with 2 × 50 ml of CH_2Cl_2. The combined org. layers were dried (Na_2SO_4), concentrated *in vacuo*, co-evaporated with toluene, and the residue was purified by CC (SiO_2; 20–50% AcOEt in hexanes to yield 157.4 mg (89%) of **10f**. TLC (50% AcOEt in hexanes): R_f 0.47. ^{1}H-NMR (200 MHz, $CDCl_3$): 1.03–1.60 (*m*, 3 CH_2); 2.05 (*m*, CH_2); 2.40 (*m*, CH_2); 2.89 (*dd*, H_β–C(5′)); 3.78 (*s*, MeO); 3.85 (*dd*, H_α–C(5′)); 4.10 (*m*, H–C(4′)); 4.89 (*m*, H(allyl)); 5.15–5.50 (*m*, C=CH_2, H–C(2′)); 5.83 (br. *s*, H–C(3′)); 5.94–6.20 (*m*, C*H*=CH_2, H–C(1′)); 6.70–8.30 (*m*, 27 arom. H, H–C(8)); 8.80 (br. *s*, NH). FAB-MS (pos., 3-NBA): 1097.3 (28, $[M+H]^+$), 303.1 (100).

*2,6-Diamino-*N^2,N^6*-dibenzoyl-9-(3′-*O*-benzoyl-4′-*O*-[bis(4-methoxyphenyl)(phenyl)methyl]-2′-*O*-{6-[(nitrophenoxy)carbonyl]hexanoyl}-β-*D*-ribopyranosyl)purine* (**10g**). In a 10-ml round-bottomed flask was placed 0.10 g (0.11 mmol) of **8g**, followed by addition of 2 ml of absolute pyridine, 14 mg (0.11 mmol) of DMAP, 0.31 g (0.78 mmol) of bis(4-nitrophenyl) heptane-1,7-dioate, and the mixture was stirred at r.t. for 24 h. The mixture was poured into 50 ml of sat. aq. $NaHCO_3$ soln. and extracted with 3 × 30 ml of CH_2Cl_2. The combined org. layers were dried ($MgSO_4$), concentrated *in vacuo*, and the residue was chromatographed (30 g of SiO_2; AcOEt : hexanes, 1:5 → 5:1) to afford 0.11 g (82%) of **10g**. TLC (SiO_2; AcOEt/hexanes 1:2 (with 1% MeOH)): R_f 0.42. ^{1}H-NMR (400 MHz, $CDCl_3$): 1.0–1.6 (*m*, 3 CH_2(pimalate)); 1.9–2.15 (*m*, CH_2(pimalate)); 2.42 (*t*, J = 7.5, CH_2C=O); 2.86 (*dd*, J = 11.0, 5.7, H_{eq}–C(5′)); 3.77, 3.78 (*s*, 2 MeO); 3.81 (*dd*, appears as *t*, J = 11.0, H_{ax}–C(5′)); 4.10 (*m*, H–C(4′)); 5.45 (*d*, J = 9.6, H–C(2′)); 5.84 (br. *s*, H–C(3′)); 6.12 (*d*, J = 9.6, H–C(1′)); 6.7–8.4 (m, 32 arom. H, H–C(8)); 9.06, 9.31 (br. *s*, 2 NH). ^{13}C-NMR (100 MHz, $CDCl_3$) 23.99, 24.08, 27.95, 33.40, 33.79 (5*t*, C(pimalate)); 55.26 (*q*, MeO); 66.15 (*t*, C(5′)); 68.53 (*d*, C(4′)); 71.19 (*d*, C(2′)); 77.22 (*d*, C(3′)); 78.50 (*d*, C(1′)); 87.44 (*s*, C(trityl)); 113.47, 113.55, 115.89 (*d*, arom. C); 122.44 (*s*, C(5)); 125.11–133.55 (*d* + *s*,

arom. C); 135.65, 135.83 (*d*, arom. C, C(8)); 140.23, 149.98, 155.43, 158.94 (4*s*, C(2), C(4), C(6), arom. C); 164.87, 165.99, 170.98, 171.62 (4*s*, C=O). FAB-MS (pos., 3-NBA): 1160 (100, $[M+H]^+$).

Bis(4-nitrophenyl) Heptane-1,7-dioate. To a soln. of 12 ml of pyridine in 25 ml of toluene was added 14 g (70 mmol) of heptane-1,7-dioyl dichloride at r.t. with stirring. The resulting orange suspension was treated with 19.5 g (140 mmol) of 4-nitrophenol, whereby the temp. of the mixture rose to 50°, and the suspension turned yellow. The suspension was filtered and washed with 150 ml of AcOEt. The combined filtrates were kept at 4°, from which 6.85 g of the first batch of yellow crystals were obtained. From the mother liquor, further recrytallization attempts afforded 9.51 g of a second batch of yellow crystals, for combined total yield of 16.36 g (47.5%) of bis(4-nitrophenyl) heptane-1,7-dioate. M.p. 84° ([60]: 84–85°). TLC (SiO_2; AcOEt): R_f 0.9. ^{1}H-NMR ($CDCl_3$): 1.6–2.1 (*m*, 3 CH_2); 2.7 (*t*, 2 CH_2); 7.3 (*d*, 4 arom. H); 8.3 (*d*, 4 arom. H).

3.2. *General Procedure for the Preparation of the Solid Supports* **11a**–**11g** (*Scheme 3*). A suspension of the nucleoside, LCAA-CPG, EtN(i-Pr)$_2$, and pyridine in DMF was shaken overnight. The solid support was filtered off, washed consecutively with 10 ml of DMF, 20 ml of MeOH, and 20 ml of Et_2O, dried in high vacuum, suspended in 2 ml of pyridine, and treated with 0.1 ml of Ac_2O. After being shaken 2 h at r.t., the solid support was filtered off and washed consecutively with 10 ml of pyridine, 10 ml of MeOH, and 15 ml of Et_2O. After drying, the loading density was determined by suspending aliquots in 70% aq. $HClO_4$/MeOH 1:1 and measuring the absorption at 498 nm (ε (DMT cation) = 70000 $cm^{-1}\,l^{-1}\,mol^{-1}$).

Solid Support with **10a** (→ **11a**). From 110 mg (0.12 mmol) of **10a**, 0.2 ml (1.2 mmol) of EtN(i-Pr)$_2$, 0.06 ml (0.07 mmol) of pyridine, and 600 mg of LCAA-CPG in 2 ml of DMF. The loading density was 21 μmol uracil-nucleoside/g solid support.

Solid Support with **10b** (→ **11b**). From 110 mg (0.12 mmol) of **10b**, 0.2 ml (1.2 mmol) of EtN(i-Pr)$_2$, 0.06 ml (0.07 mmol) of pyridine, and 600 mg of LCAA-CPG in 2 ml of DMF. The loading density was 24 μmol thymine-nucleoside/g solid support.

Solid Support with **10c** (→ **11c**). From 80 mg (0.08 mmol) of **10c**, 0.13 ml (1 mmol) of EtN(i-Pr)$_2$, 0.06 ml (0.07 mmol) of pyridine, and 250 mg of LCAA-CPG in 2.5 ml of DMF. The loading density was 19 μmol cytosine-nucleoside/g solid support.

Solid Support with **10d** (→ **11d**). From 190 mg (0.2 mmol) of **10d**, 0.34 ml (2 mmol) of EtN(i-Pr)$_2$, 0.08 ml (1 mmol) of pyridine, and 1000 mg of LCAA-CPG in 3 ml of DMF. The loading density was 24 μmol adenine-nucleoside/g solid support.

Solid Support with **10e** (→ **11e**). From 340 mg (0.32 mmol) of **10e**, 0.55 ml (3.2 mmol) of EtN(i-Pr)$_2$, 0.77 ml (1 mmol) of pyridine, and 2000 mg of LCAA-CPG in 7 ml of DMF. The loading density was 30 μmol guanine-nucleoside/g solid support.

Solid Support with **10f** (→ **11f**). From 219 mg (0.2 mmol) of **10f**, 0.34 ml (2.0 mmol) of EtN(i-Pr)$_2$, 3.0 ml of DMF, 0.8 ml (1 mmol) of pyridine, and 1000 mg of LCAA-CPG in 7 ml of DMF. The loading density was 20 μmol isoguanine-nucleoside/g solid support.

Solid Support with **10g** (→ **11g**). In a 5-ml round-bottomed flask were placed 200 mg (0.17 mmol) of **10g** and 1.0 g of CPG solid support, and the mixture was dried under high vacuum for 24 h. This mixture was treated with 3.5 ml of DMF, 0.45 ml of Et_3N, and 0.3 ml of pyridine. The mixture was shaken every 2–3 h at r.t. After 24 h, the mixture was washed with 50 ml of MeOH and then with 50 ml of Et_2O. The resulting white powder was dried under high vacuum. 2.166 mg of this CPG-support was weighed into a 10-ml volumetric flask and was made upto 10 ml with 70% aq. $HClO_4$/MeOH 1:1 soln. This orange soln. had an UV absorption of 0.41 (λ_{max} = 498 nm), which gave a loading of 27.3 μmol/g (ε = 70,000). A similar measurement with 4.406 mg of the CPG support gave a loading of 23.0 μmol/g. Average loading = 25.2 μmol/g. The CPG support was treated with 40 mg of DMAP, 1 ml of pyridine, 500 μl of Ac_2O, and allowed to stand at r.t. for 2 h. The CPG support was washed with 50 ml of MeOH, followed by 50 ml of Et_2O, and dried at r.t./high vacuum overnight.

4. ***Automated Solid-Phase Synthesis and Purification of Oligonucleotides Referring*** *to* Scheme 4. Oligonucleotide syntheses were carried out on a 1–10-μM scale on a *Pharmacia Gene Synthesizer Plus* or on an *Expedite 8909 Nucleic Acid Synthesis* system (*PE Biosystems*). The DNA/RNA synthesizer column was filled with 30–35 mg (1 μmol) or 100–120 mg (10 μmol) of CPG solid support loaded with the appropriate nucleobase. The substrates and reagents required were prepared as follows.

4.1. *Pre-automation Procedures for the* Pharmacia Gene Synthesizer Plus *System.* 4.1.1 *Phosphoramidites.* A 10% (*w*/*v*) soln. of phosphoramidate in MeCN ($n \times 160$ μl for 1 μmol and $n \times 400$ μl for 10 μmol; n = number of couplings). The phosphoramidite soln. was dried (4 Å molecular sieves, 8–12 mesh, freshly activated by heating at *ca.* 300° under high vacuum overnight) overnight at r.t. prior to use.

4.1.2. *Activator Soln.* A mixture of 0.15M 5-(4-nitrophenyl)-1*H*-tetrazole and 0.35M 1*H*-tetrazole in MeCN (180–600 μl per coupling) dried over freshly activated 3-Å or 4-Å molecular sieves.

4.1.3. *Capping A:* 1.5 g of DMAP in 25 ml of MeCN.

4.1.4. *Capping B:* 2 ml of Ac_2O and 3 ml of 2,4,6-collidine in 5 ml of MeCN.

4.1.5. *Oxidizing Soln.:* 0.1M I_2 in MeCN/2,4,6-collidine/H_2O 100:9:45.

4.1.6. *Detritylation Reagent:* 6% $Cl_2CHCOOH$ in $ClCH_2CH_2Cl$.

The synthesis of oligonucleotides with the *Pharmacia Gene Synthesizer Plus* system was accomplished with the following modifications to the protocol developed for the homo-DNA synthesis: *1*) the detritylation step was conducted over a period of 5 min for 1-μmol and 7 min for 10-μmol scale. *2*) the phosphoramidite + activator coupling step was conducted over a period of 45 min (1 μmol) and 60 min (10 μmol). Prior to the coupling step, the solid support was washed with MeCN for 4 min. Most of the oligonucleotides were synthesized in the 'Trityl-on' mode, while some were synthesized in the 'Trityl-off' mode.

4.2. *Pre-automation Procedures for the* Expedite 8909 Nucleic Acid Synthesis *System.* 4.2.1. *Phosphoramidites.* The amount of phosphoramidite soln. was determined as follows: $(n+2)\times(22.1)$ mg of phosphoramidite dissolved in $n\times 221$ μl of dry MeCN to obtain *ca.* 0.1M soln. The phosphoramidite soln. was dried (4-Å molecular sieves, 8–12 mesh, freshly activated by heating at *ca.* 300° under high vacuum overnight) overnight at r.t. prior to use.

4.2.2. *Activator Soln.* 0.35M soln. of 5-(ethylsulfanyl)-1*H*-tetrazole (1 g in 22 ml of MeCN) dried over freshly, activated 3-Å or 4-Å molecular sieves.

4.2.3. *Capping A:* 1.5 g of DMAP in 25 ml of MeCN.

4.2.4. *Capping B:* 5 ml of Ac_2O and 7.5 ml of 2,4,6-collidine in 12.5 ml of MeCN.

4.2.5. *Oxidizing Soln.:* 200 mg of I_2 in 50 ml of MeCN, followed by addition of 4.6 ml of 2,4,6-collidine and 23 ml of H_2O.

4.2.6. *Detritylation Reagent:* 6% $Cl_2CHCOOH$ in $ClCH_2CH_2Cl$.

The synthesis of oligonucleotides with the *Expedite 8909 Nucleic Acid Synthesis* system was accomplished with the following modifications to the protocol provided by the manufacturer for the RNA synthesis: *1*) the detritylation step was conducted with 500 pulses over a period of 80–400 s. *2*) The phosphoramidite + activator coupling step was conducted with 13 pulses over a period of 1160 s. Majority of oligonucleotides were synthesized in the 'Trityl-on' mode, while some were synthesized in the 'Trityl-off' mode.

4.3. *Post-automation Procedures.* 4.3.1. *Removal of Allyl Protecting Group and Removal of Nucleobase Protecting Groups with Concomitant Detachment from CPG solid Support.* After the automated synthesis was completed, the CPG solid support containing the oligonucleotide was dried *in vacuo* for 30 min, and first the removal of the allyl protecting group was effected by treatment with Pd^0 catalyst according to one of the following procedures developed by *Noyori* and co-workers [55][54][61].

Method A: Allyl Deprotection for 'Trityl-off' Sequences [55]. A mixture of 360 μl (3.7 μmol) of $BuNH_2$, 20–40 mg (22–45 μmol) of (dibenzylideneacetone)$_3Pd^0$, 60–120 mg (225–450 μmol) of Ph_3P, 140 μl (3.7 μl) of HCO_2H in 4.5 ml of THF was added to the CPG solid support and warmed to 55° for 1.5–12 h. The suspension was filtered, the CPG solid support carefully washed sequentially with 10 ml of THF, followed by 15 ml of acetone, treated with 4.5 ml of 0.1M aq. $NaCS_2NEt_2$ soln. at r.t. for 30 min, filtered and washed again sequentially with 10 ml of H_2O, 15 ml of acetone, 10 ml of EtOH, and dried in high vacuum for 15 min.

Method B: Allyl Deprotection for 'Trityl-on' Sequences [54]. A soln. of 20–90 mg (148 μmol–0.7 mmol) of $Et_2NH_2\cdot HCO_3$, 11.6–90 mg (10–77 μmol) of $(Ph_3P)_4Pd^0$, 1.3–90 mg (5 μmol–0.35 mmol) of Ph_3P in 1.0–5.0 ml of CH_2Cl_2 was added to the CPG solid support and the resulting suspension was vigorously shaken at r.t. for 3–4 h (12–24 h for isoG-containing sequences). The suspension was filtered, the CPG solid support was carefully washed sequentially with 10 ml each of CH_2Cl_2 , acetone, and H_2O, treated with 4.5 ml of 0.1 M aq. $NaCS_2NEt_2$ at r.t. for 30–45 min, filtered and washed again sequentially with 10 ml of H_2O, 15 ml of acetone, 10 ml of CH_2Cl_2, and dried in high vacuum for 15 min.

Method C: Allyl Deprotection for 'Trityl-off' sequences [61]. A homogenous soln. of 460 μl (4.5 μmol) of $Et_2NH_2\cdot HCO_3$, 177 mg (171 μmol) of (dibenzylideneacetone)$_3Pd^0$–$CHCl_3$ adduct, 432 mg (2.7 mmol) of Ph_3P, 360 μl (9.6 μmol) of HCO_2H in 6.5 ml of THF was added to the CPG solid support in a round-bottomed flask that was wrapped tightly with Al foil and shaken at 50° for 3–4 h. The suspension was filtered, the CPG solid support was carefully washed sequentially with 10 ml of THF, 10 ml of acetone, 10 ml of H_2O, treated with 4.5 ml of 0.1M aq. $NaCS_2NEt_2$ at r.t. for 30–45 min, filtered and washed again sequentially with 10 ml of H_2O, 15 ml of acetone, 10 ml of CH_2Cl_2, and dried in high vacuum for 15 min.

The dry CPG solid support containing the oligonucleotide was placed in *Eppendorf* tubes (1.5 ml), and side-by-side deprotection of nucleobase protecting groups and detachment of the oligonucleotides from the CPG solid support was effected by one of the following methods (*Table 3* lists the specific deprotection method for the specific sequence).

Method D: Detachment from CPG for Phosphate-Containing Sequences and Acyl Deprotection. Sat. aq. NH_3/EtOH, 3:1, r.t., 3–4 h.

Method E: Detachment from CPG and Acyl Deprotection. 4.5 ml of 0.2M $MeONH_2 \cdot HCl$ in aq. conc. NH_3/EtOH, r.t., 20 h.

Method F: Detachment from CPG and Acyl Deprotection for containing Sequences. 1.5 ml of 15–25% aq. $NH_2NH_2 \cdot H_2O$, 4°, 20–30 h. In the case of D-containing sequences, the deprotection was conducted at r.t. for 48 h.

Method G: Detachment from CPG and Acyl Deprotection. 5 ml of 40% (*w*/*w*) aq. $MeNH_2$/conc. aq. NH_3, 1:1, r.t., 5–6 h.

All of the above deprotections were monitored by anion exchange HPLC for optimum deprotection time.

Workup for Methods D *and* G. The CPG solid support containing *Eppendorf* vial was centrifuged. After centrifugation, the supernatant was removed and the CPG solid support was washed with 3×0.5 ml of H_2O. The combined washings and supernatant was lyophilized to dryness with a *SpeedVac* evaporator. The residue was dissolved in 1–3 ml of H_2O for analysis and purification.

Workup for Methods E *and* F: The CPG solid support containing *Eppendorf* vial was centrifuged. After centrifugation, the supernatant was removed, and the CPG solid support was washed with 3×0.5 ml of H_2O. The combined washings and supernatant were subjected to the 'desalting' procedure over a *Sep Pak C18* cartridge (*Waters*) (see *Sect. 7*) to remove excess $MeONH_2 \cdot HCl$ or $NH_2NH_2 \cdot H_2O$. The oligonucleotide-containing fractions were combined and lyophilized to dryness with a *SpeedVac* evaporator. The residue was dissolved in 1–3 ml of H_2O for analysis and purification.

Oligonucleotides synthesized in the 'Trityl-off' mode were directly taken to the next step of purification by ion-exchange HPLC.

4.3.2. *Detritylation of 'Trityl-on' Oligonucleotides.* The aq. soln. containing the acyl deprotected crude oligonucleotides (synthesized in the 'Trityl-on' mode) were concentrated *in vacuo*, the crude-residue was treated with *ca.* 10 ml of 80% aq. HCOOH (a red color appears within seconds indicating detritylation) at r.t. for 15 min and concentrated *in vacuo* to dryness. The residue was dissolved in *ca.* 2 ml of H_2O, filtered (*Nalgene* syringe filter, 0.2 μ), and taken to the next step, ion-exchange HPLC purification.

5. *Preparation of Phosphorylated Oligonucleotides* (*Scheme 5*). 5.1. *4′-Phosphate-p-RNA-Oligonucleotide Derivatives.* After the final detritylation step on the synthesizer to generate the 4′-OH end, the CPG-containing oligonucleotide was coupled with 0.1M bis(allyloxy)(diisopropylamine)phosphine in MeCN in the presence of 0.5M activator (0.15M 5-(4-nitrophenyl)-1*H*-tetrazole and 0.35M 1*H*-tetrazole in MeCN), according to the coupling protocol outlined in *Sect. 4.1.* The resulting 4′-*O*-phosphitylated oligonucleotide derivative was subjected to capping and oxidation following the usual protocols (*Sect. 4.2*). The CPG solid support was dried, deprotection of the allyl groups was performed according to *Sect. 4.3.1* (*Method A*), deprotection of acyl groups and detachment from the solid support was conducted as described in *Sect. 4.3.1.* (*Method F*), yielding the 4′-phosphorylated-p-RNA oligonucleotide. The crude oligonucleotide was purified by ion-exchange HPLC.

5.2. *2′- and 3′-Phosphate-p-RNA-Oligonucleotide Derivatives.* The oligonucleotides with the 2′- or 3′-end derivatized as phosphate were synthesized by automated solid-support synthesis with a universal solid support derivatized with a sulfone linker[25]) [62] in place of the usual pimelic acid (heptanedioic acid) linker. The 2′-end (or the 3′-end) of the nucleoside was coupled onto this solid support according to the automated synthesizer protocols (*Sect. 4.1*). The CPG solid support was dried, deprotection of the allyl groups was performed according to *Sect. 4.3.1* (*Method A* or *B*), deprotection of acyl groups and detachment from the solid support (*via* elimination of the sulfone linker) was conducted as described in *Sect. 4.3.1* (*Method F*), yielding the 2′- or 3′-phosphorylated-p-RNA oligonucleotide. The crude oligonucleotide was purified by ion-exchange HPLC.

5.3. *2′,3′- and 3′,4′-Cyclophosphate-p-RNA-Oligonucleotide Derivatives.* To a 100–500 mM soln. of the oligonucleotide-2′-phosphate (or -3′-phosphate) in H_2O, 100–200 mg/ml (0.5–1.0M, excess) of the H_2O-soluble DEC · HCl (*Fluka*, 03449) was added. The soln. was kept at r.t. for 1–3 h and monitored by HPLC (*Mono Q*). When more than 90% of the starting material had disappeared, DEC · HCl was removed by desalting of the soln. over a *Sep Pak C-18* (*Waters*) cartridge (*Sect. 7*). Oligonucleotide containing fractions were evaporated to a volume of 1–2 ml and purified by HPLC (*Mono Q*), followed by final desalting over a *Sep Pak C-18* (*Waters*) cartridge. The average isolated yields were *ca.* 70%.

6. *HPLC Purification of Oligonucleotides.* Oligonucleotides were purified by reverse-phase or ion-exchange HPLC.

Anion-exchange HPLC was performed either on *A*) *Pharmacia GP-250 Gradient Programmer* equipped with two *Pharmacia P-500* pumps, *ABI-Kratos Spectraflow 757* UV/VIS detector and a *Hewlett-Packard 3396A* analog integrator or *B*) *Pharmacia Äkta purifier (900)* controlled by *UNICORN* system. Ion-exchange columns:

a) *Mono Q HR 5/5* (*Pharmacia*) or *SAX 1000–8* (*Macherey & Nagel*); buffer *A:* 10 mM Na_2HPO_4 in H_2O, pH 10.5; buffer *B:* 10 mM Na_2HPO_4 in H_2O, 1M NaCl, pH 10.5. The product fractions were collected either in a 1M aq. AcOH soln. or in a 1M aq. $Et_3NH \cdot HCO_3$ buffer soln. *b*) *Nucleogen-DEAE 60-7* (*Macherey & Nagel*), 125 × 4 mm, flow 1 ml/min; buffer *A:* 10 mM Na_2HPO_4, H_2O/MeCN 1:4, pH 11.5; buffer *B:* 10 mM Na_2HPO_4, 1M NaCl, H_2O/MeCN 1:4, pH 11.5.

Reverse-phase HPLC was performed with a *Pharmacia-LKB-2249* gradient pump, *ABI-Kratos Spectraflow 757* UV/VIS detector, and a *Hewlett-Packard 3396A* analog integrator or *W&W 600* recorder. Reverse-phase columns: *a*) anal.: *Aquapore RP-300 C-8* (*Brownlee*), 220 × 4.6 mm, 7 μm, flow 1 ml/min; buffer *A:* 0.1M Et_3N, 0.1M AcOH, H_2O, pH 7.0; buffer *B:* 0.1M Et_3N, 0.1M AcOH, H_2O/MeCN 1:4. *b*) Prep.: *Spherisorb-S10X* RP-C18, 10 μ, 300-Å (packed by Dr. *J. Schreiber*, ETH Zürich), 220 × 12 mm, flow 3–5 ml/min; buffer *A:* 0.1M Et_3N, 0.1M AcOH, H_2O, pH 7.0; buffer *B:* 0.1M Et_3N, 0.1M AcOH, H_2O/MeCN 1:4.

7. ***Desalting of Oligonucleotides.*** The product fractions from HPLC purification were combined and diluted with 0.1–0.5M aq. $Et_3NH \cdot HCO_3$ buffer to twice the volume, and the solns. were applied to a previously conditioned[61]) reverse phase *Sep-Pak* cartridge (*C18 Waters*). Successive elution with 10 ml each of 0.1–0.5M aq. $Et_3NH \cdot HCO_3$ buffer soln., H_2O, 20–50% aq. MeCN, and lyophillization of the aq. MeCN fractions containing the product (monitored by UV at 260 nm) afforded the salt-free oligonucleotide[62]). The residue was dissolved in 1 ml of H_2O and stored at −20° as stock soln.

8. ***Ligation Experiments*** [6]. For each of the oligonucleotides in ligation experiments, a 1 ml stock aq. soln. of either 7.5 μM or 15.0 μM (0.4–1.2 OD) was prepared. Unless stated otherwise, the concentration of ligands in ligation experiments were 300 μM each, whereas the concentration of template was 150.0 μM or 75.0 μM. The corresponding volumes of aq. stock soln. of the sequences required for a particular ligation experiment were pipetted into an *Eppendorf* tube, and H_2O was removed by lyophilization; the appropriate amount (15 μl or 300 μl) of ligation buffer (0.1M aq. HEPES, 1 mM EDTA, pH 8.0 with either 1.0 or 1.5M LiCl) was added to the dry material; for ligation experiments that were exploratory and analyzed only by HPLC, the reaction volumes were 15 μl (*ca.* 1–4.5 nmol each sequence). In cases where the ligation-products were isolated and characterized by HPLC, MALDI-TOF-MS, and UV melting curves, the reaction volumes were 300 μl (*ca.* 20–90 nmol each sequence). The mixture was vortexed and briefly centrifuged and was kept either at r.t. (22–25°) or at 4° or at 10°. *Table 7* lists the reaction conditions for the various ligation experiments.

All reactions were monitored by ion-exchange HPLC: 2 μl of the vortexed and briefly centrifuged reaction mixture was diluted in 400 μl of H_2O and directly injected without any further treatment. All analyses, separations, and purifications were performed on a *Mono Q HR 5/5* column (*Pharmacia*) with a linear gradient of 0 to 1M NaCl in 10 mM sodium phosphate at pH 11.5 (detection at 260 or 270 nm).

In most cases, template and ligation product gave well separated peaks in the HPLC traces, and ligation yields were calculated as the relative amount of the ligation product with respect to the template (% area of the integrated HPLC traces; correcting for the differences in extinction coefficients of the two sequences). In some cases, the ligation-product hairpin was isolated, and the identity was confirmed by MALDI-TOF-MS and co-injection by authentic material, while, in most of the other experiments, product identification was based on the co-injection with authentic material or by comparison of t_R values with those of authentic material.

In the case of the ligation of p**r**(ATTTAAAA)-2′-p and p**r**(ATTATTAT)-2′,3′-cp in the presence of p**r**(TTTTAAATATAATAAT) as template (*Entry 14* in *Table 7*), product identification was based on co-injection with authentic material after dephosphorylation of the isolated ligation product with alkaline phosphatase (from calf intestine, EC 3.1.3.1., 30000 U/ml, Boehringer. Mannheim, #567744: dephosphorylation was achieved by adding 0.1*n* μl of 0.1M diethanol buffer pH 9.8 followed by 0.01*n* μl of alkaline phosphatase to *n* μl of a 1 to 5 μM soln. of the oligonucleotide). In this case, product yield was determined after conversion of the product to the corresponding cyclophosphate by treating the reaction mixture with DEC · HCl, as a better separation between the product-2′,3′-cyclophosphate peak and template peak was observed.

---

61) Conditioning of the *Sep Pak C18* cartridge is performed as follows: the cartridge is washed sequentially with 5 ml of MeCN (or MeOH)/H_2O 1:1, 5 ml of H_2O, and finally with 5 ml of 0.1–0.5M aq. $Et_3NH \cdot HCO_3$ buffer.

62) Co-evaporation with 1–2 ml of H_2O was necessary to remove the presence of any residual $Et_3NH \cdot HCO_3$ buffer.

REFERENCES

[1] S. Pitsch, S. Wendeborn, B. Jaun, A. Eschenmoser, *Helv. Chim. Acta* **1993**, *76*, 2161.
[2] S. Pitsch, R. Krishnamurthy, M. Bolli, S. Wendeborn, A. Holzner, M. Minton, C. Lesueur, I. Schlönvogt, B. Jaun, A. Eschenmoser, *Helv. Chim. Acta* **1995**, *78*, 1621.
[3] R. Krishnamurthy, S. Pitsch, M. Minton, C. Miculka, N. Windhab, A. Eschenmoser, *Angew. Chem.* **1996**, *108*, 1619; *Angew. Chem., Int. Ed.* **1996**, *35*, 1537.
[4] I. Schlönvogt, S. Pitsch, C. Lesueur, A. Eschenmoser, B. Jaun, R. M. Wolf, *Helv. Chim. Acta* **1996**, *79*, 2316.
[5] R. Micura, M. Bolli, N. Windhab, A. Eschenmoser, *Angew. Chem.* **1997**, *109*, 899; *Angew. Chem., Int. Ed.* **1997**, *36*, 870.
[6] M. Bolli, R. Micura, S. Pitsch, A. Eschenmoser, *Helv. Chim. Acta* **1997**, *80*, 1901.
[7] M. Bolli, R. Micura, A. Eschenmoser, *Chem. Biol.* **1997**, *4*, 309.
[8] R. Micura, R. Kudick, S. Pitsch, A. Eschenmoser, *Angew. Chem.* **1999**, *111*, 715; *Angew. Chem., Int. Ed.* **1999**, *38*, 680.
[9] F. Reck, H. Wippo, R. Kudick, R. Krishnamurthy, A. Eschenmoser, *Helv. Chim. Acta* **2001**, *84*, 1778.
[10] H. Wippo, F. Reck, R. Kudick, M. Ramaseshan, G. Ceulemans, M. Bolli, R. Krishnamurthy, A. Eschenmoser, *Bioorg. Med. Chem.* **2001**, *9*, 2411.
[11] T. Wagner, H. K. Huynh, R. Krishnamurthy, A. Eschenmoser, *Helv. Chim. Acta* **2002**, *85*, 399.
[12] O. Jungmann, M. Beier, A. Luther, H. K. Huynh, M.-O. Ebert, B. Jaun, R. Krishnamurthy, A. Eschenmoser, *Helv. Chim. Acta* **2003**, *86*, 1259.
[13] R. Krishnamurthy, S. Guntha, A. Eschenmoser, *Angew. Chem.* **2000**, *112*, 2369; *Angew. Chem., Int. Ed.* **2000**, *39*, 2281.
[14] R. Krishnamurthy, G. Arrhenius, A. Eschenmoser, *Origins Life Evol. Biosphere* **1999**, *29*, 333.
[15] F. Reck, H. Wippo, R. Kudick, M. Bolli, G. Ceulemans, R. Krishnamurthy, A. Eschenmoser, *Org. Lett.* **1999**, *1*, 1531.
[16] O. Jungmann, H. Wippo, M. Stanek, H. K. Huynh, R. Krishnamurthy, A. Eschenmoser, *Org. Lett.* **1999**, *1*, 1527.
[17] M. Beyer, F. Reck, T. Wagner, R. Krishnamurthy, A. Eschenmoser, *Science* **1999**, *283*, 699.
[18] C. Lehmann, B. Schweizer, C. Leumann, A. Eschenmoser, *Helv. Chim. Acta* **1997**, *80*, 1421.
[19] P. Lohse, B. Oberhauser, B. Oberhauser-Hofbauer, G. Baschang, A. Eschenmoser, *Croat. Chem. Acta* **1996**, *69*, 535.
[20] S. Pitsch, A. Eschenmoser, B. Gedulin, S. Hui, G. Arrhenius, *Origins Life Evol. Biosphere* **1995**, *25*, 297.
[21] S. Pitsch, A. Eschenmoser, *Pol. J. Chem.* **1994**, *68*, 2383.
[22] S. Pitsch, E. Pombo-Villar, A. Eschenmoser, *Helv. Chim. Acta* **1994**, *77*, 2251.
[23] Y.-B. Xiang, S. Drenkard, K. Baumann, D. Hickey, A. Eschenmoser, *Helv. Chim. Acta* **1994**, *77*, 2209.
[24] R. W. Fischer, A. G. Helg, K. Groebke, U. Diederichsen, A. Giger, R. Hammer, R. Krishnamurthy, C. Miculka, B. Jaun, S. Pitsch, C. Leumann, A. Eschenmoser, *Helv. Chim. Acta*, in preparation.
[25] K. Groebke, J. Hunziker, W. Fraser, L. Peng, U. Diederichsen, K. Zimmermann, A. Holzner, C. Leumann, A. Eschenmoser, *Helv. Chim. Acta* **1998**, *81*, 375.
[26] G. Otting, M. Billeter, K. Wüthrich, H.-J. Roth, C. Leumann, A. Eschenmoser, *Helv. Chim. Acta* **1993**, *76*, 2701.
[27] J. Hunziker, H.-J. Roth, M. Böhringer, A. Giger, U. Diederichsen, M. Göbel, R. Krishnan, B. Jaun, C. Leumann, A. Eschenmoser, *Helv. Chim. Acta* **1993**, *76*, 259.
[28] M. Böhringer, H.-J. Roth, J. Hunziker, M. Göbel, R. Krishnan, A. Giger, B. Schweizer, J. Schreiber, C. Leumann, A. Eschenmoser, *Helv. Chim. Acta* **1992**, *75*, 1416.
[29] A. Eschenmoser, M. Dobler, *Helv. Chim. Acta* **1992**, *75*, 218.
[30] D. Müller, S. Pitsch, A. Kittaka, E. Wagner, C. E. Wintner, A. Eschenmoser, *Helv. Chim. Acta* **1990**, *73*, 1410.
[31] E. Wagner, Y.-B. Xiang, K. Baumann, J. Gück, A. Eschenmoser, *Helv. Chim. Acta* **1990**, *73*, 1391.
[32] S. Drenkard, J. Ferris, A. Eschenmoser, *Helv. Chim. Acta* **1990**, *73*, 1373.
[33] G. Ksander, G. Bold, R. Lattmann, C. Lehmann, T. Früh, Y.-B. Xiang, K. Inomata, H.-P. Buser, J. Schreiber, E. Zass, A. Eschenmoser, *Helv. Chim. Acta* **1987**, *70*, 1115.
[34] A. Eschenmoser, 'Kon-Tiki-Experimente zur Frage nach dem Ursprung von Biomolekülen', in 'Materie und Prozesse. Vom Elementaren zum Komplexen', Eds. W. Gerok *et al.*, Verh. Ges. Dtsch. Naturforsch. Ärzte, 116. Versammlung, Berlin 1990, Wissenschaftl. Verlagsges.mbH, Stuttgart, 1991, p. 135–172.
[35] A. Eschenmoser, *Nachr. Chem. Tech. Lab.* **1991**, *39*, 795.

[36] A. Eschenmoser, 'Toward a Chemical Etiology of the Natural Nucleic Acids' Structure', in Proceedings R. A. Welch Foundation, Conference on Chemical Research XXXVII, '40 Years of the DNA Double Helix', Robert A. Welch Foundation, Houston/Texas, 1993, p. 201 – 235.
[37] A. Eschenmoser, *Pure Appl. Chem.* **1993**, *65*, 1179.
[38] A. Eschenmoser, *Origins Life Evol. Biosphere* **1994**, *24*, 389.
[39] A. Eschenmoser, *Origins Life Evol. Biosphere* **1997**, *27*, 535.
[40] A. Eschenmoser, *Science* **1999**, *284*, 2118.
[41] R. W. Fischer, 'Allopyranosyl-Nukleinsäure: Synthese, Paarungseigenschaften und Struktur von Adenin-/Uracil-haltigen Oligonukleotiden', Diss. No. 9971, ETH Zürich, 1992; A. G. Helg, 'Allopyranosyl-Nukleinsäure: Synthese, Paarungseigenschaften und Struktur von Guanin-/Cytosin-enthaltenden Oligonukleotiden', Diss. No. 10464, ETH-Zürich, 1994; K. Groebke, 'Über Purin-Purin-Paarungen bei Hexopyranose-Nukleinsäuren', Diss. No. 10149, ETH Zürich, 1993; U. Diederichsen, 'A. Hypoxanthin-Basenpaarungen in Homo-DNA-Oligonucleotiden. – B. Zur Frage des Paarungsverhaltens von Glucopyranosyl-Oligonucleotiden', Diss. No. 10122, ETH Zürich, 1993; A. Giger, 'Untersuchungen über Oligonucleotide mit 2-Deoxy-D-Ribose, 2,3-Dideoxy-D-Glucopyranose und D-Allopyranose als Zuckerbausteine', Diss. No. 9975, ETH-Zürich, 1992.
[42] R. Krishnamurthy, 'Synthesis and Characterization of Altrose-Hexose and Ribo-Pyranosyl based Oligonucleotides', Postdoctoral Report, ETH-Zürich, 1994.
[43] A. Van Aerschot, I. Verheggen, C. Hendrix, P. Herdewijn, *Angew. Chem., Int. Ed.* **1995**, *34*, 1338; C. Hendrix, H. Rosemeyer, I. Verheggen, F. Seela, A. Van Aerschot, P. Herdewijn, *Chem. Eur. J.* **1997**, *3*, 110.
[44] B. Allart, R. Busson, J. Rozenski, A. Van Aerschot, P. Herdewijn, *Tetrahedron* **1999**, *55*, 6527.
[45] N. Hossain, B. Wroblowski, A. Van Aerschot, J. Rozenski, A. de Bruyn, P. Herdewijn, *J. Org. Chem.* **1998**, *63*, 1574.
[46] R. Hammer, 'Synthesis and Characterization of Hexose Pyranosyl Nucleic Acids', Postdoctoral Report, ETH Zürich, 1992.
[47] C. Miculka, '1. Paarungseigenschaften von 2′-Deoxy-allopyranosyl-(6′ → 4′)-oligonucleotiden ('Homo-RNA') und L-Ribopyranosyl-(4′ → 2′)-oligonucleotiden ('p-RNA'). 2. Eine Synthese der racemischen Ribose und des racemischen Ribopyranosyladenins', Postdoctoral Report, Institute for Pharmaceutical Chemistry, University of Frankfurt (Prof. C. Noe), 1995.
[48] A. A. Koshkin, P. Nielsen, M. Meldgaard, V. K. Rajwanshi, S. K. Singh, J. Wengel, *J. Am. Chem. Soc.* **1998**, *120*, 13252.
[49] S. Knapp, W. C. Shieh, *Tetrahedron Lett.* **1991**, *32*, 3627; S. Niitsuma, Y. Ichikawa, K. Kato, T. Takita, *Tetrahedron Lett.* **1987**, *28*, 3967; T. Hashizume, K. Yoshida, *Agric. Biol. Chem.* **1976**, *40*, 2001; A. M. Kritzyn, A. Holy, *Collect. Czech. Chem. Commun.* **1975**, *40*, 3211; H. Iwamura, M. Miyakado, T. Hashizume, *Carbohydr. Res.* **1973**, *27*, 149; Y. H. Pan, R. K. Robins, L. B. Townsend, *J. Heterocycl. Chem.* **1967**, *4*, 246.
[50] H. Vorbrüggen, B. Bennua, *Chem. Ber.* **1981**, *114*, 1279.
[51] H. G. Fletcher Jr., R. K. Ness, *J. Am. Chem. Soc.* **1955**, *77*, 5337; R. Jeanloz, H. G. Fletcher Jr., C. S. Hudson, *J. Am. Chem. Soc.* **1948**, *70*, 4052.
[52] P. Ermert, Diplomarbeit ETH (1990); S. Pitsch, C. Spinner, K. Atsumi, P. Ermert, *Chimia* **1999**, *53*, 291.
[53] P. Garner, J. V. Yoo, R. Sarabu, *Tetrahedron* **1992**, *48*, 4259.
[54] Y. Hayakawa, M. Hirose, R. Noyori, *J. Org. Chem.* **1993**, *58*, 5551.
[55] Y. Hayakawa, S. Wakabayashi, H. Kato, R. Noyori, *J. Am. Chem. Soc.* **1990**, *112*, 1691.
[56] M. Ashwell, C. Bleasdale, B. T. Golding, I. K. O'Neill, *J. Chem. Soc., Chem. Commun.* **1990**, 955; B. L. Gaffney, R. A. Jones, *Tetrahedron Lett.* **1982**, *23*, 2253.
[57] G. M. Visser, V. van Westrenen, C. A. A. von Boeckel, J. H. van Boom, *Recl. Trav. Chim. Pay-Bas* **1986**, *105*, 528.
[58] N. Baggett, K. W. Buck, A. B. Foster, M. H. Randall, J. M. Webber, *J. Chem. Soc.* **1965**, 3394, 3401; C. Li, A. Vasella, *Helv. Chim. Acta* **1993**, *76*, 211; D. M. Clade, *Chem. Rev.* **1979**, *79*, 491.
[59] S. Wolfe, *Acc. Chem. Res.* **1972**, *5*, 102.
[60] Y. Okuno, K. Horita, O. Yonemitsu, K. Shibata, T. Amemiya, R. H. Holm. *J. Chem. Soc.*, *Perkin Trans. 1* **1984**, *5*, 1115; H.-J. Roth, 'HOMO-DNS, Herstellung, Paarungseigenschaften und Struktur von Adenin-Thymin-Haltigen Oligonukleotiden', Diss. No. 9591, ETH-Zürich, 1991.
[61] Y. Hayakawa, M. Hirose, M. Hayakawa, R. Noyori. *J. Org. Chem*. **1995**, *60*, 925.
[62] V. A. Effimov, A. A. Buryakova, S. V. Reverdato, O. G. Chakhmakcheva, Y. A. Ovchinnikov, *Nucleic Acids Res.* **1983**, *11*, 8369.

[63] U. Pieles, W. Zürcher, M. Schär, H. E. Moser, *Nucleic Acids Res.* **1993**, *21*, 3191.
[64] G. Quinkert, E. Egert, C. Griesinger, 'Aspects of Organic Chemistry', Verlag Helvetica Chimica Acta, Basel, 1996, Chapt. 7.2.
[65] D. G. Gorenstein, J. B. Findlay, B. A. Luxon, D. Kar, *J. Am. Chem. Soc*. **1977**, *99*, 3473.
[66] S. Ilin, I. Schlönvogt, M.-O. Ebert, B. Jaun, H. Schwalbe, *ChemBioChem* **2002**, *3*, 93.
[67] H. Schwalbe, J. Wermuth, C. Richter, S. Szalma, A. Eschenmoser, G. Quinkert, *Helv. Chim. Acta* **2000**, *83*, 1079.
[68] G. Karig, A. Fuchs, A. Büsing, T. Brandstetter, S. Scherer, J. W. Bats, A. Eschenmoser, G. Quinkert, *Helv. Chim. Acta* **2000**, *83*, 1049.
[69] L. A. Markey, K. J. Breslauer, *Biopolymers* **1987**, *26*, 1601
[70] P. N. Borer, B. Dengler, I. Tinocco Jr., O. C. Uhlenbeck, *J. Mol. Biol.* **1974**, *86*, 843.
[71] M. Tarköy, M. Bolli, B. Schweizer, C. Leumann, *Helv. Chim. Acta* **1993**, *76*, 481.
[72] C. Leumann, *Bioorg. Med. Chem*. **2001**, *9*, 1.
[73] P. Herdewijn, *Biochim. Biophys. Acta* **1999**, *1489*, 167.
[74] M.-O. Ebert, A. Luther, H. K. Huynh, R. Krishnamurthy, A. Eschenmoser, B. Jaun, *Helv. Chim. Acta* **2002**, *85*, 4055.
[75] M. Renz, R. Lohrmann, L. E. Orgel, *Biochem. Biophys. Acta* **1971**, *240*, 463; L. E. Orgel, *Nature (London)* **1992**, *358*, 203.
[76] R. Naylor, P. T. Gilham, *Biochemistry* **1966**, *5*, 2722.
[77] O. A. Federova, M. B. Gottikh, T. S. Oretskaya, Z. A. Shabarova, *Nucleosides Nucleotides* **1996**, *15*, 1137.
[78] G. V. Kiedrowski, *Angew. Chem.* **1986**, *98*, 932.
[79] A. R. Hill Jr., L. E. Orgel, T. Wu, *Origins Life Evol. Biosphere* **1993**, *23*, 285.
[80] M. Kurz, K. Göbel, C. Hartel, M. W. Göbel, *Angew. Chem*. **1997**, *109*, 873.
[81] M. Renz, R. Lohrmann, L. E. Orgel, *Biochim. Biophys. Acta* **1971**, *240*, 463.
[82] D. A. Usher, A. H. Hale, *Proc. Natl. Acad. Sci. U.S.A.* **1976**, *73*, 1149; D. A. Usher, *Nature New Biol.* **1972**, *235*, 207.
[83] D. Sievers, G. v. Kiedrowski, *Chem. Eur. J.* **1998**, *4*, 629 and refs. cit. therein.
[84] A. Luther, R. Brandtsch, G. v. Kiedrowski, *Nature* **1998**, *396*, 245.
[85] A. Saghatelian, Y. Yokobayashi, K. Soltani, R. Ghadiri, *Nature* **2001**, *409*, 797.
[86] N. Paul, G. F. Joyce, *Proc. Natl. Acad. Sci. U.S.A* **2002**, *99*, 12733; K. E. McGinness, G. F. Joyce, *Chem. Biol*. **2003**, *10*, 5; W. K. Johnston, P. J. Unrau, M. S. Lawrence, M. E. Glasner, D. P. Bartel, *Science* **2001**, *292*, 1319.
[87] A. Eschenmoser, *Origins Life Evol. Biosphere* **1997**, *27*, 535.
[88] J. Ferris, G. Ertem, *Science* **1992**, *257*, 1384; J. P. Ferris, A. R. Hill, R. Liu, L. E. Orgel, *Nature* **1996**, *381*, 59; J. P. Ferris, *Origins Life Evol. Biosphere* **2002**, *32*, 311.
[89] A. Kanavarioti, P.-A. Monnard, D. W. Deamer, *Astrobiology* **2001**, *1*, 271.
[90] K.-U. Schöning, P. Scholz, X. Wu, S. Guntha, G. Delgado, R. Krishnamurthy, A. Eschenmoser, *Helv. Chim. Acta* **2002**, *85*, 4111.

Received October 6, 2003